NNT : 0000AIXM0000

THÈSE DE DOCTORAT

Soutenue à Aix-Marseille Université
le 09 Septembre 2024 par

Nour-Islem Yanis SAIDANI

Role of CELSR2 in tumor progression and its targeting in triple negative breast cancer

Discipline
Biologie-Santé

Spécialité
Oncologie

École doctorale
ED62 – SCIENCES DE LA VIE ET DE LA SANTE

Laboratoire/Partenaires de recherche
Centre de Recherche en Cancérologie de Marseille

Composition du jury

Ines Liebscher Leipzig University, Allemagne	Rapporteure
Julie PANNEQUIN Institut de Génomique fonctionnelle, Université de Montpelier, France	Rapporteure
Franck Vandermoere Institut de génomique fonctionnelle, Université de Montpelier, France	Examinateur
Emmanuelle Charafe-Jauffret Aix-Marseille Université	Présidente
Jean-Paul BORG Aix-Marseille Université	Directeur de thèse
Alexandra WALTON Aix-Marseille Université	Co-directrice de thèse

Affidavit:

I, undersigned, Nour Islem Yanis SAIDANI, hereby declare that the work presented in this manuscript is my own work, carried out under the scientific supervision of Alexandra WALTON and Jean-Paul BORG, in accordance with the principles of honesty, integrity and responsibility inherent to the research mission. The research work and the writing of this manuscript have been carried out in compliance with both the French national Charter for Research Integrity and the Aix-Marseille University Charter on the fight against plagiarism.

The work presented in this manuscript has not been submitted previously either in France or in another country in the same or in a similar version as part of another examination or defense process.

Marseille May 30th 2024

Signature :



Liste de publications et/ou brevets et participation aux conférences

Liste des publications et/ou brevet réalisées dans le cadre du projet de thèse :

SAIDANI NIY, Josselin E, Castellano R, Ly J, Verenerey J, Audebert S, Walton A and Borg JP. CELSR2 is a potent biomarker and druggable target in triple negative breast cancer (to be submitted)

Participation aux conférences et écoles d'été au cours de la période de thèse :

- 5ème PhD Day du Centre de Recherche Cancérologie de Marseille - Communication Orale
- 6th IPC symposium 2021, Marseille France
- Challenges in Onco-Immunology Société Française d'Immunologie (SFI), Paris
- ImmunoSEM 2021 Bristol Myers Squibb
- Development of an educational program for autoimmune diseases and immunotherapies National and Kapodistrian University of Athens, Athens, Greece
- Summer schoool in Immunotherapy of Cancer, Tubingen Germany - Poster
- Summer School "Single-cell approaches and omics, Bucharest Romania - Poster
- Symposium de l'institut cancer immunologie 2023, Marseille France - Communication orale
- Symposium du département COMET 2024, Marseille France - Communication orale
- Adhesion GPCRs - present and future, Split Croatia - Poster

Résumé en français :

Le cancer du sein triple négatif (TNBC) pose un défi majeur de santé publique. C'est une maladie caractérisée par une hétérogénéité, des métastases fréquentes et une résistance au traitement par chimiothérapie. Bien que quelques thérapies ciblées aient été approuvées ces dernières années pour la prise en charge des patientes, telles que les inhibiteurs de PARP et les inhibiteurs de checkpoint immunitaires, la plupart des patientes demeurent inéligibles pour ces nouvelles thérapies. Dans le but de développer de nouveaux traitements pour le traitement du cancer du sein triple négatif, nous nous sommes intéressés à Cadherin EGF LAG seven-pass G-type receptor 2 (CELSR2), un récepteur couplé aux protéine G (RCPG) d'adhésion qui a été principalement étudié dans le développement neuronal, les maladies cardiovasculaires, la scoliose, les anomalies du métabolisme,…etc. Dans notre étude, nous avons constaté qu'une surexpression de CELSR2 est positivement corrélée à la fois à une survie sans métastases significativement réduite et à la survie globale des patientes atteintes de TNBC. De plus, en analysant les données transcriptomiques des patientes, nous avons constaté que l'expression de CELSR2 est augmentée dans le site métastatique comparé à la tumeur primaire. Au niveau single cell, nous avons constaté que CELSR2 est principalement exprimé par cellules malignes, tandis que les tissus sains présentent une faible expression, ce qui fait du récepteur une cible potentiellement prometteuse en clinique. Dans la présente étude, nous avons élucidé le rôle fonctionnel du récepteur en le downrégulant avec des siRNA ou des shRNA dans des lignées cellulaires TNBC (MDA-MB468, HCC1806, BT20) . : nous avons observé une diminution significative de la prolifération cellulaire, de la migration cellulaire et de l'invasion à travers la matrice extracellulaire. Nous avons également découvert que CELSR2 active la voie AMPc/PKA/CREB afin de favoriser la phosphorylation oxydative. De plus, nous avons xénogreffé des cellules TNBC prélablement transduites avec des shRNA dirigé contre CELSR2 sur les glandes mammaires des souris NSG immunodéficientes chez lesquelles nous avons observé

un ralentissement de la croissance tumorale et une diminution globale de l'activité Ki67. Dans le but d'évaluer le ciblage thérapeutique du récepteur avec des nanobodies, nous avons immunisé des lamas avec des membranes cellulaires de MCF7, une lignée cellulaire exprimant de haut niveau de CELSR2. Après la construction de la librairie, nous avons effectué des criblages en alternant cellules exprimant CELSR2 et la protéine recombinante de la partie extracellulaire du récepteur et sélectionné deux nanobodies spécifiques de CELSR2. Lors du traitement des cellules avec les nanobodies spécifiques de CELSR2, nous avons observé une diminution de la prolifération et de la migration cellulaire, imitant ainsi les phénotypes observés lorsqu'on downrégule le récepteur. En résumé, cette étude dévoile un nouveau rôle de CELSR2 dans la progression tumorale ainsi qu'une preuve de concept que ce récepteur pourrait être une cible thérapeutique potentielle dans le traitement du TNBC.

Mots clés : Cancer du sein triple négatif (TNBC), RCPG d'adhésion, CELSR2, nanobodies

Abstract :

Triple negative breast cancer (TNBC) poses a major public health challenge. It is a disease characterized by heterogeneity, frequent distant metastasis and resistance to conventional treatment. Although a number of targeted therapies have been approved in recent years for the treatment of TNBC such as PARP inhibitors and immune checkpoint inhibitors, most patients do not benefit from these novel therapies. With the aim of developing novel therapeutics for the treatment of triple negative breast cancer, we investigated Cadherin EGF LAG seven-pass G-type receptor 2 (CELSR2), an adhesion G-protein coupled receptor which has been mostly studied in neural development, coronary artery disease, scoliosis, metabolism defects, etc. Yet, we found that an overexpression of CELSR2 correlates positively with both a significantly decreased metastasis free survival and overall survival of triple negative breast cancer patients. Moreover, by analyzing patient transcriptomics data we found that CELSR2 expression is increased in the metastatic site when compared with the primary tumor.

At a single cell level, we found that CELSR2 is mostly expressed on malignant cells in tumors, while healthy tissue exhibits a low expression, potentially making the receptor a desirable target in the clinic. We elucidated the functional role of the receptor by knocking down the receptor with siRNA or shRNA : the resulting phenotypes were significantly dampened cell proliferation, cell migration and invasion through the extracellular matrix. We also aimed to investigate the molecular pathway to explain the observed phenotype; we found that CELSR2 signals through the cAMP/PKA/CREB pathway to promote oxidative phosphorylation in TNBC cells. Moreover, we xenografted TNBC cells knocked down for CELSR2 in immunodeficient NSG mice in which we observed a hindered tumor growth and an overall decrease of Ki67 activity. With the aim of assessing the druggability of the receptor with nanobodies, we immunized lama with cell membranes of MCF7, a highly expressing cell line for CELSR2. After library construction, we performed screens by alternating between cells expressing CELSR2 and the recombinant protein of the extracellular fragment of CELSR2. We selected two nanobodies specific for CELSR2. Upon treatment of cells with the nanobodies specific to CELSR2, we observed a hindered cell proliferation and migration, mimicking the observed phenotypes when the receptor was silenced. Altogether, this study unveils a novel role for CELSR2 in tumor progression along with a proof of concept of its potential as a targeted therapy candidate for triple negative breast cancer.

keywords : Triple negative breast cancer (TNBC), adhesion GPCRs, CELSR2, nanobodies

General public abstract in English :

A cell is the fundamental unit of all living organisms. It is an almost self-sufficient factory, in which organic and inorganic molecules are treated and transformed. A cell undergoes many morphological changes throughout its life, and just like a human, it reproduces, but in an asexual manner. While the reproduction of cells is crucial, it happens that it becomes uncontrolled, therefore causing the infamous disease : cancer. For a cell to become uncontrolled, there needs to be catastrophic events which alter the genome, which is somehow the operating system of a cell. The alteration of the genome leads to an abnormal expression of proteins favorable to the growth of cancer. In the present study, we identified a previously unsuspected protein, CELSR2, expressed on the surface of cancer cells and which plays a potent role in the proliferation of cells and their migration capacity. Beyond our investigation of the role played by CELSR2, we developed nanobodies, small antibodies, aimed at the protein. We can think of these nanobodies as bullets used to shoot very precisely at our protein of interest, CELSR2. Altogether, this study provides novel insights on the biology of this protein in a cancer context and offers original tools to target it in further preclinical and clinical settings.

Abstract vulgarisé en Français :

Une cellule est l'unité fondamentale de tout organisme vivant. C'est une usine quasi-autosuffisante, dans laquelle sont traitées et transformées des molécules organiques et inorganiques. Une cellule subit de nombreux changements morphologiques tout au long de sa vie et, tout comme l’être humain, elle se reproduit, mais de manière

asexuée. Alors que la reproduction des cellules est cruciale, il arrive qu'elle devienne incontrôlée, provoquant ainsi la fameuse maladie : le cancer. Pour qu’une cellule devienne incontrôlée, il faut qu’il y ait des événements catastrophiques qui altèrent le génome, qui est en quelque sorte le système d’exploitation d’une cellule. L'altération du génome entraîne une expression anormale de protéines favorables à la croissance du cancer. Dans la présente étude, nous avons identifié une protéine jusqu'alors insoupçonnée, CELSR2, exprimée à la surface des cellules cancéreuses et qui joue un rôle considérable dans la prolifération des cellules et leur capacité de migration. Au-delà de notre étude sur le rôle joué par CELSR2, nous avons développé des nanobodies, de petits anticorps dirigés contre la protéine. Nous pouvons considérer ces nanobodies comme des balles utilisées pour tirer très précisément sur notre protéine d’intérêt, CELSR2. En résumé, cette étude met en lumière la biologie de cette protéine dans un contexte cancéreux et offre des outils originaux pour la cibler dans le futur dans des contextes précliniques et cliniques.

Acknowledgements :

The present work was conducted at the cancer research center of Marseille U1068, affiliated with the INSERM, CNRS, Aix Marseille Université and l'institut Paoli Calmettes.
Alexandra, you have been a lot of things for me, a mentor, a gossip partner, a friend, a lawyer… Thank you for passionately supervising my PhD thesis, and thank you for all the monumental efforts in shaping and proofreading this present piece of work. I am very happy to be your first doctoral student. I have no doubt we will have the chance to work together one day.
I would like to thank the head of our research group and my thesis co-supervisor Jean-Paul Borg for welcoming me in the team and the provided means which enabled me to pursue my PhD project.

Huuuuuge thanks to Sylvie and Avais. Thank you for your efforts in administrative management which made our work seamless. I have learned a lot from you two. Thank you Sylvie for all the advice and discussions, the history lessons about the institute and all the local scientific community.

I shall express my greatest gratitude to Andrew Kruse and Luca Lignitto. You are both role models for me. I profoundly admire your intelligence and passion for science and fundamental questions and the efforts you put in your works. I guess for every PhD candidate, there are a number of people we look up to, in my case, it's you two.

What has become an evil axis, Bashir, Ines, Nassim, The Pierre-Louis, The Jeck. What a bunch of free and easy numbskulls. Words would not express the depth of our relationships. More than friendship, brotherhood.

At the CRCM, an interesting platform called "In vivo studies made easy with Remy and Emmanuelle" exists. I could not thank you enough Remy for your advice and the time spent on talking, sharing and helping me mature as a junior researcher. My thankfulness for you Emmanuelle is tremendous, thanks a lot for all the goodwill, time and efforts spent.

I would like to thank the members of the Antibody therapeutics and immunotargeting platform, where I spent some time and learned a considerable part of what I know today. Patrick, you were always present, with great inputs and advice. Remi and Thimotée you both have been full of concern and kindness towards me and my project. Thanks a lot.

Marghé, Nicolas, Nathan, Sébastien, Rania et Raph LeCamembert, Charlotte, all of you have participated either scientifically or emotionally to make my thesis a happy chapter.
My team, the Borg-Maina, AKA JPB-FM 103.5 MHz. Although some would think we are a radio station, we actually do science, discover novel biomarkers, make antibodies AND nanobodies, engineer mouse models, develop new therapeutic approaches…In a nutshell, we fight cancer. Thanks a lot to all of the team members who have participated in setting a positive mood and growing our science.

vghigh adinigh tanmirth tamo9rant imawlaniw i imma, d baba, ayathma, tamatouth iw d tafamilt akith wahi d ait n tadarth negh que ce soit egue Bbouandes negh egue Vgayeth, eg Setif i les encouragements nwen, dayen dachou iyijen adla79agh anda ligh tura.

“Luck is what happens when preparation meets opportunity”

Seneca

"Natural forces within us are the true healers of disease.”
Hippocrates

نَحْنُ طُـــلَّابُ الْجَزَائِرْ ..... نَحْنُ لِلْمَجْدِ بُنَـــاةْ

نَحْنُ آمَـــالُ الْجَـزَائِـــرْ ..... فِي اللَّيَالِي الْحَالِكَاتْ

لبلدي,بلد الأحرار, بلد المليون ونصف مليون شهيد

بلادي أحبك فوق الظنون

لأجل بلادي عصرت النجوم

 # i tmurthiw - ⵉ ⵜⴰⵎⵓⵔⵜⵀⵉⵡ

Table of contents :

Affidavit: 1

Résumé en français : 3

Abstract : 4

General public abstract in English : 6

Abstract vulgarisé en Français : 6

Abbreviations list : 12

Chapter 1 : 15

A brief history of breast cancer and its care 15

Breast cancer epidemiology : 16

Breast cancer risk factors : 21

Age : 22

Ethnicity : 23

Menopause and menarche : 23

Genetic predisposition : 23

Radiations and environmental elements exposure: 25

Hormonal contraception : 26

Lifestyle : 26

Pregnancy and breastfeeding : 27

Breast cancer biology, histology and molecular subtyping 27

The breast : 27

Pathology of invasive breast cancer : 28

Breast cancer molecular subtyping : 30

Triple negative breast cancer : 34

TNBC biology : 34
TNBC microenvironment : 37
TNBC study models : 39
BC and TNBC therapeutics : current and ongoing 43
Chapter 2 : 57
Re-activation of developmental programs in cancer: 57
The Hedgehog pathway : 58
The NOTCH pathway : 59
Wnt pathway : 59
Other pathways : 61
Chapter 3 : 62
An overview of the GPCRs family : 62
GPCR signaling 68
G-protein dependent and independent signaling : 69
Downstream effectors of GPCR signaling : 71
Biased signaling of GPCRs : 73
GPCR structure : 74
Adhesion GPCRs : 77
aGPCRs in cancer : 84
Chapter 4 : 87
CELSR2 receptor : 87
CELSR2 tissue distribution and functions : 88
Chapter 5 : 90
Antibody - nanobody therapeutics 90
Nanobodies from discovery to application 92
The pipeline to nanobody discovery : 95
Objectives of this thesis: 96

Results : 98

Original research paper : Cancer promoting mechanism of CELSR2 and its targeting in triple negative breast cancer 99

Introduction : 101

Material and methods : 103

Results : 114

CELSR2 expression in healthy tissues and breast tumors and correlation with patient prognosis 114

CELSR2 promotes tumor growth in TNBC mouse xenograft 115

CELSR2 drives proliferation, migration and invasion of TNBC cells 116

CELSR2 induces CREB phosphorylation : 117

CELSR2 activates the TCA cycle and oxidative phosphorylation 118

CELSR2-targeting nanobodies significantly inhibit cell migration 119

Discussion : 120

Study limitations : 124

Acknowledgements : 124

Author contribution : 124

Declaration of Interest 125

Funding sources : 125

Figures : 125

Tables : 138

Supplementary materials : 139

References : 159

CELSR2 mediates cell adhesion to the matrix : 166

Tethered agonist exposure does not induce CELSR2 activation : 168

CELSR2 silencing does not sensitize cells to chemotherapies : 171

Discussion 174

CELSR2 expression in TNBC tumors : 176
A new role for CELSR2 in breast tumor development: 176
CELSR2 acting as an adhesion molecule : 177
Biased agonism of CELSR2 : 179
Mechanism of CELSR2 in orchestrating tumor cells metabolism, proliferation and migration: 182
CELSR2 specific nanobodies discovery : 183
CELSR2 variants : 185
Study limitations : 186
A cancer cell centered approach : 186
CELSR2 orphan status : 187
Risks and limitations of targeting CELSR2 with nanobodies : 187
References : 189

Abbreviations list :

5HT1A : serotonin 1A receptor

aGPCR : adhesion G-protein coupled receptor

AD: anno domini

ADC : antibody drug conjugate

AML : acute myeloid leukemia

AR : androgen receptor

BALB/c : Bagg Albino C

BC : before Christ

BCS : breast conserving surgery

BL1: basal like 1

BL2 : basal like 2

BMP : bone morphogenetic peptides

cAMP : Cyclic adenosine monophosphate

CDK : cyclin dependent kinase

CELSR2 : Cadherin EGF LAG seven-pass G-type receptor 2

DAG : diacylglycerol

D2 : dopamine receptor 2

DFS : disease free survival

DLL : delta like ligand

ECD : extracellular domain

EMA : European medicines agency

ER : estrogen receptor

EMT : epithelial-mesenchymal-transition

FISH : fluorescent in situ hybridization

GAIN : GPCR autoproteolysis-inducing domain

GDP : guanosine diphosphate

GTP : guanosine triphosphate

GLPs : glucagon like peptides
GPCR : G-protein coupled receptor
GPS : GPCR proteolysis site
GSK3 : glycogen synthase kinase-3
HDI : high developing index
HER2 : human epidermal receptor 2
ICI : immune checkpoint inhibitor
IDC : invasive duct carcinoma
IHC : immunohistochemistry
IP3 : inositol triphosphate
JAG : Jagged
LAR : luminal androgen receptor
LDI : low developing index
M : mesenchymal
MLC : myosin-light-chain phosphatase
MMAE : monomethyl auristatin E
NSG : Nod SCID gamma
OS : overall survival
PAR : protease activated receptor
PARP : Poly (ADP-ribose) polymerase
pCR : pathologic complete response
PIP2 : phosphatidylinositol 4,5- bisphosphate
PFS : progression free survival
PR : progesterone receptor
PLC : phospholipase C
PTH : parathyroid hormone
ROR1 : receptor Tyrosine Kinase Like Orphan Receptor 1
ROR2 : receptor Tyrosine Kinase Like Orphan Receptor 2
ROS : reactive oxygen species
RT : radiotherapy
RTK : receptor tyrosine kinase
RYK : related to receptor tyrosine kinase
RRSO : risk reducing salpingo-oophorectomy

SMO : smoothened

TMB : tumor mutational burden

TME : tumor microenvironment

TNBC : triple negative breast cancer

VIP : vasoactive intestinal peptide

WHO : world health organization

γ-SEC : gamma secretase

Chapter 1 :

A brief history of breast cancer and its care

Breast cancer has been identified as early as 3000 BC in the writings of Imhotep, an Egyptian physician and architect (Cases 39 through 46 of the Edwin Smith surgical papyrus)[1]. Fast forward to ancient Greece, Hippocrates stipulated that breast carcinoma develops upon a disequilibrium of humours. Then during the 1st AD Leonides of Alexandria masterfully described a surgical approach to excise only the tumor with very narrow margins, instead of removing large parts of the breast, thus, prognosticating what would become a gold standard in breast cancer surgery 2 millennia later[2]. While science and medicine stagnated in Europe, muslim scholars sustained medicine and science in the islamic world, most notably Ibn Sina (10th century AD) and Abu al-Qasim (10th century AD), who first sought to reduce the tumor burden by cauterizing it, then proceeded to surgery[3]. Little to no progress was made in the following centuries until the advent of the aseptic surgery paradigm and anesthesia application around the 18th and 19th centuries, which helped ease the surgical burden both on patients and surgeons. Different approaches were then implemented, among which the dissection of axillary lymph nodes along with radical mastectomy performed by the Johns Hopkins hospital surgeon Halsted[4]. The 20th century would go on to be the era where surgery was not the only resort anymore, as light was shed on the pathogenesis of the disease, the discovery of hormone receptors, the introduction of medical radiation, the clinical use of chemotherapy and targeted therapies towards the end of the century[5–7]. Thus, surgery is now used in some sort of therapeutic sequence along with other modalities, such as an adjuvant chemoradiotherapy complementing the surgical procedure. Breast cancer treatment up to the end of the 20th century focused mainly on eradicating the disease, with little attention given to the psychological repercussions that mastectomy had on female patients. Most often, total or partial mastectomy induced psychological disorders notably anxiety, depression and insomnia. The 21st century is finally the century when

a human and psychological dimension was instituted in breast cancer care with the introduction of breast conservation surgery and mammary reconstruction[8]. This evolution in surgical practice showed an important psychological benefit and satisfaction among patients[9]. Additionally, axillary lymph nodes were not systematically dissected, rather only those positive mostly[10]. As we understood better the biology of cancer itself, more therapies paved their way to clinical practice, most notably PARP inhibitors, monoclonal antibodies and immunotherapies[11]. **Contemporary research focuses on at least two objectives : restrain breast cell proliferative pathways and identify proteins that can either have a prognostic value or be a target for treatment.**

Breast cancer epidemiology :

Breast cancer, along with colorectal, lung and prostate cancers, are the accounted as the “big four” as per their incidence[12]. By 2020, female breast cancer has become the most commonly diagnosed cancer, thus surpassing lung cancer[13]. More than 2.3 million cases (11%) are diagnosed yearly out of the ~19 million cancer cases. Breast cancer is the most frequently diagnosed cancer in at least 159 countries. Breast cancer is the leading cause of death related to cancer and accounts for almost 700,000 deaths (15.5% among female deaths and 6.9% of all cancer deaths) (Figure 1). Currently, the WHO recommends a screening mammography for women aged between 50 and 69 every 2 years[14].

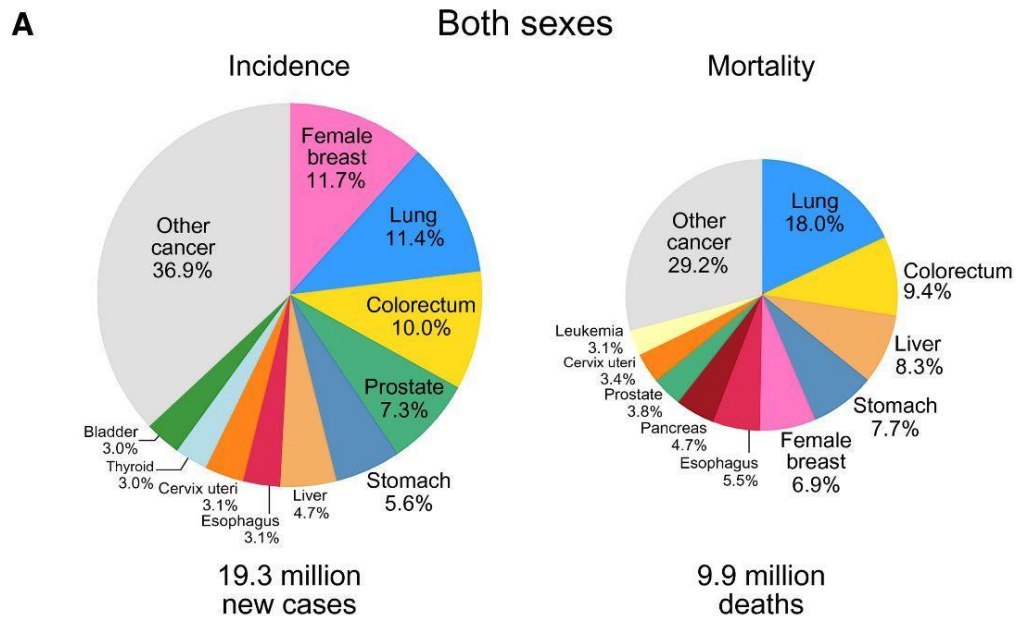
A
Both sexes
Incidence
Mortality
Female breast 11.7%
Lung 11.4%
Colorectum 10.0%
Prostate 7.3%
Stomach 5.6%
Liver 4.7%
Esophagus 3.1%
Cervix uteri 3.1%
Thyroid 3.0%
Bladder 3.0%
Other cancer 36.9%
19.3 million new cases
Lung 18.0%
Colorectum 9.4%
Liver 8.3%
Stomach 7.7%
Female breast 6.9%
Esophagus 5.5%
Pancreas 4.7%
Prostate 3.8%
Cervix uteri 3.4%
Leukemia 3.1%
Other cancer 29.2%
9.9 million deaths

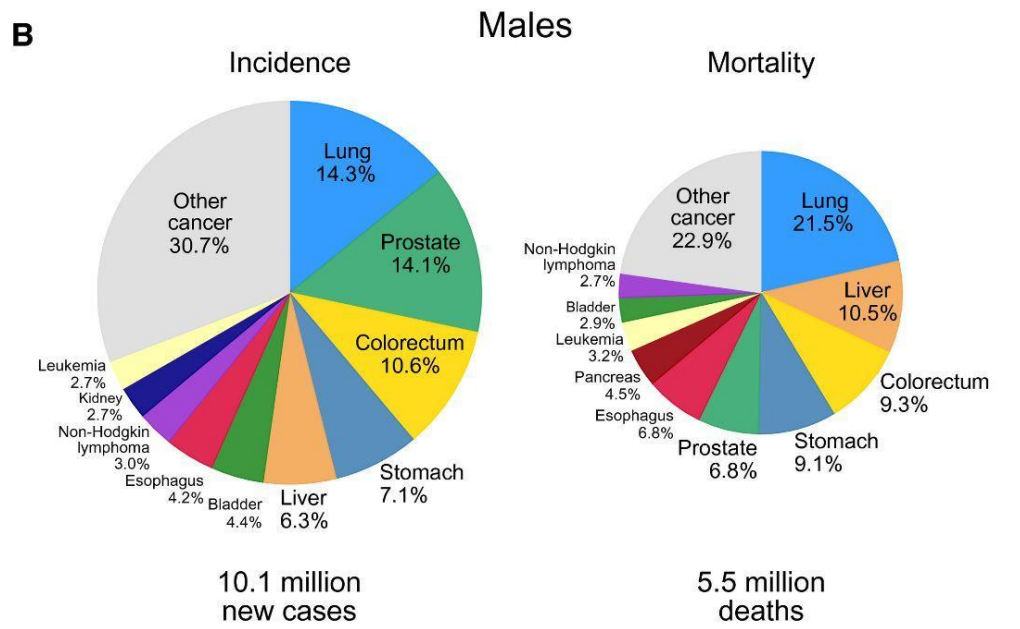
B
Males
Incidence
Mortality
Lung 14.3%
Prostate 14.1%
Colorectum 10.6%
Stomach 7.1%
Liver 6.3%
Bladder 4.4%
Esophagus 4.2%
Non-Hodgkin lymphoma 3.0%
Kidney 2.7%
Leukemia 2.7%
Other cancer 30.7%
10.1 million new cases
Lung 21.5%
Liver 10.5%
Colorectum 9.3%
Stomach 9.1%
Prostate 6.8%
Esophagus 6.8%
Pancreas 4.5%
Leukemia 3.2%
Bladder 2.9%
Non-Hodgkin lymphoma 2.7%
Other cancer 22.9%
5.5 million deaths

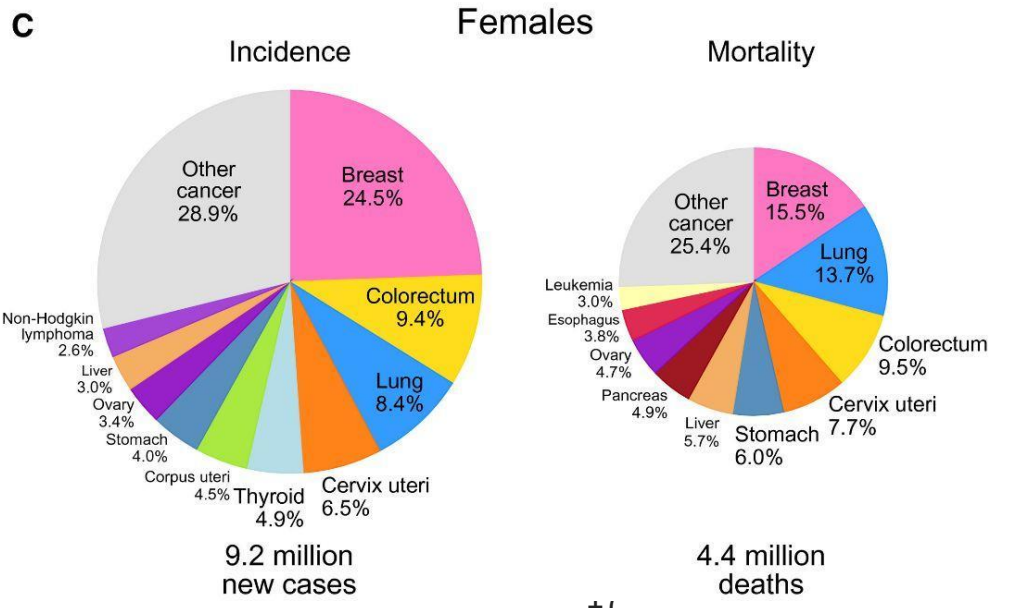
C
Females
Incidence
Mortality
Breast 24.5%
Colorectum 9.4%
Lung 8.4%
Cervix uteri 6.5%
Thyroid 4.9%
Corpus uteri 4.5%
Stomach 4.0%
Ovary 3.4%
Liver 3.0%
Non-Hodgkin lymphoma 2.6%
Other cancer 28.9%
9.2 million new cases
Breast 15.5%
Lung 13.7%
Colorectum 9.5%
Cervix uteri 7.7%
Stomach 6.0%
Liver 5.7%
Pancreas 4.9%
Ovary 4.7%
Esophagus 3.8%
Leukemia 3.0%
Other cancer 25.4%
4.4 million deaths

Figure 1 :Worldwide number of cancer cases. (A) Incidence and mortality of 10 most common cancers in both sexes, (B) in men, (C) in women[13].

Important disparities in incidence are however observed, based on various factors. Incidence is usually higher in high developing index (HDI) than low/medium (L/MDI) developing countries such as in the US, Australia, New Zealand and Canada (55.9 cases/100000 versus 29.7/100000 respectively) (Figure 2).

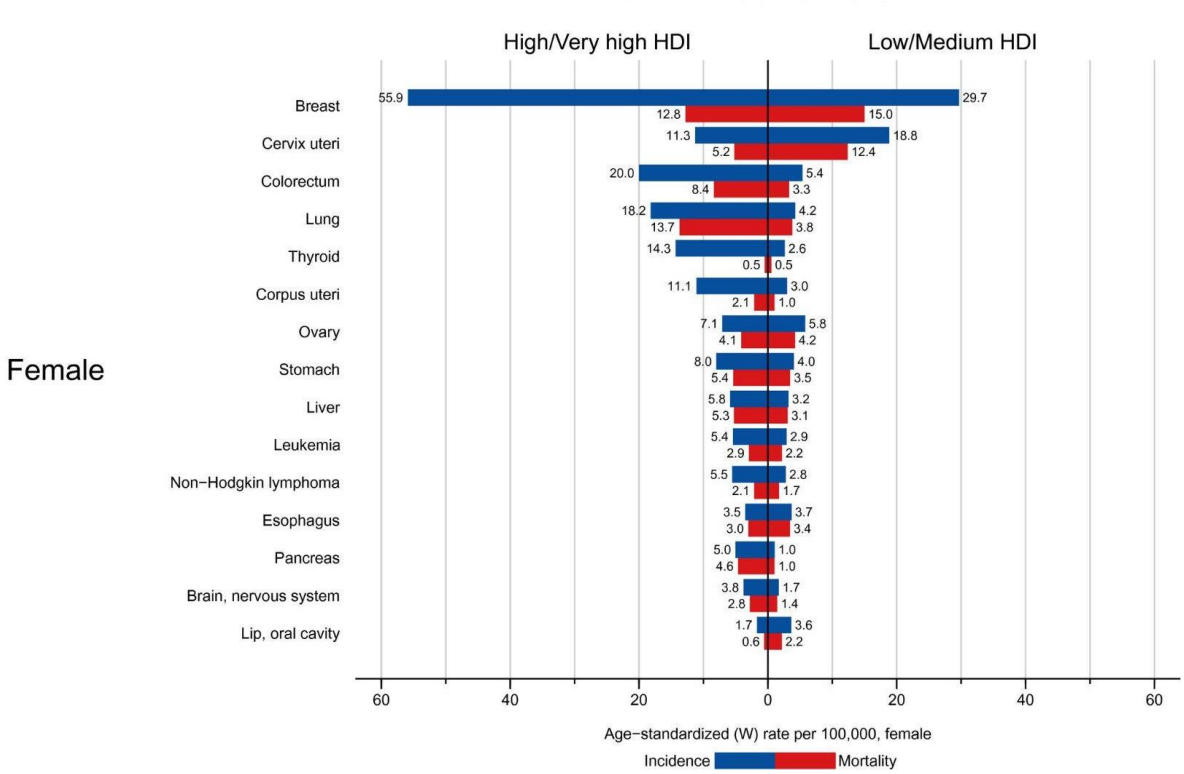

Figure 2 : Incidence rates of the 15 most prevalent malignancies observed in women in high or very high Human Development Index (HD) countries vs low or medium HDI countries[13].

This higher observed incidence reflects the higher access to medical facilities and prevention screening programs by mammography in HDI countries. This pattern is further reflected in mortality which is inverted in developing countries in which the mortality is higher than in developed countries. This situation could have many roots of which we can cite 2 major ones. First, the complicated or even absent access to mammography for early screening which delays the diagnosis, and once the patients present themselves to the clinic, the disease has already reached an advanced stage.

Second, the lower access for new therapies such as targeted drugs and immunotherapies which represent a major breakthrough in cancer management[15]. Furthermore, the higher incidence in developed countries is supported by the exposure to a number of risk factors such as the use of oral contraceptives, late menopause, alcohol consumption, physical inactivity…etc. Screening programs seem to have reached an enrollment plateau since two decades, thus giving way to campaigns encouraging breastfeeding, physical activity and limiting alcohol use in order to complement the population based screening programs[16,17]. Beyond the present-day landscape, the projected incidence of breast cancer should not significantly change over the next few years, unlike pancreas and thyroid cancers. Projected deaths show a net negative value, nevertheless, breast cancer is projected to remain the most deadly by 2030 (Figure 3)[18] .

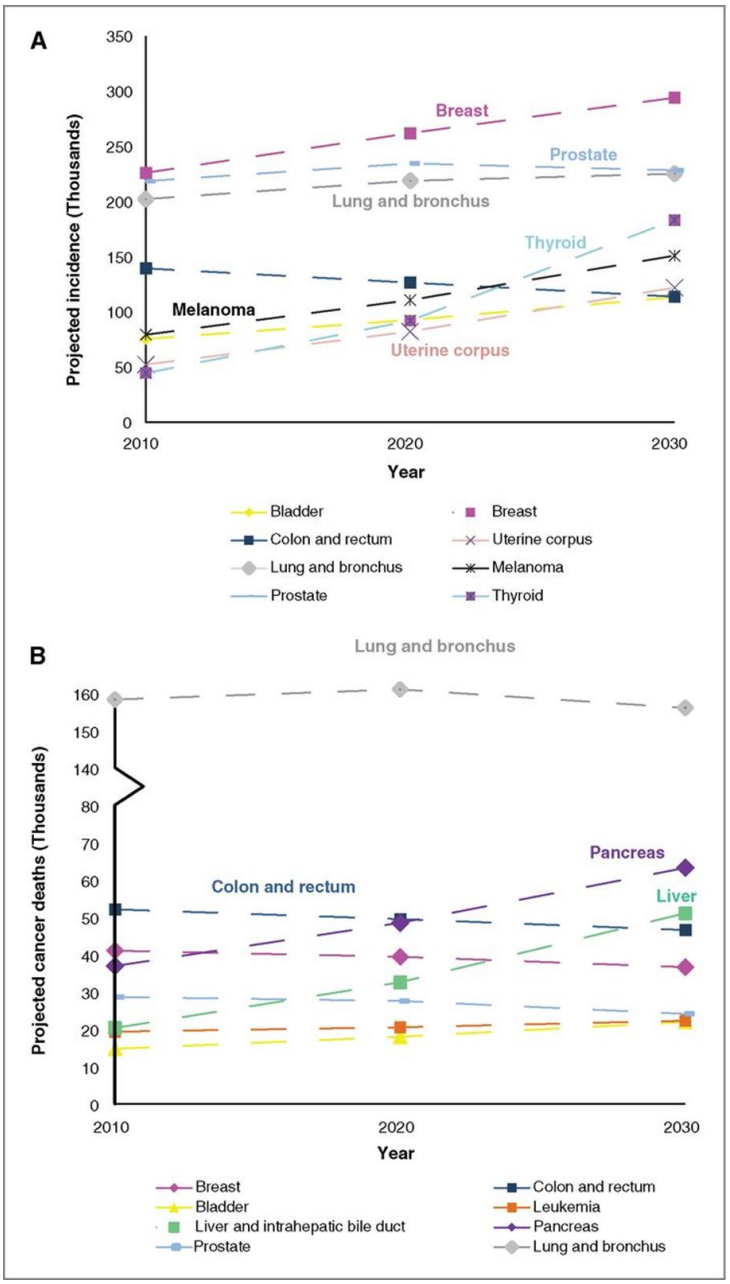

Figure 3 : Projected incidence and deaths in both sexes. (A) incidence projection of 8 most prevalent cancers by 2030. (B) mortality projection of the deadliest cancers by 2030[18].

For all these factors, breast cancer gets a generous amount of funds towards preclinical and clinical research totaling more than $2.3 billion every year out of a total of $24.5 billion (11.5%) (Table 1) , which is more than any other site specific cancer research program[19].

Table 1 : Table showing the total allocated funds worldwide by cancer for the period 2016 to 2020[19].

	Number of awards (n=66 388)	Funding ($US 24 451 417 116)	Median funding ($US)	Mean funding ($US)
Type of science (excluding Cancer Research UK data)				
Pre-clinical research	57 816 (87·1%)	17 969 719 237 (73·5%)	87 689 (38 663–263 304)	314 183 (885 349)
Phase 1–4 trials	2427 (3·7%)	1 802 086 858 (7·4%)	301 250 (59 658–729 375)	749 932 (1 574 177)
Public health research	4809 (7·2%)	2 286 966 656 (9·4%)	99 391 (38 459–421 080)	485 555 (1 338 086)
Cross-disciplinary research	1336 (2·0%)	1 225 644 480 (5·0%)	329 417 (81 535–855 760)	918 774 (2 947 519)
Site of cancer				
Bladder	731 (1·1%)	208 101 857 (0·9%)	56 638 (35 000–164 320)	271 609 (728 409)
Bone	699 (1·1%)	213 449 408 (0·9%)	81 409 (36 854–201 320)	296 892 (1 036 170)
Brain	3575 (5·4%)	1 341 358 513 (5·5%)	105 237 (39 872–373 282)	357 082 (714 391)
Breast	7146 (10·8%)	2 732 461 588 (11·2%)	95 469 (39 243–402 315)	364 694 (789 856)
Cancer (general)	17 581 (26·5%)	7 127 890 199 (29·2%)	102 010 (39 872–338 904)	411 469 (1 446 547)
Cervical	778 (1·2%)	221 377 352 (0·9%)	60 227 (35 231–194 288)	278 197 (691 238)
Cholangiocarcinoma	211 (0·3%)	28 975 497 (0·1%)	42 444 (37 504–90 315)	139 305 (426 158)
Colorectal	3971 (6·0%)	1 250 675 380 (5·1%)	82 789 (37 861–247 101)	280 365 (644 656)
Haematological	5281 (8·0%)	2 295 537 884 (9·4%)	121 061 (46 410–449 260)	412 226 (1 201 920)
Head and neck	2267 (3·4%)	488 894 517 (2·0%)	41 650 (36 640–117 416)	210 104 (563 056)
Liver	2842 (4·3%)	589 266 188 (2·4%)	77 000 (33 472–108 385)	200 731 (506 269)
Lung	4120 (6·2%)	1 284 540 483 (5·3%)	78 401 (36 640–177 909)	280 730 (678 243)
Mesothelioma	140 (0·2%)	46 630 600 (0·2%)	117 416 (41 080–392 842)	333 075 (690 148)
Multiple cancers	3972 (6·0%)	2 120 387 780 (8·7%)	120 942 (42 444–466 322)	543 410 (1 468 287)
Other	1189 (1·8%)	467 159 643 (1·9%)	38 663 (38 663–297 495)	313 621 (774 672)
Ovarian	1563 (2·4%)	525 279 183 (2·1%)	83 602 (38 054–348 040)	307 027 (625 598)
Pancreatic	2290 (3·4%)	834 323 932 (3·4%)	83 139 (38 907–229 194)	325 827 (812 544)
Prostate	2777 (4·2%)	1 257 476 285 (5·1%)	128 000 (40 375–477 266)	428 329 (7 935 660
Renal	684 (1·0%)	195 958 550 (0·8%)	77 000 (37 257–213 940)	253 977 (618 093)
Skin	1793 (2·7%)	766 667 040 (3·1%)	137 093 (41 621–449 568)	408 342 (782 547)
Testicular	49 (0·1%)	11 858 646 (<0·1%)	110 706 (40 304–298 292)	252 311 (343 705)
Thyroid	382 (0·6%)	69 829 408 (0·3%)	43 968 (34 197–89 703)	175 405 (422 939)
Upper gastrointestinal	2347 (3·5%)	373 317 556 (1·5%)	44 893 (31 833–89 484)	342 619 (135 971)

Breast cancer risk factors :

Cancers are multifactorial diseases (Figure 4), a number of causative agents and risk factors are shared among different tumors, and some are specific for a given cancer. Onset of breast cancer has been associated with many risk factors which can be divided into modifiable factors, mostly related to lifestyle, and non-modifiable factors related to one's genetics and physiological processes.

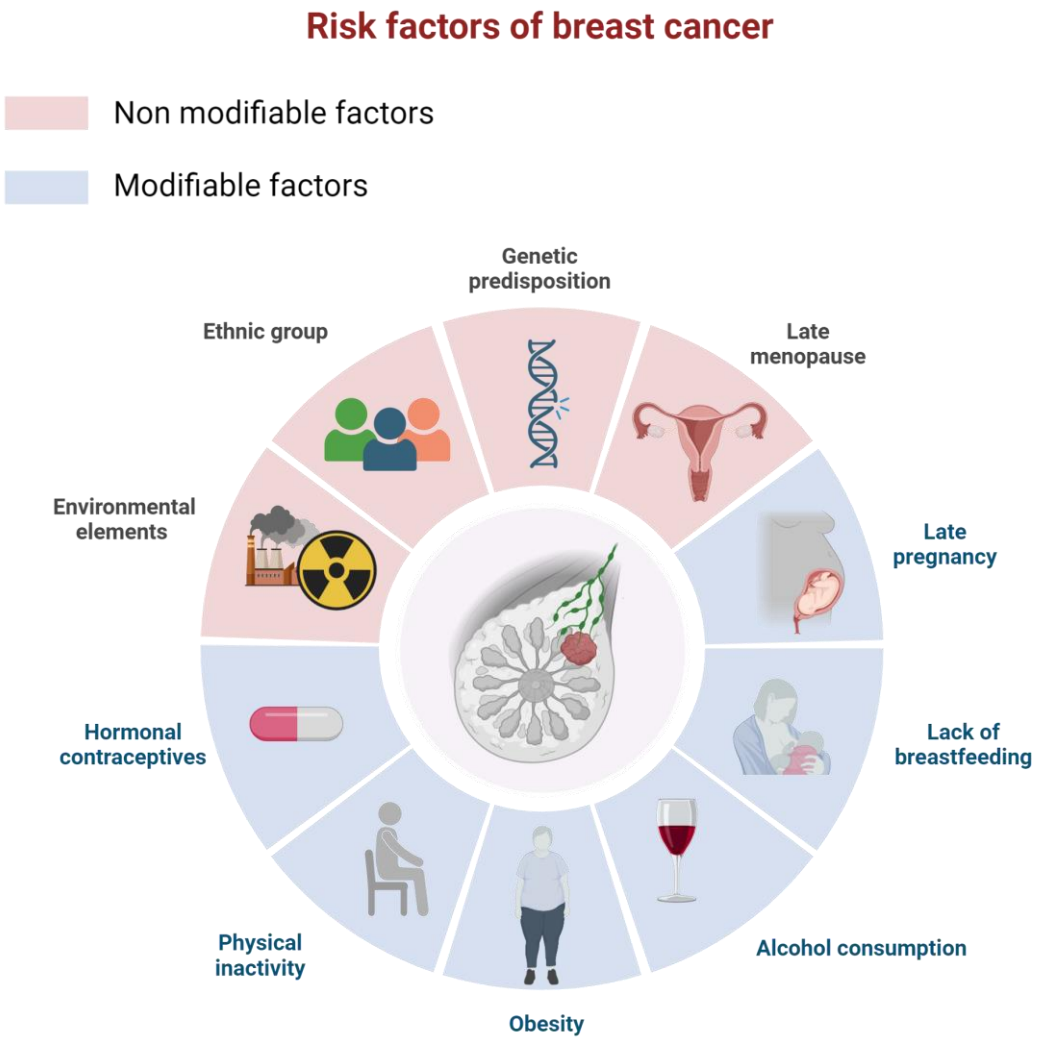

Figure 4 : schematic diagram of modifiable and non modifiable risk factors of breast cancer onset (Created with Biorender).

Age :

Age is a significant risk factor of breast cancer onset. The majority of cases being diagnosed among women aged more than 50 years. Less than 15% of patients are younger than 45 years old. The mortality is also significantly higher among the older population, as more than 99% of reported deaths are patients older than 60 years old[20].

Ethnicity :

In the United States where race and ethnicity are systematically reported, incidence of breast cancer varies from a group to the other. Incidence is highest in white women (140.8 per 100000), intermediate in african american women (121.7 per 100000) and lower hispanic women (89.8 per 100000)[21]. Disease progression and mortality are also different. White women are more likely to present with a localized disease compared with other ethnic groups 5-6% of white women present metastatic breast cancer compared with 9% of African American[22]. Ethnicity has also implications on aggressiveness and breast cancer subtype incidence. African American women showcased the highest rates of poorly differentiated tumors. Moreover, TNBC incidence is highest in this group[23]. These observed disparities can be explained partially by differences in mammography screening rates which are usually higher among white women, but also genetic predisposition, lifestyle which is closely related to socio-economic class and environmental factors.

Menopause and menarche :

Exposure to estrogen activity is a major risk factor of breast cancer onset. This activity is reflected by the age of the onset of both menarche and menopause. Indeed breast cancer is associated with an increased risk factor of 1.05 for every year younger at menarche, and by a factor of 1.29 for every year older at menopause[24]. Menarche initiates the first menstrual cycle but induces long term systemic hormone activity that can be traced throughout the adult life[25]. Likewise, menopause marks the end of menstruation which is associated with a swift decrease in estrogen levels, which is associated with a lower risk for breast cancer onset.

Genetic predisposition :

Based on the model developed by Knudson which postulates that every individual bears 2 alleles of every single gene, and for a tumor to develop, the two alleles of specific genes, known as tumor suppressor genes, must be hit (Figure 5). Among certain families and groups of the general population, one allele can be inherited already “hit” and behaves recessively in a tumorigenic process. A second hit on the healthy allele, which can occur at any given moment of life, must occur so a tumor develops. The process of tumor development in a case of an individual with an inherited mutation is therefore significantly accelerated[26,27].

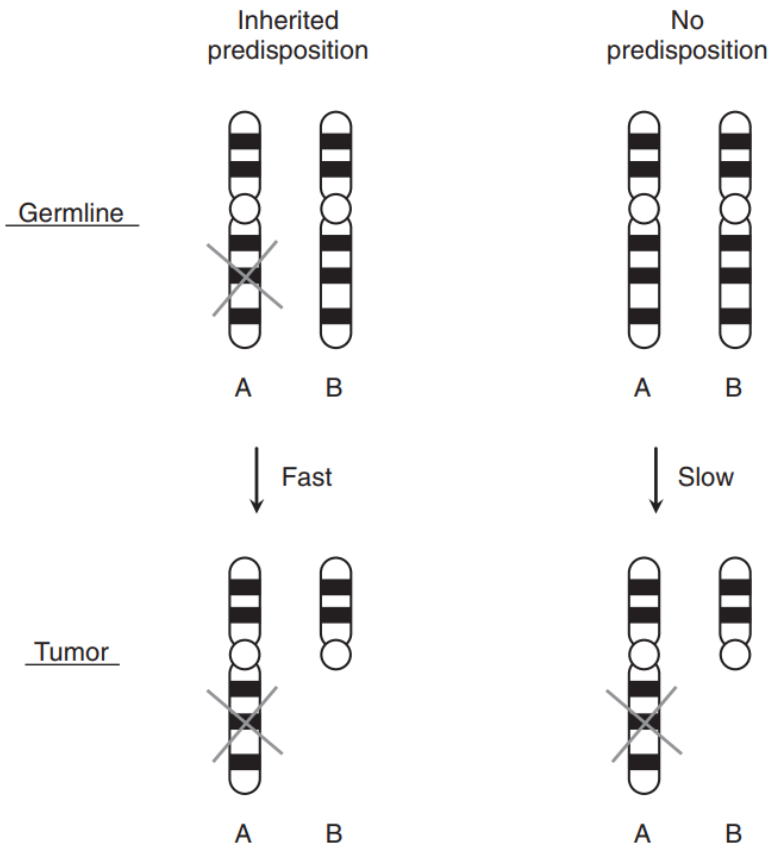

Figure 5 : Model of tumor suppressor genes. A pair of autosomal alleles A and B is indicated for individuals with (left) or without (right) a germline mutation. Tumor development happens faster in an individual with a genetic predisposition following the inactivation of the healthy allele.

It is estimated that around 10% of all diagnosed breast cancers are of family origins, while the rest are sporadic. Several genes have been associated with breast cancer onset and that are inherited through the family. Most prominently, we find BRCA1 and BRCA2. Both act as tumor suppressors genes. Meta analysis showed a breast cancer onset risk of 57% in cases BRCA1 is mutated, and 49% in BRCA2 mutations [28] [29]. Findings reported by Kauf and colleagues concluded on the positive impact of a risk reducing salpingo-oophorectomy (RRSO) among BRCA1/2 mutation carriers. In this prospective study where BRCA1/2 mutations carriers were either assigned to surveillance or the RRSO group. The RRSO showed a significant decrease in the onset of gynecological tumors, of which breast tumors (Figure 6), further highlighting

the defining role of these mutations on the onset of the disease and the interplay between different organs of the female reproductive system[30].

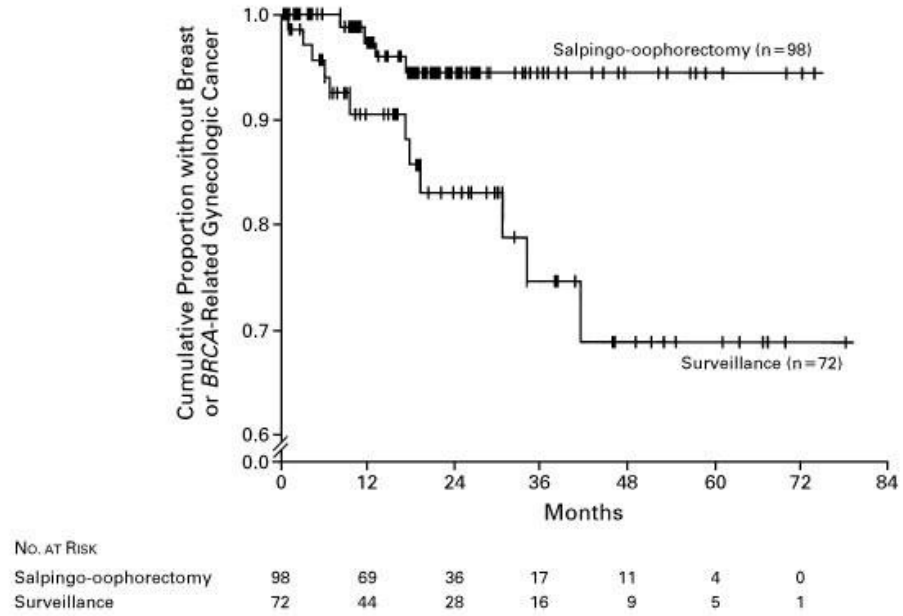

Figure 6 : Kaplan-Meier survival estimate of time to breast cancer onset in women undergoing risk-reducing salpingo-oophorectomy vs surveillance[30].

Several other genes are associated with breast cancer if mutated but to a lesser extent than BRCA1/BRCA2, of which we cite CHEK, PALB2, PTEN, RAD51C, RAD51D and TP53[31].

Radiations and environmental elements exposure:

Ionizing radiation, namely X and gamma rays exposure has been recognized as a causative factor of cancer since 2000 by the International Agency for Cancer Research[32]. X and gamma rays cause a DNA break, which can be repaired, but if not, leads to deep alteration of cellular processes. Although radiation was perceived as an effective way of imaging the inner parts of the body, its hazardous long term consequences went unsuspected. For instance, Wilhelm Rontgen, unaware of the effects of X rays, used his wife's hand, Anna Bertha Ludwig, to produce the first ever X-ray cliché[33]. Many studies have subsequently associated ionizing radiation with cancer onset. The most striking evidence was reported in the Japanese population exposed to the atomic bomb explosions in Hiroshima and Nagasaki. The risk of

developing breast cancer among females aged <20 years in 1945 was 4 times higher than the general population[34]. Algeria's Reggane region in the Sahara desert has also known atomic detonations in the early 1960s, both local populations and French servicemen were exposed to ionizing radiation and subsequently developed different tumors of which breast cancer[35,36]. Occupational exposure to ionizing radiation, although very low, has also been associated with a slight increase in breast cancer incidence[37]. Other environmental elements contribute to breast cancer onset but to a lesser extent than radiations. Most notably, exposure to pesticides, chemicals and artificial light [38,39].

Hormonal contraception :

Long term effects of hormonal contraception have been extensively studied. In 1996, a meta analysis included more than 53000 women in 25 countries who either never used, are users or past users of hormonal contraceptives. It was revealed that hormonal contraceptives increased the risk of breast cancer by 1.24, but this risk seemed alleviated 10 years after contraceptive discontinuation[40]. An analysis of the Danish sex hormone registry which included more than 1.8 million women aged between 15 - 49 years, of which there were more than 11000 breast cancers. Ongoing or recent use of hormonal contraceptives had an increased risk of 1.20 when compared with women who never used contraceptives[41].

Lifestyle :

Several lifestyle factors contribute to the onset of breast cancer. For instance, a meta analysis showed that a sedentary lifestyle is associated with a 15% increased risk of breast cancer onset[42]. Regular physical activity on the other hand is a protective factor in several cancers, of which breast tumors, reducing the risk by 14%[43]. The biological mechanism associated with these observations remains elusive. Closely related to physical activity, obesity, especially after menopause, is recognized as an important risk factor for breast cancer onset and aggressiveness[44]. The intensified effects of obesity after menopause can be explained by the higher levels of fat which raise estrogen levels. Moreover, obesity is associated with a poor clinical outcome and resistance to therapies[45].

Alcohol is classified as a class 1 carcinogen by the IARC. Several studies have provided evidence linking alcohol intake with an increased risk for a number of cancers. The WHO estimates that more than 100000 breast cancer cases out of the 2 million globally are attributed to alcohol intake. Moreover, the risk is increased with each unit consumed[16].

Pregnancy and breastfeeding :

Pregnancy effects on breast cancer are somehow paradoxal. Although pregnancy correlates transiently with the onset of the disease in the few following years, pregnancy at an early age is associated with a reduced long term risk. Uniparous women younger than 25 years old have a lifetime reduced risk of 36%[46].

Moreover, a meta-analysis comprising studies from 30 countries concluded a decreased risk of breast cancer of 4.3% for each 12 months of breastfeeding, when considering all breast cancer subtypes. The risk was further reduced by 20% in triple negative breast cancer (TNCB)[40,47]. Furthermore, lack of breastfeeding was associated with an increased risk of 191% of TNBC[48].

Breast cancer biology, histology and molecular subtyping

The breast :

The mammary gland is the common feature shared among the Mammalia class. In humans, the female breast is part of the reproductive system. Its primary aim is to produce milk for newborn breastfeeding. The breast is a dynamic gland that undergoes considerable postnatal development and cyclic morphological changes throughout a woman’s reproductive life. At a microscopic level, the mammary gland is formed by about 20 lobes that converge to open up to the nipple (Figure 7). Each lobe is formed by lobules which contain secretory alveoli and the terminal ducts. These ducts and alveoli are formed by apical luminal ductal and alveolar cells respectively and a

myoepithelial layer on the basal side of the epithelium. The muscle layer responds to the oxytocin stimulus to contract, thus expelling the milk from the alveoli and the ducts. This functional unit of the breast is embedded in a rather dense connective matrix. In non-lactating women, breast is dominated by fat, while during lactation, glandular tissue becomes predominant. The development of the mammary gland starts in utero, then puberty induced estrogen and progesterone stimulate the growth of the mammary glands. The breast receives a multitude of endocrine and paracrine signals throughout these developmental stages and requires endocrine and paracrine signals . The systemically available estrogen and progesterone are sensed by hormone receptor-positive cells and respond by producing growth factors which in turn induce the expression of adhesion, cytoskeletal and extracellular matrix proteins[49,50]. This cascade of events tightly regulates the homeostasis of mammary gland development and changes throughout the life course of a woman. However, breaches in physiological events lead to different lesions such as Paget's disease, papillomas, cysts and breast cancer.

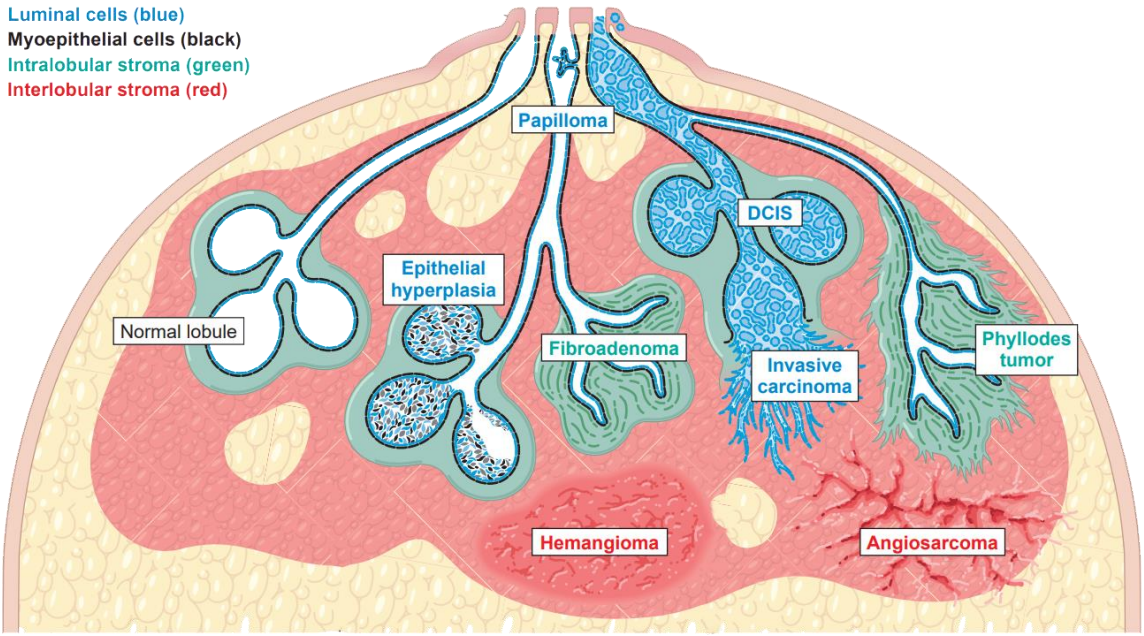

Figure 7 : anatomy of the female breast with preneoplastic and neoplastic lesions.

Pathology of invasive breast cancer :

Breast cancer has been intimately associated with hormonal activity for over a century. Thomas William Nunn reported in 1882 a case of breast cancer which regressed 6 months after the cessation of her menstruation[51]. It was only a couple years later that

Albert Schinzinger in 1889 proposed to perform surgical oophorectomy as a way to control breast cancer progression. Ovarian activity would then be translated more precisely to estrogen exposure, and the observation of an increased risk for breast cancer associated with late menopause and early menarche solidified the causality of estrogen receptor activity on disease onset.

Invasive breast cancer is defined as malignant cells breaking out of the stroma of the breast, thus no longer controlled within the boundaries of the basement membrane. Most breast cancers arise either from the ducts or the lobules. According to the WHO classifications, there are at least 19 major histological subtypes[52,53]. Invasive duct carcinoma (IDC), also known as no special type (NST) is the most frequent histotype of infiltrative breast malignancy, accounting for more than 75%[54]. IDC originates either from the ducts or the terminal ductolobular unit. IDC as are characterized by large tumor cells with abundant, lightly eosinophilic cytoplasm, with varying degrees of nuclear pleomorphism and mitotic activity. Morphologically, IDC is formed by glands appearing to infiltrate the stroma, with variable degrees of tubule formation. Onset of IDC frequently induces a strong inflammatory response accompanied by a desmoplastic reaction. The second most prevalent histotype is the invasive lobular carcinoma (ILC) which accounts for 10-15% of breast tumors. ILC grows around the lobules of the mammary glands. The cytology is structurally different from the IDC, ILC is characterized by relatively small cells with reduced cytoplasmic volume, large but nonpleomorphic nuclei, and few if any mitoses. Interestingly, when cells of ILC invade the surrounding adipose tissue, it does not induce a fibrous reaction which causes desmoplasia as frequently observed with IDC[55].Several studies that compared the overall survival of IDC and ILC from the data registry databases found no significant differences[56–58]. One of the prognostic factors routinely used in the clinic relies on histological grading according to Elston and Ellis modified Scarff-Bloom-Richardson (SBR), which is based on the proportion of cancer cells that are in tubule formation, the nuclear pleomorphism and the number of mitoses defines well, moderately or poorly differentiated tumors[59]. While there's still a debate as to whether the identified histotypes are always relevant for prognosis assessment and treatment choice, the identified histological subtypes allow the pathologists to recognize a primary breast tumor. Additionally, the recognized subtypes in the WHO breast cancer bluebook

continuously change over time; while 10 were initially identified in 1968, the list went up to 59 in 2012, before coming down to 44 subtypes[60].

Besides the histological grading, TNM system which was designed by French surgeon Pierre Denoix in 1952 has been widely accepted and is still a gold standard to stage the tumor based on the continuously updated recommendations of the Cancer Staging Manual published by the American Joint Cancer Committee[61]. Currently, TNM includes features of the T for tumor, primarily the size, N for lymph node involvement and M for metastasis. Moreover, it has been recommended that breast tumor staging includes a description of estrogen receptor (ER), progesterone receptor (PR) and human epidermal receptor 2 (HER2) status[62].

Breast cancer molecular subtyping :

Ever since the advent of novel DNA sequencing technologies, cancer features have been meticulously dissected and disease specific genotypes have been established. Prominent researchers Dr. Charles Perou and Theresa Sorlie were first to comprehensively classify breast tumors based on their molecular taxonomy (Figure 8). Starting from surgical samples of breast tumors, they performed a cDNA microarray assay in which more than 8000 genes were identified. By performing a hierarchical clustering, two main branches were separated based on the expression of the ER, thereby resulting in an ER+ group, which comprises the luminal A and luminal B. Luminal A is ER+ and PR+ while HER2-. Luminal B is ER+, PR+ and HER+. The second branch negative for ER comprises the ERBB2+ subtype and the basal-like subtype. ERBB2+HER2 enriched subtype is characterized by a high expression of several genes of the ERBB2 amplicon at 17q22.24 which obviously includes ERBB2 (ERBB2 being the gene encoding for HER2). **Finally, the basal-like subtype, which was subsequently labeled as triple negative, is negative both for hormone receptors and low HER2, while showcasing high expression of basal markers such as keratins 5 and 17, laminin…etc.** Normal-like breast cancer subtype was identified at the time but was subsequently suspected to be an experimental artifact in which a low number of tumor cells were isolated compared with the healthy normal cells of the breast[63,64].

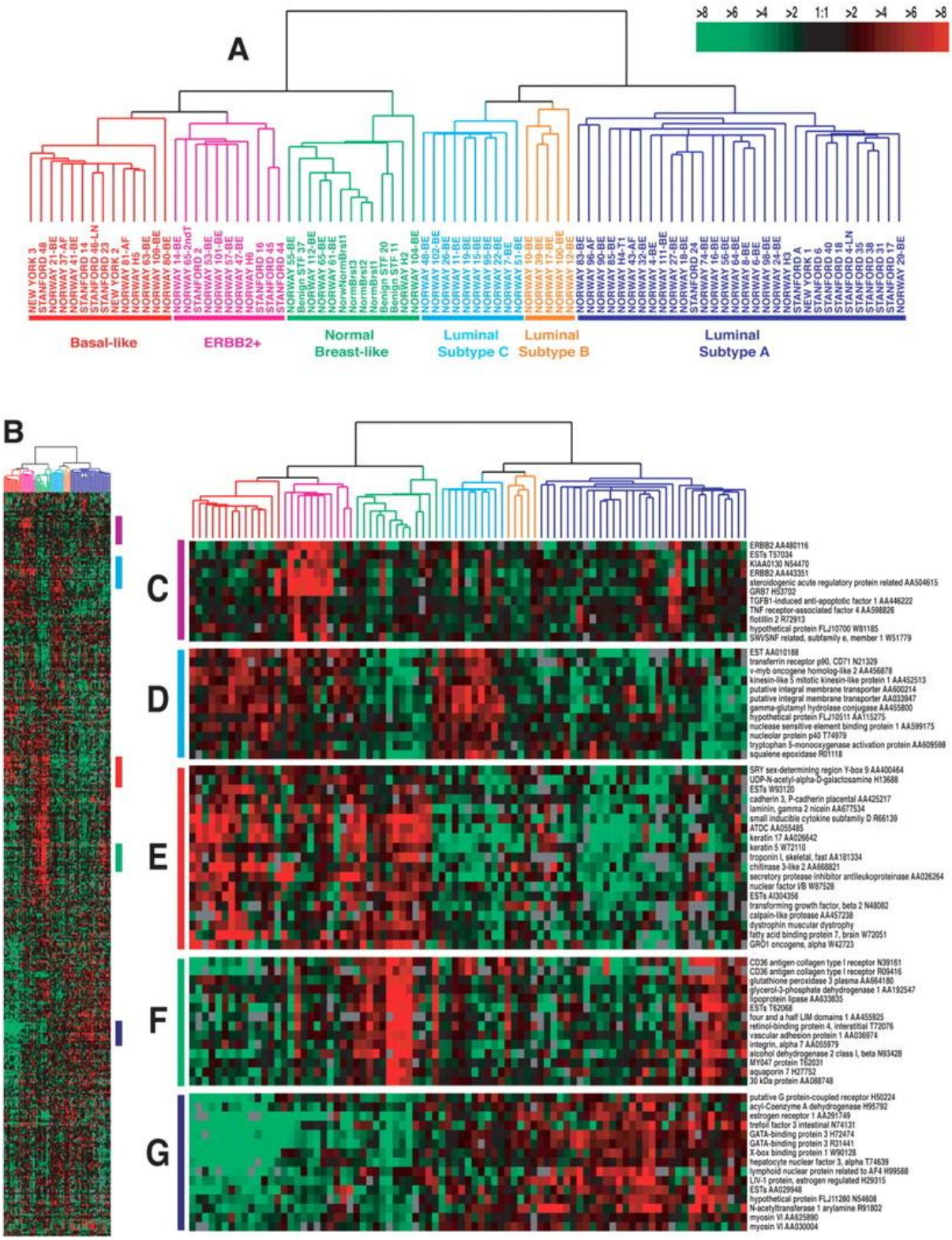

Figure 8: Gene expression levels of breast carcinomas analyzed by hierarchical clustering. (A) breast tumors divided into 6 subtypes based on gene expression differences. (B) Full cluster diagram. (C-G) most enriched genes in each subtype[64].

While the histological subtyping did not provide a great insight into the prognosis of patients, molecular subtyping proved to be a more robust method to stratify patients. Indeed, in Perou and Sorlie's study, survival analysis showed significantly different outcomes for patients clustered in different subtypes, with the worst prognosis in the HER2 and basal-like groups, and a significant difference between luminal A and luminal B (Figure 9). This study provided the most powerful tool in identifying specific intratumoral features capable of predicting the prognosis and to govern therapeutic choice. This clustering was coherently reproduced from independent microarray studies[65]. While the initial clustering relied on very large cDNA microarray screens, it has been proven that the different subtypes can be reproducibly identified by limiting the screen to genes/protein of ER, PR and HER2 across different platforms such as FISH and immunohistochemistry[66]. Positivity of ER and PR is defined as at least 1% of positive cells, while 10% of membrane staining cut-off HER2 positive is defined as positive[67]. The systematic assessment of ER, PR and HER2 status in the care of invasive mammary tumors became the cornerstone of clinical management of patients.

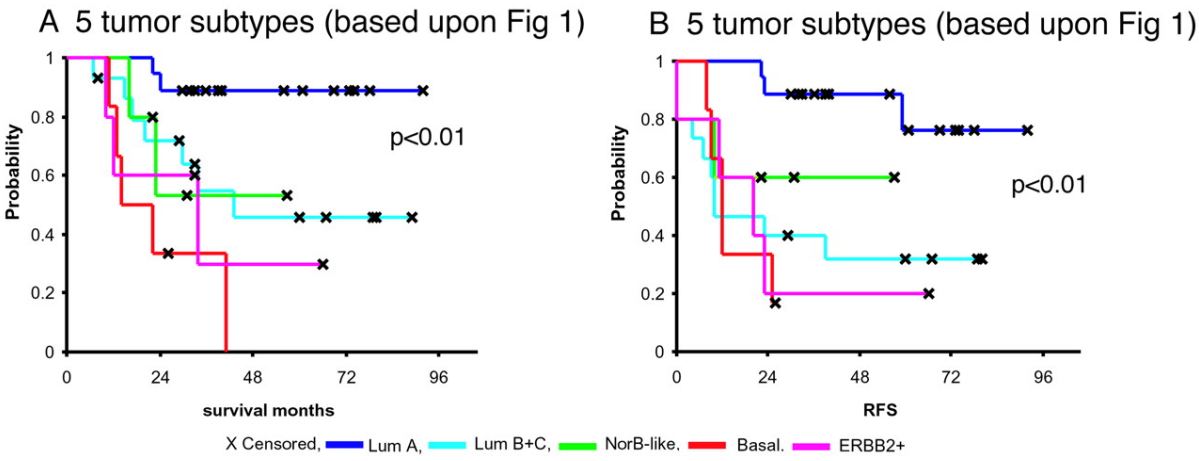

Figure 9 : Overall and relapse free survival of breast cancer patients based on the molecular subtype. (A) overall survival, (B) relapse free survival[64]

A large number of systemic and targeted therapies are now approved and marketed for the various breast cancer subtypes (Figure 10). Luminal tumors are treated with endocrine therapy which aims to decrease estrogen availability to hormone positive tumor cells. Endocrine therapy is generally administered in sequence with

chemotherapy. ERBB2+ tumors, while initially labeled as a particularly aggressive subtype, with the introduction of high affinity humanized monoclonal antibody Trastuzumab highly improved the clinical outcome of patients. Trastuzumab has been shown to be effective either as a monotherapy or in combination with multiple agents[68–70]. **Finally, TNBC tumors lack a ubiquitous marker allowing for a specific and effective targeting strategy, thus making them "target-less", leaving solely chemotherapeutic agents, especially anthracyclines and taxanes, the main therapeutic choice in the clinic, in addition to some novel therapies that will be discussed further.**

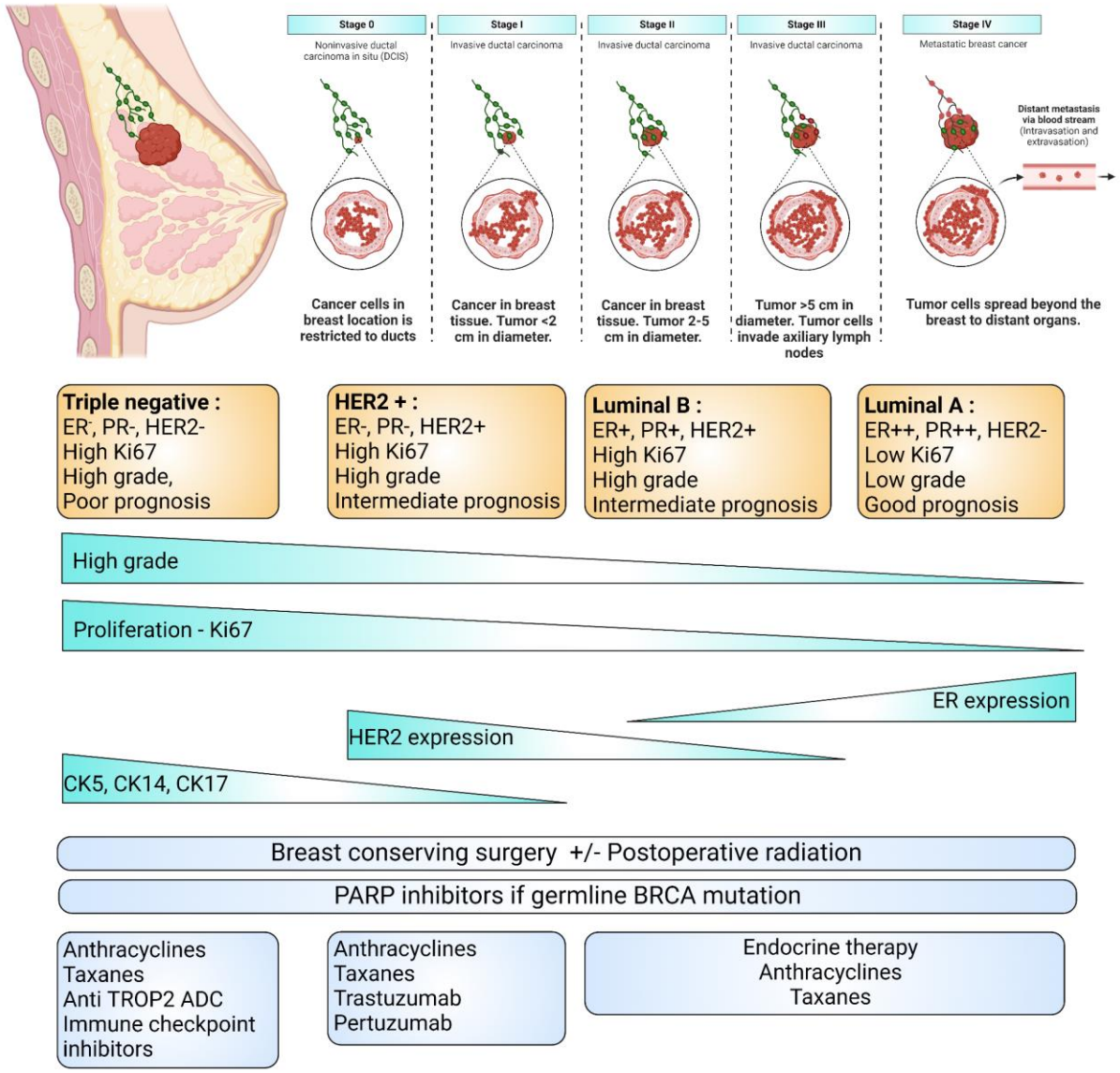

Figure 10 : Schematic diagram summarizing tumor staging, the different breast cancer subtypes, the histological features, the molecular signature and therapeutic approach

Triple negative breast cancer :

TNBC biology :

The first mention of “triple negative breast cancer” was reported in 2005, a few years after Perou and Sorlie reported the molecular patterns of breast tumors.. TNBC tumors are defined by what they do not express, a breast cancer subtype that does not express ER, PR nor overexpress HER2. TNBC tumors account for around 10-15%, corresponding to more than 170000 cases of all diagnosed breast cancer worldwide. TNBC is most frequently diagnosed in young premenopausal females, with an overrepresentation of Hispanic and African American women[71,72] . Genomic instability is highly prevalent in TNBC with numerous gains, losses, and small tandem duplications resulting in a highly segmented profile and contributing to a large heterogeneity. 75% of BRCA mutated breast cancer are of triple negative phenotype, and more than 25% of TNBC tumors carry a BRCA mutation[73]. TNBC tumors are larger in size, are most often of high grade and grow rapidly and are particularly aggressive[72,74] . A number of reports show a significantly decreased overall survival of TNBC patients when compared with the other breast cancer subtypes, especially luminal tumors[65,71,74]. There is a well documented increased likelihood of both early recurrences and distant recurrence of TNBC tumors within 5 years of diagnosis, with a peak between the first and 3rd year, followed by a decline (Figure 11)[74].

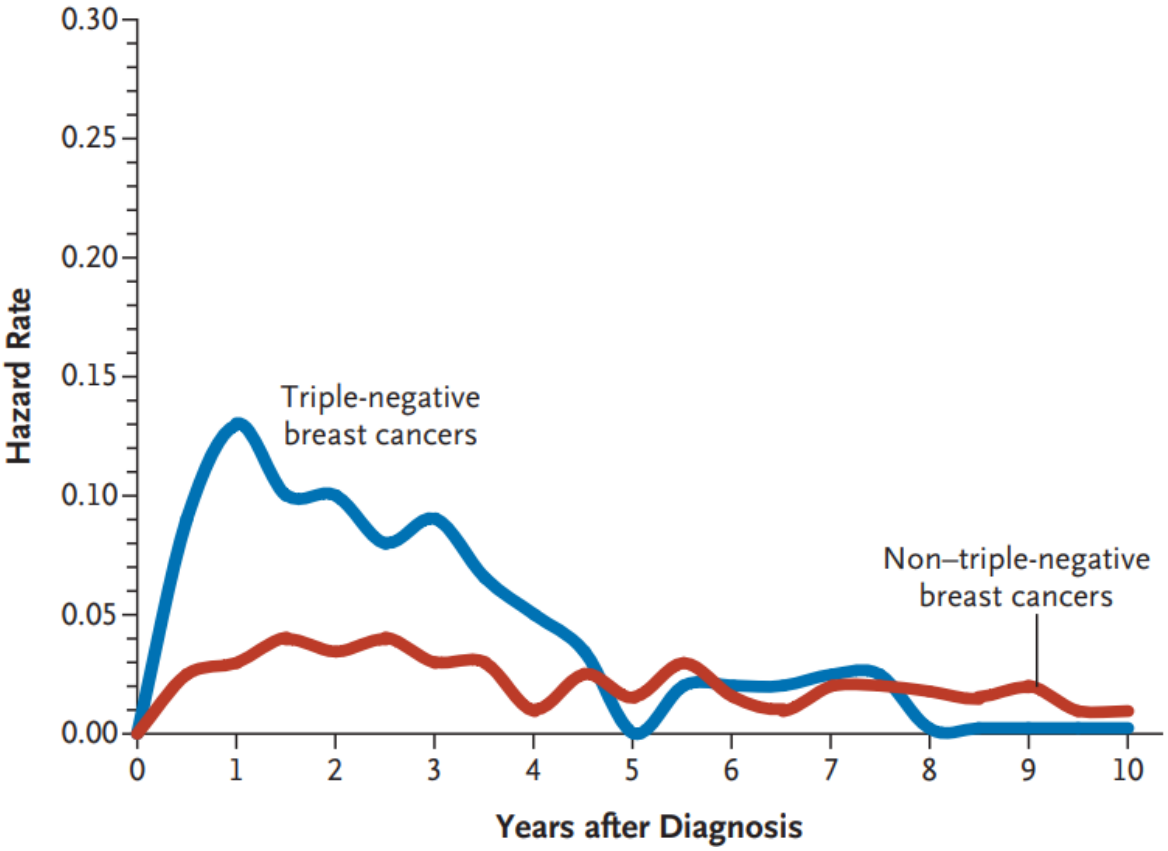

Figure 11 : hazard rates for distant recurrence of TNBC and non non TNBC in the years following diagnosis[73].

The metastatic pattern of TNBC is distinct from the other breast tumors, the organotropism of these tumors is particularly oriented to the viscera, especially the lungs, the liver and the brain; most often patients will present with many lesions across different organs[75]. On the contrary, bone metastasis is much less likely for TNBC patients than other breast cancer subtypes (Figure 12)[76]. Metastatic TNBC patients have a lower overall survival when compared with non TNBC breast tumors, as the median survival was 9 vs 22 months respectively[74].

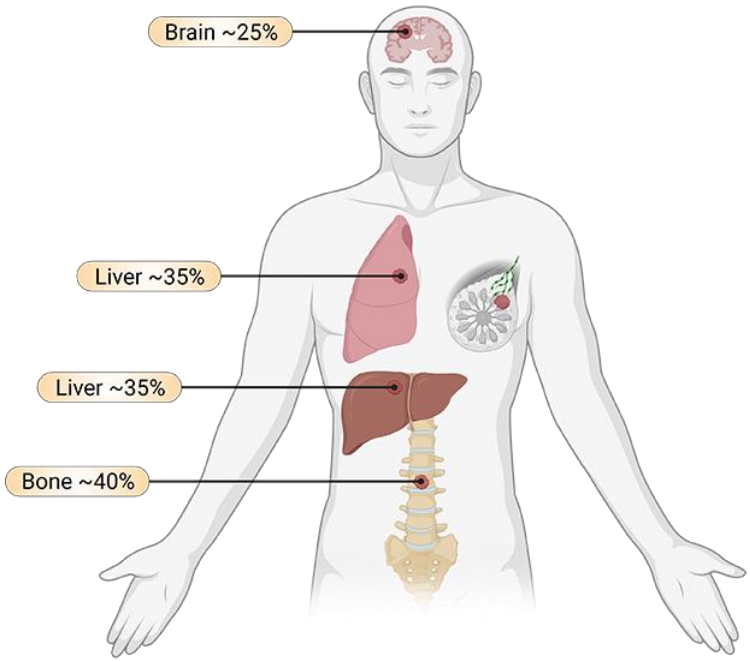

Figure 12 : Schematic diagram of the most frequently metastasized body sites in TNBC patients.

TNBC is characterized by an important heterogeneity both interpatient and intrapatient. The complexity of these tumors is highlighted by the further subclassification of TNBC into four subtypes based on histopathological and molecular features. Indeed, Lehmann and his colleagues used surgical samples and performed a gene expression analysis identified 6, then refined to 4 distinct TNBC subtypes, namely basal like 1 (BL1), basal like 2 (BL2), mesenchymal (M) and luminal androgen receptor (LAR)[77,78]. This classification became known as TNBCtype-4. Each subtype

has its specificity. BL1 is characterized by an elevated cell cycle and DNA damage response gene expression (*MYC*, *PIK3CA*, *CDK6*, *AKT2*, *KRAS*, *FGFR1*, *IGF1R…)*. BL2 is enriched in growth factor signaling and myoepithelial markers (EGFR, MET, NGF, Wnt/β-catenin, and IGF-1R pathways…). M subtype is characterized by an elevated expression of genes involved in epithelial-mesenchymal-transition (EMT), cell motility and migration and extracellular matrix remodeling. Lastly, LAR is substantially different from the other subtypes, it is characterized by an overexpression of the androgen receptor (AR) and a highly activated hormone-related signaling pathways (steroid synthesis, porphyrin metabolism…). Alternative studies have proposed TNBC subtyping based on gene signatures similarly to Lehmann's study. These investigations conclude most to a model often close enough to the TNBCtype-4 model[79–81]. The subtyping has both a clinicopathological relevance and a prognostic value. Indeed, LAR is associated with a lower grade than BL-1. But lymph node spread is more prevalent in LAR tumors (47% of cases) compared with other subtypes. The metastatic pattern varies as well; the LAR subtype is associated with a higher bone metastasis incidence compared with other subtypes (46% vs 16%), while the M subtype demonstrates a higher frequency of lung metastasis (46% vs 25%). The overall survival is also dependent on the subtype, BL1 shows the most prolonged survival and the highest rate of complete pathologic response (pCR), in contrast, BL1 displays the lowest pCR and overall survival[77,82].

TNBC microenvironment :

In the last two decades, many technological advances such as bulk and single cell RNA-sequencing, multiplex imaging, spectral and mass cytometry facilitated the in depth characterization of the tumor microenvironment (TME) composition[83]. The microenvironment of a tumor is a complex and a proper ecosystem comprising a plethora of cell types, ranging from immune cells, endothelial cells, scaffolding cells such as fibroblasts but also the extracellular matrix and a whole network of signaling molecules (Figure 13)[84]. The complexity of the tumor microenvironment is such that the presence of microbial communities has been reported within many tumors, of which breast cancer[85]. In regards to the emergence of treatment resistance and the recurrence of TNBC due to the activation of genes involved in self-renewal and

immune suppression, scrutinizing the TME is of prime importance for further refinement of the therapeutic choice[86]. In depth investigation of the TME has revealed important contributions of the cell populations to cancer development. TME cells can be roughly divided into pro-tumoral and anti-tumoral. In the pro-tumoral compartment, first we find the adipocytes and cancer associated fibroblasts (CAFs). These populations have a seminal role in the TME as they promote extracellular matrix remodeling, modulate angiogenesis and support tumor cell proliferation, migration and invasion[87]. The pro-tumoral immune cells present in the TME include neutrophils, tumor associated macrophages (TAMs), myeloid derived suppressor cells (MDSCs) and regulatory T-cells (Tregs). These cells have a function of regulating the immune response by dampening the activation of infiltrating cytotoxic lymphocytes. Anti-tumoral components of the TME include M1 macrophages, dendritic cells (DC), natural killer cells (NK), tumor infiltrating B and T cells. In a nutshell, these cells are responsible for tumor cells recognition and clearance through various mechanisms such as antigen recognition and presentation by DCs and B cells, engulfing and phagocytosis by macrophages, direct killing by T cells…etc[88–91]. Generally, TNBC tumors have been found to maintain a high number of tumor infiltrating lymphocytes T cells compared to other breast tumors. TILs have been shown to have a positive prognostic value in multiple tumors[92–95]. In TNBC, a high TILs infiltration was found to be correlated with a significantly prolonged overall survival. Moreover, the infiltration of cytotoxic lymphocytes is associated with an improved response to both chemotherapy and ICIs[96]. A scoring of TILs infiltration has been suggested to help refine and inform on the prognosis and recurrence risk of TNBC patients[97]. Tumor associated macrophages are also found in high numbers in TNBC tumors, comprising up to 25% of the TME. This immune subset is generally found to be a negative marker of the overall survival and contribute to creating a permissive environment to metastasis[98]. Next to T cells and macrophages, B cells are the most prevalent subset, approximately 11% of the infiltrate. They could be found to form either tertiary lymphoid structures or as isolated cells. Their role in the infiltrate is yet to be unequivocally postulated, yet a number of studies report on their association with a favorable prognosis[99,100].

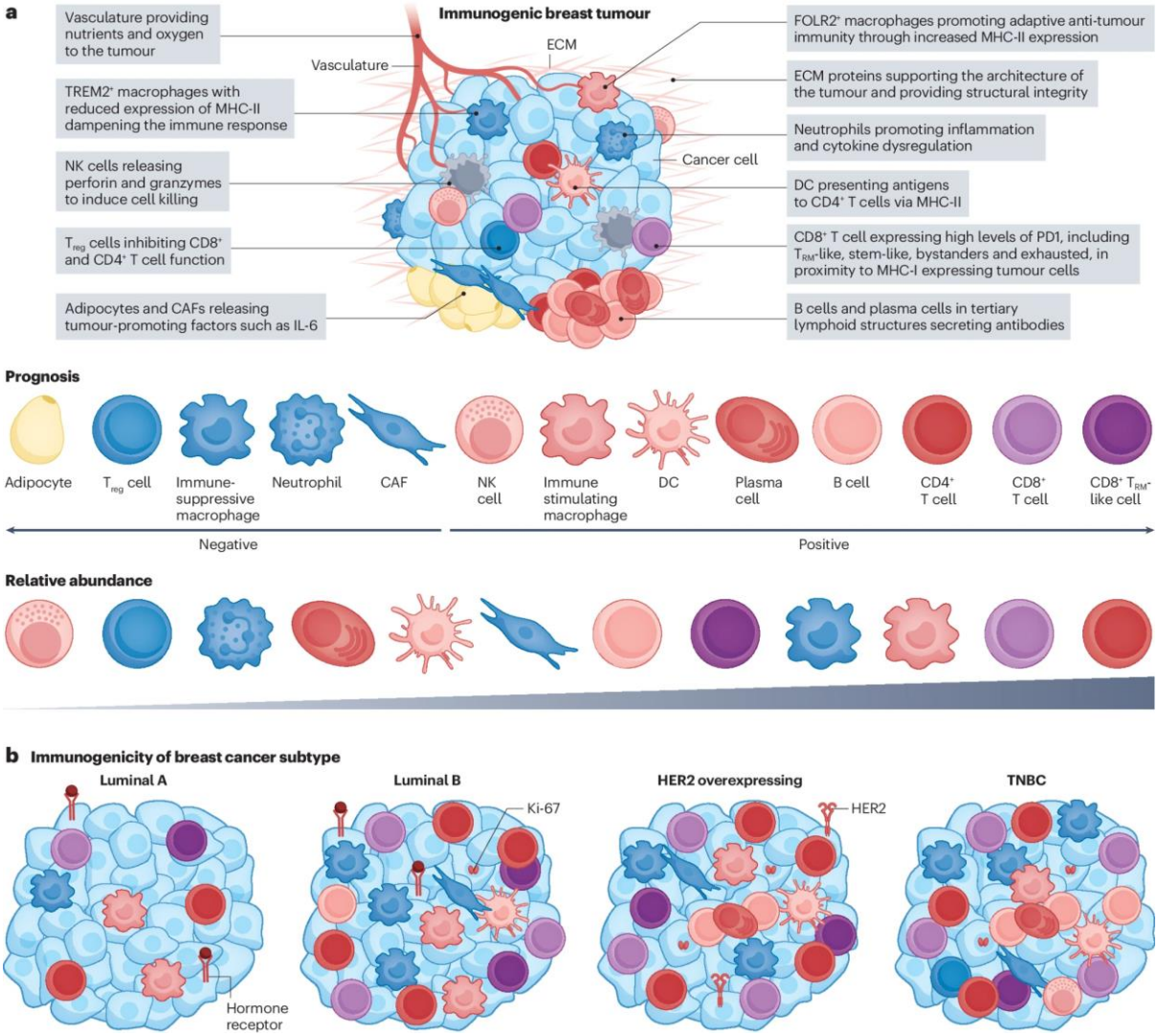

Figure 13 : Overview of the breast tumors microenvironment. (a) Tumor microenvironment components and their role in tumor progression. (b) Representative abundance of immune cells in the four breast cancer subtypes.

TNBC study models :

Most breast cancer biology research has been conducted using 2D cell culture and in vivo models. Both human and murine TNBC cell lines that provide a virtually unlimited source of homogenous cells have been established through the years (Table 2) . A number of studies aimed to characterize the molecular and histological subtype of the available cell lines. For instance, group leader Professor Charaffe and colleagues at our hospital the Institut Paoli Calmettes grouped 31 breast cancer cell lines into 3 subgroups, luminal, basal and mesenchymal[101]. Subsequent studies have

characterized the genomic profile such as BRCA and TP53 status as well the TNBC subtype as described by Lehmann and colleagues into BL1, BL2, M and LAR

Table 2 : Molecular and genetic classification of frequently used TNBC cell lines. PT = primary tumor, PE= pleural effusion, M = mesenchymal, BL1= basal-like 1, BL2 = basal like 2, LAR = luminal androgen receptor, Mut = mutated, WT = wild type

Cell line	Site of origin	Molecular classification	P53 status	BRCA status
BT20	PT	Unclassified	Mut	WT
BT549	PT	M	Mut	WT
CAL51	PE	M	WT	WT
MDA-MB157	PE	M	Mut	WT
MDA-MB231	PE	M	Mut	WT
MDA-MB436	PE	M	Mut	Mut
MDA-MB468	PE	BL1	Mut	WT
SUM149PT	PT	BL2	Mut	Mut
SUM102PT	PT	BL2	WT	WT
SUM185PE	PE	LAR	Mut	WT
SUM-159PT	PT	M	Mut	WT
HCC38	PT	BL1	Mut	WT
HCC70	PT	BL2	Mut	Mut
HCC1187	PT	BL2	Mut	WT

HCC1806	PT	BL2	Mut	WT
HCC1937	PT	BL1	Mut	Mut

Although a growing number of cell lines has been proposed to the breast cancer community, a staggering majority of studies utilize some of the most well known cell lines, such as MCF7, MDA-MB231 and T47D, all of which have been used in our current study[102]. While TNBC cell lines provide a powerful tool for the study of breast cancer biology, they remain a crude model, with many inconsistencies between these 2D models and endogenous tumors. Indeed, it has been shown that cell lines bear a fold increase in DNA alteration, supposedly due to the fact that these cell lines have been isolated from high grade tumors, which are more prone to accumulate DNA aberrations[103]. Additionally, cell lines found in different labs end up deriving from their source, which is translated in different cell behaviors reported in the literature, such as differences in sensitivity to drugs[102]. Moreover, cells in 2D culture do not recapitulate the natural course of cancer which accumulates mutations and molecular features across different stages, instead they represent a homogeneous clonal cell population which has been selected according to the cultivation method. Sensitive, but yet crucial cell populations such as cancer stem cells may not survive in culture due to defects in specific nutrients or their incapacity to attach to culture plasticware. The major drawback of these cell lines remains their clonal origin. Indeed, as discussed above, TNBC is a very heterogeneous disease which encompasses major differences within the same tumor and across different tumors. While cell lines have been subclassified according to the Lehmann's classification, only a few cell lines are available in each subtype. Finally, cancer itself is a multicellular disease which involves all cells of the TME such as fibroblast, myoepithelial cells, immune cells, endothelial cells… are lacking in 2D experimental settings[104,105]. To address these challenges, the community developed both 3D organoid models and genetically engineered mice which develop spontaneous TNBC tumors. In fact, 3D models provide a strong tool which recapitulates to a certain extent the complexity of the tumor microenvironment with its different components. First attempts at 3D culture date back at least to the late 70s. Indeed, Emerman and colleagues reported that epithelial cells isolated from mammary

glands of midpregnant mice and cultured them either onto plastic or in a collagen matrix. The two settings vary in the growth and differentiation of cells and a differential soluble factors availability is observed[106]. This study points to the potential differences and bias that could be encountered in studies aimed to study the biology of a given tissue or tumor as 2D culture grows significantly faster and in a linear manner rather than being influenced by molecules and cells of the microenvironment.

Finally, in vivo models have been the gold standard to validate any in vitro finding. In vivo investigation can either be carried out by using xenograft / allograft models or genetically engineered models. Xenograft studies utilize either patient derived cells or established cell lines, which would be grafted or injected either subcutaneously, orthotopically or intravenously in immunodeficient models such as the Nod SCID gamma (NSG) or nude mice. The orthotopic xenograft was a model that has been utilized in the present study to assess tumor growth and metastasis formation. Allograft models differ from the xenograft only in the used mice, instead of using immunodeficient mice, allograft can be carried in immunocompetent mice such as C57BL/6 or BALB/c[107]. While the xenograft model is the standard model for translational cancer research and biomarker investigation, the lack of the immune microenvironment, the loss of heterogeneity and the clonal nature of the tumors constitute altogether the limit of these models[108,109]. Genetically engineered mouse models (GEMMs) tackle some of the challenges posed by the graft models. GEMMs, if properly engineered, could recapitulate to large extent the human TNBC and provide a potent platform to further understand the tumor biology, the interaction of the tumor cells with components of the TME and attempt therapeutic approaches. Many models have been engineered but fail to mimic important stages of the TNBC such as metastatic progression, advent of specific histological subtypes, few heterogeneity and non representative genetic drivers[110–112]. More recently, at least two models have been engineered with a better integration of TNBC characteristics. A model has been engineered in our group by Lamballe and colleagues which is based on a subtle increase in the RTK MET. The model develops TNBC tumors exclusively, recapitulates the primary drug resistance observed in patients, forms metastasis and recapitulates the intertumoral heterogeneity such as described by Lehmann and colleagues[113]. Another recent study reported an exclusive TNBC model based on a

MYC amplification and PTEN deletion which are both dysregulated in a large number of TNBC tumors. The model recapitulates to large extent the features of TNBC observed in the clinic[114]. Although these models can be criticized due to the very low tumor incidence for the first, and the forced pathogenesis with specific gene alterations rather than an accumulation and genomic instability for both, they still provide the most reliable preclinical model to better understand the TNBC biology and test therapeutic approaches.

BC and TNBC therapeutics : current and ongoing

The management of breast cancer has consistently evolved since the middle of the 20th century. Indeed, breast cancer patients had an OS of around 20% after 10 years in the mid 1940s to mid 1950s . The OS went all the way up to almost 80% 50 years later (Figure 13) [115].

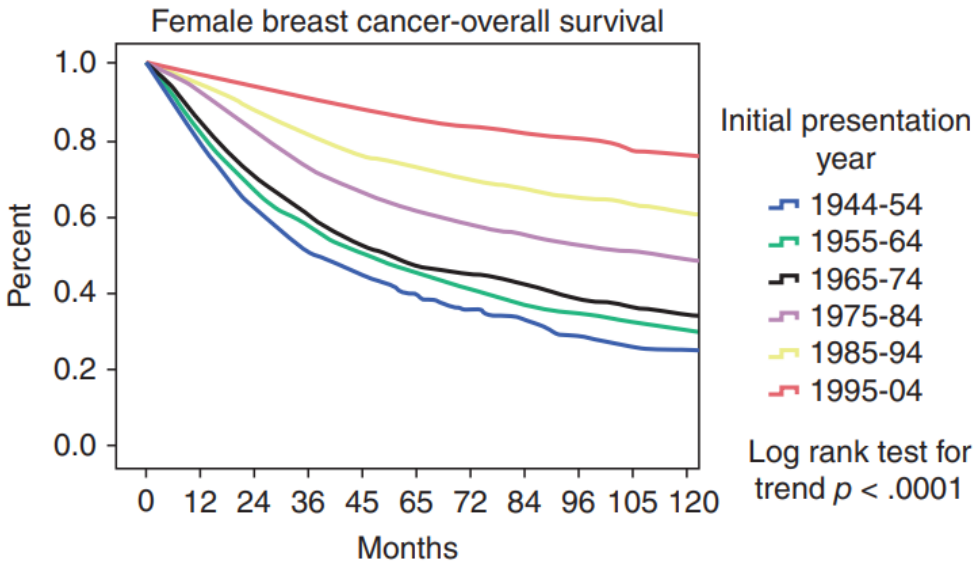

Figure 13 : Survival curve of breast cancer patients since the mid 40s.

The alleviation of the survival curves is multifactorial : appropriate population based screening programs, development of diagnostic tools, sensitization of women to the pathology which drives clinician consultation upon suspicions mass in the breast and most importantly the better understanding of the breast cancer biology with its clinicopathological and molecular complexities as discussed above and the subsequent development of adequate therapies. In the following chapter, we will focus

on major advances made towards both local and metastatic breast cancer management.

Surgery :

Surgical removal of breast tumors remains the option to go for in eligible patients given its curative nature and long term efficacy. Radical mastectomy was for an extended period of time the sole surgical approach, but breast conserving surgery (BCS) has been favored for its moderate burden and cosmetically acceptable approach. It has been shown that BCS results in similar OS and DFS as radical mastectomy[116]. Nevertheless, a number of patients are ineligible for BCS such as tumors > 4 cm, multicentric tumor, previous history of radiation to the breast, pregnancy…etc.

Radiotherapy :

Radiation therapy (RT) is well established for breast cancer patients, TNBC and non TNBC alike. In a meta-analysis which included more than 10000 patients found that radiotherapy reduced the 10 year risk of recurrence from 35 to 19.3% and reduced the breast cancer death rate by about a sixth[117]. RT can either be administered in adjuvant settings or for palliative purposes. Nevertheless, RT is not yet a predominant disease modifying element, instead, the relatively accepted and reported evidence of the clinical benefit systemic therapies make them the go-to option in the clinic.

Chemotherapy :

Chemotherapeutics based therapy for breast cancer treatment has been continuously evolving ever since the 1960s. It aims to prolong life, alleviate or delay symptoms, improve life quality and prepare a tumor for resection. Initially, single agent regimens such as cyclophosphamide and melphalan had limited effects in improving the DFS and OS[118]. The paradigm subsequently shifted to regimens based on 2 or more chemotherapeutic agents. Numerous trials focused on evaluating a regimen based on cyclophosphamide, methotrexate and 5FU (CMF) or some alternative regimen containing anthracyclines[119]. It has been found that anthracyclines containing

regimens provide a prolonged recurrence and overall survival when compared with CMF regimen. Chemotherapy has been used both in the adjuvant and neoadjuvant settings for the care of TNBC. Of note, it has been reported in independent reports that both adjuvant and neoadjuvant chemotherapy provide the same long term distant recurrences and overall survival[120,121]. Adjuvant chemotherapy is currently the main adjuvant therapy given to patients and it has provided substantial improvement of the DFS and OS. A randomized clinical trial at the MD Anderson investigated the effects of adjuvant chemotherapy in breast cancer patients. In ER negative tumors, chemotherapy reduced the risk of recurrence by 21 to 25% and the mortality rate by 55%[122]. Alternatively, chemotherapy has been used in the neoadjuvant settings with the purpose of downsizing the often large tumors prior to surgical removal. Neoadjuvant chemotherapy could render an inoperable tumor operable and allows in some cases a breast conservative surgery after tumor regression[123]. Many regimens have been proposed for the care of TNBC patients both in the adjuvant and neoadjuvant settings. The routinely used regimens contain an anthracycline such as doxorubicin and epirubicin, a taxane such as paclitaxel, and an alkylator, most often cyclophosphamide. The administration of chemotherapies can either be administered concurrently or sequentially[124,125]. Although the treatment of subcentimeter TNBC tumors can be effective, the management of metastatic tumors, which often showcase visceral and soft tissue relapse is much more challenging. Indeed, due to a lack of potent targeted therapies for the large part of TNBC patients, systemic chemotherapy is the foundation of patients care. Unlike local tumors, it has been shown that for the management of metastatic TNBC, a sequential chemotherapy regimen is preferred as it provides the same long term effects while having limited side effects when compared with concurrent regimens[126]. Of the most frequently administered drugs we find anthracyclines and taxanes as used for local TNBC, antimetabolites such as as gemcitabine and capecitabine, microtubule inhibitors such as vinorelbine and erublin, most of which are used in case of anthracyclines and taxanes failure[127].

Nevertheless, treatment of metastatic TNBC with chemotherapy provides mitigated results, with high relapse rates in the first years post treatment as discussed above, shortening of PFS after each line of treatment and limited impact on OS. **This hazardous situation led to substantial funds and efforts being invested in**

unraveling TNBC biological features in order to identify vulnerabilities and biomarkers to be targeted (Figure 14).

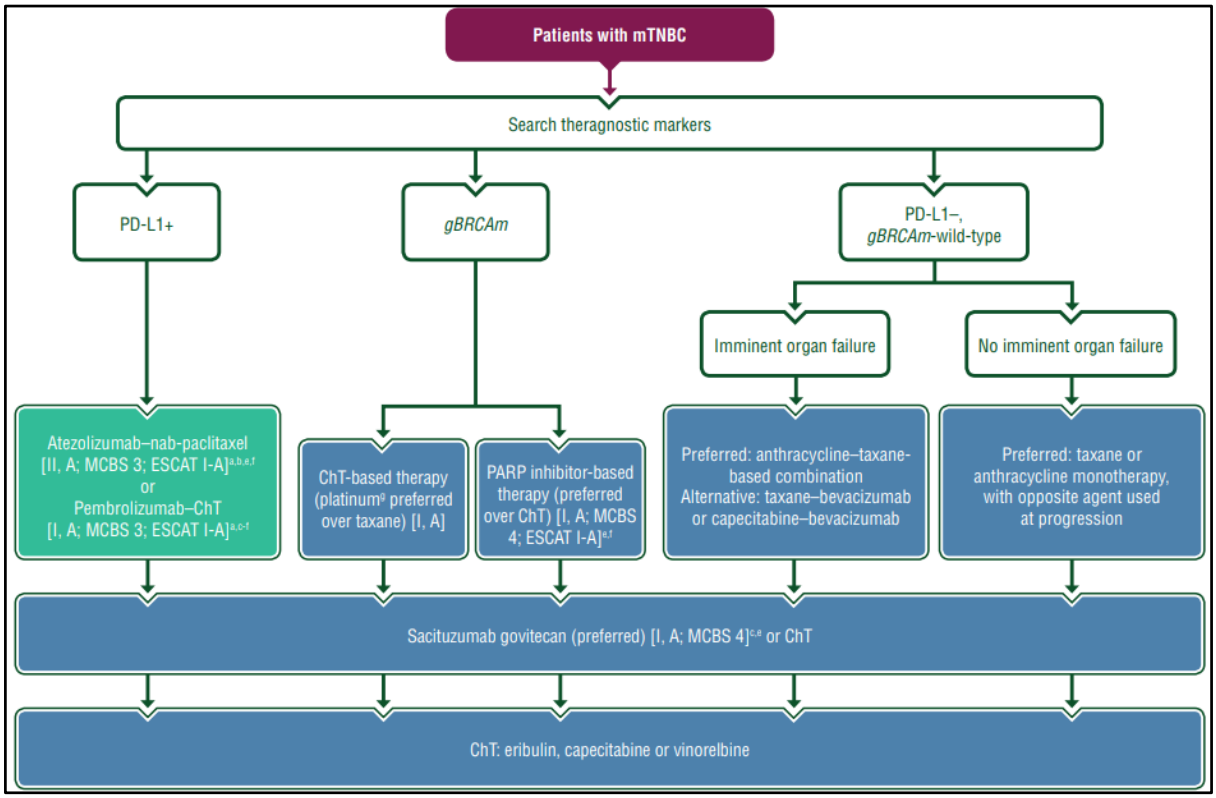

Figure 14 : Decision tree of the metastatic TNBC therapeutic management in the clinic[127].

Targeted therapies :

Targeted therapies have been a game changer in cancer care. Their importance is further highlighted in the astonishing number of targeted therapies approved for clinical use from 2000 until 2022 . Indeed, a study has found that less than 10% of approved drugs are cytotoxic chemotherapies, which were and are still the gold standard for many tumors. Meanwhile, more than 90% of the approved drugs by the FDA for the treatment of various cancers are targeted therapies, whether they are small compounds such as kinase inhibitors or biologics such as antibodies (Figure 15)[128].

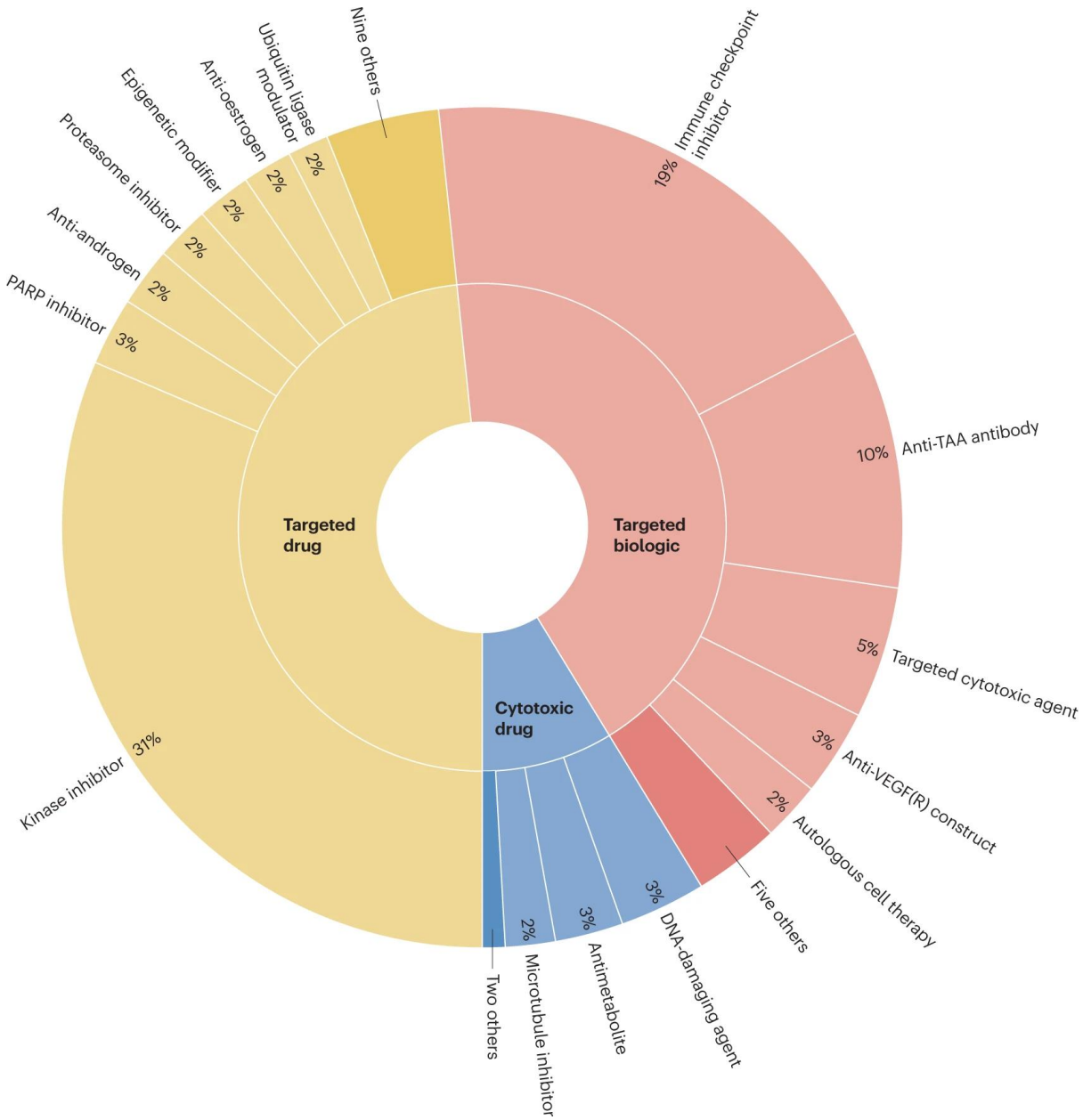

Figure 15 : overview of therapies categorized by mechanism of action approved by the FDA since 2000 for the treatment of various tumors[128].

The introduction of trastuzumab, a high affinity humanized monoclonal antibody that targets the HER2/neu receptor, is probably one of the best examples of the success of targeted therapies. The HER2 positive breast cancer was associated with the shortest DFS and OS. Additionally, multivariate analysis of diagnosed patients between 1990 and 2002 showed that HER2 positive cases had 5.09 times the rate of recurrence and 7.81 times the rate of distant recurrences after 5 years compared with

hormone positive cases. Trastuzumab has been investigated for the treatment of metastatic HER2 positive breast tumors both as a single agent or in combination with many chemotherapeutic agents. Patients treated with chemotherapy in addition to trastuzumab had a 37% improved OS and an increase of 10 year OS from 75.2% to 84% when compared with patients treated with chemotherapy alone[129].

Various strategies have been applied for the development of potent targeted therapies for the treatment of metastatic TNBC. But as discussed above, TNBC poses a particularly arduous public health challenge because of the disease heterogeneity and the lack of a shared therapeutic target in patients. Until very recently, no targeted therapy was approved for TNBC. This situation changed with the introduction of PARP inhibitors, immune checkpoint inhibitors and the ADC targeted at TROP-2.

Olaparib and talazoparib, two PARP inhibitors, were both investigated for the treatment of BRCA1/2 mutant breast cancer. Robson et al investigated the efficacy of olaparib for the treatment of HER2 negative metastatic breast tumors. Olaparib was found to significantly improve the PFS (7 vs 4.2 months) when compared with the standard treatment (Figure 16). Response to treatment was also significantly increased in the olaparib group (59.9% vs 28.8%), disease progression or death was 42% lower in the olaparib group[130].

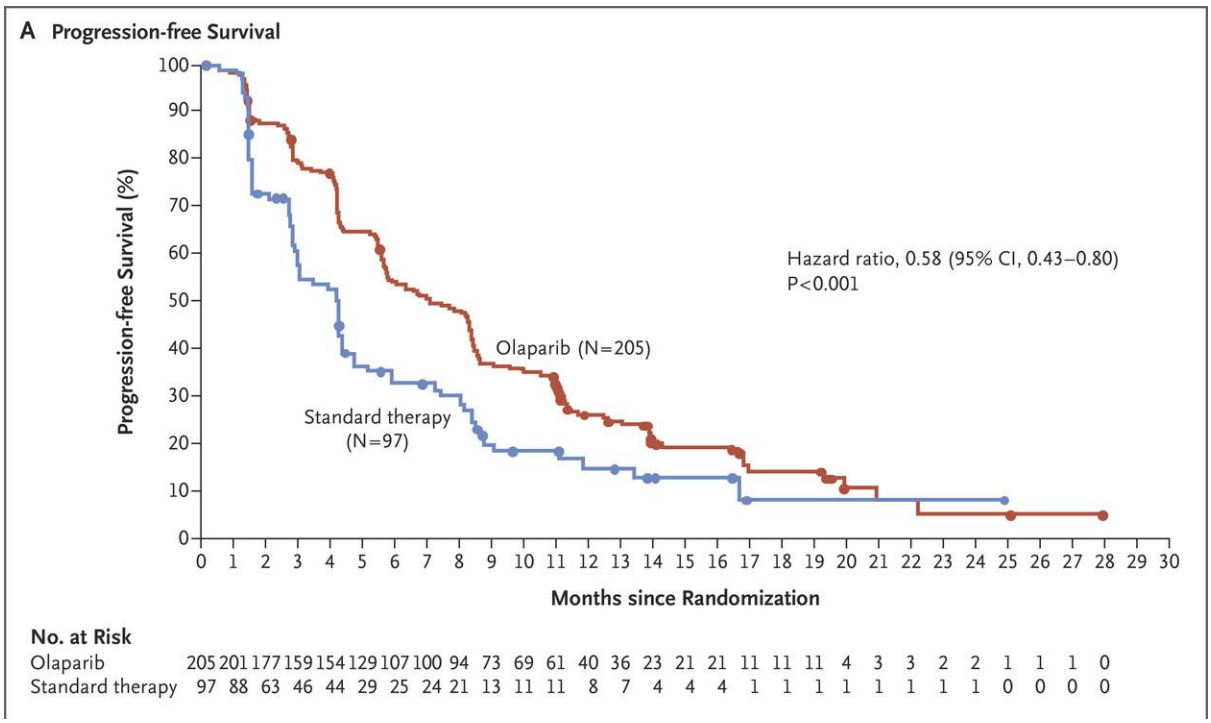

Figure 16 : Kaplan-Meier estimates of progression free survival of TNBC patients treated with olaparib (in red) or with standard therapy (in blue)[130]

In a second study by Litton et al. investigating talazoparib for the treatment of advanced breast cancer with BRCA 1/2 mutation, talazoparib showed similar results to olaparib with a prolonged PFS in the talazoparib group (8.6 vs 5.6 months) and a higher objective response rate (62.6% vs. 27.2%) when compared with standard therapy which included second line capecitabine, vinorelbine, eribulin or gemcitabine (Figure 17)[131].

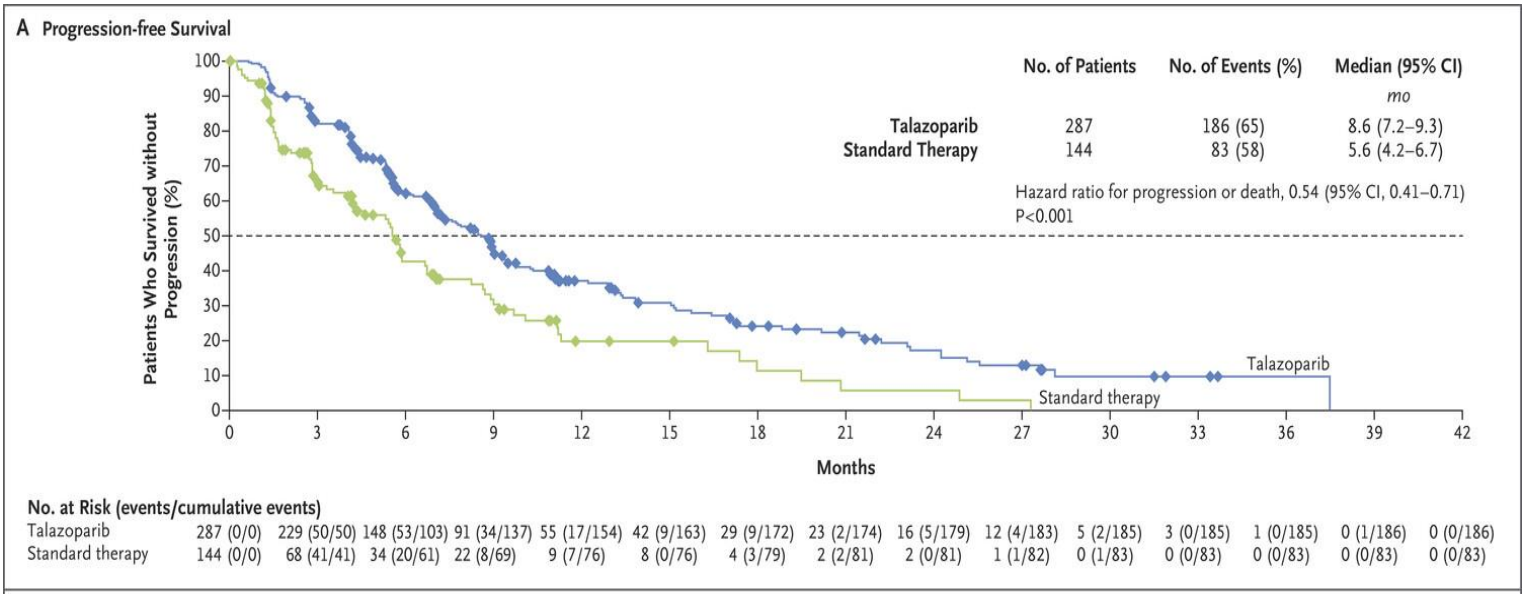

Figure 17 : Kaplan-Meier estimates of progression free survival of TNBC patients treated with talazoparib (in blue) or with standard therapy (in green)

Although PARP inhibitors showed some efficacy in prolonging the PFS of TNBC patients, this improvement remains timid and benefits only those patients with BRCA mutations. It remains highly insufficient to substantially improve the management of TNBC in the clinic.

ICIs :

The last decades have witnessed the discovery of immune checkpoint blockers, which have revolutionized the cancer treatment field, especially in non-resectable and metastatic solid tumors. Programmed death-1 (PD-1) and Cytotoxic T-lymphocyte Antigen-4 (CTLA-4) are immunoglobulins expressed on T cells to limit the cytotoxic activity and enhance self-tolerance. Tumor cells are found to be able to express ligands to these receptors as a mechanism to evade the immune response. Targeting these molecules with Immune Checkpoint inhibitors (ICI) has proven to have a major effect on halting tumor progression. ICIs even became the mainstay of most advanced melanoma and non small cell lung cancer treatments[132,133].

ICB are monoclonal antibodies that target immune checkpoint proteins in order to enhance the immune system response to tumors. The PD-1/PDL-1 blockers mainly stimulated CD8+ T cell infiltration and cytotoxicity to the tumor. It has proven efficacy when administered to patients whose tumors express the checkpoint, have a relatively infiltrated tumor and a high mutational burden(TMB) tumors. The latter is defined by the number of somatic mutations per megabase occurring in the gene coding sequence[134] such as melanoma, and non-small cell lung carcinoma. Theoretically, patients presenting a high TMB tumor are eligible candidates for these immunotherapies, however on the bedside, patients with the same cancer stage who have been administered these treatments responded differently (Figure 18). Additionally to the levels of PD-L1 and TMB, many other factors influence the response to ICIs, of which we can cite the infiltration of the tumor by cytotoxic lymphocytes, exposure to UVs and smoking, systemic effects of gut microbiome, obesity, use of beta-blockers…etc[135].

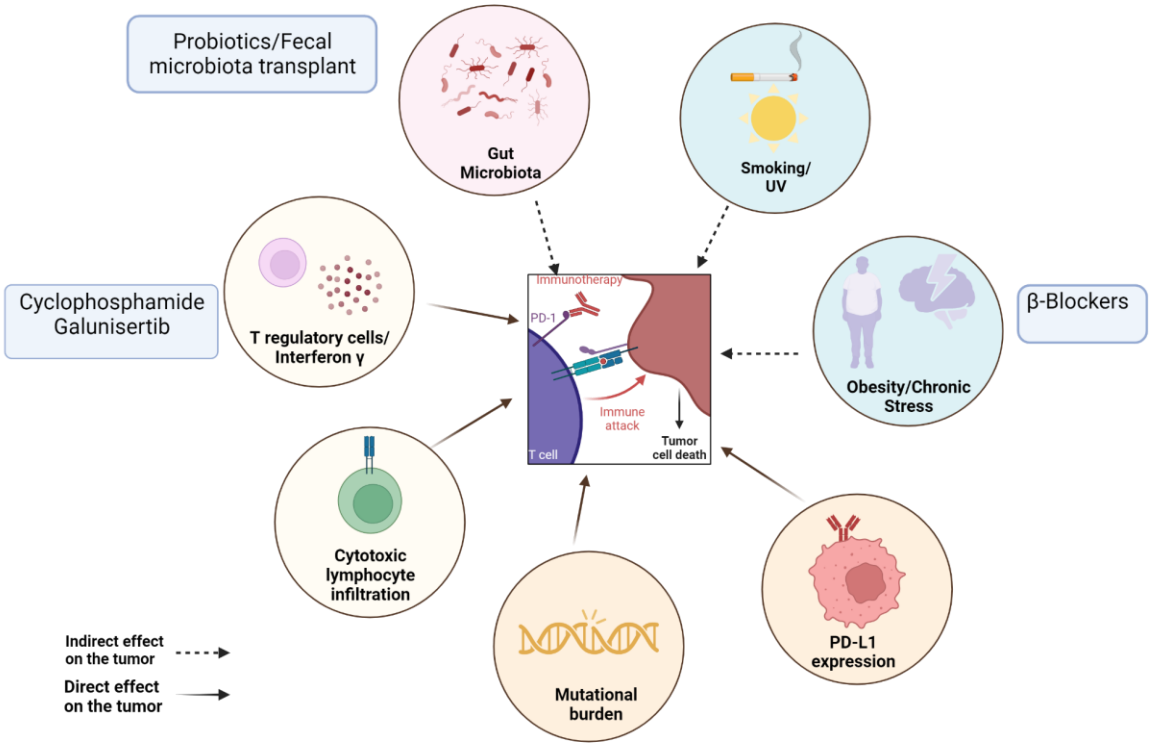

Figure 18 : Schematic diagram highlighting factors influencing response efficacy to immune checkpoint inhibitors (Created with Biorender)

Numerous factors are implicated in patients' response to Immune Checkpoint inhibitors, whether directly throughout tumor mutational burden, PD-L1 expression, Immune cell infiltration, different cytokine secretion, or indirectly by microbiota, smoking, UV light, obesity, and chronic stress. Of note, many treatments are found to be able to target these factors and eventually improve treatment outcomes.

In TNBC, a number of clinical trials were conducted to assess the safety and efficacy of ICIs. Keynote-522 trial evaluated pembrolizumab, an anti-PD1, in neoadjuvant settings of stage 2 and stage 3 TNBC patients in combination with chemotherapy against chemotherapy alone. The pathological complete response was significantly higher in the pembrolizumab group (64.8% vs 51.2%). The treatment related adverse events were comparable in both groups (78% vs 73%)[136]. In the Keynote-355 trial which included 847 patients, pembrolizumab was assessed for the treatment of unresectable metastatic TNBC. It was administered in combination with chemotherapy and compared with chemotherapy alone. The pembrolizumab treated group had a

median progression free survival of 9.7 months versus 5.6 months in the chemotherapy alone group. The efficacy of pembrolizumab correlated with the enrichment of PD-L1 expression in the tumor which was systematically assessed by IHC. Moreover, the addition of pembrolizumab to the chemotherapy regimen did not result in more toxicities[137].

Application of antibody drug conjugates (ADCs) for the treatment of TNBC :

an ADC is complex formed by a monoclonal antibody bound to a cytotoxic drug via a linker. The ADC acts by targeting a surface antigen, is then internalized by endocytosis and the drug is released from the antibody within the cell, causing cell death (Figure 19).

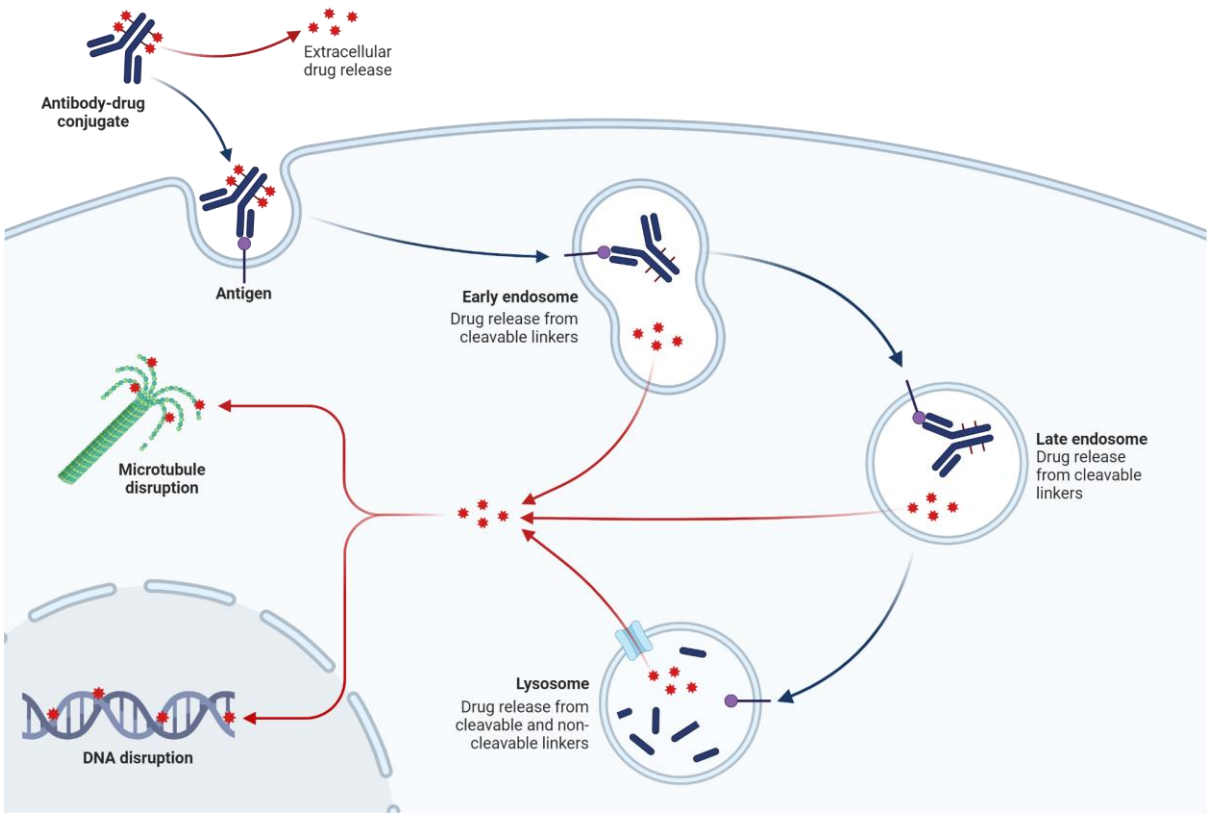

Figure 19 : Schematic representation of the mechanism of release of the bound cytotoxic agent and induction of cell death by the antibody–drug conjugates (ADCs)

Sacitizumab govitecan is an ADC targeting TROP-2 and is coupled to SN-38, a very potent antineoplastic drug. The ADC was assessed for the treatment of metastatic

TNBC patients who were previously treated with taxanes. Anti-TROP2 was evaluated against single agent chemotherapy (eribulin, vinorelbine, capecitabine, or gemcitabine). The group of patients receiving Sacituzumab govitecan had a significantly prolonged PFS (5.6 vs 1.7 months) and OS (12.1 vs 6.7 months). The objective response was higher in the ADC group (35% vs 5%) (Figure 20). These results led to the approval of Sacitizumab govitecan for the treatment of metastatic TNBC patients who were previously treated with 2 lines of chemotherapy[138].

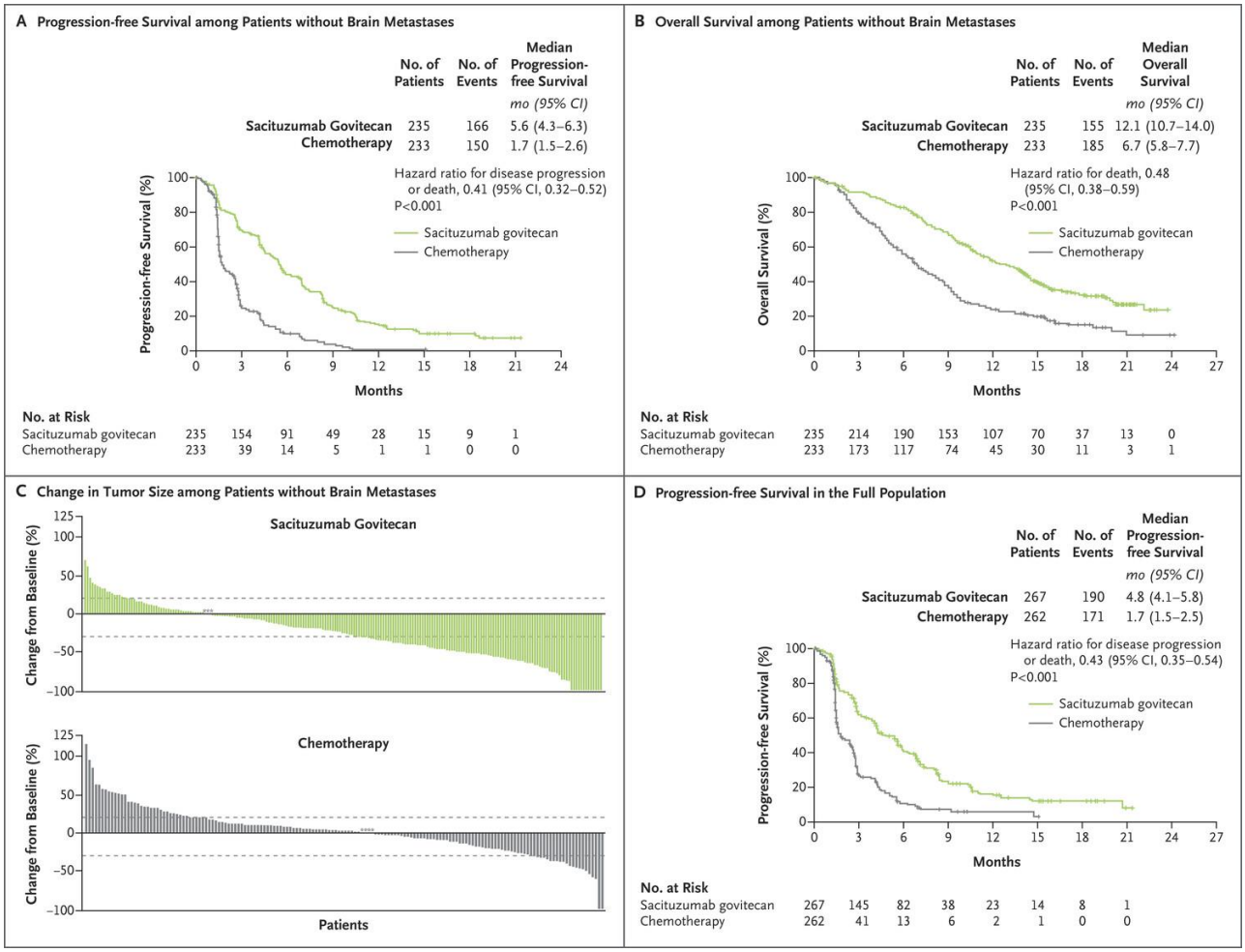

Figure 20 : Progression free and overall survival of patients treated with Sacituzumab Govitecan. (A and) PFS and OS respectively of patients without brain metastasis treated with Sacituzumab Govitecan (in green) or treated with standard therapy (in gray). (C) change in tumor size (D) PFS of all patients treated with Sacituzumab Govitecan (in green) or standard therapy (in grey)[138].

Ladiratuzumab vedotin is another ADC directed against SLC39A6 linked to MMAE, which is currently being investigated for the treatment of metastatic TNBC, in possible combination with ICIs. Preliminary results of the single arm trial showed a PFS of 11.3 weeks, with controllable adverse events[139].

Targeted therapies offer a robust therapeutic platform for aggressive tumors. In TNBC, all sort of strategies are being investigated, ranging from targeting DNA damage repair within the nucleus, targeting signaling pathways such as MEK, AKT and mTOR within the cytoplasm of tumor cells, to targeting surface proteins such as receptor tyrosine kinases and immune checkpoints (Figure 21).

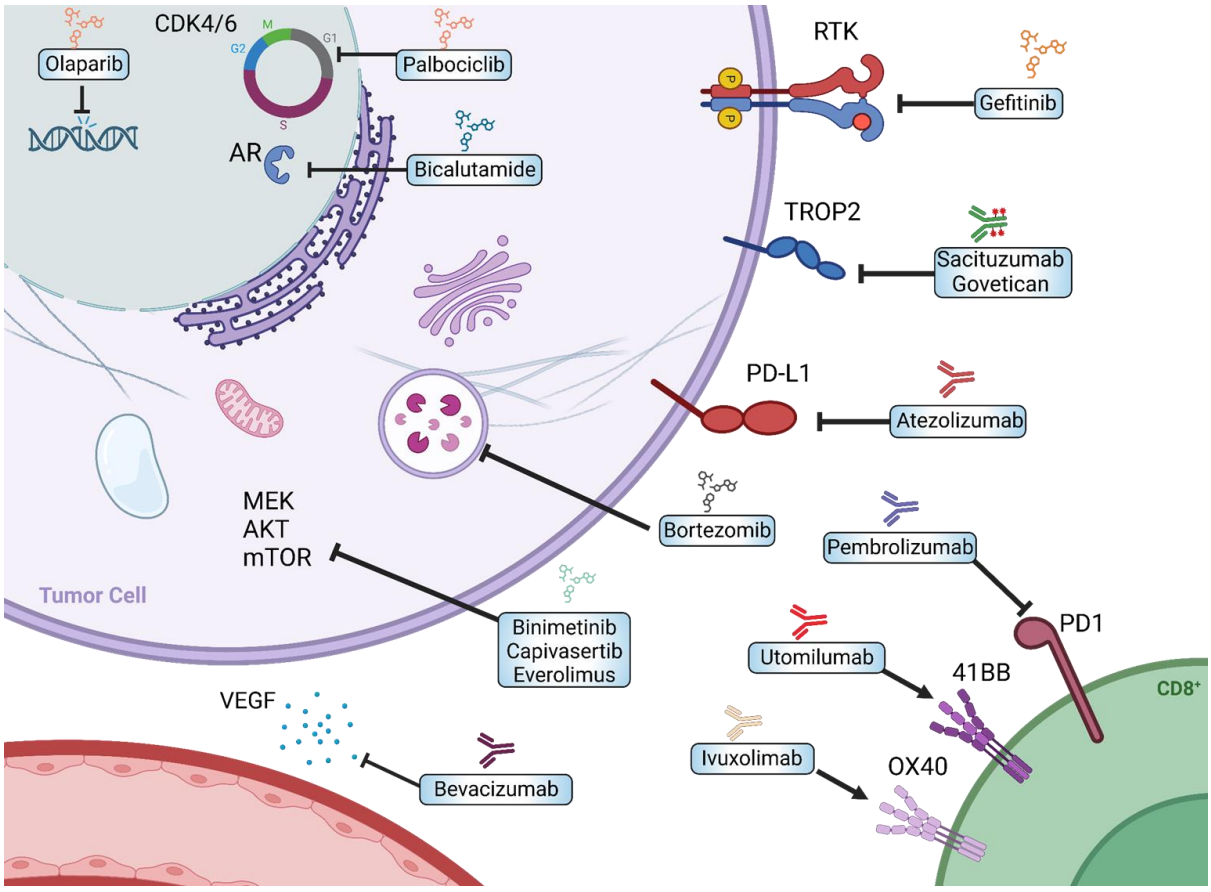

Figure 21 : Schematic diagram of investigated drugs for the treatment of TNBC (Created with Biorender)

As of June 2024, a search on Clinicaltrials.gov of “Triple negative breast cancer” or “TNBC” retrieved more than 300 trials. Of those, 116 trials are in phase 1, 183 are in phase 2 and 38 are in phase 3. A strict majority of the ongoing trials investigate a

targeted therapy alone or in combination with a cytotoxic agent or another targeted therapy such as PARP inhibitors, tyrosine kinase inhibitors or ICIs (Table 3)

Table 3 : non exhaustive list of ongoing trials of targeted therapies in TNBC

Investigated drug	Mechanism	Trial settings	Phase	Trial ID
Olaparib	PARP inhibitor	Alone or in combo with chemo (paclitaxel, carboplatin, cyclophosphamide) or with immunotherapy (durvalumab)	I to III	NCT02032823 NCT00707707 NCT03801369
Bicalutamide	Androgen receptor inhibitor	Alone	II	NCT02353988
Palbociclib	CDK4/6 inhibitor	In combo with chemo (Paclitaxel) or with immunotherapy (Avelumab)	I to II	NCT05067530 NCT04360941
Alpelisib	PI3K inhibitor	In combo with nab-paclitaxel	II to III	NCT04251533 NCT04216472
GSK2141795	AKT inhibitor	In combo with trametinib	II	NCT01964924
Dactolisib	PI3K/mtor inhibitor	In combo with MEK162	I	NCT01337765
Cetuximab	EGFR inhibitor (mAB)	In combo with ixabepilone	II	NCT01097642
Erlotinib	EGFR inhibitor	In combo with chemo (cisplatin, temsirolimus, metformin, veliparib)	I to II	NCT01097642 NCT00998036 NCT01650506
Bintrafusp Alfa	TGF-β / PD-L1 inhibitor	Alone	II	NCT04489940

Investigated drug	Mechanism	Trial settings	Phase	Trial ID
Bevacizumab	VEGF-A inhibitor	Alone or in combo with chemo (docetaxel, paclitaxel, nab-paclitaxel, erlotinib)	II to IV	NCT03577743 NCT01094184 NCT00733408
Pembrolizumab	PD-1 inhibitor	Alone or in combination with chemo (gemcitabine, carboplatin, paclitaxel)	I to III	NCT02447003 NCT02819518 NCT03036488
Atezolizumab	PD-L1 inhibitor	Alone or in combination with chemo (nab-paclitaxel, doxorubicin, capecitabine)	I to III	NCT01375842 NCT03197935 NCT03371017
Ivuxolimab	OX-40 agonistic antibody	In combination with avelumab	II	NCT03971409

Of the growing number of trials conducted aiming to develop novel therapeutic agents or find synergies between existing drugs on the market, many fail to reach their endpoint (Table 3). Many factors influence the success of trials for the treatment of TNBC of which the development of drug resistance, the investigation of drugs in patients who failed 3 or 4 lines of treatment already and the lack of prognostic biomarkers which can be used to potentially predict treatment response.

Table 3 : Non exhaustive list of failed clinical trials in TNBC

Investigated drug	Phase	Patients number	Primary endpoint	Trial outcome	Trial ID
Cobimetinib[140]	II	106	PFS	5.5 (trial) vs 3.8 (Std) mo	NCT02322814
Sorafenib in combo with capecitabine	III	537	PFS	5.5 (trial) vs	NCT01234337

				5.4 (Std) mo	
Metformin[141]	II	40	PFS	5.4 (trial) vs 6.3 (Std) mo	NCT01310231
Ceralasertib and Adavosertib[142]	II	273	PFS	5.3 (trial) vs 3.6 (Std) mo	NCT03330847
Ipatasertib in combo with paclitaxel[143]	III	255	PFS	7.4 (trial) vs 6.1 (Std) mo	NCT03337724
Durvalumab[144]	II	82	PFS	5.7 (trial) vs 3.6 (Std) mo	NCT02299999
Veliparib in combo with paclitaxel and carboplatin[145]	III	634	pCR	53% (trial) vs 58 (Std)	NCT02032277

https://link.springer.com/book/10.1007/978-3-030-20301-6

Chapter 2 :

Re-activation of developmental programs in cancer:

As discussed previously, the mammary gland is a particularly dynamic organ, characterized by cellular plasticity and undergoes multiple morphological changes as early as in the womb[146]. The mammary gland starts its development with the formation of the primary mammary gland bud then a mammary rudiment is formed. The growth of this rudiment is subsequently stimulated by the recruitment of cells of the ectoderm, a process very much similar to the in situ development of a tumor. Fast forward many weeks still in utero, the gland enlarges its boundaries and pushes against the basement membrane, in the same way as a tumor which would proliferate and invade

the stroma surrounding it. Embryonic pathways are particularly prone to growth, bulking and expansion. Indeed, it is worth considering that the embryonic pathways enable the development of a microscope zygote all the way to a human being of around 3kg in a record time of 40 weeks. Embryonic pathways are put in place to ensure the appropriate development of the embryo, under strict spatial and temporal control. In adulthood, the molecular machinery governing embryonic development is mostly silenced and sometimes reoriented towards homeostasis maintenance, particularly tissue regeneration upon injury (Figure 22).

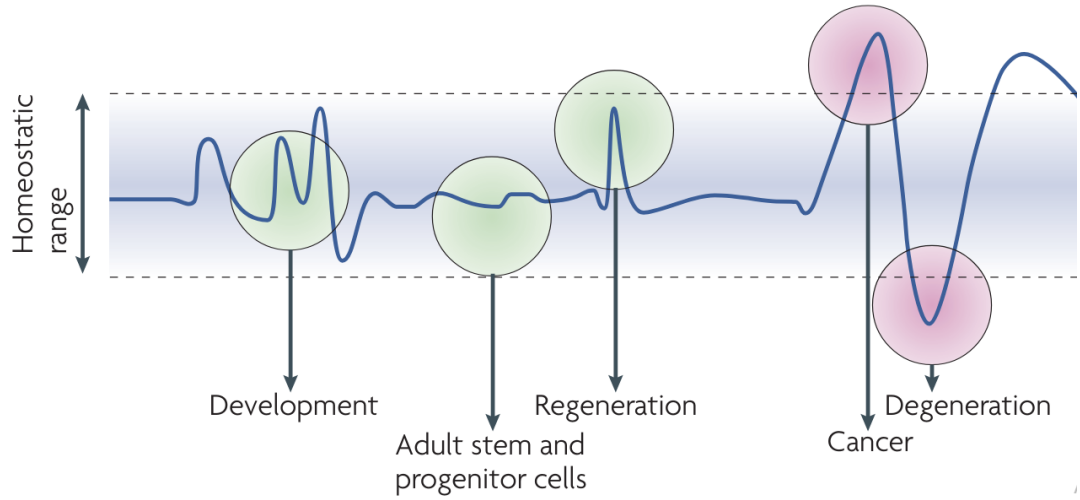

Figure 22 : Change of the Wnt signaling throughout life and in pathological conditions[147]

However, these observations led to the hypothesis that cancer leverages embryonic pathways in order to prevent differentiation or reverse differentiated cells that sustain malignancy, stemness, a mesenchymal state and promote invasion and metastasis (Figure 23)[148]. The following are among the most studied pathways :

The Hedgehog pathway :

There are 3 ligands in this pathway, Sonic hedgehog, Indian hedgehog and Desert hedgehog. The ligands bind to Patched-1 receptor which alleviates repression of the GPCR smoothened (SMO), which results in stabilization of GLI proteins and their translocation to the nucleus and regulation of gene expression. The ligands play distinct roles in the development of limbs, teeth, viscera and the central nervous system. In a cancerous context, hedgehog ligands are found to be overexpressed in virtually all different cancers, especially digestive tract cancers such as stomach,

biliary tract and pancreatic tumors[149]. Moreover, mutations of both SMO and Patched-1 have been documented, leading to a constitutive pathway activation[150,151]. The activation of the hedgehog pathway results in the expression of proliferation proteins such as Cyclin D, Cyclin E and Myc[152,153]. Owing to the potent role of the hedgehog pathway, multiple drugging strategies have been attempted, and two inhibitors, Vismodegib and Sonidegib are approved for the treatment of basal cell carcinoma[154,155].

The NOTCH pathway :

It has the four NOTCH receptors at its core. The pathway is activated upon contact between a cell expressing one of the NOTCH receptors and a cell expressing a NOTCH ligand, such as DLLs (1-3) and JAG (1 and 2). Once the ligand binds to its receptor, γ-secretase (γ-SEC) cleaves the intracellular part of the NOTCH receptor (NICD), which would convey the signal to the nucleus by translocation and induce its transcriptional regulation[156]. The NOTCH pathway is particularly involved in cell fate determination, stem cell niche maintenance and plays a pivotal role in the development of the endocrine system, such as the development of pancreatic and bowel glands[157–159]. Unlike the hedgehog pathway, NOTCH has been reported to play a role of both an oncogene (breast cancer, T-ALL) and a tumor suppressor (skin cancer), depending on the context and tumor background[160–162]. The drugging strategy of the NOTCH pathway consisted in inhibiting the activity of γ-SEC for the treatment T-ALL and ductal adenocarcinoma, although a limited efficacy was reported, patients suffered significant gastrointestinal adverse effects such diarrhea, vomiting and nausea, owing to the activity of the NOTCH pathway in the regulation of glands in the gut[163,164].

Wnt pathway :

It regulates key developmental processes. It contributes to myogenesis, cell fate, axis patterning, cell proliferation and migration[165–168]. The pathway further branches into 3 distinct pathways, a canonical pathway which regulates gene expression by the means of β-catenin, and two other non-canonical pathways, the planar cell polarity and calcium influx[169]. The ligands of this pathway are the 19 members of the WNT family

glycoproteins, and possibly others, which bind to receptors expressed on cells such as the frizzled family and LRP co-receptors. In the canonical pathway, the absence of WNT translates to a continuous phosphorylation of β-catenin which is sequestered in a complex of APC and axin and is degraded by GSK3. Upon Wnt binding to a frizzled and its co-receptor LRP5/6, β-catenin is released from the degradation complex and accumulates in the cytoplasm, it is then translocated to the nucleus, thus initiating its transcriptional regulation[169,170]. The non canonical pathways are β-catenin independent. The Wnt calcium pathway is mostly activated by the interaction between Wnt5a and frizzled 2. The pathway induces Ca^{2+} accumulation in the cytoplasm which subsequently activates PKC, Cdc42 and induce gene transcription and actin polymerization[171,172]. Lastly, the Wnt/PCP pathway has been demonstrated to signal through frizzled receptors, in cooperation with other co-receptors such as ROR1, ROR2 and RYK[173,174]. **Quite interestingly, this pathway has been reported to be activated by other receptors such as CELSR1-3 and VANGL1-2**[175,176]. The different signaling pathways have been extensively reviewed here[177]. Wnt PCP pathway plays a potent role in cell migration and polarization both during embryogenesis and in cancer[178,179].

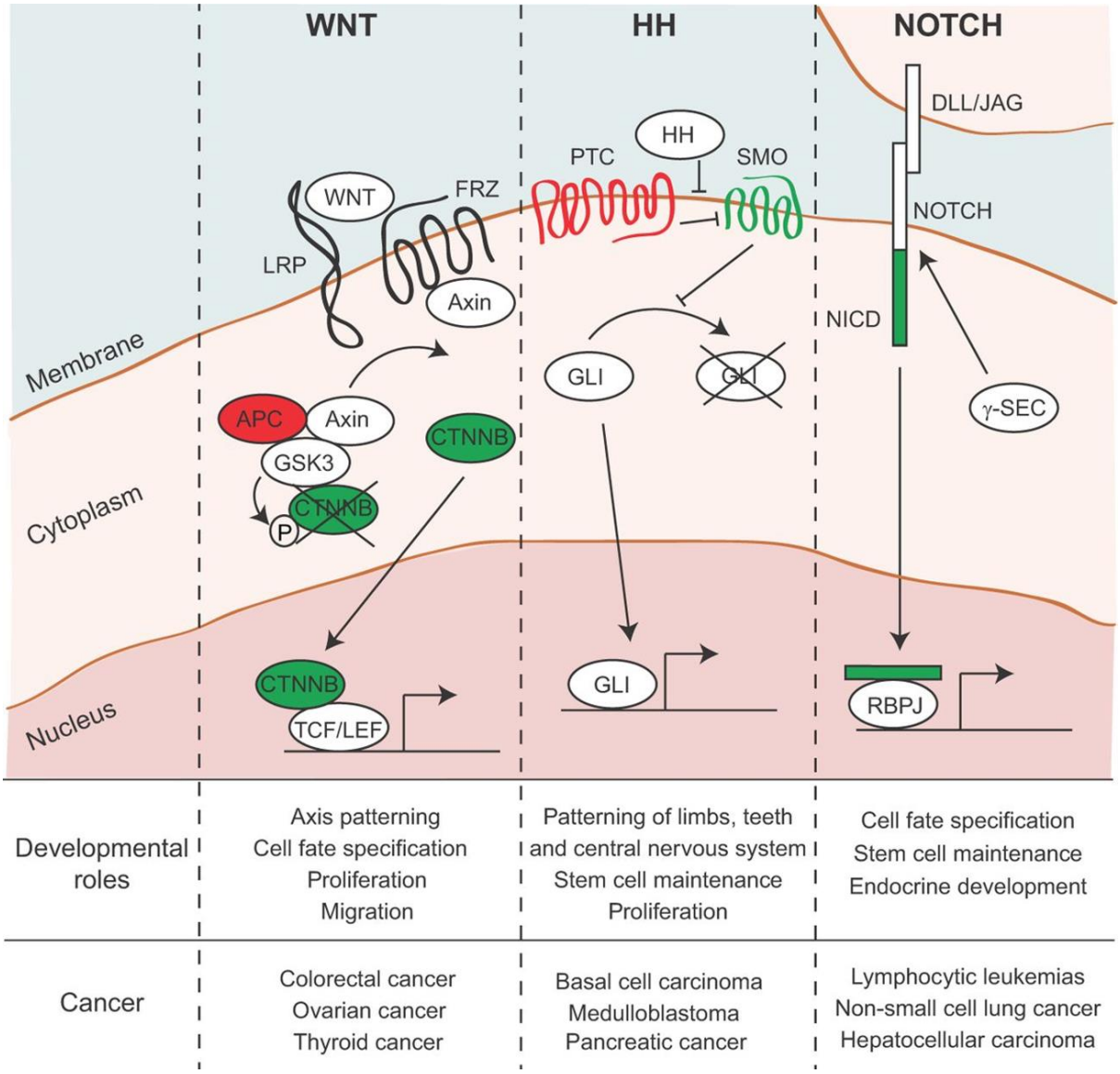

Figure 23 : Developmental pathways frequently activated and/or altered in cancer[148]**.**

Other pathways :

Other pathways shared between embryogenesis and cancer development include the protease activated receptors (PARs), the bone morphogenetic peptides (BMP), the transforming growth factor (TGF-β) pathways…etc[148].

Because of the strong involvement of these embryological pathways in tumor development, many research groups, including ours, work to elucidate the extent of the role of these mechanisms. In our lab, we are particularly interested in one of the Wnt/PCP pathway receptors, CELSR2, a G-protein coupled receptor, as strongly correlated with a decreased metastasis free survival and overall survival of TNBC

patients. To our best knowledge, no previous study has ever investigated the involvement of CELSR2 in breast cancer development nor attempted to target the receptor therapeutically. The receptor, its physiology and the results of this study will be discussed following an overview of the family of receptors to which CELSR2 belongs.further.

Chapter 3 :

An overview of the GPCRs family :

The very simple idea that some proteins act as receptors for other molecules to permit intercellular communication was still controversial just 4 decades ago. Indeed, the existence of such proteins was not obvious and no scientific data backed the proof of their presence within the cell. Henry Dale, a prominent English pharmacologist who would go on to receive the Nobel prize in physiology or medicine in 1936 stated "...It is a mere statement of fact to say that the action of adrenaline picks out certain such effector-cells and leaves others unaffected ; it is a simple deduction that the affected cells have a special affinity of some kind for adrenaline ; but I doubt whether the attribution to such cells of "adrenaline-receptors" does more than re-state this deduction in another form…"[180]. No clear biochemical experiment settings nor technology allowed to study or structure these receptive proteins. Some of the "assumed" receptors that were meticulously studied for an extended length of time were the adrenergic receptors. In the early 1980s, Robert Lefkowitz's lab performed radioligand labeling of agonist and antagonist of the β-adrenergic receptor, isoproterenol and alprenolol respectively. They showed a different binding competition pattern for the two molecules, suggesting different affinities for the receptor, a low and a high affinity. Addition of guanine nucleotides interconverted the two curves, bringing the high affinity molecule binding capacity down to one similar to a low affinity molecule (Figure 24)[181].

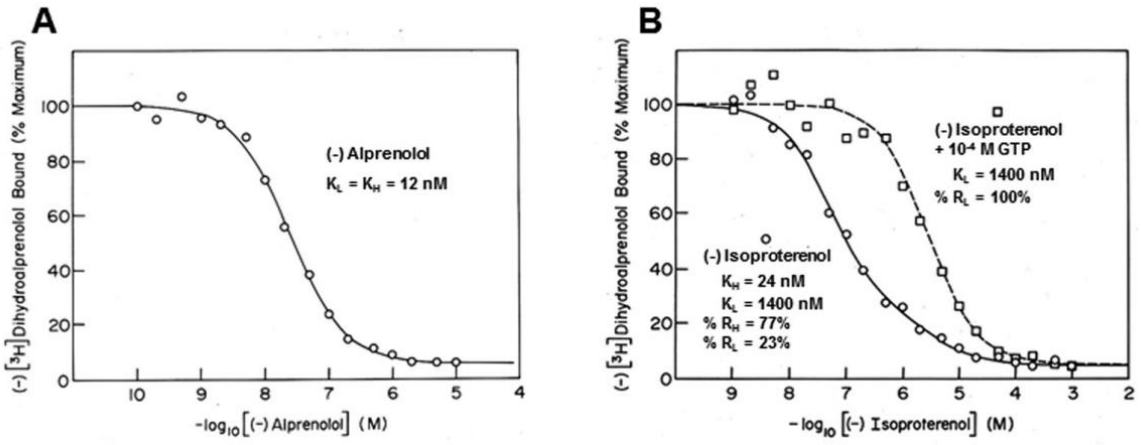

Figure 24 : (A) curve fitting binding from displacement of dihydroalprenolol by the antagonist alprenolol. (B) displacement by the agonist isoproterenol in the presence (□–□) or absence (○–○) of GTP[182].

This finding suggested this low affinity state is translated by the binding of the molecule to the receptor, while the high affinity state represents the binding of the molecule to the receptor and a third component would add up to this complex. The guanine nucleotide effect clearly hinted to the third component as the guanine nucleotide regulatory protein, otherwise known as a G-protein[183]. These findings would pave the way for the rise of the ternary model. This operational model postulates that an event involving signaling through a receptor must encompass at least 3 elements, a ligand, a receptor and an intracellular signaling partner , G-proteins, arrestins among others (Figure 25)[183].

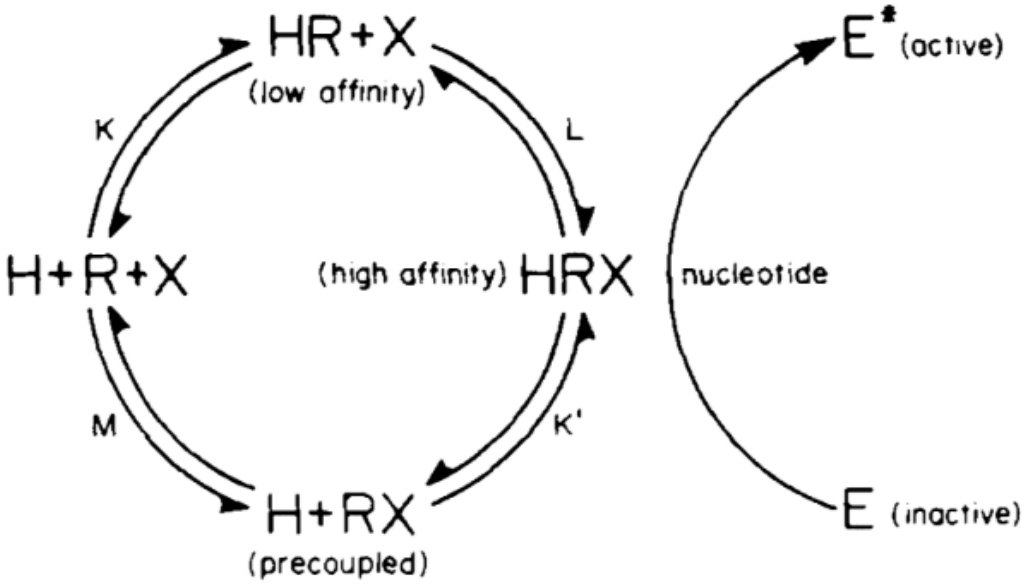

Figure 25 : schematic diagram of the full version of the ternary complex[183]. H= hormone, R= receptor, X= additional component required for the signaling

G proteins themselves were, then, recently discovered by Ross and Gilman[184]. These findings were the foundations to establish what would be known as G-protein coupled receptors (GPCRs). More efforts to study these receptors focused on their sequence and structure. Cloning of the β-adrenergic receptor and partial sequencing revealed homologies with the then known rhodopsin, a light sensitive, 7 transmembrane receptor that was sequenced in 1982[185]. The transmembrane domain was hypothesized to be at the origin of light sensitivity of rhodopsins. With the sequencing of the β-adrenergic receptor, it became an accepted consensus that these transmembrane receptors were a canonical feature of the GPCR family instead of light sensitive proteins[186]. More adrenergic receptors would be cloned and sequenced in the subsequent years[187–190] . The discovery of these receptors and their structure was rewarded with the chemistry Nobel prize in 2012 to Robert Lefkowitz and Brian Kobilka[191]. Today, we come to realize that GPCRs form a superfamily of over 800 identified receptors[192,193]. This superfamily is virtually involved in all known physiological and pathological events, most notably sensory processes, namely taste, smell and vision, behavior regulation, early development, energy metabolism, cardiac functions and immune response [194–196]. **Thus it is not surprising that pharmaceutical companies harnessed for the last decades chemical and**

biological compounds to target GPCRs, resulting in about a third of the drugs approved for different pathologies by the FDA[197].

The human GPCR family of receptors is divided into 4 major classes based on sequence homology and functional similarity :

Class A : the rhodopsins family which is the biggest GPCR class consisting of more than 700 members. They are further subdivided into subclasses based on the nature of the associated ligand such as peptides, amino acids, proteins, lipids, melatonin, photons…etc. The druggability of this class of GPCRs is particularly successful (Figure 26). More than 500 drugs targeting GPCRs are aimed at this specific class and more than 500 others are in clinical trials[198].

Class B is further divided into two subfamilies, the secretin family (B1) which currently has 15 known members and the adhesion family (B2) which has 33 members. The members of class B are characterized by large extracellular domains for the most. The secretin family members serve as receptors mostly for peptide hormones such as parathyroid hormone (PTH), glucagon, glucagon like peptides (GLPs), vasoactive intestinal peptide (VIP)…etc[199]. T**he other arm of the class B receptors, the adhesion subfamily (aGPCRs) has multiple unique features such as diverse extracellular motifs, a GPCR autoproteolysis-inducing domain (GAIN), and a tethered agonist. Although a growing number of studies report the involvement of aGPCRs in multiple diseases, no therapeutic agent has entered clinical trials**[200].
CELSR2, the receptor of interest in the present study belongs to this subfamily of receptors. Its characteristics and role in various physiological and pathological processes are discussed further.

Class C otherwise known as the glutamate subfamily has 22 members. This subfamily has a distinctive large extracellular domain and their activation requires constitutive dimerization of the receptor. Despite the low number of members of this subfamily, at least 16 drugs targeting these GPCRs are marketed by the FDA[201].

Class F, the Frizzled and SMO subfamily which has 11 members and are known to be mediators of Wnt signaling and play a critical role in embryonic development. These are sometimes labeled as atypical GPCRs as they activate disheveled in the cytosol instead of inducing the canonical signaling cascade of GPCRs[202]. Among this subfamily, SMO has been successfully targeted by a small molecule antagonist to act as a neoplastic agent[203].

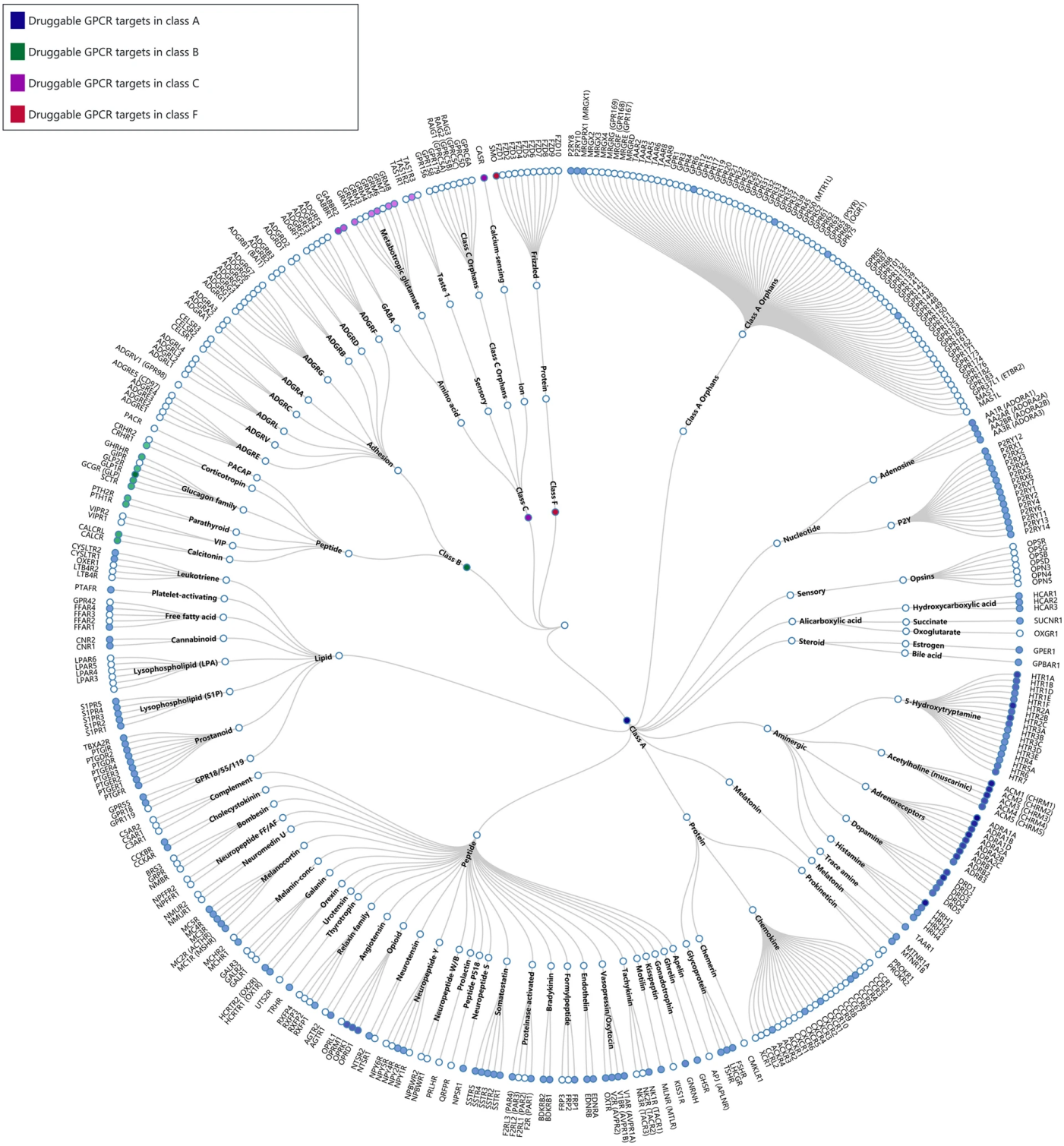

Figure 26 : Tree of GPCRs. Node represents GPCR. Solid color represents receptors with approved drugs[204].

GPCR signaling

GPCRs are remarkably versatile in function, with this diversity comes a large diversity in ligands and signaling partners. The range of activators of GPCRs is truly striking and encompasses all known molecular structures, and beyond (Figure 27). For instance, within the Family A of receptors alone, amines activate a large number of receptors, of which adrenergic; muscarinic, dopaminergic and 5- hydroxytryptamine, are activated by adrenaline, acetylcholine, dopamine, serotonin and respectively. More ligands include peptides such as angiotensin and somatostatin, proteins such as chemokines, lipids such as endocannabinoids and free fatty acids…etc[205]. The diversity is such that rhodopsins are activated by photons, which are not even physical compounds. **Although important efforts and major discoveries led to the identification of a large number of ligands, yet the endogenous ligands of more than 140 receptors are still unknown**[206]. Thus making the natural function of these orphan GPCRs ambiguous but also granting the opportunity of drugging these receptors once their ligands are known.

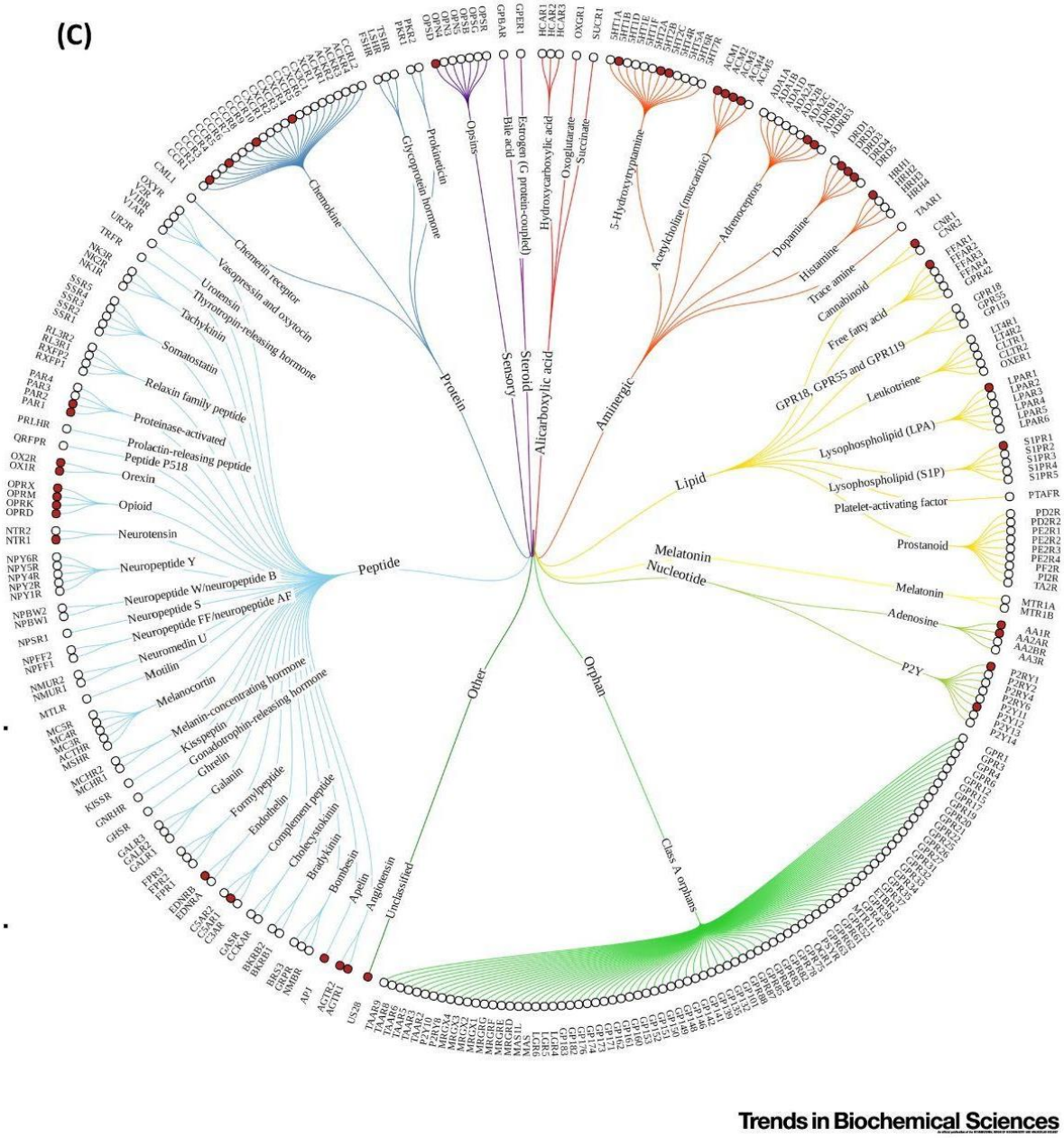

Figure 27 : Classification of GPCRs according to their endogenous ligands[207].

G-protein dependent and independent signaling :

Upon activation of a GPCR, the signaling cascade can either undergo a G-protein dependent or G-protein independent pathway. The canonical pathway is the G-protein dependent, which is mediated by a heterotrimeric G-protein complex composed of a G-alpha, a G-beta and a G-gamma subunit[208]. In contrast to the very large diversity of the GPCR family, G-proteins make only 4 families (Gs, Gi/o, Gq/11 and G12/13)[209].

The low number of G-proteins compared to the number of GPCRs reflects the conserved mechanism of activation of the receptors independently of the diverse functions they execute and ligand nature.

It has been shown that GPCRs have a basal activity independent of a ligand binding[210]. The basal activity of GPCRs could be modulated by ligands that could be maximal agonists, which induce a maximal response, partial response agonist, which induce an intermediate response, an antagonist or an inverse agonist that would decrease the basal activity of the receptor (Figure 28)[211].

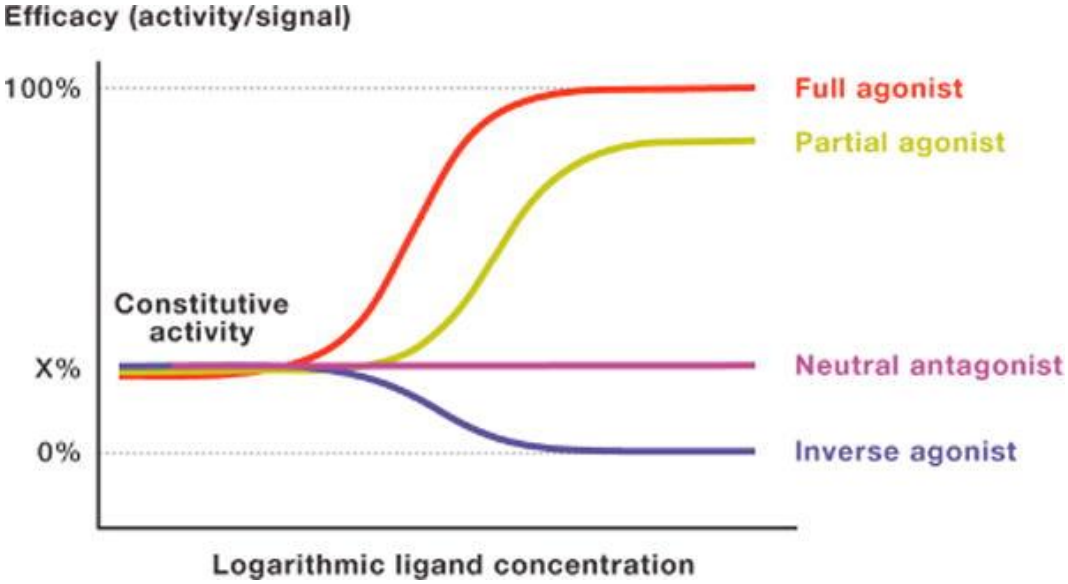

Figure 28 : GPCR activation upon different ligands binding[211].

In the inactive state of the receptor, the alpha subunit remains bound to GDP, and upon activation, the GPCR initiates a nucleotide exchange, thus rapidly dissociating the GDP and making place for a GTP, a very abundant component in cells, to bind, and further induce the dissociation of the trimeric complex due to a conformational change of the G-alpha subunit, resulting in two subunits : a G-alpha bound to GTP, and another formed by G-beta and G-gamma (Figure 29). **These resulting subunits induce very diverse downstream signaling cascades, of which we can cite signaling through MAPK, cAMP, phospholipases, ion channels…etc**[212]. The activation cycle is terminated once the G-alpha, which is a weak GTPase, hydrolyzes the GTP to GDP, leading to the recoupling of the G-alpha subunit with the G-beta and G-gamma subunit.

Alternatively, GPCR can signal through other intracellular proteins than G-proteins such as beta-arrestins and G-protein receptor kinases (GRK). Arrestins are a family of 4 members (arrestin 1-4). Arrestins 1 and 4 are the proteins responsible for visual perception in the retina where they're mostly expressed, while arrestins 2 and 3 are ubiquitously expressed. Similarly to G-proteins, arrestins undergo conformational change upon binding to a receptor, which induces the exposure of the concave surface of the N-terminal lobe that holds phosphointeraction sites, which engage GRK phosphorylated serines and threonines and activate the downstream signaling (Figure 29)[213].

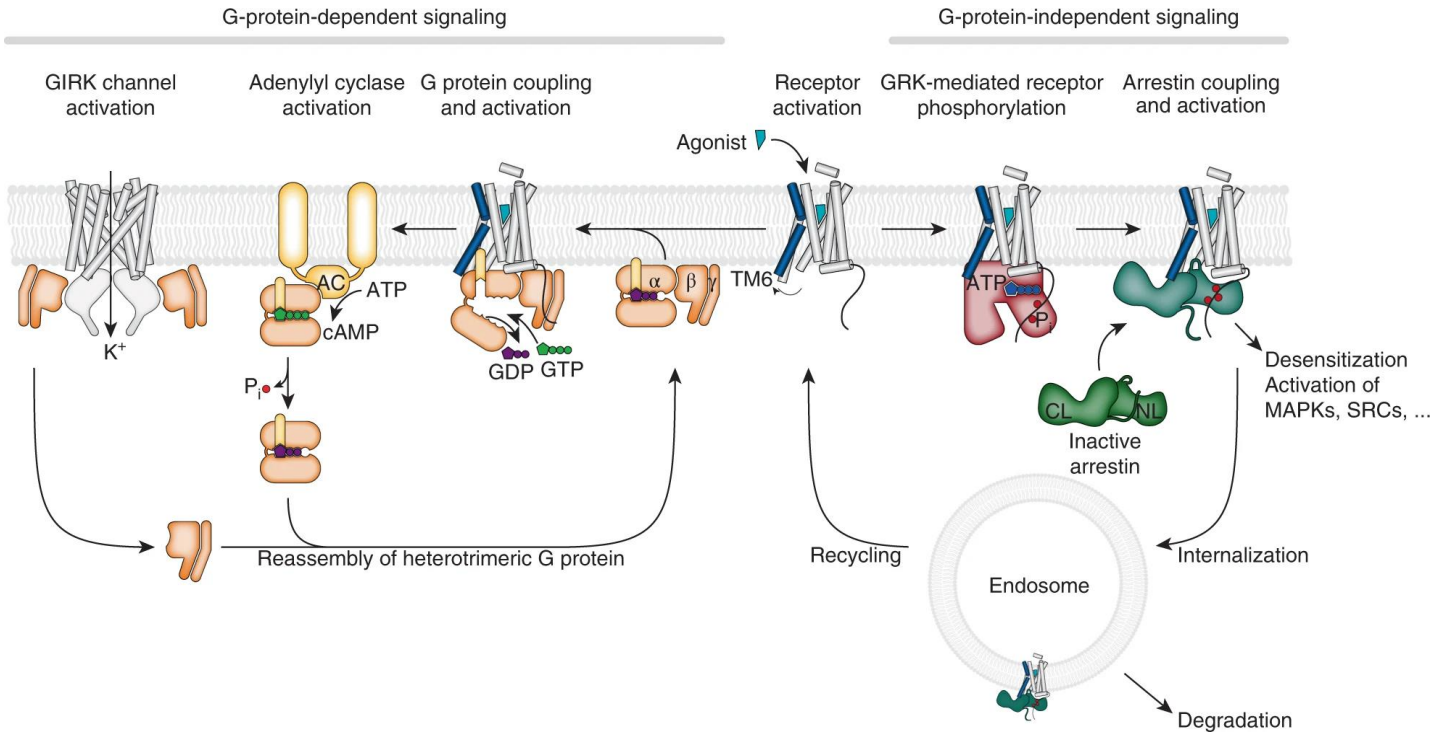

Figure 29 : G-protein dependent and independent signaling[208].

Downstream effectors of GPCR signaling :

The four Gα proteins associated with GPCRs induce different signaling pathways within the cell (Figure 30). Gαs stimulates adenylate cyclase, thus inducing the accumulation of cAMP, which in turn activates protein kinase A and leads to the phosphorylation of CREB and its translocation to the nucleus in order to induce the expression of its target genes. Gαi, on the other hand, inhibits adenylate cyclase, thus

decreasing cAMP levels and inhibiting the PKA/CREB pathway. Gαq activates the phospholipase C (PLC) which hydrolyzes phosphatidylinositol 4,5- bisphosphate (PIP2) to diacylglycerol (DAG) and inositol triphosphate (IP3). Ultimately IP3 leads to the release of calcium from the ER to the cytoplasm[214]. The accumulation of calcium and DAG activate protein kinase C (PKC). Among the functions of PKC is the activation of NfKB[215]. Finally, Gα12/13 directly activates RH-RhoGEFs to regulate the activity of the GTPase Rho which in turn phosphorylates substrates such as MLC phosphatase, ERM, LIMK…etc[216]. Although the canonical pathways remain predominant, alteration in downstream signaling and alternative pathways exist depending on the receptor and pathophysiological context.

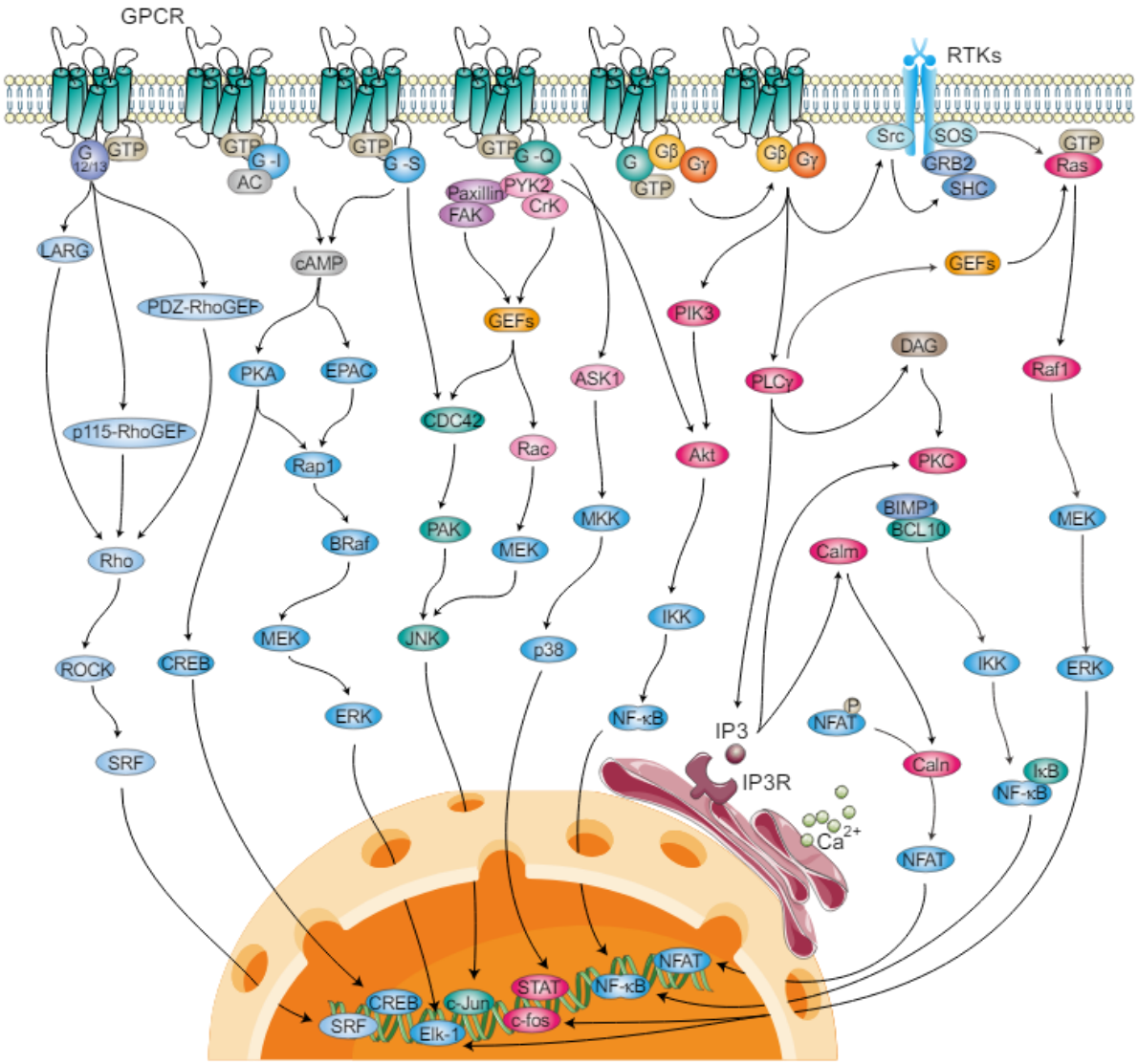

Figure 30 : Downstream signaling pathways following GPCR activation

Biased signaling of GPCRs :

It has been documented that a given GPCR does not necessarily signal through an unique pathway, rather different ligands exhibit a functional selectivity or else known as a biased signaling (Figure 31)[211]. For example, arrestins have been found to compete with G-proteins for signal transduction[217]. Indeed, the selectivity for a given binding partner can influence both the response rate but also its nature, where a ligand could be an agonist in a given signaling setting and an antagonist in another. For example, aripiprazole was postulated to be a partial agonist of 5-HT1A and D2 receptors as well as a 5-HT2A antagonist. Aripiprazole is currently marketed by the FDA for the treatment of schizophrenia. Subsequent studies have found that aripiprazole actions range from agonism to antagonism depending on the cell line used for the study[218]. The reported results are not incoherent if we consider the multiple layers of complexity surrounding GPCR signaling.

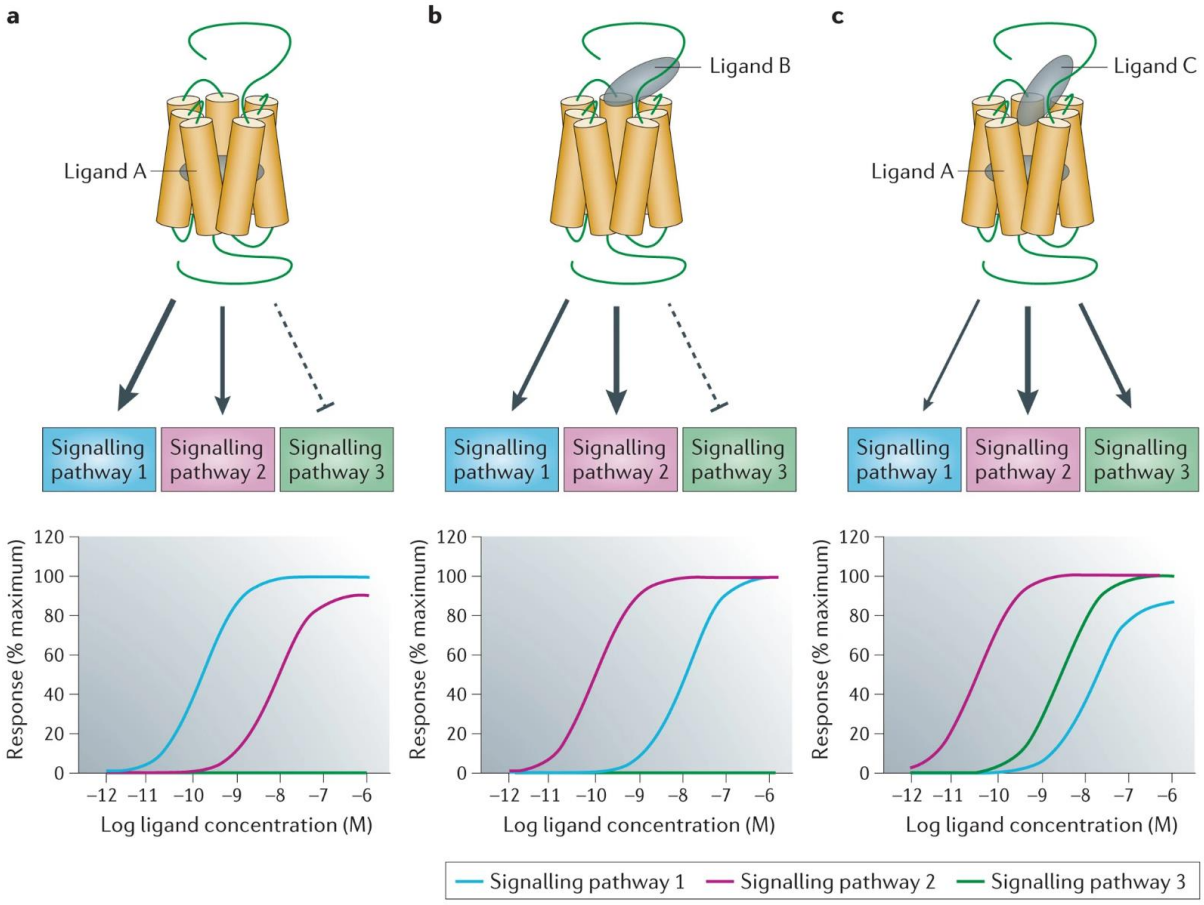

Figure 31 : Signaling bias describes the ability of different ligands acting on the same receptor to activate various signaling pathways.

GPCR structure :

Additionally to the investigation of the function and activation of a given GPCR, major efforts have been deployed to solve the structure of these receptors as it provides invaluable insights into the molecular mechanism and greatly facilitates the understanding of ligand recognition and drug discovery. The first ever crystal structure of a GPCR was solved in 2000 when an inactive rhodopsin was purified from the bovine eye and structured[219]. Subsequently, the structure of the β2-adrenergic receptor bound to an antagonist was solved in 2007[220]. This led to an interest in purifying and solving the structure of the GPCRs bound to their intracellular signaling partners. In 2011, the β2-adrenergic receptor was purified in complex with the associated G-protein (Gas)[221].

GPCR structure solving benefited greatly from progress made in protein purification and the application of nanobodies[222,223] along with the advent of cryo-EM which had a determinant role on solving the structure of over 90% of GPCRs bound to signaling partners structures. More than 450 structures of 82 GPCRs from the different classes, except the class B, have been solved by cryo-EM[204]. Nevertheless, solving the structure of GPCRs in their active state remains highly challenging, and most of the structures reported in the literature are in the inactive state of the receptor (Figure 32).

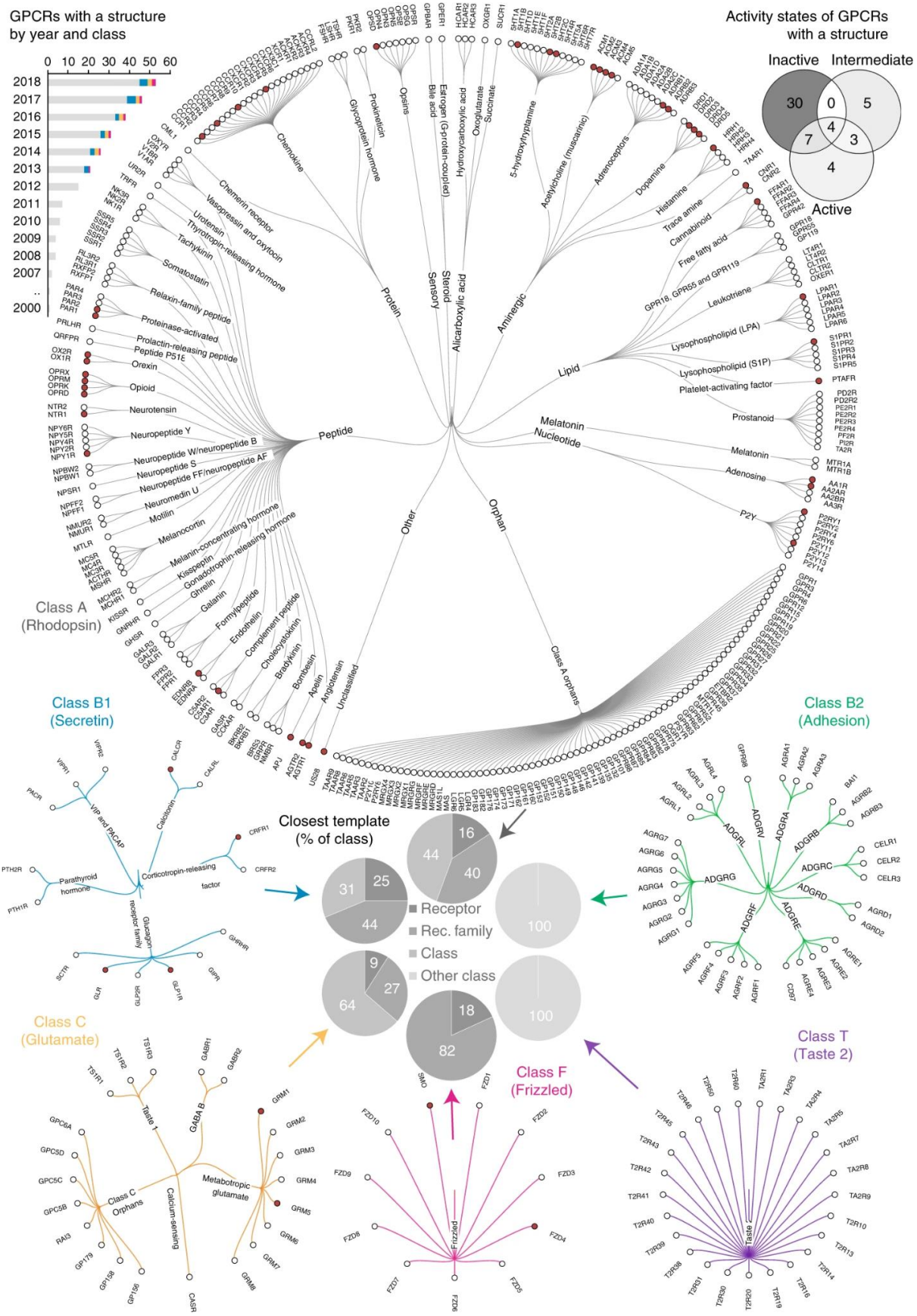

Figure 32 : Reported solved structures of GPCRs. Red circles represent structured receptors[224].

The structure of these receptors is conserved to a large extent : we note the presence of the canonical 7 transmembrane helices embedded in the phospholipid bilayer, a disulfide bond,three extracellular loops (ECLs) and three intracellular loops (ICLs) (Figure 33). **Unlike most receptors, GPCRs ligands bind to the transmembrane helices 3, 5, 6 or 7 instead of the extracellular region. The ECLs are particularly important as they can occlude or expose the binding pocket on the helices by a change of conformation**[225].

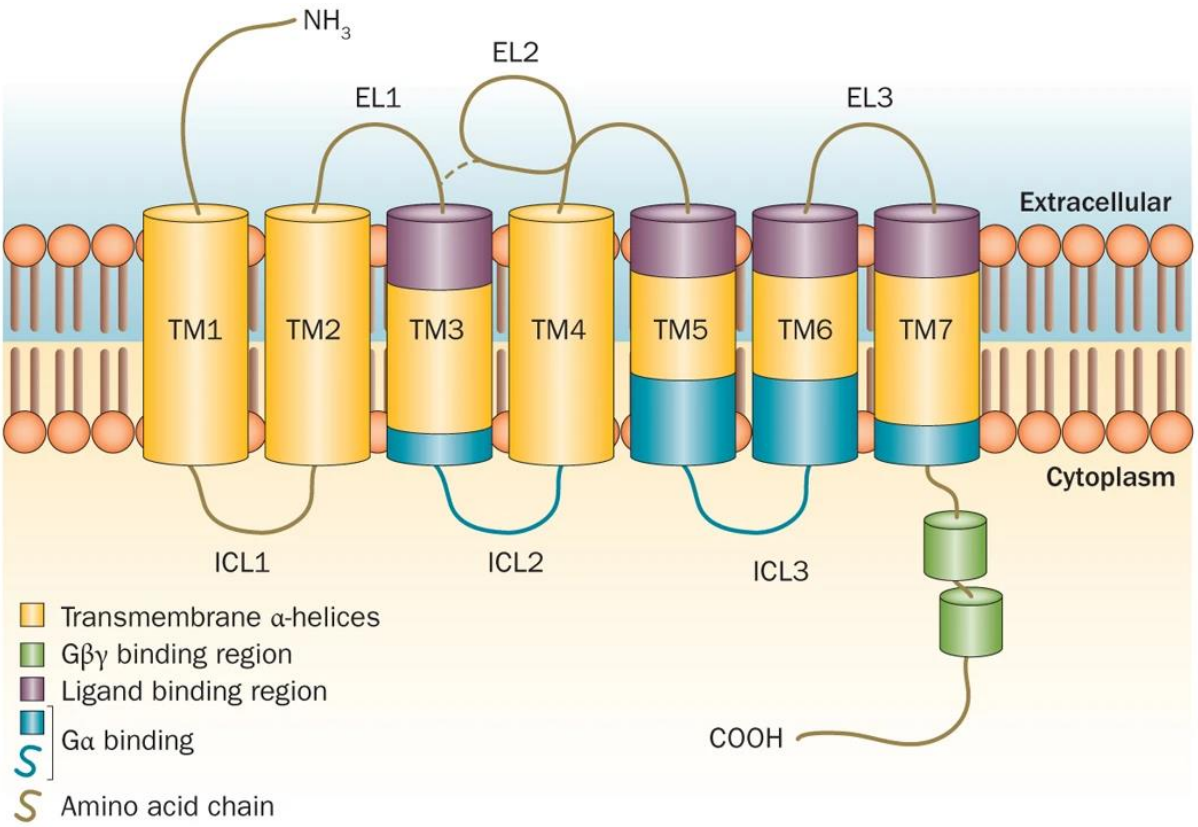

Figure 33 : Schematic diagram of a GPCR structure with seven transmembrane domains, extracellular and intracellular loops (ECLs and ICLs respectively)[226]

Functionally, GPCRs are represented in the landscape of virtually all physiological processes, ranging from metabolism, immune function and sensory function but also play a role in the pathogenesis and chronicity of many diseases, such as metabolic

diseases (obesity, diabetes, osteoporosis…etc) immunological disorders, neurodegenerative diseases and cancer[227].

Adhesion GPCRs :

The identification of the adhesion group of receptors was the result of the progress made in cDNA cloning techniques in the 80s (Figure 34). The first members to be cloned were CD97 and EMR1, both being largely expressed on leukocytes. The structure of these newly cloned receptors was found to comprise the canonical 7TM feature of all GPCRs, and importantly, a large extracellular domain with several epidermal growth factor (EGF) like domains[228,229].

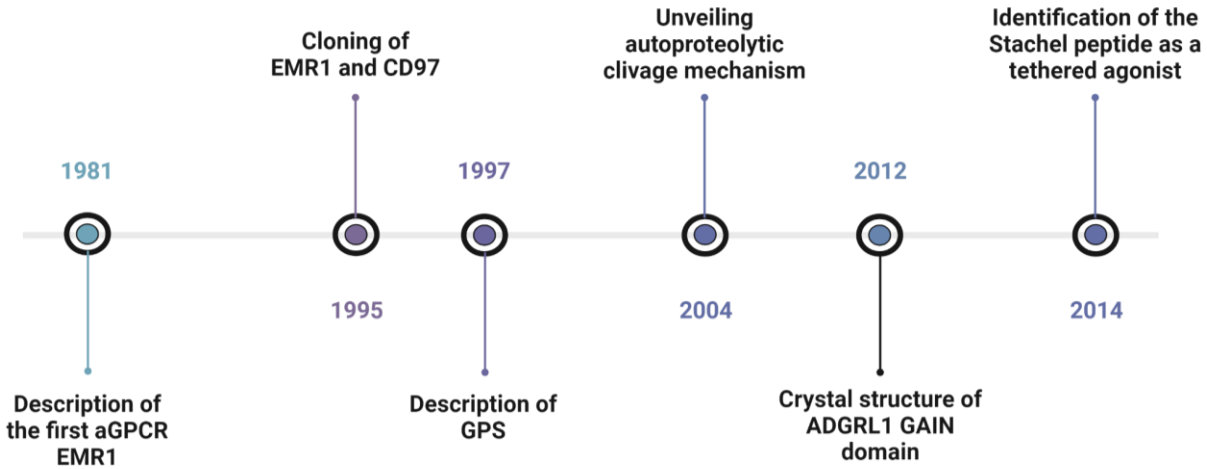

Figure 34 : Selected key findings and discoveries in the adhesion GPCR field since their discovery. (Created with Biorender.com)

The presence of these two features supported the branding of this class of receptors EGF-TM7[230]. Subsequently, many other members enclosing the same features were identified such as the other members of the EMR group, BAIs (Brain angiogenesis inhibitors), latrophilins, CELSRs…[231–234]. More research on these receptors shed light on another key feature of the adhesion GPCRs consisting of the segregation of each receptor into two non covalently attached fragments that originate from the full length

receptor. The cleavage localization on the receptor happens at the GPCR proteolysis site (GPS), located immediately on the extracellular portion of the receptor[235]. The GPS motif which is in some sort a linker between the adhesive domains and the 7TM is highly conserved among the members of the human adhesion GPCRs subfamily, thus making this motif another canonical feature of the group of receptors[236]. More extensive research on this group of receptors and the integration of structural biology revealed that the GPS motif is an integral part of a broader domain termed GPCR-Autoproteolysis INducing (GAIN) domain. It has been shown that the GAIN domain is both sufficient and necessary for the autoproteolysis to happen [237]. The activation mechanisms of the aGPCR family remain challenging to investigate as the natural ligands are difficult to identify. Nevertheless, it has been shown that mechanical cures could trigger the activity of aGPCRs, going against the paradigm that GPCRs are quasi exclusively chemosensors[238–240]. Other possible activation pathways include the engagement with the extracellular matrix or other cell membrane receptors (Figure 35)[241–244]. Another layer of complexity was added with the proposal of the existence of a tethered agonist termed the Stachel peptide; which would be exposed with the cleavage of the N-terminal fragment at the GPS site. **Many studies have used synthetic Stachel peptides and could effectively activate various aGPCRs upon treatment both in vitro and in vivo**[242,245–248].

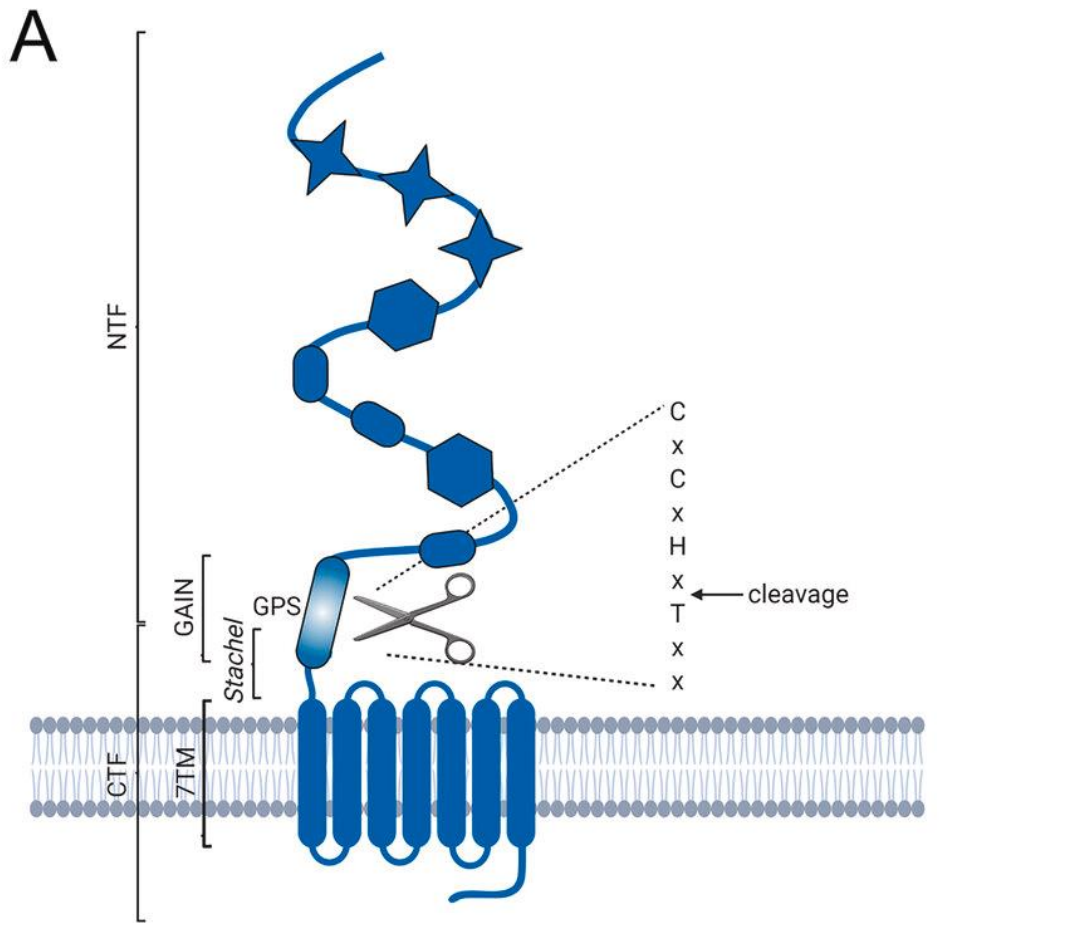
A
NTF
GAIN
GPS
Stachel
CTF
7TM
C
x
C
x
H
x
T
x
x
cleavage

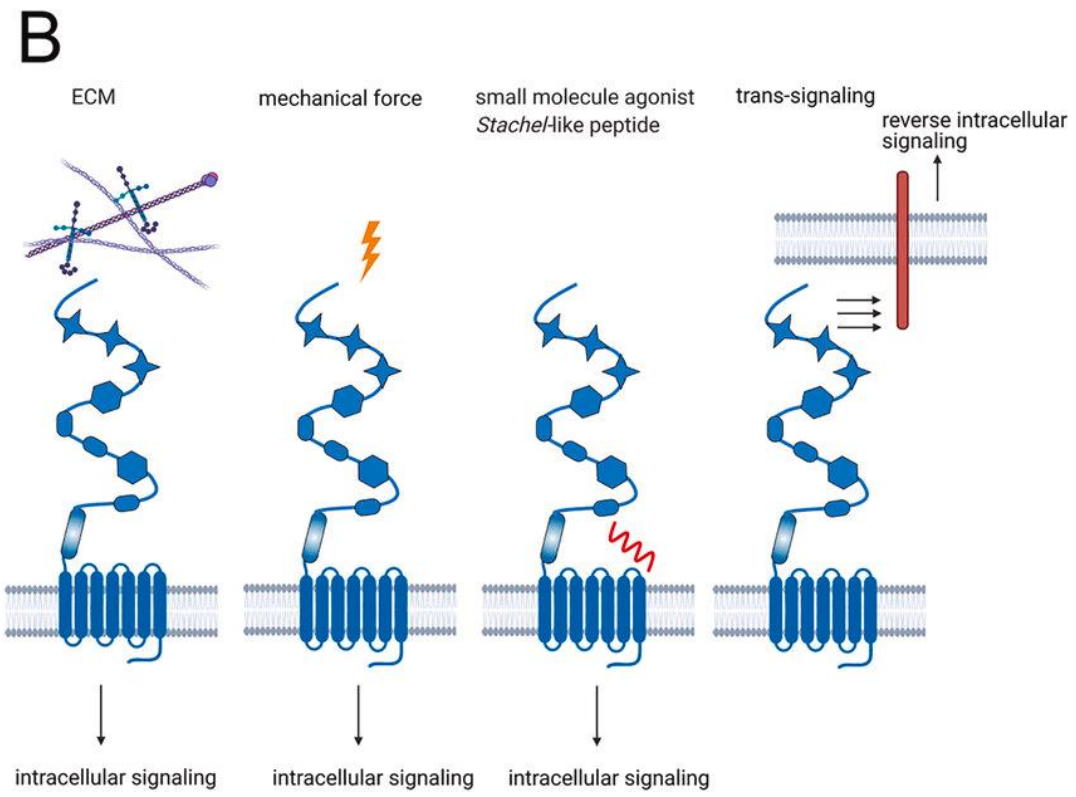
B
ECM
mechanical force
small molecule agonist
Stachel-like peptide
trans-signaling
reverse intracellular
signaling
intracellular signaling
intracellular signaling
intracellular signaling

Figure 35 : (A) Schematic representation of the aGPCR structure. (B) activation of aGPCRs by interaction with extracellular matrix, Stachel peptide or by interaction with receptors from other cells[249].

Up to date, the adhesion subfamily of GPCRs comprises 33 members in humans divided into nine subfamilies based on sequence homologies in the canonical 7 transmembrane domains and the extracellular fragments (Figure 36). The nomenclature of the receptors was initially based on the structure or the function but was subsequently unified by the Adhesion GPCR Consortium and the International Union of Basic and Clinical Pharmacology Committee. The current nomenclature includes a common root ADGR followed by the subfamily identifying letter and member identifying number. The functions of the aGPCR members are very diverse. Roles of aGPCRs include sensory functions, development and function of immune cells, development of the central nervous system, regulation of endocrine functions.. etc. The aberrant activation of the receptors has been reported to be implicated in a multitude of diseases, of which neurodegenerative syndromes, psychiatric and endocrine diseases, developmental defects…etc. (Table 4)

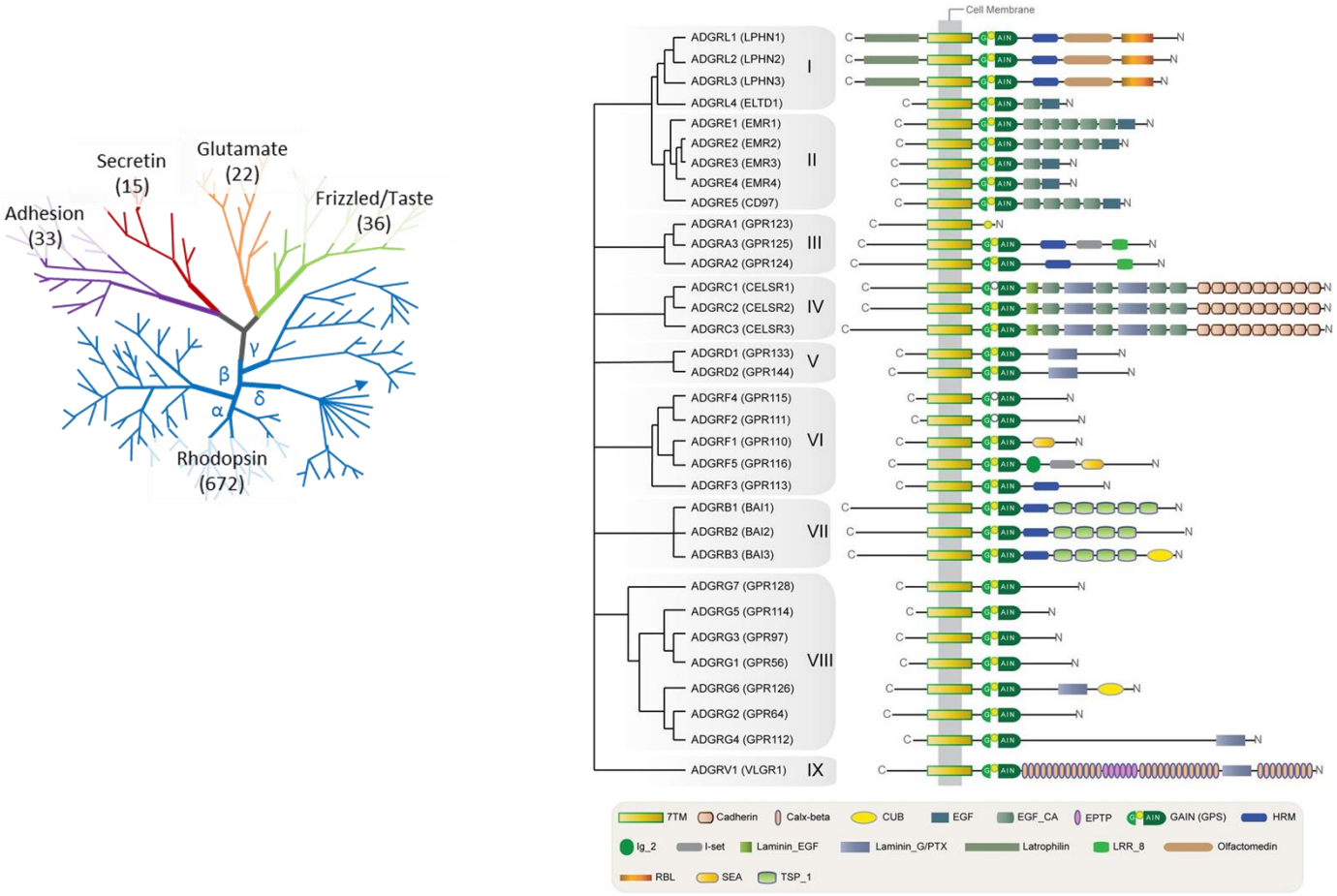

Figure 36 : Schematic representation of the phylogenetic representation of aGPCRs and their structure[250].

Table 4 : list of aGPCRs, their associated signaling pathway and involvement in health and disease

aGPCR	Subgroup	Cleavage /Stachel activation	Signaling pathway	Role in health and disease
ADGRL1	1	Yes	Gaq	Neuron morphogenesis/ Obesity/ receptor of α-latrotoxin[251–253]
ADGRL2	1	Yes	G12/13	Synapse organization/ heart development[254,254,255]

ADGRL3	1	Yes	G12/13 Gas	Attention deficit with hyperactivity[256]
ADGRE1	2	No	Gaq Gai[257]	Macrophage marker, eosinophilic disorders
ADGRE2	2	Yes	Gaq Gas	Vibratory urticaria[258]
ADGRE3	2	Yes	Gas Gai[259,260]	Marker of granulocytes / Nephropathy
ADGRE5	2	Yes	G12/13[244,261,262]	Granulocyte and dendritic cell homeostasis / rheumatoid arthritis / multiple sclerosis
ADGRA3	3	No	G12/13	Choroid plexus homeostasis / apicobasal polarity[263,264]
ADGRA2	3	No	ELMO/Dock	Blood brain barrier integrity / pericyte polarization [265,266]
ADGRA1	3	No (No GAIN)		Thermogenesis / pluripotent stem cell reprogramming [267,268]
ADGRC1 (CELSR1)	4	No	Gas	Epilipsy / Cell-cell adhesion[269,270]
ADGRC2 (CELSR2)	4	Yes	Gas	Ependymal ciliogenesis[271]
ADGRC3	4	No	Gas	Ependymal

(CELSR3)				ciliogenesis[271]
ADGRD1	5	Yes	Gas	Embryo transit in utero / phagocytosis mediation[272,273]
ADGRD2	5	No	Gaq	Unknown
ADGRF1	6	Yes	Gaq Gas Gai	Non alcoholic fatty liver disease / Blood brain barrier permeability[274,275]
ADGRF2	6	No		Enamel hypomineralization[276]
ADGRF3	6	Yes	Gaq	Taste [277]
ADGRF4	6	No	Gaq Gai	Epidermal differentiation / enamel mineralization [278,279]
ADGRF5	6	Yes	Gaq	Somatostatin regulation / retinal endothelial layer patterning[280,281]
ADGRB1	7	Yes	G12/13 B-arrestin	Synaptic plasticity / Parkinson's disease[282,283]
ADGRB2	7	Yes	G12/13	Angiogenesis regulation / depression[284,285]
ADGRB3	7	Yes	Gaq	Synaptic connection / schizophrenia[286]
ADGRG1	8	Yes	Gaq G12/13	Depression / Epilepsy / NK activation [287,288]

ADGRG2	8	Yes	Gaq G12/13 B-arrestin	Azoospermia / Male fertility [289,290]
ADGRG3	8	Yes	Gai G12/13	Antimicrobial function[291]
ADGRG4	8	Yes	Gas Gai	Mechanical force sensing[292]
ADGRG5	8	No	Gas Gai	Unknown
ADGRG6	8	Yes	Gas	Chronic obstructive pulmonary disease/ scoliosis / myelination / glial cell development [293,294]
ADGRG7	8	No	Gas	Intestinal contraction frequency / Sezary syndrome [295,296]
ADGRV1 (VLGR1)	9	Yes	Gai Gaq	Autophagy regulation /epilipsy / Usher syndrome [297–299]

aGPCRs in cancer :

GPCRs have been shown to play a critical role in the progression and metastasis of many different tumors. Tumor cells can hijack the activation of GPCRs and their downstream signaling to boost their proliferation[300], immune evasion[301], angiogenesis[302], invade the surrounding tissue and metastasize to distant organs[303]. GPCRs in tumors can be activated through gain of function mutations, independent of the presence of their ligand[304] or by the overexpression of the receptors and their

agonists produced by either the tumor or stromal cells. A foundational discovery was made in 1986 when the MAS oncogene was identified and was described to have the canonical 7 transmembrane domains. MAS was shown to induce cell transformation of NIH 3T3, a fibroblast cell line[305]. Subsequent studies showcased the role of GPCRs in driving tumorigenesis. The virtually unlimited bioavailability of the agonist of the muscarinic acetylcholine receptor was found to induce NIH 3T3 cellular transformation[306]. Moreover, the ectopic expression of the serotonin receptor 5HT1c was found to drive a similar cell transformation[307]. These studies point out to the potency of the GPCR signaling in driving crucial phases of tumorigenesis. More GPCRs have since been implicated in tumor cell proliferation, migration and invasion such as the protease activated receptors (PARs), chemokine receptors, G-protein estrogen receptor…etc[308–310]. The adhesion GPCRs have also attracted a significant interest for their potential role in tumor development. CD97 / ADGRE5 was the first aGPCR to be correlated with cancer. A de novo expression of CD97 was found in thyroid carcinoma, and this expression was strongly correlated with the progression of thyroid cancer and the level of differentiation of the tumors[311]. CD97 has been explored in glioblastoma and was found to be expressed mostly on tumor cells while healthy neurons exhibit a low expression. An ADC was developed against CD97 and was shown to have a high efficacy in selectively killing tumor cells in vitro[312]. Interestingly, ADGRE2 has recently been targeted with CAR-T cells for the treatment of acute myeloid leukemia (AML) . ADGRE2 was found to be expressed on leukemic blasts while normal hematopoietic stem cells exhibited low to no expression. The CAR-T cells exhibited a high potency in clearing tumor cells both in vitro and in vivo. These CAR-T cells targeting ADGRE2 could represent an attractive target for the treatment of AML[313]. The role of the other aGPCRs in different cancers is described below :

Table 5 : comprehensive list of aGPCRs involved in various cancers

aGPCR	Cancer	Expression	Impact on tumor cells / tumor development
ADGRL2	Breast cancer[314]	Increased	Immune suppression
ADGRL4	Colorectal cancer, renal cell carcinoma, breast cancer, neuroblastoma[315–	Increased	Migration, invasion, EMT, immune suppression

	[318]		
ADGRE1	AML[319]	Increased	Unknown
ADGRE2	Breast cancer, lung cancer[320,321]	Increased	Stem cell repression, Improved patient survival
ADGRE3	Glioblastoma[322]	Increased	Cell invasion
ADGRE5	Glioblastoma, colorectal cancer, ovarian cancer, gastric cancer, AML[312,323–326]	Increased	Decreased patient survival, cell proliferation, migration, invasion, drug resistance
ADGRA2	Glioblastoma, osteosarcoma, lung cancer[327–329]	Increased or decreased	Cell proliferation, cell cycle progression, drug resistance,
ADGRA3	Colorectal cancer[330]	Increased	Improved patient prognosis
CELSR2	Hepatocellular carcinoma[331,332]	Increased	Decreased overall survival, drug resistance
ADGRD1	Glioblastoma, AML[242,333]	Increased	Decreased overall survival, cell proliferation
ADGRF1	Lung cancer, prostate cancer, breast cancer, osteosarcoma[334–336]	Increased	Drug resistance, tumor initiation
ADGRF5	Colorectal cancer, breast cancer, gastric cancer [337–339]	Increased	Decreased overall survival, tumor cell proliferation and invasion
ADGRB1	Lung cancer, glioblastoma, breast cancer[340–343]	Decreased	Angiogenesis, inversely correlated with metastasis,
ADGRG1	Colorectal cancer, melanoma, AML[344–346]	Increased	Positively correlated with metastasis, EMT, cell proliferation, migration, invasion,
ADGRG2	Breast cancer, endometrial cancer, Ewing sarcoma[347–349]	Increased	Cell adhesion, migration, invasion, tumor suppressor,
ADGRG6	Breast cancer, colorectal cancer[350,351]	Increased	Decreased overall survival, cell proliferation tumor growth,

Chapter 4 :

CELSR2 receptor :

CELSR2 is a member of the group 4 of the adhesion GPCR family. It has been initially identified in the drosophila and termed Flamingo. It has been initially shown to play a critical role in the planar polarity of wing cells[352]. In humans, 3 orthologs have been identified : CELSR1, CELSR2 and CELSR3. CELSR2 gene covers a region of 26 kb on chromosome 1 and the protein has a molecular weight of around 320kDa, which is among the largest of aGPCRs family. CELSR1 and CELSR3, both share most features similar extracellular motifs and molecular weight. The 3 paralogs have around 60% sequence homology. CELSR2 has the putative 7TM, a GAIN domain, and a large extracellular fragment of around 260kDa comprising an arrangement of 9 atypical cadherin repeats,6 EGF like, 2 LAG like and 1 laminin EGF like motifs[353]. The intracellular part of CELSR2 includes 3 intracellular loops (ICLs) and a C-terminal tail of 305 amino acids. The C-terminal part is enriched in serines, threonine, proline, and encompasses several PEST sequences, hinting at the potential degradation mechanism (Figure 37). The overall architecture of these receptors is poised to relay both intercellular signals based on the homotypic interaction with receptors on neighboring cells, and intracellular signals via heterophilic interactions of soluble ligands binding.

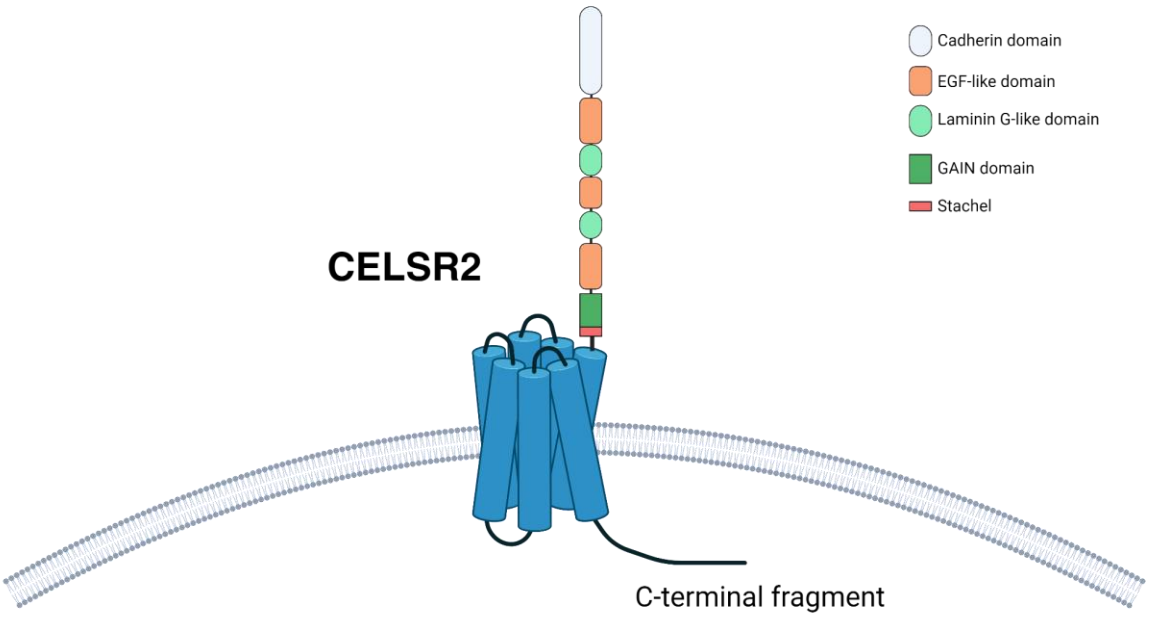

Figure 37 : Schematic representation of the domains of CELSR2 (Created with Biorender)

The downstream signaling pathway has been very recently elucidated. CELSR2 has been found to undergo cleavage at the GPS site, and point mutation of the threonine positioned at residue 2357 was sufficient to block the cleavage. Furthermore, by utilizing nano bret assays, CELSR2 has been found to couple to Gαs in transfected HEK293 (Figure 38). This coupling required autoproteolysis, and the acute exposure to the tethered agonist did not augment the activation of the receptor[354].

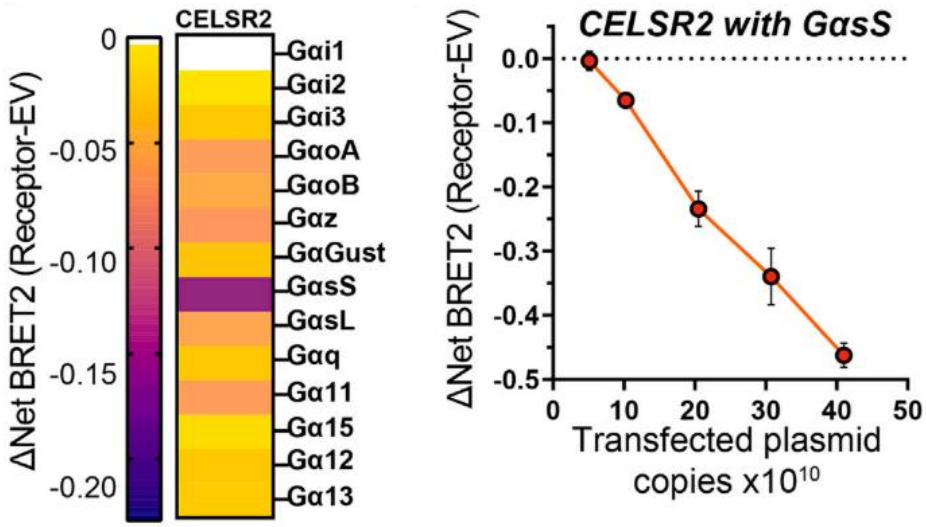

Figure 38 : (Left) Heatmap illustrating G protein coupling of full-length CELSR2. (Right) Copy-dependent full-length CELSR2 coupling to GasS[354].

CELSR2 tissue distribution and functions :

Originally, Flamingo was reported to be expressed in the epithelium and nervous system of the drosophila[352]. Subsequently, it has been reported to be expressed in other mammalian organs and tissues such as the esophagus, stomach, lungs, heart…etc[355–357]. In our study, we report a very high expression of CELSR2 in the brain, specifically in oligodendrocytes when compared with other body sites. Much of the understanding of the functions of CELSR2 as well as the other CELSRs originates from studies conducted in drosophila on the orthologue Flamingo. Until now, the role

of CELSR2 remains quiet elusive as very few studies studied in depth its implications in physiological and pathological processes, instead, CELSR2 is often found among top hits in GWAS studies of various diseases, most notably ciliopathies, lipid imbalance and cardiovascular syndromes[358–361]. In more experimental studies, CELSR2 has been found to induce cell aggregation upon ectopic expression with the full length. This phenotype was diminished when the protein lacked most of the extracellular domain, highlighting the functional relevance of the adhesive properties of the extracellular adhesion motifs [352]. Another study showed that a defect of flamingo in drosophila induced a neuronal dendrite growth and a tiling defects. The ectopic expression of wild type flamingo rescued a normal phenotype. In order to investigate whether there is functional diversity and difference of role between the N-terminal and C-terminal fragments, truncated versions of the receptor have been expressed. The flamingo lacking the N-terminal could rescue the dendrite growth, while the flamingo lacking the C-terminal fragment rescued the tiling phenotype[362]. This study unveiled for the first time a functional difference of the N-terminus and the C-terminus. More studies have reported the central role of CELSR2 in mediating various processes of the planar polarity[269,363–365].

CELSR2, as a central protein of the PCP and a large aGPCR remains understudied in a cancerous context. CELSR2 expression has been reported to be correlated with a decreased overall survival of hepatocellular carcinoma patients, and an upregulated expression in tumors when compared with adjacent normal tissue[331]. Another study investigating mechanisms of glucocorticoid resistance in acute lymphoblastic leukemia revealed CELSR2 as a key mediator in the onset of therapeutic resistance both in vitro and in vivo[332]. Although these studies hint at an interesting phenomenon of the cancer biology, they are based on transcriptional signatures and do not uncover the underlying molecular mechanisms governing the reported observation. In our current study, some of the raised questions we attempted to answer were the underlying mechanisms governing the involvement of CELSR2 in tumorigenesis and the associated processes. Moreover, the large extracellular fragment opens the door for a potential therapeutic targeting with biologics such as antibodies and nanobodies, which we also investigated as part of this study.

Chapter 5 :

Antibody - nanobody therapeutics

Antibodies have been considered and used as weapons, Paul Elrhich himself described antibodies as “Magic bullets”, thus promoting the idea of making them a weapon of high precision[366]. Monoclonal antibodies have prompted a milestone revolution in cancer theranostics. Although major challenges were met with the idea of administering antibodies generated in mice and the observed immune response of the host against the therapeutic antibodies.

Historically, polyclonal antisera were used for the treatment of infectious diseases such as rabies, varicella, tetanus…etc[367]. It was considered for a lengthy period of time as the gold standard for numerous infections, and its proponent, the german physiologist Emil Von Behring was awarded the first ever Nobel prize in physiology or Medicine in 1901[368]. This therapeutic approach, otherwise known as “serum therapy” persisted until the advent and large marketing of antibiotics[369]. While being supplanted by antibiotics in infectious diseases, polyclonal antisera made their comeback as a possible therapeutic strategy in cancer. One of the first attempts was the purification of antisera raised against ferritin and subsequently labeled with radioactive Iodine 131 for the effective targeting of tumors known for their high expression levels[370]. This approach delivered poorly as there were major issues with response consistency among patients, quality control, heterogeneous deposition across different healthy tissues and host immune response, as these antibodies were not humanized yet. The big scientific leap forward was the discovery and characterization of monoclonal antibodies.

Persistence led to the modification of murine antibodies to generate chimeric murine-human antibodies very much similar to the naturally occurring human IgG, then humanized and then fully human antibodies. These monoclonal antibodies were approved for use in clinical settings, such as the anti CD20 (Rituximab), and many others such immune checkpoint inhibitors (Pembrolizumab), anti VEGF (Bevacizumab), anti HER2 (Trastuzumab)...etc[136,371–373]. Nevertheless, a number of investigated antibodies fail as monotherapy, which prompted researchers more than 50 years ago to arm antibodies with toxins in order to increase the cytotoxic effects of

the therapy. Toxins such as abrin, ricin, pseudomonas exotoxin and diphtheria toxin were the first to be conjugated, making an immunotoxin[374–377]. These immunotoxins act on tumor cells first by binding to the antigen of interest, get endocytosed within the cell and kill from within. Although the approach is original, the toxicity was quite dramatic and the toxins themselves are highly immunogenic. This drawback paved the way for the reflexion on ways to refine this approach, but instead of arming the antibody with a toxin, it would be armed with approved small molecules such as anthracyclines, a sort of second generation ADCs. This approach alleviated the immunogenicity but did not induce great cell death nor provide a great clinical benefit as the used drugs were not the most potent one could think of. A third generation of ADCs are currently used and benefit from very specific monoclonal antibodies conjugated with a highly potent drug which is toxic at very low doses[378]. Important innovations in ADC development were made in the used linker which conjugates the drug to the antibody. The used linkers must guarantee that it does not interfere with the antibody recognition of the target, remains conjugated and stable in circulation and is released only when internalized and in the proper tumor cell compartment[379].
The benefit of radiation therapy was already established, and the use of Iodine 131 proved to be very effective in thyroid cancer. Another approach to attack tumor cells consisted in the use of radioactive elements instead of chemical components as for ADCs.

Monoclonal antibodies solved some of the faced issues, and we have now in clinical use for example an anti CD20 with labeled with radioactive iodine 131 (tositumomab) or Yttrium 90 (ibritumomab tiuxetan) for the treatment of non Hodgkin lymphoma[380]. These radioimmunoconjugates act by emitting β-particles and little ɣ-radiation. However, major challenges remain in the use of the radioimmunoconjugates, most prominently the complex logistics, the decay of radioactivity over time, the need to have specialized institutions…etc. Another investigated alternative to conjugating antibodies with a drug or radioligand are the cytokines, otherwise known as antibody cytokine conjugates. Indeed, aggressive tumors tend to have a highly immunosuppressive microenvironment, which dampens the activity of cytotoxic lymphocytes. The paradigm of coupling antibodies with cytokines aims to stimulate the immune response while preventing the large side effects of systemic administration of

cytokines[381] . Among the investigated cytokines, we have IL-2, IL-12, and TNF-a[382–384]. Most ongoing trials couple one of these cytokines with antibodies aimed at different tumor antigens such as EDB, GD2, FAP…etc. IL-2 for example is a central player in the activation of anti-tumoral immune cells such as cytotoxic T-cells and NK cells. The proposed mechanism of these conjugates is that IL-2 induces the local activation of lymphocytes while the antibody binding to the tumor cell antigen induces an antibody dependent cell toxicity through its Fc fragment[385].

Beyond arming antibodies with drugs, another strategy to prompt a therapeutic response was to simultaneously target the tumor cells and an activating receptor on cytotoxic t cells with bispecific antibodies. These bispecifics harbor one arm aimed at each target. The challenge in the early investigations was the high activation of T-cells when using full antibodies because of the presence of the Fc fragment. Subsequent investigations successfully engineered a fusion protein consisting of two single chain variable fragments (scFvs), these would be called bispecific T-cell engagers (BiTEs). The most prominent example is blinatumomab, a BiTE aimed at CD3 ε-chain on T-cells and the tumor antigen CD19.

Nanobodies from discovery to application

The challenges to develop potent antibodies include very high developmental and production costs, long lead time for manufacturing, low penetration in tumors and an extended half-life of several weeks which increases risks of adverse events[386]. A promising alternative are nanobodies, which are small fragments with similar binding affinities and are a tenth the size of conventional antibodies. Their discovery in the 90s in camels and subsequently in sharks was totally random, yet they immediately raised the interest of the community[387,388]. Other studies on the camelid family revealed the presence of nanobodies in alpaca, llama and vicuna[389–391].

Nanobodies present interesting features for their use in clinical practice, yet with some drawbacks (Table 4). Because nanobodies use a single immunoglobulin variable domain for the recognition of antigens, they can have access to epitopes out of reach for conventional antibodies. For instance, nanobodies can penetrate in tight catalytic

pockets or protein-protein binding domains. Another attractive feature of nanobodies is the flexibility in the administration route, as these can be used in IV injection, subcutaneously, as an aerosol and a topical application[392–395]. Moreover, unlike conventional antibodies, nanobodies have a high homology with the human VH domain, which renders the humanization and translation to clinical practice easier and cheaper. The humanization of a nanobody requires a straightforward mutagenesis on very few residues, in the order of 10 aa[396]. The drawbacks of using nanobodies for therapeutic purposes include the lack of an Fc fragment, therefore nanobodies cannot provide Fc dependent cell cytotoxicity. Additionally, its half-life, which is very short, limits the potential uptake by the tumor. Nevertheless, this opens a therapeutic window of possibly using multiple doses as compared with antibodies, and because nanobodies are the smallest possible unit capable of mimicking antibody functions, they provide a design flexibility to augment the half-life. Various strategies have been used, most notably creating a tandem of two nanobodies, the addition of an Fc fragment and conjugation to polyethylene glycol[392].

Table 5 : Advantages and limitations of nanobodies compared with conventional full length antibodies[397].

	Antibodies	**Nanobodies**
Size	150 kD	15 kD
Development costs	High	Moderate
Administration	i.v., s.c.	i.v., s.c., aerosol, topical
Specificity	High	High
Off target adverse effects	None	None
On target adverse effects	Depends on target	Depends on target
In Vivo half-life	Can be adjusted by Fc-engineering	Can be adjusted by PEGylation or fusion to albumin-specific Nb
Metabolites	Non-toxic, biodegradable	Non-toxic, biodegradable
Tissue penetration	Slow	Excellent in periphery
Tissue specificity	Targetable (bi-specific Abs)	Targetable (bi- specific Nbs)
Albumin binding	Usually not	Via albumin-specific Nb to extend half life, usually no effect on potency

The number of studies reporting the use of nanobodies as a therapeutic platform has grown exponentially for the last 2 decades, going from just under 10 studies in the late 90s to almost 700 by 2023. Caplacizumab, a nanobody targeting the Von Wilbrand

factor for the treatment of acquired thrombotic thrombocytopenic purpura, was approved by the FDA[398]. It was followed by the approval of Ciltacabtagene Autoleucel, a CAR-T cell therapy which expresses a nanobody at its surface for the recognition of BCMA for the treatment of multiple myeloma[399]. At least two other nanobodies have been approved by agencies other than the FDA and the EMA. Ozoralizumab, an anti-TNF alpha nanobody was approved for the treatment of rheumatoid arthritis in Japan[400]. Envafolimab is an anti PD-L1 nanobody approved for the treatment of solid tumors such as colorectal, biliary tract and soft tissue tumors in China[401]. Many clinical trials investigating nanobodies either for their functional effects, or as bispecific T-cell engagers, or as the antigen recognition component of CAR-T cells are being conducted in various tumors in preclinical and clinical settings(Table 6) [402] .

Table 6 : Non exhaustive table of reported nanobodies in the literature targeting tumor antigens :

Target	Tumor targeted	Tested model	Application
CAIX[403]	Breast cancer	In vitro / NSG mice	Therapy
CapG[404]	TNBC	In vitro / Nude mice	Diagnosis / Therapy
CD20[405]	Non Hodgkin lymphoma	C57BL6 / NSG mice	Therapy
CD33[406]	Acute myeloid leukemia	NSG mice	Imaging
CTLA4[407]	Melanoma	C57BL6 mice	Therapy
Mesothelin[408]	Breast cancer	NSG mice	Imaging
EGFR[409–411]	Epidermoid carcinoma / Lung cancer /	In vitro / NSG mice	Therapy / Imaging
CD105[412]	Hepatocellular carcinoma	In vitro / NSG mice	Therapy
BCMA[413]	Multiple myeloma	In human CAR-T cells trial	Therapy
CD7[414]	T-lymphoblastic	In human CAR-T	Therapy

	lymphoma	cells trial	
CD22[415]	B-cell lymphoma	In human CAR-T cells trial	Therapy
EpCAM[416]	Epithelial tumors	In human CAR-T cells trial	Therapy
VEGFR/ANG2[417]	Solid tumors	In human bispecific trial	Therapy
PDL1/CTLA4[418–420]	Hepatocellular carcinoma / Lung adenocarcinoma / TNBC	In human bispecific trial	Therapy

The pipeline to nanobody discovery :

Most reported nanobodies in the literature have been discovered from naive, immunized or synthetic libraries. Animal immunization and selection remains the most effective way of identifying potent nanobodies with high affinity. This strategy consists of immunizing a camelid with a given antigen : recombinant protein, plasma membranes, whole cells..etc. The immunization induces an immune response of the animal which raises high affinity nanobodies against the target. The circulating lymphocytes are then harvested, and the mRNA is extracted. By reverse transcription, cDNAs are obtained and nanobodies sequences are amplified by nested polymerase chain reactions. The PCR products are then cloned into a vector and transformed in an expression system such as bacteria. This step allows for the appreciation of the library size; 10^7 transformants is considered to be good[421]. The subsequent selection of nanobodies consists of alternating strategies by phage display between cells expressing the antigen of interest, the recombinant protein, another cell line expressing the antigen…etc. Recently, the concerns over animal use pushed for the advent of synthetic libraries which are constructed by mutagenesis of the CDR regions and yield diverse libraries. The limitation of the synthetic library lies in the complex library construction process and the need for a very large library quality of 10^9 to 10^{15}

transformants [422].In the present study, we opted for llama immunization to discover nanobodies specific to CELSR2

Objectives of this thesis:

The CRCM is a laboratory located for the most part within the Institut Paoli Calmettes, a regional specialized hospital for the care of HemOnc patients. The hospital has a longstanding expertise in the management of breast cancer patients and has been frequently regarded as one of the top institutions for the treatment of this pathology in the country[423].

My research group led by Pr. Jean-Paul Borg and Dr. Flavio Maina explores molecular circuits operating in solid tumors, focusing particularly on components of signaling networks. My PhD project was part of a larger program aiming at identifying vulnerabilities in TNBC, specifically the Wnt/PCP related proteins. The projects of the group were supported and funded through the years by several organizations including “La Ligue Contre Le Cancer”, “Fondation pour la Recherche Médicale - FRM”, “l'Institut Universitaire de France”...etc.

During my thesis, I pursued two main objectives :

The first was to understand the role of CELSR2 in TNBC development, if there is any and unveil the underlying mechanism. This aGPCR has been described briefly in hepatocellular carcinoma patients with no deep investigation of the mechanism and the function of the receptor in cells. As a surface receptor, it should convey cues from the extracellular environment and signal within the cell to induce a response. We aimed at conducting the most exhaustive possible study, by interrogating patients data of our hospital and the public datasets, by conducting in vivo studies to assess the tumorigenic role of CELSR2 in vivo and using knockdown and overexpression strategies in vitro to evaluate its effect on various cellular processes. These investigations should apprise whether CELSR2 could be an attractive therapeutic target in TNBC.

The second objective consisted in discovering nanobodies specific to CELSR2 extracellular fragment which could modulate the signaling activity of the receptor. The choice of nanobodies was motivated by several factors :

The affordability : llama immunization costs range anywhere between 2500 and 10000 euros, which are relatively low cost compared with other immunization strategies for the development of monoclonal antibodies.

The growing interest and potential in the future : 2 nanobodies have so far been approved in the clinic. One of them is used in oncology as the targeting domain of a CAR-T cell therapy directed against BCMA in multiple myeloma. Nanobodies have particular features discussed in the thesis, but most importantly the possibility of binding a conformational epitope, the ease of production and manipulation and the straightforward humanization process for potential future studies.

The local environment : within the CRCM, a core facility “Antibody therapeutics and immunotargeting” with a longstanding expertise is accessible to work on discovering nanobodies against surface antigens. Particularly, the core facility has previously worked and discovered nanobodies specific to GPCRs such as the glutamate receptors.

The rationale of using nanobodies as a therapeutic platform, additionally to their comparable recognition capacity with monoclonal antibodies, is the ease of development and subsequent customization depending on the future needs.

Altogether, the project aimed to unveil the function of CELSR2 in tumor cells, thus deepening our knowledge of the orphan class of adhesion GPCRs, and proposing the receptor as a potential novel therapeutic target in TNBC.

Results :

Research paper :

Original research paper : Cancer promoting mechanism of CELSR2 and its targeting in triple negative breast cancer

Authors :

SAIDANI NIY[1], Josselin E[2], Castellano R[2], Ly J[1], Verenerey J[3], Audebert S[4], Finneti P[3], Bertucci F[3], Chames P[3], Walton A[1] and Borg JP[1,4,5].

Affiliations :
1 : Aix Marseille Univ, CNRS, INSERM, Institut Paoli-Calmettes, CRCM, Equipe labellisée Ligue 'Cell polarity, Cell signaling and Cancer', Marseille, France.
2 : Aix Marseille Univ, CNRS, INSERM, Institut Paoli-Calmettes, CRCM, TrGET Preclinical Platform, Marseille, France
3 : Aix Marseille Univ, CNRS, INSERM, Institut Paoli-Calmettes, CRCM, Marseille, France.
4 : CRCM, Marseille Proteomics, Aix-Marseille Univ, INSERM, CNRS, Institut Paoli-Calmettes, Marseille, France.
5 : Institut Universitaire de France (IUF), Paris, France. jean-paul.borg@inserm.fr.

Contact information :
Jean-Paul Borg, PU-PH
Centre de Recherche en Cancérologie de Marseille, Inserm, CNRS, Aix-Marseille Université, Institut Paoli-Calmettes
27 BD Leï Roure BP30059
13273 MARSEILLE CEDEX 09 FRANCE
tel 33 (0)4 86 97 72 01 /fax 33 (0)4 86 97 74 99
e-mails: jean-paul.borg@inserm.fr

Keywords : Triple negative breast cancer, CELSR2, adhesion GPCR, nanobody

6 figures

Graphical abstract :

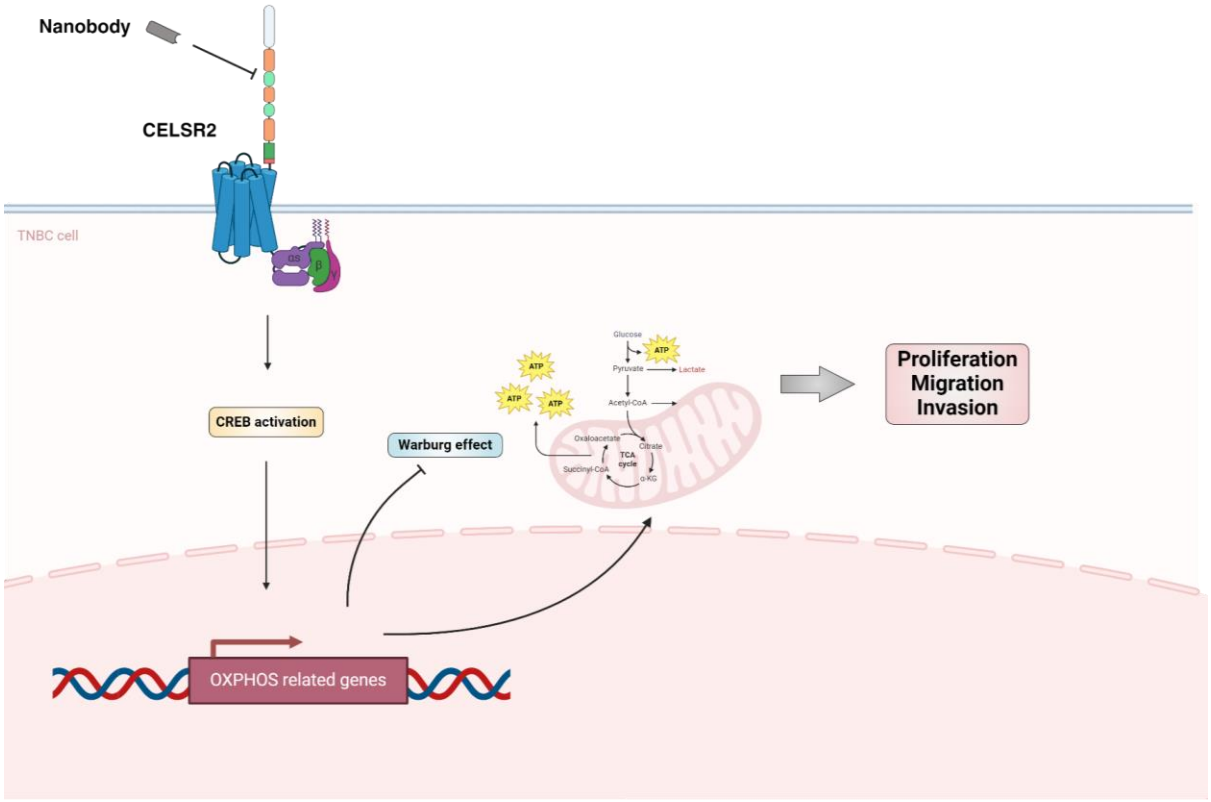

Abstract :

Triple negative breast cancer (TNBC) is an aggressive subtype characterized by a high heterogeneity, increased relapse hazard and resistance to approved therapies. Adhesion G protein coupled receptors have attracted attention recently in various tumors for their druggability. In the present study, We report that CELSR2 is associated with a decreased overall survival and metastasis free survival of TNBC patients. Moreover, we find CELSR2 mostly expressed in malignant cells in the tumor microenvironment, while its expression in the healthy tissues is relatively low, rendering it a promising target in TNBC. CELSR2 knockdown significantly impairs many tumorigenic processes such as cell proliferation, migration and invasion in vitro, and tumor growth in vivo. Mechanistically, we find that CELSR2 promotes oxidative phosphorylation via the CREB pathway. Finally, we observe a significant decrease of cell migration upon treatment with two in house discovered nanobodies. Altogether, our data sheds light on CELSR2 signaling, its involvement in tumor

cell processes, its role in enhancing oxidative phosphorylation, and provide a rationale for future development of nanobodies for the treatment of TNBC.

Introduction :

Triple negative breast cancer (TNBC) lacks estrogen receptor, progesterone receptor and human epidermal receptor 2 (HER-2) amplification[1]. Worldwide, TNBC tumors account for around 10-15%, corresponding to more than 170000 cases of all diagnosed breast cancer[2]. TNBC has further been categorized into 4 subtypes based on their molecular signature : basal like 1, basal like 2, luminal androgen receptor and mesenchymal[3]. Clinically, TNBC patients present aggressive tumors most often of high grade with a considerable proliferation capacity[4]. Moreover, these tumors show an increased likelihood of early and distant recurrences within 5 years of diagnosis[5]. The metastatic burden of TNBC renders the care of these tumors particularly challenging as more than 90% of cancer related deaths are associated with metastasis[6]. It is established that TNBC is both the most immunogenic based on the infiltration of tumor infiltrating lymphocytes and the most genetically unstable as these tumors have a high frequency of tumor suppressor genes mutations such as BRCA1/2 and TP53[7,8]. These characteristics, along with the identification of a tumor antigen, TROP2, led to the approval of a few targeted therapies for the care of TNBC patients of which are the immune checkpoint inhibitors, PARP inhibitors and the anti-TROP2 antibody drug conjugate (ADC)[9]. Regrettably, most metastatic TNBC patients cannot profit from these novel targeted therapies, and could only benefit from chemotherapeutic regimens, thus making the need to identify novel targets one of the hotspots of cancer research[10]. Owing to this lack of therapeutic options and the important heterogeneity observed between patients and within the same patient, the survival of TNBC patients is today the lowest among all breast cancer subtypes[2]. Several studies shed light on the involvement of embryonic pathways in all stages of cancer development, from initiation to metastasis[11]. Indeed, these pathways are particularly potent in promoting cell proliferation, migration and invasion[12]. Under strict

spatiotemporal control, these pathways enable a proper embryo development. Yet, when activated in cancerous lesions, they highly heighten the aggressiveness of tumor cells[13]. Wnt/Planar cell polarity (PCP), a non canonical branch of the Wnt pathway plays a role in morphogenesis by regulating convergent-extension cell movement during development, has been associated with breast cancer development and metastasis[14–16]. Downregulation of core PCP proteins such as VANGL2, Prickle1 and Frizzled 2 results in growth and migration defects[14,16,17]. CELSR2, a core component of the Wnt/PCP pathway, is an atypical cadherin and an adhesion GPCR. It plays a crucial role in neural pathfinding and ciliogenesis[18]. CELSR2 is the human homolog of Flamingo in drosophila[19]. It has two paralogs, CELSR1 and CELSR3. CELSR2 has the canonical 7 transmembrane domain of the GPCRs, a GPCR autoproteolysis inducing domain, and a large extracellular fragment comprising an arrangement of 9 cadherin repeats, 6 EGF like, 2 LAG like and 1 laminin EGF like motifs. The cytoplasmic end of the receptor is enriched in serines, threonines and prolines[20]. Recent findings report that the CELSRs constitutively couple to the G protein Gαs to activate the cyclic AMP (cAMP)[21]. CELSR2 has been reported to be positively correlated with a decreased overall survival of hepatocellular carcinoma patients and an increased receptor expression in tumor cells when compared with the adjacent healthy tissue[22].

Here, we deciphered that an overexpression of CELSR2 in TNBC patients is correlated with a decreased overall survival and metastasis free survival. Moreover, the expression was found to be upregulated in the metastatic site. By analyzing single cell RNA-seq data, we showed that CELSR2 is predominantly expressed on tumor cells, while its expression in most healthy tissues was low except in the nervous system. Moreover, we showed that silencing CELSR2 in multiple TNBC cell lines decreases cell motility, proliferation and invasion through the matrix and impairs tumor growth in vivo. Mechanistically, we described that CELSR2 expression induced CREB activation, promoting expression of oxidative phosphorylation related genes in TNBC. Indeed, by analyzing the total proteome by mass spectrometry of cells silenced for CELSR2, we confirmed a downregulation of a large number of mitochondrial proteins associated with the tricarboxylic cycle and oxidative phosphorylation, some of which are the expression products of CREB target genes.

Moreover, by revisiting patient transcriptomics data, we found that the overexpression of CELSR2 in metastatic sites was correlated with an increased expression level of OXPHOS genes. Finally, we showed that two in-house developed nanobodies, which bind to the receptor's extracellular fragment, impaired cell motility as strongly as genetic silencing strategies. Altogether, our data provides novel insights of the functions of CELSR2 in a cancerous context, demonstrate novel signaling mechanisms employed by CELSR2 to promote tumor progression via the regulation of tumor metabolism in TNBC, and shed light on CELSR2's potential as a therapeutically targetable vulnerability in TNBC.

Material and methods :

Plasmids :

Plasmid encoding human codon optimized full length CELSR2 bearing GFP tag at its C-terminus was kindly provided by Tadashi UEMURA (Kyoto University). In order to generate the loss of function CELSR2, the extracellular fragment of CELSR2 was deleted between the residues 32 and 2380, keeping the signal peptide and the C-terminal fragment. Q5 high fidelity polymerase was used to perform the PCR and the product was purified with Nucleospin columns (Macherey-Nagel Cat#740609.50) and transformed in thermocompetent DH5α e.coli.

The truncated version of CELSR2 representing the loss of function was synthesized Plasmid for expressing recombinant human extracellular CELSR2 bearing a 6xHis tag was cloned into a pHL-sec expression vector with a secretion signal using the NEBuilder HiFi assembly kit. Briefly, pHL-sec was digested by AgeI HF and BsteII HF, overhanging primers between the backbone and the cDNA of human extracellular CELSR2 were designed. PCR was performed with Phusion enzyme and the product was purified. Purified PCR product was subsequently cloned in thermocompetent DH5α. The plasmids were sequence confirmed by whole plasmid sequencing (Eurofins Scientific).

Luciferase reporter plasmid of Cre, SRE, SRF, NFAT and NFκB were kindly provided by Ines Liebscher (Leipzig University).

Cell culture and reagents :

All used cell lines in this study were obtained from the ATCC. Cell lines were maintained in DMEM (Cat #11965092, Gibco) supplemented with 10% heat inactivated fetal bovine serum (FBS), penicillin streptomycin (Cat #15070063, Gibco), non essential amino acids (cat #11140035, Gibco) and sodium pyruvate (Cat# 11360070, Gibco). SUM149 and SUM159 were maintained in Ham's F12 supplemented with 5% heat inactivated FBS, penicillin streptomycin, insulin (5 µg/ml), hydrocortisone (1 µg/ml).

Cell lines were regularly tested for mycoplasma using MycoAlert (Cat#LT07-318, Lonza).

siRNA transfections and shRNA transductions :

Cells were transfected with siRNA duplexes using lipofectamine RNAiMax (Cat #13778075, Thermo Scientific) as per the manufacturer instructions. Thep rotein expression was assessed between 24 to 72h post transfection.

Alternatively, shRNA targeting CELSR2 were packaged in lentiviral particles by co-transfecting HEK293T with VSV-G, ps-PAX2 along with the shRNA. 48 hours later, supernatant containing lentiviral particles was collected and filtered in 0.45µm filters. Breast cancer cell lines were grown to 60% confluence, washed in PBS. Polybrene was added to 1/1000 ratio to the previously collected lentiviral particles containing supernatant and then was added to cells. 24h later, cells were washed in PBS, fresh media was added and proceeded with puromycin selection.

Immunofluorescence imaging :

Cells were grown on glass coverslips for 24-48 hours then fixed with 4% formaldehyde (Cat # 28908, Thermo Scientific) for 15 min at room temperature. Cells were washed in PBS and permeabilized with 0.1% triton x-100, washed in PBS and blocked in 3%

BSA for 30 min. Antibodies against GFP 1/1000 (Thermo Fisher, Cat #11120), Phalloidin 1/500(Thermo fisher, Cat # A22287), P-CREB 1/400 (Cell signaling Cat#9198) were incubated overnight at 4°c. Coverslips were then washed in PBS tween at room temperature and subsequently incubated with secondary antibodies for 1h at room temperature. Alternatively, mitotracker dyes (Thermo Fisher, Cat# M7514) were incubated for 20 min at a concentration of 200nM with the cells prior to the fixation step, and subsequently treated as described above Coverslips were washed with PBS tween and mounted on ProLong™ Gold medium (Thermo Scientific, Cat #P36931,). Images were taken using Zeiss laser scanning
confocal LSM880.

Wound healing assay :

Cells were transfected with siRNA targeting CELSR2 and grown for 24h. Cells were then detached, counted and 90000 cells were seeded in each compartment for the wound healing chamber (Cat #80209, IBIDI). Cells were let to adhere for a further 24h. 2h prior to the start of the migration, cells were treated with Mitomycin C at 5µM final concentration (Cat# 226940020, Thermo fisher) in order to prevent cell proliferation. Wound healing chambers were then removed and cells were washed twice in PBS to remove cell debris. Brightfield or fluorescence photographs across the wound were taken every 10 min for a period spanning from 6 to 48h, depending on the migration speed of the cell line. Analysis was performed in FIJI 1.54G, as previously described[23].

Boyden migration assay :

Cells were transfected with either siCELSR2 or siCTRL for 24h. The cells were then trypsinized, resuspended in serum free DMEM and subsequently added to the Boyden chambers at a density of 20000 cells per well. Complete media containing serum was added to the lower chamber to serve as a chemoattractant. Cells were allowed to migrate across the 8µm polycarbonate membrane for 18h at 37°c 5% CO2. At the endpoint, migrated cells were fixed with 4% PFA for 15min at RT. The remaining cells on the top end of the membrane were removed by a cotton swab. Crystal violet was added to each well to stain the migrated cells. The Boyden chambers were washed 3 times in PBS. Photographs were taken using a Nikon Ts2 microscope. Finally, SDS

1% was added to each membrane in order to dissolve the crystal violet which stained the migrated cells and optical density was measured using a CLARIOstar Plus microplate reader.

Invasion assay :

Invasion assay was carried as previously described[24]. Briefly, cells were transfected and seeded at a density of 5000 cells per well in ultra low attachment 96 well plates. 48 hours later, media was removed and replaced with matrigel (Corning Cat#354234). The plate was placed at 37°C in order to allow the matrix to solidify. Fresh media was added on top of the matrix. Spheroids were photographed every 10min in a multi-position Zeiss Videomicroscope.

Luciferase reporter assay :

we performed luciferase reporter assays (Promega) as per the manufacturer's protocol in order to investigate the downstream signaling pathways of CELSR2 : NFAT-luc and NFκB-luc for Gαq, CRE-luc for Gαs and Gαi, SRF-luc for Gα12/13 and SRE-luc for Gβγ. Assays were performed by cotransfecting in HEK293T the luciferase reporter with the receptor or GFP vector as control and incubated 18h at 37°C 5% CO2. The following day cells were lysed with passive lysis buffer, firefly luciferase was added and read on a CLARIOstar Plus microplate reader.

Animal studies :

All animal experiments were performed in agreement with the French Guidelines for animal handling and approved by the local ethic committee (C2EA14) for Animal Experimentation (Agreement no. APAFIS#13349-2018013116278149). NOD/SCID/γc null mice (NSG) were obtained from Dr. C. Rivers (Margate, UK). Mice were housed under sterile conditions with sterilized food and water provided *ad libitum* and maintained on a 12-h light and 12-h dark cycle. MDA-MB-468 (1×10^6 cells/mice) in a 1/2 (v/v) Matrigel (Becton Dickinson Bioscience) suspension were injected into mammary fat pads of 6-10-week-old female NSG mice. Tumor growth was monitored by digital caliper measurements and by calculating volumes (length × width x height × p/6).

Seahorse experiments :

Seahorse Cell Energy Phenotype assay Seahorse XFe24 Analyzer (Agilent) and the Seahorse XF Cell Energy Phenotype Test Kit (Cat# 103325-100, Agilent) were used to perform assays according to the manufacturer's protocol. In brief, a Seahorse cell culture plate was treated with PLO/laminin and 10,000 dissociated GBM cells were plated per well, with five technical replicates per condition accompanied with a blank control well. Cells were incubated overnight at 37C in a CO2 incubator to allow for attachment. Meanwhile, a Seahorse Utility plate/sensor cartridge was hydrated and calibrated using Calibration buffer (Cat# 100840-000, Agilent) in a non-CO2 incubator at 37C overnight. Cell medium was aspirated and replaced with 500 mL Assay medium [Agilent Base Medium (Cat# 102353-100, Agilent), 1 mM pyruvate (Cat# 103578-100, Agilent), 2 mM glutamine (Cat# 103579-100, Agilent), 10 mM glucose (Cat# 103577-100, Agilent)] and was incubated for 1 h in a non-CO2 incubator at 37C. The mitochondrial stressors carbonyl cyanide p-(tri-fluoromethoxy)phenyl-hydrazone (FCCP) and oligomycin were prepared to a final molar concentration of 1.25 mM and 10 mM, respectively, and were added to Port A of the sensor cartridge. The Seahorse cell plate and sensor cartridge were run on a Seahorse XF Cell Energy Phenotype Assay program using Agilent Wave software. Both OCR and ECAR were measured at three baseline timepoints and six timepoints after the addition of the mitochondrial stressors.

LC/MS :

Total proteomes from CELSR2 depleted cells (MDA-MB468 siCELSR2) were compared to control cells (MDA-MB468 siCTRL) by label free quantitative mass spectrometry analysis. 15µg of cell lysates were loaded on NuPAGE™ 4–12% Bis–tris acrylamide gels according to the manufacturer's instructions (Invitrogen, Life Technologies). Running of samples was stopped as soon as proteins stacked as a single band and following imperial blue staining (Life Technologies), the upper part of the gel containing the proteins was cut and processed for classical in gel digestion (washes, thiols reduction with 10 mM DTT and cystein alkylation with 55 mM iodoacetamide). Each band was further digested as previously described with trypsin and analyzed by liquid chromatography (LC)-tandem MS (MS/MS) using an Orbitrap

Fusion Lumos Tribrid Mass Spectrometer (ThermoFisher Scientific, San Jose, CA) online with a nanoRSLC Ultimate 3000 chromatography system (ThermoFisher Scientific, Sunnyvale, CA). First, peptides were concentrated and purified on a pre-column PepMap100 C18, 2cm × 100µm I.D, 100Å pore size, 5µm particle size in solvent A (0.1% formic acid in 2% acetonitrile). In the second step, peptides were separated on a reverse phase LC EASY-Spray C18 column PepMap RSLC C18, 50cm × 75µm I.D, 100Å pore size, 2µm particle size (ThermoFisher) at 300nL/min flow rate and 40°C. After column equilibration using 4% of solvent B (20% water - 80% acetonitrile - 0.1% formic acid), peptides were eluted from the analytical column by a two-step linear gradient (2-20% acetonitrile/H2O; 0.1% formic acid for 90min and 20-45% acetonitrile/H2O; 0.1% formic acid for 20min). For peptide ionization in the EASY-Spray nanosource in front of mass spectrometer, spray voltage was set at 2.2 kV and the capillary temperature at 275 °C. The Orbitrap Lumos was used in data-independent mode with the following parameters. First, MS spectra were acquired in the Orbitrap in the range of m/z 375-1500 at a FWHM resolution of 120,000 measured at 400 m/z. AGC target was set at standard parameters with an automatic Maximum Injection Time. MS2 spectra were acquired in the Orbitrap with a resolution of 30,000, in the mass range of 200-1800 m/z after isolation of parent ion in the quadrupole and fragmentation in the HCD cell under collision Energy of 30%. DIA parent ion range was from 400 to 1000 m/z divided into 40 windows 16 Da wide and from 1000 to 1500 m/z divided into 10 windows 50 Da wide.

Data Processing Protocol :

Relative intensity-based label-free quantification (LFQ) was processed using the DIA-NN 1.8 algorithm. Raw files were searched against the Human database extracted from UniProt on the 10th of January 2023 and containing 20404 entries (reviewed) with the addition of a protein contaminant bank (J Proteome Res 2022;21(9):2104-2113. Protein Contaminants Matter: Building Universal Protein Contaminant Libraries for DDA and DIA Proteomics; Ashley M Frankenfield, Jiawei Ni, Mustafa Ahmed, Ling Hao). The following parameters were used for searches: (i) trypsin allowing cleavage before proline; (ii) one missed cleavages were allowed; (iii) cysteine carbamidomethylation (+57.02146) as a fixed modification and methionine oxidation

(+15.99491) and N-terminal acetylation (+42.0106) as variable modifications; (iv) a maximum of 1 variable modification per peptide allowed; and (v) minimum peptide length was 7 amino acids and a maximum of 30 amino acids. The match between runs option was enabled to transfer identifications across different LC-MS/MS replicates based on their masses and retention time. The precursor false discovery was set to 1%. DIA-NN parameters were set on Single-pass mode for Neural Network classifier, Robust LC High precision for quantification strategy and RT-dependent mode for Cross-run normalization. Library was generated using Smart profiling set up. The main output file from DIA-NN was further filtered at 1% FDR and LFQ intensity was calculated using our DIAgui package at 1% *q*-value (https://github.com/marseille-proteomique/DIAgui [Gerault et al., 2024]).

The statistical analysis was done with Perseus program (version 1.6.15.0) from the MaxQuant environment (www.maxquant.org), Tyanova & Cox, 2018 . Quantifiable proteins were defined as those detected in above 70% of samples in one condition or more. Missing values were replaced using data imputation by randomly selecting from a normal distribution centered on the lower edge of the intensity values that simulates signals of low abundant proteins using default parameters (a downshift of 1.8 standard deviation and a width of 0.3 of the original distribution). To determine whether a given detected protein was specifically differential, a two-sample t-test was done using permutation-based FDR-controlled at 0.01 and employing 250 permutations. The p value was adjusted using a scaling factor s0 with a value of 1. Analysis was done on biological triplicates, each injected twice on mass spectrometers.

Plasma membrane isolation :

Cell fractionation was performed with the ProteoExtract® kit (Merck Cat#539790) as per the manufacturer protocol. Briefly, adherent cells were seeded until they reached full confluence. Cells were washed with wash buffer twice. Extraction buffer 1 was added with a protease inhibitor cocktail and incubated under shaking for 10 min. The fraction 1, containing the cytosolic proteins was transferred and stored on ice. Extraction buffer 2 was added with protease inhibitors and incubated under shaking for 30 min. The fraction 2 representing the membrane proteins was transferred and

stored on ice. Extraction buffer 3 was added and incubated under shaking for 10 min. The fraction 3 which represents nuclear proteins was transferred and stored on ice. Finally, extraction buffer 4 was added to the cells and the 4th fraction was immediately transferred. The different fractions were analyzed by western blot.

Knockout cells generation :

The gene sequence of CELSR2 was downloaded from NCBI and uploaded to Benchling. 5 gRNAs were designed to target the first exon of the gene. The gRNAs with the best on target score and off target score were selected. gRNA were synthesized by Eurofins Scientific. pSpCas9-2A-GFP plasmid (Addgene Cat#48138) was digested with BbsI and the gRNAs were cloned using the T7 ligase. The resulting constructs were run on an agarose gel and subjected to a Sanger sequencing to check for the proper cloning of the gRNAs. Subsequently, the constructs were transfected in MCF7 cells. After 24h, cells were sorted to 1 GFP positive cell per well. A total of 96 clones were sorted per guide. Finally, all the clones were screened for the expression of CELSR2 by western blot.

Expression and purification of N-terminal fragment of CELSR2 :

Expi293 cells (Thermo Fisher Cat #A14635) were cultured in Expi293 medium at 37°C/8% CO2 under shaking. 30µg of extracellular CELSR2 plasmid was transfected using expifectamine as per manufacturer protocol. Expifectamine enhancers 1 and 2 were added to the transfected cells 18 hours later. The supernatant was collected 5 days later, centrifuged and dialyzed to PBS overnight at 4°C. The dialysis product was applied on HisPur™ Cobalt Resin columns (Thermo Fisher Cat #89965). The bound proteins to the resin were washed twice with cold NaCl 300mM and twice with cold PBS. The column was finally eluted with imidazole 150mM. Concentration of eluted proteins was estimated with a nanodrop spectrophotometer.

Binding affinity measurements on recombinant antigen

CELSR2-HA-His (10µg/mL) was coated overnight at 4°C on Maxisorp Elisa 96 flat bottom microplates. The plate was saturated with 5% milk for 1 hour at RT then washed 3 times. Serial dilutions of nanobodies were added for 2 hours at RT. Nanobodies bound to the recombinant CELSR2 were detected using anti c-myc antibody followed by an HRP-conjugated goat anti mouse. The detection of peroxidase was carried using TMB substrate; the reaction was stopped with the stop solution and subsequently OD450 was measured on the CLARIOstar Plus microplate reader.

Binding affinity measurements on cells

Cell lines were detached, counted and saturated using BSA 2% for 1 hour at 4°C to avoid non specific binding of the nanobodies. Cells were then incubated for 1 hour at 4°C with serial dilutions of the nanobodies. Subsequently cells were stained with mouse anti-His tag antibody (Novagen, 70796-4), cells were washed 3 times and revealed with secondary alexa 647 anti mouse antibody (Thermo Fisher A-21235), after 3 washes cells were analyzed with LSRFortessa.

Resources table :

Reagent and resources	Source	Reference
Antibodies		
CELSR2 (D2M9H) XP	Cell signaling	47061
AKT	Cell signaling	4691
Phospho-AKT(Ser473)	Cell signaling	9271s
ERK 1/2	Cell signaling	9102L
Phospho-ERK	Cell signaling	4370
MEK1/2	Cell signaling	8727S
Phospho-Mek 1/2(ser217/221)	Cell signaling	9154
CREB	Cell signaling	9197
Phospho-CREB (Ser133) (87G3)	Cell signaling	9198
GSK3	Cell signaling	12456
Phospho-GSK3	Cell signaling	5558
SAPK/JNK	Cell signaling	9252
Phospho-SAPK/JNK	Cell signaling	4668
Tubulin	SIGMA-ALDRICH	T9026-.2ML
Ki-67	Agilent	GA626
His-Tag	MERCK	70796-4
GFP	Thermo Fischer	A11122
Goat anti-Mouse Secondary Antibody HRP	Thermo Fischer	31430
Goat anti-Mouse Secondary Antibody, Alexa Fluor™ 647	Thermo Fischer	21235
siRNA		
siRNA ID	siRNA sequences	
siCELSR2#1	CGACAACAAUCCAACCUUU	Horizon Discovery
siCELSR2#2	GGGAGGAAGUUGAUUUCU A	Horizon Discovery
shRNA		
shRNA ID	shRNA target sequence	
shCELSR2#1	TAGGATTCCACCTCTTCCC	Horizon Discovery
shCELSR2#2	TTTACATTCCTTTTCCGAC	Horizon Discovery
Bacterial strains		
5-alpha Competent E. coli	New England Biolabs	C2987H
TG1 Electrocompetent Cells	Lucigen	60502-2
BI21 chemically competent	Thermofischer	C606003
Cell culture media and reagents		
DMEM High glucose	Thermofischer	21068028
100ML	Thermofischer	15140122
TRYPSIN 0.25% EDTA 100ML	Thermofischer	25200056
500ML	Thermofischer	14190094
SODIUM PYRUVATE MEM 100MM(CE) 100ML	Thermofischer	11360039
MATRIGEL EHS 5ml	Dutscher	356230
NON ESS AMINO ACIDS (100X) 100ML	Thermofischer	11140035
Lipofectamine LTX	Thermofischer	15338100

Mitomycin C	Thermofischer	226940020

Commercial kits		
Seahorse XF Cell Energy Phenotype Tes	Agilent	103325–100
Silver stain kit	Thermofischer	24612
BCA Protein Assay Kit	Thermofischer	#23225
Softwares		
GraphPad Prism 8	GraphPad	
ImageJ v1.42	NIH	
Gephi 0.10.1	NetBeans	

Results :

CELSR2 expression in healthy tissues and breast tumors and correlation with patient prognosis

An extended view of the genetic expression from 115 tumors shows that CELSR2 is ubiquitously expressed in the different breast tumor subtypes. A high expression in the luminal A tumors, and an intermediate expression in the other subtypes, TNBC and HER2 enriched was reported (Figure 1A). Consistent with these results, gene expression data from the cancer genome atlas (TCGA) shows an upregulation of the expression of CELSR2 in the luminal group when compared with the normal tissue, while the expression is intermediate in the basal and HER2 positive groups (Figure 1B, left panel). Similarly, CELSR2 protein level in the different breast tumor subtypes was found to be correlated with the mRNA levels in the Clinical Proteomic Tumor Analysis Consortium (CPTAC) database (Figure 1B, right panel). Taken together, CELSR2 appears to be considerably overexpressed mainly in luminal tumors. The Kaplan Meier analysis revealed that the expression of CELSR2 was correlated with a significantly decreased overall survival of all TNBC patients. Considering the TNBC subtypes, we found a significantly decreased overall survival of basal like 2 patients, while there are tendencies for the basal like 1 and mesenchymal subtypes. Equally importantly, the overexpression of CELSR2 is associated with a significantly improved survival in the luminal androgen receptor subtype (Figure 1C). Furthermore, the overexpression of CELSR2 was found to be correlated with a shorter metastasis free survival in TNBC patients (5 year MFS, 71% for low expression versus 58 for high expression; p = 6.74E-03) (Figure 1D). We analyzed in parallel the paralogs of CELSR2, CELSR1 and CELSR3, both showed no prognostic value in TNBC patients (Supplementary figure 1A). Next we intended to investigate the expression of CELSR2 across the primary tumor and metastatic sites. . We analyzed the gene expression in the study presented by Garcia-Recio et al[25] . When gene expression in metastatic tissue was paired with the primary site, it revealed an upregulation of CELSR2 in the metastatic sites of TNBC. We did not observe the same upregulation pattern in the other breast tumor subtypes (Figure 1E). We performed once again the same analysis for CELSR1 and CELSR3, both showed no change in expression in the metastatic site compared with the primary site, suggesting distinct roles for the paralogs in TNBC development (Figure S1B and S1C). To further investigate the expression of CELSR2

in TNBC, we performed a single cell analysis of basal tumors which showed that the expression is predominantly found in malignant cells, while the expression in the tumor microenvironment cells such as fibroblasts, endothelial cells and immune cells is modest (Figure 1F-G). Furthermore, we performed a single cell analysis of healthy tissues which revealed an overall low expression of CELSR2 in the different organs and tissues, besides the nervous system which has a high expression in oligodendrocytes (Figure 1H-I). Altogether, these results indicate that CELSR2 has a prognostic value in TNBC, and could play an important role both in the primary and the metastatic sites. Moreover, the prevailing expression in cancer cells and low expression in healthy tissue could render it a target which would induce limited side effects.

CELSR2 promotes tumor growth in TNBC mouse xenograft

In order to further investigate the functions of CELSR2 in vivo and to confirm what has been previously observed in TNBC patients, we established 2 short hairpin RNA clones (shRNA) targeting the first exon of CELSR2 (Figure 2A). Western blot of whole cell lysates confirmed the downregulation of CELSR2 in the TNBC cell line MDA-MB468 (Figure 2B). To determine the role of CELSR2 in tumorigenesis, we grafted the fourth right mammary fat pad of Nod-SCID gamma mice (n=6 in each group) with shSCR or shCELSR2 MDA-MB468 cells (1.10^6 cells in Matrigel) (Figure 2C). Tumor volume was measured weekly, over a period of 4 weeks. Mice grafted with shSCR MDA-MB468 had a higher tumor volume than the shCELSR2 group (Figure 2D). At the endpoint, tumors of the shSCR group were visually larger (Figure 2E), and the measured weight was higher than shCELSR2 group(Figure 2F). Upon sacrifice, metastasis formation was assessed by bioluminescence at the endpoint of the protocol. Notably, we observed a non-significantly higher tendency of metastasis to the lymph nodes in the shSCR group compared to the shCELSR2 group (Figure S2-A).We found that all lungs were already invaded by tumor cells, despite the orthotopic injection of cells and the relatively short protocol time, revealing the high metastatic potential of MDA-MB468. We then confirmed by immunohistochemistry the knockdown of CELSR2 in the xenograft tumor with a specific antibody directed at the extracellular fragment of the receptor. Interestingly, the staining of the shSCR tumors was also observed in the extracellular matrix, hinting at a possible cleavage

and capture of the extracellular fragment within the matrix (Figure 2G). Upon staining of the tumors by hematoxylin, eosin and safran, we observed distinct tumor morphologies and stromal involvement between the 2 groups (Figure 2H). Additionally, we stained for the proliferation marker Ki-67 by IHC, we observed a higher staining positivity in the shSCR group as compared with shCELSR2 group, confirming the growth defect observed in vivo (Figure 2I). Our findings indicate that CELSR2 plays an important role in driving tumor growth in vivo.

CELSR2 drives proliferation, migration and invasion of TNBC cells

We aimed to characterize the expression levels of CELSR2 by western blot in normal breast and cancer cell lines, ranging from triple negative cell lines (BT20, MDA-MB468, HCC1806, MDA-MB231, SUM149, SUM159, MDA-MB436, HCC38), HER2+ (MDA-MB453), luminal (MCF7, BT474, T47D, MDA-MB157) and normal (MCF10A). The expression level of CELSR2 is heterogeneous across basal tumors, while it is higher in luminal cell lines, consistent with the previous cDNA microarray result. The expression in MCF10A was intermediate (Figure 3A). The TNBC cell lines BT20, MDA-MB468 and HCC1806 showed strong expression of CELSR2, so we therefore decided to use these 3 cell lines to study the involvement of CELSR2 in proliferation, migration and invasion of TNBC cells. We knocked down CELSR2 by RNA interference (siRNA). CELSR2 knockdown was verified by western blot (Figure 3B-D). Migration capacity was assessed by wound healing assays where cells were seeded and followed overtime until wound closure. The migration was significantly slowed in CELSR2 knockdown cells of MDA-MB468, BT20 and HCC1806 (Figure 3E-G). While wound healing assay mimics the collective migration of cells, we intended to further investigate the individual migration in a Boyden chamber assay. Similarly to the wound healing results, migration capacity was impaired in CELSR2 knockdown MDA-MB468 cells (Figure 3H). Moreover, in order to confirm the tumor growth defect observed in vivo, we performed a proliferation assay of MDA-MB468 by knocking down CELSR2 and seeding 20000 cells. 24h later cells were fixed and quantified. Interestingly, knockdown of CELSR2 produced a substantial defect in cell proliferation in vitro (Figure 3I). The effects of CELSR2 knockdown were further observed in invasion assays. We used the BT20 cell line, capable of forming spontaneous 3D spheroids in ultra low attachment plates. Upon embedding the

spheroids in a collagen-methylcellulose matrix, we observed a significant decrease of the invasion capacity of cells (Figure 3J). Overall these results demonstrate that the loss of CELSR2 compromises the tumorigenic processes, most importantly proliferation, migration and invasion of TNBC cells.

CELSR2 induces CREB phosphorylation :

As the downstream signaling cascade of CELSR2 was still poorly investigated in the literature, we aimed to identify the activated pathways by the receptor in tumor cells which could be responsible for the observed phenotypes. We performed immunoblot stainings of various signaling pathways following The downregulation of CELSR2 with two different siRNA. We investigated the pathways commonly activated by GPCRs. We found that silencing CELSR2 does not activate or repress GSK3, MAPK, nor AKT signaling . Interestingly, silencing CELSR2 was found to highly repress CREB phosphorylation (Figure 4A). Our result was subsequently confirmed by immunofluorescence (Figure 4B). Our finding is in line with what has been recently reported by Bui and colleagues regarding CELSR2 coupling to Gαs[237]. Next, we aimed to overexpress CELSR2 with a C-terminal GFP tagged construct and checked for CREB activation. First, we transfected GFP-CELSR2 in order to assess the proper localization at the plasma membrane. We found that ectopic expression of GFP-CELSR2 was mostly at the plasma membrane, and in the cytoplasm to a lesser extent (Figure 4C). We observed CREB activation upon overexpression of CELSR2 (Figure 4D). In order to gain a deeper understanding of the coupling of the receptor to G-proteins, we carried a luciferase reporter system assays in which we used : NFAT-luc and NFκB-luc for Gαq, CRE-luc for Gαs and Gαi, SRF-luc for Gα12/13 and SRE-luc for Gβγ (Figure 4E) . CELSR2 overexpression showed Gαs signaling activity compared with cells transfected with GFP. Interestingly, unlike what has been reported by Bui and colleagues, the overexpression also induced the activation of Gα12/13 and Gβγ, potentially owing these differences to the cancerous context (Figure 4F). Taken together, our results indicate that CELSR2 signals through Gαs to induce the phosphorylation of CREB in TNBC cells. While this signaling pathway appears to be responsible for the

oncogenic potential of CELSR2, it is probably not the only one, as our results indirectly show the recruitment of other G proteins than Gαs.

CELSR2 activates the TCA cycle and oxidative phosphorylation

In order to further investigate the underlying mechanism of CELSR2 in TNBC progression, total proteome analysis was performed following the knockdown of CELSR2 with siRNA in MDA-MB468 cells (Figure 5A). Over 800 proteins were found to be downregulated in the siRNA group. We found CELSR2 among the significantly downregulated proteins (Supplementary table 1), confirming the knockdown of the receptor (Figure 5B). WikiPathway analysis was used to identify the pathway associated with the differentially expressed proteins. Interestingly, amino acid metabolism, Krebs cycle and oxidative phosphorylation were the most enriched pathways (Figure 5C). Among the most downregulated proteins, we identified COX5B, SDHA, NDUFV2, NDUFS1, ATP5F1A, COX17, ATP5ME and ATP5F1D proteins which are key components of the mitochondrial respiratory chain (Figure 5D). Interestingly, a number of the downregulated proteins implicated in OXPHOS found in our mass spectrometry results are expression products of CREB target genes such as OGDH, NUBPL, NDUFV3, ARG2, ATP5D among others (Supplementary table 1). This finding was notable because it has been reported that TNBC tumors which have an increased reliance on OXPHOS metabolism exhibit aggressive tumors associated with the worse prognosis. Moreover, metabolic switch to OXPHOS has been shown to reduce sensitivity to chemotherapies[26–28]. TThis led us to hypothesize that CELSR2 enables tumor cell aggressiveness through the promotion of mitochondrial metabolism in TNBC. We thus first revisited the patient data from the AURORA cohort[25]. This led us to hypothesize that CELSR2 enables tumor cell aggressiveness through the promotion of mitochondrial metabolism in TNBC. We thus first revisited the patient data from the AURORA cohort. We performed a differential expression analysis between patients who exhibit a high and low CELSR2 expression. Strikingly, we found aerobic respiration and OXPHOS and other pathways related to mitochondrial functions among the top pathways enriched in patients with a high CELSR2 expression, further supporting the hypothesis that CELSR2 drives tumor progression by bolstering mitochondrial metabolism (Figure 5E). We then analyzed the active mitochondria with mitotracker probes in TNBC

cells upon CELSR2 silencing with siRNA. We found a decreased overall active mitochondria staining following CELSR2 knockdown (Figure 5F). In order to gain an overview on the metabolic regulation by CELSR2, we measured mitochondrial respiration using the Seahorse XFe24 Analyzer (Figure 5G). The assay allows the measurement of the oxygen consumption rate (OCR) upon the addition of the mitochondrial stressors oligomycin and FCCP. Following CELSR2 knockdown, both basal and maximal respiration were significantly reduced (Figure 5H). These findings unveil a novel unsuspected role of CELSR2 in promoting OXPHOS, potentially through the activation of CREB, contributing to TNBC progression.

CELSR2-targeting nanobodies significantly inhibit cell migration

As we have shown that CELSR2 is mostly expressed by malignant cells in the tumor microenvironment and its silencing impairs tumor progression, we tested whether CELSR2 could be targeted therapeutically. To this end, we aimed to discover nanobodies specific to the CELSR2 extracellular fragment with a lama immunization strategy (Figure 6A). We chose to immunize the llama with MCF7, which exhibits a high expression of CELSR2, as previously reported (Figure 2A). We isolated plasma membranes with ProteoExtract® as per the manufacturer protocol. We injected into the llama the highly enriched CELSR2 membranes fraction (Figure 6A-B). In order to select nanobodies specific to the extracellular fragment of CELSR2, we generated MCF7 knockout cells with CRISPR-Cas9 sgRNAs (Figure 6C) and produced the extracellular fragment of CELSR2 in Expi293 (Figure 6D). A first round of selection consisted in depleting positive nanobodies on CELSR2 knockout cells. The output was subsequently screened on wild type cells by FACS. After a second round of selection on immobilized recombinant extracellular CELSR2 by a direct ELISA (Figure 6A), we identified the two nanobodies D7 and G6 (Figure 6E). The two nanobodies were screened by FACS on different cell lines with varying expression levels of CELSR2 and its two paralogs, CELSR1 and CELSR3 . The two nanobodies were found to recognize cells in accordance with CELSR2 levels and not according to the expression levels of its paralogs, CELSR1 and CELSR3 (Supplementary figure 3A-B). Elisa on recombinant protein of CELSR2 showed different binding

affinities for the nanobodies D7 and G6 with Ec50 of 490 and 320nM respectively (Figure 6F). The affinity of the two nanobodies were then tested on cell lines by flow cytometry : MCF7, MDA-MB468 and MDA-MB231 cell lines and MCF7-CELSR2 knockout cells (Figure 6G-H). The binding of the two nanobodies was efficient on all cell lines except CELSR2-knockout cells. The binding was in the micromolar range (Table 1). Finally, we aimed to investigate a potential role of the nanobodies in altering cell motility as observed with the knockdown strategies. We treated migrating MDA-MB468 with the two nanobodies specific to CELSR2 and a control nanobody which is found to be negative in flow cytometry at a concentration of 1µM. Our results show that the D7 and G6 are effectively impairing cell migration in wound healing assay (Figure 6 I-J). These findings represent a promising proof of concept towards assessing the potential of utilizing nanobodies targeting and modulating CELSR2 activity for therapeutic intervention in TNBC.

Discussion :

Triple negative breast cancer continues to pose a major public health challenge due to a considerable heterogeneity, resistance to chemotherapeutic regimens and lack of targeted therapies[9,10,29]. Identifying new druggable targets is necessary to ameliorate TNBC care. aGPCRs are a group of 33 transmembrane receptors that have been recently described for their involvement in tumor biology[30–35]. We identified in the present study CELSR2, a receptor at the crossroad between the aGPCR family and the Wnt/PCP pathway as a potential targeted therapy for the treatment of TNBC patients[18,20,36]. We show that CELSR2 overexpression is correlated with a significantly decreased overall survival of specific subtypes of TNBC patients. We confirm its implication in TNBC progression both in vitro and in vivo and provide insights on the mechanism of action probably involved, which until now was elusive. Indeed, we propose a model where CELSR2 expression is associated with the activation of the cAMP/PKA/CREB signaling pathway, promoting the expression of oxidative phosphorylation related genes in TNBC cells thus promoting tumor progression.

A previous study conducted in a cancer context found that CELSR2 is significantly overexpressed in hepatocellular carcinoma patient tumors, while the expression in

adjacent healthy tissue was close to none. Furthermore, patients with a CELSR2 overexpression were found to have a significant decrease in the overall survival[22]. Along the same lines, in the present study, we demonstrate that CELSR2 expression is predominant in malignant cells in TNBC patients and that the expression is low or absent in most healthy tissues, except in the nervous system.

Interestingly, when considering the different subtypes of TNBC based on the Lehman's classification[3], we found a significant decrease of the overall survival in basal like 2 patients, while there was a tendency for mesenchymal and basal like 1 patients. Surprisingly overexpression of CELSR2 was associated with an increased overall survival of luminal androgen receptor patients. In light of these findings, CELSR2 appeared to have diverging effects on different subtypes of TNBC. Moreover, we report an increased expression of CELSR2 in the metastatic site. The gain of expression in the metastatic site opens substantial opportunities for the onset of a therapeutic strategy for metastatic patients whose subtype appears to be significantly affected by CELSR2 expression. Notably, the reported prognostic value in TNBC of CELSR2 was not observed with the receptor's paralog : CELSR1 and CELSR3. Moreover, the gain of expression of CELSR2 in the metastatic site was also unique, suggesting a non redundant role of the 3 receptors.

CELSR2 has been reported to alter Schwann cells proliferation and migration following receptor silencing[37]. Accordingly, in the preclinical and in vitro TNBC models we used in our study, we unveiled a significant cell proliferation, motility and invasion defects in vitro (Figure 3) and a delayed tumor growth in vivo (Figure 2E) following CELSR2 silencing. Our xenograft model did not allow us to accurately capture the differential in metastasis formation. The xenograft of a less metastatic TNBC cell line could be used in order to assess the implications of CELSR2 in invading distant organs. Indeed, such a model would be beneficial to assess whether the modulation of CELSR2 would have an impact on metastasis formation in addition to altering tumor growth.

Most of the previous reports investigating CELSR2 were restricted to functional studies in neurological models, leaving an important gap in understanding the mechanism of the receptor and the associated signaling pathways[38–43]. Recently, CELSR2 has been

shown to couple to Gαs in BRET assays[21]. We report in our study that CELSR2 induces the phosphorylation of CREB at the residues Ser133. Unsurprisingly, by utilizing luciferase reporter systems, we find that CELSR2 in addition to activating CRE, a Gαs coupling readout, activates SRE and SRF in TNBC cells (Figure 4F). Indeed, it is well established that ligands secreted by the tumors can induce a functional selectivity of a GPCR depending on the context and immediate needs of the cells[44].

Tumor cell metabolism has been well established as one of the cancer hallmarks[45,46]. Tumor cells rely on nutrients collected from their environment to produce the needed energy for their growth and survival. Multiple drugs targeting tumor cell metabolism have been investigated in various cancers[47–50]. Unlike many malignancies which rely on glycolytic metabolism known as the Warburg effect, TNBC has been shown to induce a metabolic switch to OXPHOS. This metabolic switch has been reported to elicit an aggressive phenotype and a resistance to chemotherapeutic regimens[26,27,51–53]. Nevertheless, the mechanisms governing this TNBC metabolic switch remain elusive. OXPHOS is a more efficient energy production pathway than glycolysis. Moreover, it has been previously reported that CREB activation potentiates OXPHOS in various cell types such as fibroblasts and neuronal cells[54,55].

Our data suggest that CELSR2 and its signaling through the cAMP/PKA/CREB pathway contribute to sustaining an OXPHOS metabolism in TNBC cells. Indeed, silencing CELSR2 resulted in a profound downregulation of proteins of the TCA cycle and OXPHOS (Figure 5C-D), including the expression products of CREB target genes, and reduced baseline and maximal respiration using Seahorse analyzer. OXPHOS has been reported to facilitate cell proliferation and motility. Indeed, cell treatment with drugs sustaining mitochondrial metabolism induces an increase of cell motility[56]. Moreover, the induction of OXPHOS has been shown to induce the proliferation of colorectal cells[57]. Our data suggest that CELSR2 activation and its signaling through the cAMP/PKA/CREB pathway contributed to sustaining an OXPHOS metabolism in TNBC cells. Indeed, silencing CELSR2 results in a profound downregulation of proteins of the TCA cycle and OXPHOS (Figure 5C-D), including the expression products of CREB target genes, and reduced baseline and maximal respiration using Seahorse analyzer. Further studies could investigate the metabolome of the cells in

order to assess whether the decrease of OXPHOS in TNBC cells silenced for CELSR2 results in an increase of glycolytic metabolites as a compensatory mechanism.

Targeting the receptor could have the dual effect of impairing crucial tumorigenic processes and sensitizing tumor cells to chemotherapeutic regimens[26,53]. Moreover, the identification of a CELSR2 agonist, antagonist ligand or allosteric modulator could be highly valuable in further investigating processes mediated by the receptor. Many tools could be developed to study receptor-mediated cellular processes such as antibodies, aptamers and nanobodies.

Nanobodies have been a particularly attractive therapeutic platform for cancer care in recent years[58]. As single immunoglobulin variable domain antibodies, they can target conformational epitopes inaccessible to conventional antibodies due to their large size. Moreover, nanobodies have relatively low developmental costs and an easy humanization process[59]. By the means of llama immunization, we discovered two specific nanobodies directed at the extracellular fragment of CELSR2 (Figure 6E). We find they are capable of recognizing both the recombinant protein and the endogenously expressed receptor (Figure 6F-H). We further wondered whether the nanobodies had any effect on cellular processes. We note they are both capable of significantly inhibiting cell motility in wound healing assays (Figure 6I-J). More assays should be conducted in order to assess the effect of the nanobodies on other cellular processes such as proliferation and adhesion, as well CREB activation and the transcription of the genes related to OXPHOS.

Our data are a proof of concept of the potency of CELSR2 in tumorigenesis and its targetable nature by virtue of its large extracellular domain. An important next step in assessing CELSR2 as a potent target in TNBC treatment would be the treatment of orthotopically grafted tumors with the nanobodies. Another therapeutic platform that could be investigated is the linking of the nanobodies with highly cytotoxic drugs to make a nanobody drug conjugate[60]. The treatment protocol would require considerable optimization given the short half life of the nanobodies in vivo. Some of the strategies to increase the half life are the coupling of the nanobody to a Fc-fragment or the design of a biparatopic construction. The side effects of a targeted

therapy against CELSR2 should in theory be uptaken by the tumor and elicit limited adverse events, given the overall low expression of the receptor in healthy tissues (Figure 1H-I)

Overall, this study expands our current understanding of CELSR2 molecular mechanisms in a cancerous context and opens new venues of future investigation into CELSR2 biological function and modulation of its activity in TNBC.

Study limitations :

Our study highlights the general mechanism of action of CELSR2 in TNBC models but does not recapitulate the full signaling cascade. Moreover, future investigations are required to extrapolate the in vitro findings regarding cell energy metabolism to the in vivo models used. A number of technologies such as MetFlow and SCENITH have recently emerged which can be used for investigating energy metabolism of tumor ex vivo[61,62].

Acknowledgements :

We thank Dr. Ines Liebscher for her contribution to critical discussions about the project. We thank Remi Bonjean for his assistance and advice on the nanobody discovery. We wish to thank Evelyn Thi Tien for her assistance in the seahorse experiments setup. We would like to thank the core facilities of the laboratory : ICEP, Imaging and flow cytometry. We thank Dr. Nassim Salem for his critical inputs on the manuscript. We thank the Adher'n Rise COST action for its funding of participation in training schools and scientific meetings. We wish to thank the Institut Cancer Immunologie for their funding of the PhD fellowship of NIYS.

Author contribution :

Conception or design of the work: NIYS, AW, RC, JPB

Experimental execution : NIYS, EJ, JL, SA

Data collection: NIYS, EJ, JV

Data analysis and interpretation: NIYS, EJ, RC, SA

Funding acquisition : JPB

Drafting the article: NIYS, AW

Critical revision of the article: AW

Declaration of Interest

The authors declare that they have no further financial or other conflicts of interest in relation to this research and its publication.

Funding sources :

This work was funded by Ligue Nationale Contre le Cancer (Label Ligue), Institut Universitaire de France awarded to JPB and Institut Cancer Immunologie awarded to NIYS.

Figures :

Figure 1 : CELSR2 expression in healthy tissues and breast tumors and correlation with patient prognosis. (A) heatmap of gene expression in breast tumors. Tumors subtypes are colored as : green = normal like, orange = luminal subtype C, pink = ERBB2 amplified, light blue = luminal subtype B, red = basal like, dark blue = luminal subtype A (Adapted from Sorlie et al[63]). (B) Left panel = CELSR2 mRNA levels evaluated in different breast cancer subtypes and normal tissue. Right panel = CELSR2 protein level in different breast cancer subtypes retrieved from the CPTAC database. (C) Impact of CELSR2 expression on the overall survival of all TNBC patients and the different subtypes of TNBC. (D) Impact of CELSR2 expression on metastasis free survival of all breast cancer patients (left) and TNBC patients only (right). (E) CELSR2 expression change between paired primary tumors and metastasis. (F) Left = UMAP of single cell RNA-seq data of TNBC. Single cells are color coded based on the cell subtype. Right = UMAP of CELSR2 expression in TNBC. Single cells are colored based on their level of CELSR2 expression. (G) Bubble

heatmap of CELSR2 expression in different cell subtypes in TNBC. Bubble size reflects percentage of positive cells. Bubble color reflects transcript average per cell. (H) Left = UMPA of single cell RNA-seq data of healthy tissues. Single cells are color coded based on the tissue of origin. (I) Bubble heatmap of CELSR2 expression in different healthy tissues. Bubble size reflects percentage of positive cells. Bubble color reflects transcript average per cell.

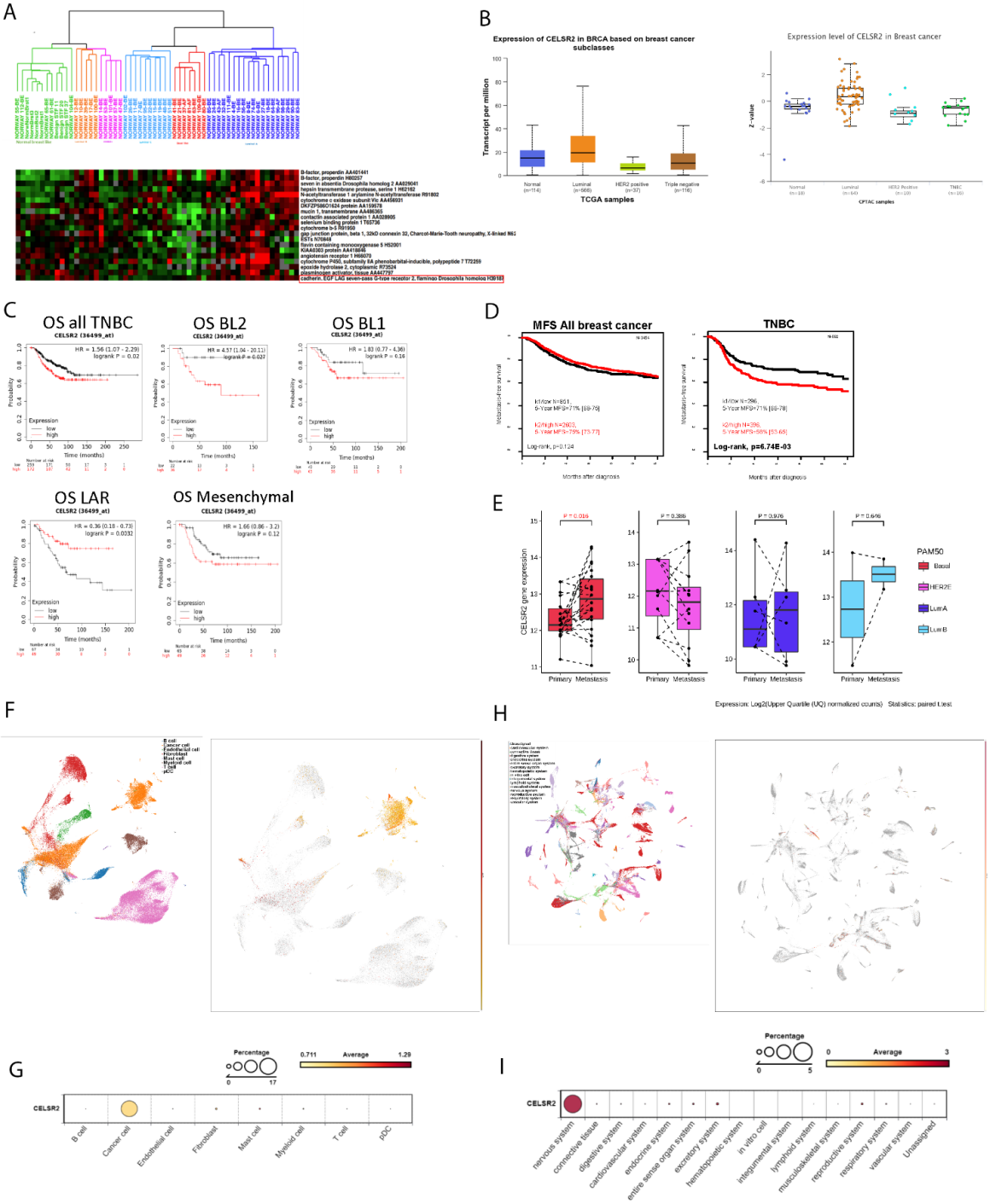
A
B
Expression of CELSR2 in BRCA based on breast cancer subclasses
Transcript per million
Normal (n=114)
Luminal (n=668)
HER2 positive (n=37)
Triple negative (n=116)
TCGA samples
Expression level of CELSR2 in Breast cancer
Z-value
Normal (n=18)
Luminal (n=64)
HER2 Positive (n=10)
TNBC (n=16)
CPTAC samples
C
OS all TNBC
OS BL2
OS BL1
OS LAR
OS Mesenchymal
CELSR2 (36499_at)
Probability
Expression
low
high
Time (months)
D
MFS All breast cancer
TNBC
Metastasis-free survival
Months after diagnosis
Log-rank, p=6.74E-03
E
CELSR2 gene expression
Primary
Metastasis
PAM50
Basal
HER2E
LumA
LumB
F
H
G
I
Percentage
Average
CELSR2
B cell
Cancer cell
Endothelial cell
Fibroblast
Mast cell
Myeloid cell
T cell
pDC
nervous system
connective tissue
digestive system
cardiovascular system
endocrine system
entire sense organ system
excretory system
hematopoietic system
in vitro cell
integumental system
lymphoid system
musculoskeletal system
reproductive system
respiratory system
vascular system
Unassigned

Figure 2 : CELSR2 promotes tumor growth in TNBC mouse xenograft. (A) Schematic representation of the shRNA constructs used to knock down CELSR2. (B) Western blot of CELSR2 following receptor silencing in MDA-MB468. (C) Schematic representation of the orthotopic xenograft of MDA-MB468 and the endpoint assessments of the primary tumor and metastasis formation. (D) Measurements of tumor volume in mm3 at the indicated time points. (E) Representative images of the tumors excised from mice at the endpoint. (F) Measure of tumor weight at the endpoint. (G) Immunohistochemistry staining of CELSR2 in shSCR and shCELSR2 tumors. (H) Hematoxylin eosin safran staining of shSCR and shCELSR2 tumors. (I) Immunohistochemistry of Ki67 in shSCR and shCELSR2 tumors.

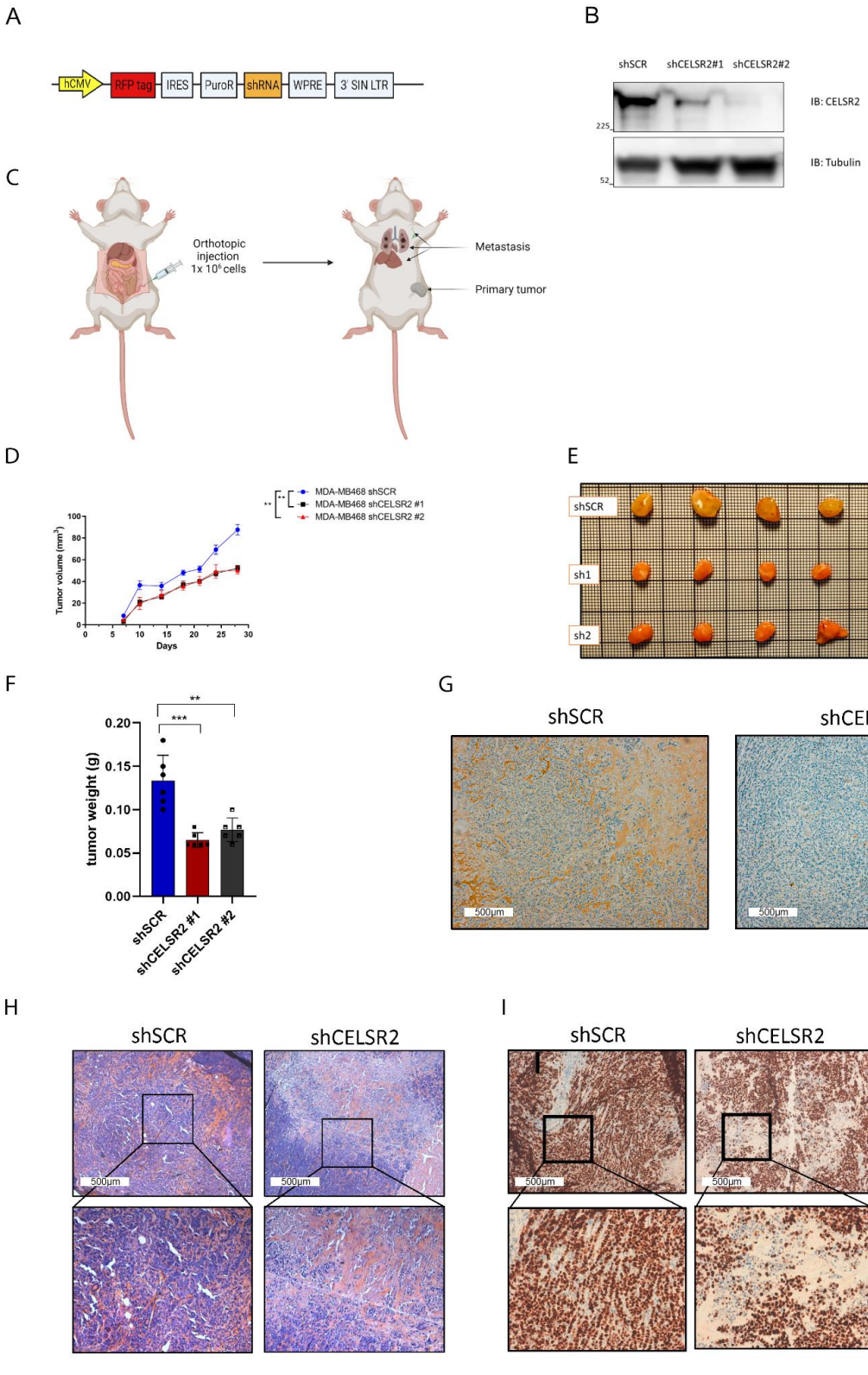
A
hCMV
RFP tag
IRES
PuroR
shRNA
WPRE
3' SIN LTR
B
shSCR
shCELSR2#1
shCELSR2#2
225
52
IB: CELSR2
IB: Tubulin
C
Orthotopic injection
1x 10^6 cells
Metastasis
Primary tumor
D
MDA-MB468 shSCR
MDA-MB468 shCELSR2 #1
MDA-MB468 shCELSR2 #2
Tumor volume (mm^3)
Days
E
shSCR
sh1
sh2
F
tumor weight (g)
shSCR
shCELSR2 #1
shCELSR2 #2
G
shSCR
shCELSR2
500µm
H
shSCR
shCELSR2
500µm
I
shSCR
shCELSR2
500µm

Figure 3 : CELSR2 promotes proliferation, migration and invasion of TNBC cells. (A) Expression of CELSR2 in a panel of breast cancer cell lines and a normal-like mammary epithelial cell line. In red = TNBC cell lines, in pink = ERBB2 amplified cell line, in dark blue = luminal A cell lines, in light blue = luminal B cell line, in black = normal like mammary epithelial cell line. (B-D) Western blot of CELSR2 following receptor silencing in MDA-MB468, BT20 and HCC1806 with siRNA. (E-G) Upper panel = Wound closure rate of TNBC cell lines MDA-MB468, BT20 and HCC1806 following CELSR2 knockdown. Lower panel = representative images of the wound healing assay quantified in the upper panel. t0 = time point 0, te = endpoint (H) Left panel = quantification of migrated MDA-MB468 cells through the microporous membrane following CELSR2 knockdown. Right panel = representative images of migrated cells quantified in the left panel. (I) Left panel =quantification of proliferated cells following CELSR2 knockdown. Right panel = representative images of proliferated cells stained with crystal violet quantified in the left panel. (J) Left panel =spheroid invasion rate of the matrix following CELSR2 knockdown. Right panel = representative images of spheroid invasion following CELSR2 knockdown quantified in the left panel.

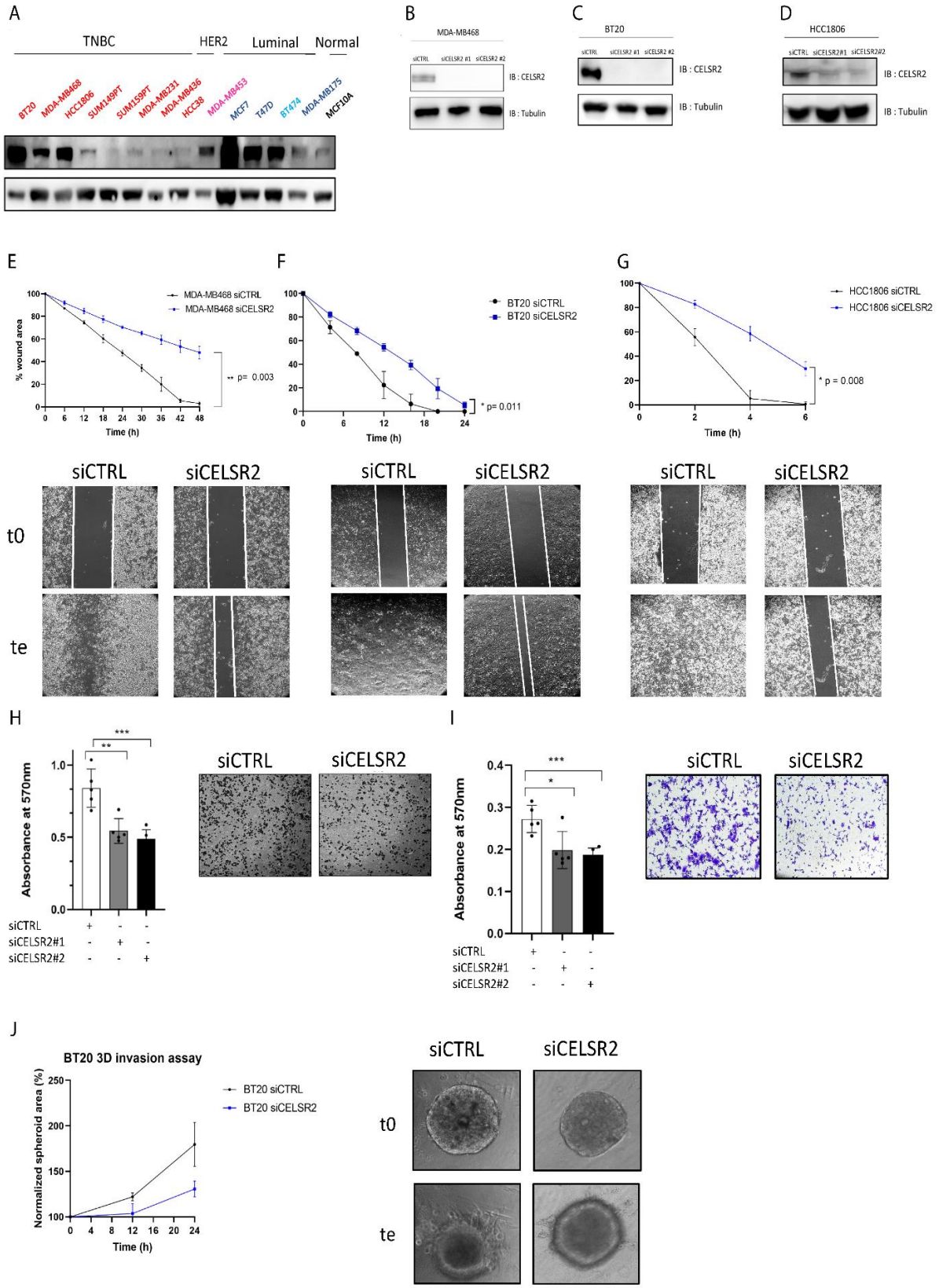
A
TNBC
HER2
Luminal
Normal
BT20
MDA-MB468
HCC1806
SUM149PT
SUM159PT
MDA-MB231
MDA-MB436
HCC38
MDA-MB453
MCF7
T47D
BT474
MDA-MB175
MCF10A
B
MDA-MB468
siCTRL
siCELSR2 #1
siCELSR2 #2
IB : CELSR2
IB : Tubulin
C
BT20
siCTRL
siCELSR2 #1
siCELSR2 #2
IB : CELSR2
IB : Tubulin
D
HCC1806
siCTRL
siCELSR2#1
siCELSR2#2
IB : CELSR2
IB : Tubulin
E
MDA-MB468 siCTRL
MDA-MB468 siCELSR2
% wound area
** p= 0.003
Time (h)
F
BT20 siCTRL
BT20 siCELSR2
* p= 0.011
Time (h)
G
HCC1806 siCTRL
HCC1806 siCELSR2
* p = 0.008
Time (h)
siCTRL
siCELSR2
t0
te
H
Absorbance at 570nm
siCTRL
siCELSR2#1
siCELSR2#2
I
Absorbance at 570nm
siCTRL
siCELSR2#1
siCELSR2#2
J
BT20 3D invasion assay
Normalized spheroid area (%)
BT20 siCTRL
BT20 siCELSR2
Time (h)
siCTRL
siCELSR2
t0
te

Figure 4 : CELSR2 promotes CREB phosphorylation. (A) Western blot of CREB, p-CREB, AKT, p-AKT, ERK1/2, p-ERK1/2, MEK, p-MEK, Jnk, p-Jnk, GSK3 and p-GSK3 following CELSR2 knockdown. (B) p-CREB immunostaining following CELSR2 knockdown. (C) GFP-CELSR2 staining at the plasma membrane. (D) western blot of p-CREB following CELSR2 overexpression. (E) SRF, CRE, SRE and NFAT luciferase gene reporter assays illustrating the activated pathways downstream of G-proteins signaling. (F) CRE, NFAT, SRE, SRF and NfKB luciferase reporter activity of cells transfected with GFP-CELSR2. Data normalized to the mean value of cells transfected with GFP and are presented as mean ± SEM (n=3)

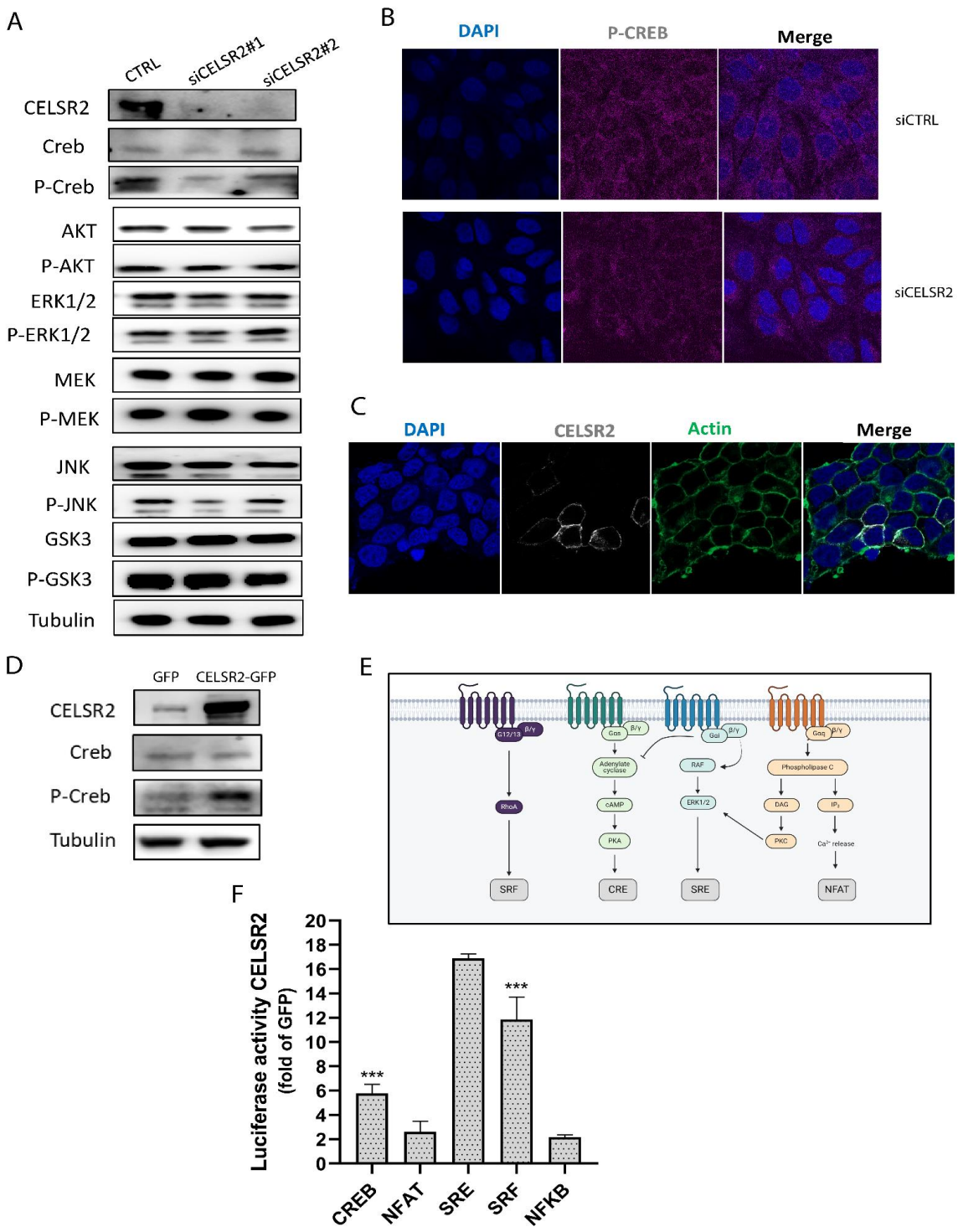
A
CTRL
siCELSR2#1
siCELSR2#2
CELSR2
Creb
P-Creb
AKT
P-AKT
ERK1/2
P-ERK1/2
MEK
P-MEK
JNK
P-JNK
GSK3
P-GSK3
Tubulin
B
DAPI
P-CREB
Merge
siCTRL
siCELSR2
C
DAPI
CELSR2
Actin
Merge
D
GFP
CELSR2-GFP
CELSR2
Creb
P-Creb
Tubulin
E
Adenylate cyclase
cAMP
PKA
RhoA
RAF
ERK1/2
Phospholipase C
DAG
PKC
SRF
CRE
SRE
NFAT
F
Luciferase activity CELSR2 (fold of GFP)
20
18
16
14
12
10
8
6
4
2
0
***
***
CREB
NFAT
SRE
SRF
NFKB

Figure 5 : CELSR2 activates the TCA cycle and oxidative phosphorylation. (A) Western blot of CELSR2 in MDA-MB468 following receptor knockdown. Each condition had 3 replicates. (B) Volcano plot of total proteome change following CELSR2 knockdown. In blue = significantly downregulated proteins, in red = significantly upregulated proteins. (C) Top 10 enriched pathways following CELSR2 knockdown using WikiPathway enrichment analysis. (D) Bubble heatmap of downregulated OXPHOS proteins following CELSR2 knockdown. (E) Heatmap of gene ontology analysis of CELSR2 high TNBC patient tumor transcripts, log-p value is indicated in blue color gradient and gene count in black color gradient. (F) Mitotracker staining following CELSR2 knockdown. (G) Real time cell oxygen consumption rate (OCR) measurements following CELSR2 knockdown. (H) Baselineand maximal respiration quantification.

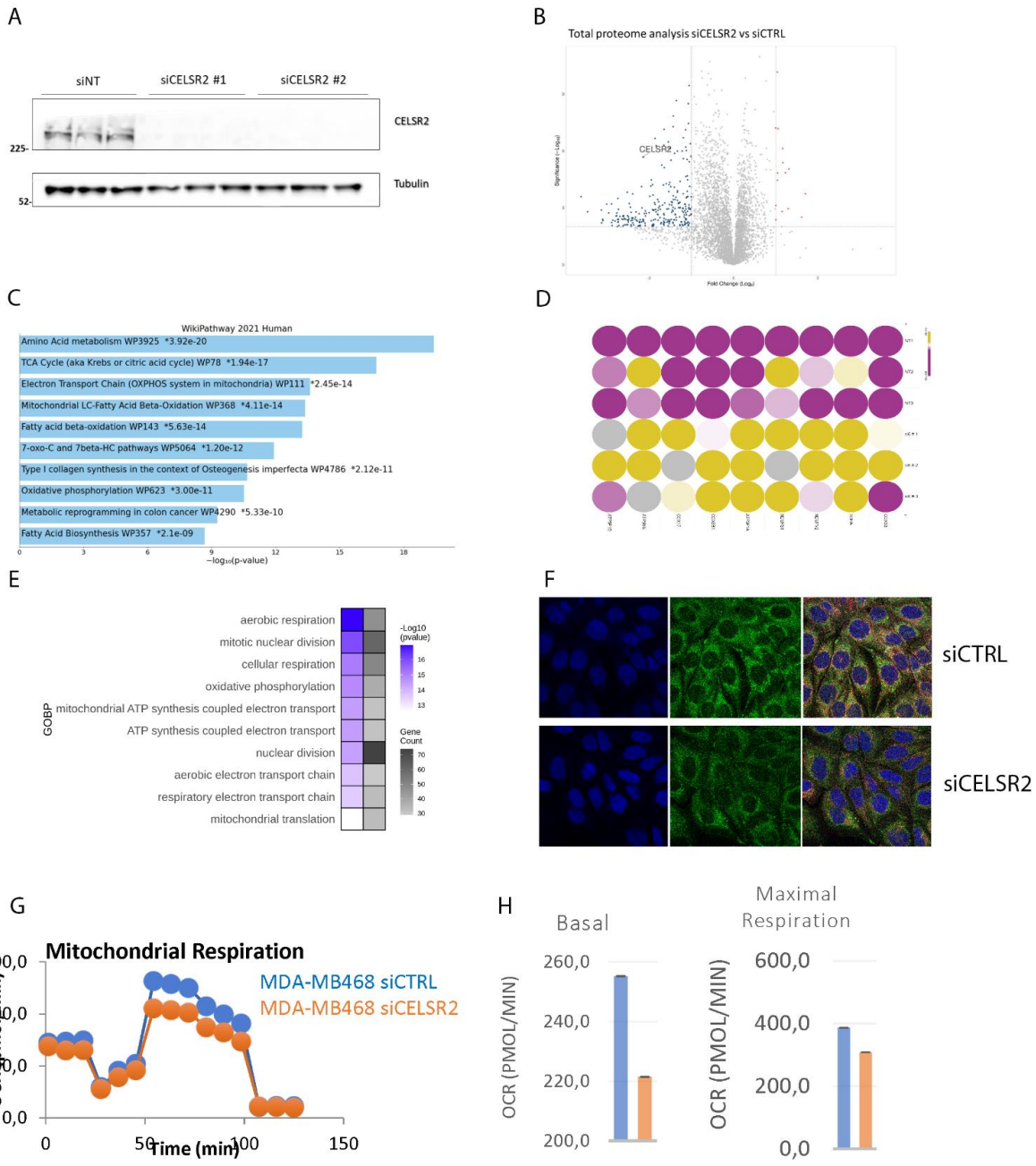
A
siNT
siCELSR2 #1
siCELSR2 #2
CELSR2
225-
Tubulin
52-
B
Total proteome analysis siCELSR2 vs siCTRL
CELSR2
C
WikiPathway 2021 Human
Amino Acid metabolism WP3925 *3.92e-20
TCA Cycle (aka Krebs or citric acid cycle) WP78 *1.94e-17
Electron Transport Chain (OXPHOS system in mitochondria) WP111 *2.45e-14
Mitochondrial LC-Fatty Acid Beta-Oxidation WP368 *4.11e-14
Fatty acid beta-oxidation WP143 *5.63e-14
7-oxo-C and 7beta-HC pathways WP5064 *1.20e-12
Type I collagen synthesis in the context of Osteogenesis imperfecta WP4786 *2.12e-11
Oxidative phosphorylation WP623 *3.00e-11
Metabolic reprogramming in colon cancer WP4290 *5.33e-10
Fatty Acid Biosynthesis WP357 *2.1e-09
0
3
6
9
12
15
18
−log₁₀(p-value)
D
E
GOBP
aerobic respiration
mitotic nuclear division
cellular respiration
oxidative phosphorylation
mitochondrial ATP synthesis coupled electron transport
ATP synthesis coupled electron transport
nuclear division
aerobic electron transport chain
respiratory electron transport chain
mitochondrial translation
-Log10 (pvalue)
16
15
14
13
Gene Count
70
60
50
40
30
F
siCTRL
siCELSR2
G
Mitochondrial Respiration
MDA-MB468 siCTRL
MDA-MB468 siCELSR2
600,0
400,0
200,0
0,0
OCR (pmol/min)
0
50
100
150
Time (min)
H
Basal
Maximal Respiration
OCR (PMOL/MIN)
260,0
240,0
220,0
200,0
600,0
400,0
200,0
0,0

Figure 6 : CELSR2-targeting nanobodies significantly inhibit cell migration. (A) schematic representation of nanobodies discovery. (B) Western blot of CELSR2, E-cadherin and tubulin following cell fractionation. (C) Western blot of CELSR2 in wild type and knockout MCF7 cells. (D) Blue coomassie gel of recombinant extracellular CELSR2. (E) SDS-page gel of the nanobodies D7 and G6. (F) Elisa titration of D7 and G6 nanobodies against plastic immobilized extracellular CELSR2. (G-H) dose-dependent binding curve of D7 and G6 nanobodies respectively to the cell surface of CELSR2 expressing cells by FACS. (I) wound closure rate of MDA-MB468 treated with the nanobodies D7, G6 or a control nanobody. (J) representative images of the wound healing closure quantified in (I).

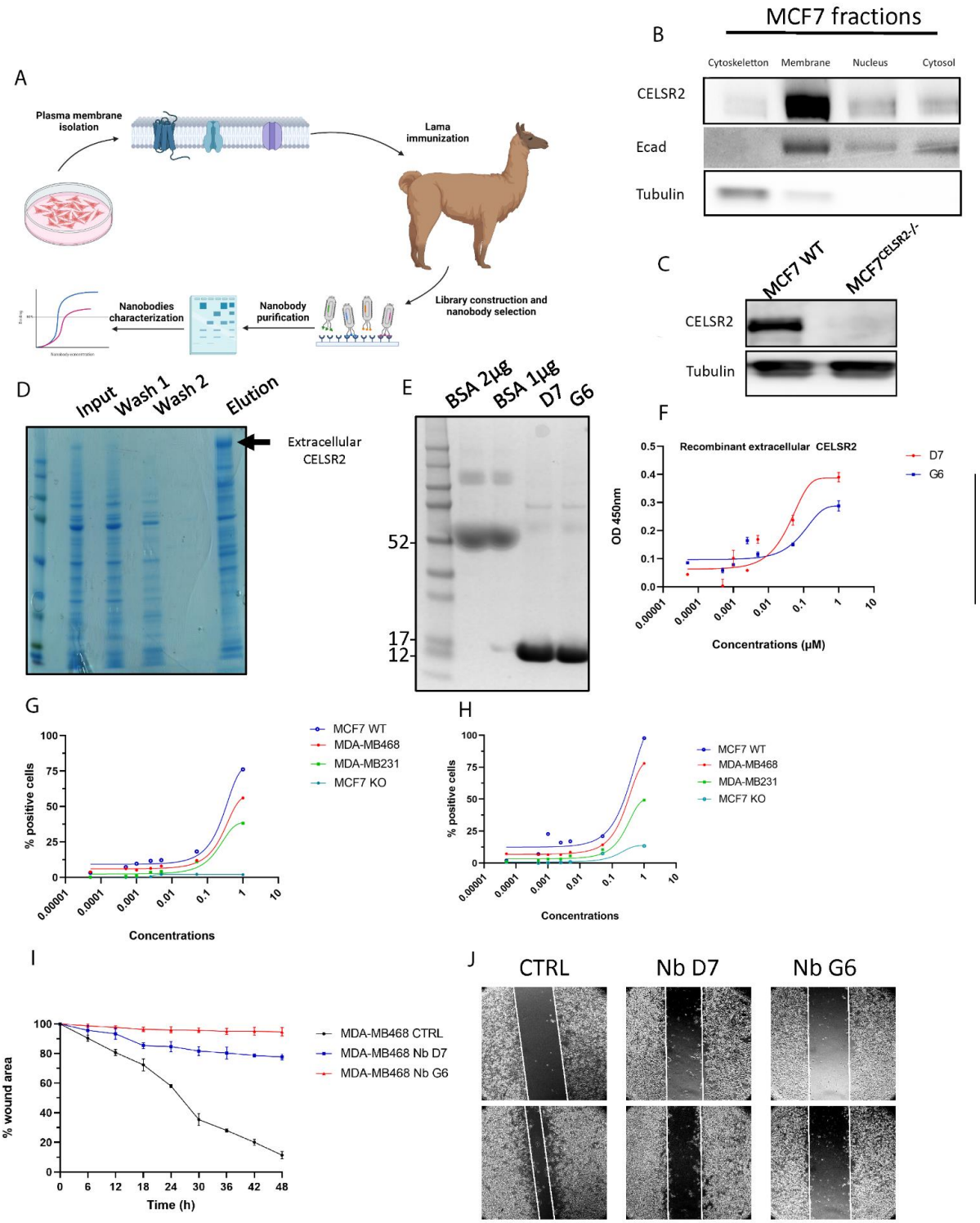
A
Plasma membrane isolation
Lama immunization
Library construction and nanobody selection
Nanobody purification
Nanobodies characterization
B
MCF7 fractions
Cytoskeletton
Membrane
Nucleus
Cytosol
CELSR2
Ecad
Tubulin
C
MCF7 WT
MCF7CELSR2-/-
CELSR2
Tubulin
D
Input
Wash 1
Wash 2
Elution
Extracellular CELSR2
E
BSA 2µg
BSA 1µg
D7
G6
52
17
12
F
Recombinant extracellular CELSR2
D7
G6
OD 450nm
Concentrations (µM)
G
MCF7 WT
MDA-MB468
MDA-MB231
MCF7 KO
% positive cells
Concentrations
H
MCF7 WT
MDA-MB468
MDA-MB231
MCF7 KO
% positive cells
Concentrations
I
MDA-MB468 CTRL
MDA-MB468 Nb D7
MDA-MB468 Nb G6
% wound area
Time (h)
J
CTRL
Nb D7
Nb G6

Tables :

Table 1 : Binding parameters on CELSR2-positive cell lines from curves of figure 6 panels G and H.

	EC50 (µM)	
	Nb D7	**Nb G6**
MCF7 WT	0.33	1.59
MDA-MB468	1.41	1.6
MDA-MB231	1.43	1.56

Supplementary materials :

Table S1 : Total proteome of MDA-MB468 following CELSR2 downregulation. Protein levels are compared to wild type cells treated with siCTRL. In pink = donwregulated proteins / In green = upregulated proteins

First,Protein,Description	Genes
Polymerase delta-interacting protein 2	POLDIP2
Isovaleryl-CoA dehydrogenase, mitochondrial	IVD
Mitochondrial import inner membrane translocase subunit TIM4	TIMM44
Delta(3,5)-Delta(2,4)-dienoyl-CoA isomerase, mitochondrial	ECH1
Very long-chain specific acyl-CoA dehydrogenase, mitochondrial	ACADVL
tRNA methyltransferase 10 homolog C	TRMT10C
Isochorismatase domain-containing protein 2	ISOC2
Succinate--CoA ligase [GDP-forming] subunit beta, mitochondrial	SUCLG2
Protein NipSnap homolog 1	NIPSNAP1
NADH dehydrogenase [ubiquinone] 1 alpha subcomplex subunit	NDUFA6
Serine--tRNA ligase, mitochondrial	SARS2
Polyribonucleotide nucleotidyltransferase 1, mitochondrial	PNPT1
Delta-1-pyrroline-5-carboxylate dehydrogenase, mitochondrial	ALDH4A1
Trifunctional enzyme subunit beta, mitochondrial	HADHB
NADPH:adrenodoxin oxidoreductase, mitochondrial	FDXR
Glutathione S-transferase kappa 1	GSTK1
Monofunctional C1-tetrahydrofolate synthase, mitochondrial	MTHFD1L
2,4-dienoyl-CoA reductase [(3E)-enoyl-CoA-producing], mitochor	DECR1
Thioredoxin reductase 2, mitochondrial	TXNRD2
Ornithine aminotransferase, mitochondrial	OAT
Succinate--CoA ligase [ADP-forming] subunit beta, mitochondrial	SUCLA2
NADH dehydrogenase [ubiquinone] iron-sulfur protein 3, mitoch	NDUFS3
Tyrosine--tRNA ligase, mitochondrial	YARS2
Iron-sulfur protein NUBPL	NUBPL
Aldehyde dehydrogenase X, mitochondrial	ALDH1B1
Hydroxyacyl-coenzyme A dehydrogenase, mitochondrial	HADH
3-hydroxyisobutyrate dehydrogenase, mitochondrial	HIBADH
Isocitrate dehydrogenase [NAD] subunit gamma, mitochondrial	IDH3G
Methionine--tRNA ligase, mitochondrial	37316.00
Glutaminase kidney isoform, mitochondrial	GLS
Acetyl-CoA acetyltransferase, mitochondrial	ACAT1
Citrate synthase, mitochondrial	CS
FAST kinase domain-containing protein 4	TBRG4
Succinate--CoA ligase [ADP/GDP-forming] subunit alpha, mitoch	SUCLG1
Single-stranded DNA-binding protein, mitochondrial	SSBP1
Mitochondrial ribonuclease P catalytic subunit	PRORP
Elongation factor Ts, mitochondrial	TSFM
Peroxisomal acyl-coenzyme A oxidase 1	ACOX1
Histone deacetylase complex subunit SAP18	SAP18
Malonyl-CoA-acyl carrier protein transacylase, mitochondrial	MCAT
NADH dehydrogenase [ubiquinone] 1 alpha subcomplex subunit	NDUFA10
Enoyl-CoA hydratase, mitochondrial	ECHS1
Isocitrate dehydrogenase [NADP], mitochondrial	IDH2
Elongation factor G, mitochondrial	GFM1
Adenosine 5'-monophosphoramidase HINT2	HINT2

Aspartate aminotransferase, mitochondrial	GOT2
Adrenodoxin, mitochondrial	FDX1
28S ribosomal protein S27, mitochondrial	MRPS27
Superoxide dismutase [Mn], mitochondrial	SOD2
Pyruvate dehydrogenase E1 component subunit alpha, somatic f	PDHA1
Aconitate hydratase, mitochondrial	ACO2
Methylglutaconyl-CoA hydratase, mitochondrial	AUH
Elongation factor Tu, mitochondrial	TUFM
Electron transfer flavoprotein subunit alpha, mitochondrial	ETFA
28S ribosomal protein S34, mitochondrial	MRPS34
Iron-sulfur cluster assembly enzyme ISCU	ISCU
Succinyl-CoA:3-ketoacid coenzyme A transferase 1, mitochondria	OXCT1
Isocitrate dehydrogenase [NAD] subunit alpha, mitochondrial	IDH3A
DnaJ homolog subfamily A member 3, mitochondrial	DNAJA3
Mitochondrial intermediate peptidase	MIPEP
Bifunctional methylenetetrahydrofolate dehydrogenase/cyclohy	MTHFD2
Complement component 1 Q subcomponent-binding protein, mi	C1QBP
Malate dehydrogenase, mitochondrial	MDH2
NADH dehydrogenase [ubiquinone] iron-sulfur protein 2, mitoch	NDUFS2
Very-long-chain (3R)-3-hydroxyacyl-CoA dehydratase 3	HACD3
Enoyl-CoA delta isomerase 1, mitochondrial	ECI1
Methylmalonyl-CoA mutase, mitochondrial	MMUT
Heat shock protein 75 kDa, mitochondrial	TRAP1
Presequence protease, mitochondrial	PITRM1
Isoleucine--tRNA ligase, mitochondrial	IARS2
Palmitoyl-protein thioesterase ABHD10, mitochondrial	ABHD10
3-hydroxyacyl-CoA dehydrogenase type-2	HSD17B10
Ribosome-recycling factor, mitochondrial	MRRF
Mitochondrial-processing peptidase subunit beta	PMPCB
Actin-binding protein WASF1	WASF1
Trifunctional enzyme subunit alpha, mitochondrial	HADHA
Phosphatidate cytidylyltransferase, mitochondrial	TAMM41
Phosphoenolpyruvate carboxykinase [GTP], mitochondrial	PCK2
Aspartate--tRNA ligase, mitochondrial	DARS2
Dihydrolipoyl dehydrogenase, mitochondrial	DLD
ATP-dependent RNA helicase SUPV3L1, mitochondrial	SUPV3L1
Mitochondrial-processing peptidase subunit alpha	PMPCA
2-oxoadipate dehydrogenase complex component E1	DHTKD1
10 kDa heat shock protein, mitochondrial	HSPE1
ADP/ATP translocase 3	SLC25A6
Xaa-Pro aminopeptidase 3	XPNPEP3
Peroxiredoxin-like 2A	PRXL2A
Malonate--CoA ligase ACSF3, mitochondrial	ACSF3
Cytochrome b-c1 complex subunit Rieske, mitochondrial	UQCRFS1
Succinate-semialdehyde dehydrogenase, mitochondrial	ALDH5A1
Succinate dehydrogenase [ubiquinone] flavoprotein subunit, mit	SDHA
Cadherin EGF LAG seven-pass G-type receptor 2	CELSR2
Alanine aminotransferase 2	GPT2
Membrane-associated tyrosine- and threonine-specific cdc2-inhi	PKMYT1
Putative transferase CAF17, mitochondrial	IBA57

Transmembrane protein 109	TMEM109
Cysteine desulfurase	NFS1
Complex I assembly factor ACAD9, mitochondrial	ACAD9
Mitochondrial genome maintenance exonuclease 1	MGME1
ATP synthase subunit d, mitochondrial	ATP5PD
Protein transport protein Sec61 subunit alpha isoform 1	SEC61A1
Coiled-coil-helix-coiled-coil-helix domain-containing protein 1	CHCHD1
DNL-type zinc finger protein	DNLZ
Serine hydroxymethyltransferase, mitochondrial	SHMT2
3-beta-hydroxysteroid-Delta(8),Delta(7)-isomerase	EBP
Isocitrate dehydrogenase [NAD] subunit beta, mitochondrial	IDH3B
Very-long-chain enoyl-CoA reductase	TECR
Glutamate dehydrogenase 1, mitochondrial	GLUD1
Threonine synthase-like 1	THNSL1
Glutaredoxin-2, mitochondrial	GLRX2
Solute carrier family 2, facilitated glucose transporter member 1(	SLC2A10
Ferrochelatase, mitochondrial	FECH
60 kDa heat shock protein, mitochondrial	HSPD1
1-acylglycerol-3-phosphate O-acyltransferase ABHD5	ABHD5
Corrinoid adenosyltransferase MMAB	MMAB
Lon protease homolog, mitochondrial	LONP1
Serine palmitoyltransferase 1	SPTLC1
Desumoylating isopeptidase 1	DESI1
Protein ABHD11	ABHD11
28S ribosomal protein S29, mitochondrial	DAP3
Probable glutamate--tRNA ligase, mitochondrial	EARS2
Threonine--tRNA ligase, mitochondrial	TARS2
39S ribosomal protein L46, mitochondrial	MRPL46
ATP synthase subunit g, mitochondrial	ATP5MG
Pyruvate dehydrogenase E1 component subunit beta, mitochon(	PDHB
Calcium load-activated calcium channel	TMCO1
Probable arginine--tRNA ligase, mitochondrial	RARS2
Serine palmitoyltransferase small subunit B	SPTSSB
NADH dehydrogenase [ubiquinone] flavoprotein 2, mitochondria	NDUFV2
NADH dehydrogenase [ubiquinone] 1 beta subcomplex subunit 9	NDUFB9
Haloacid dehalogenase-like hydrolase domain-containing protein	HDHD3
RNA-binding protein 38	RBM38
NFU1 iron-sulfur cluster scaffold homolog, mitochondrial	NFU1
Ankyrin repeat domain-containing protein 27	ANKRD27
Derlin-1	DERL1
m-AAA protease-interacting protein 1, mitochondrial	MAIP1
Putative methyltransferase-like protein 7A	METTL7A
Translocon-associated protein subunit gamma	SSR3
GrpE protein homolog 1, mitochondrial	GRPEL1
Putative GTP-binding protein 6	GTPBP6
Proline-rich protein 11	PRR11
Prohibitin-2	PHB2
Delta-1-pyrroline-5-carboxylate synthase	ALDH18A1
Stress-70 protein, mitochondrial	HSPA9
L-2-hydroxyglutarate dehydrogenase, mitochondrial	L2HGDH

4-aminobutyrate aminotransferase, mitochondrial	ABAT
Thioredoxin-dependent peroxide reductase, mitochondrial	PRDX3
Translational activator of cytochrome c oxidase 1	TACO1
Cytochrome c oxidase subunit 4 isoform 1, mitochondrial	COX4I1
Ribosome-releasing factor 2, mitochondrial	GFM2
Medium-chain specific acyl-CoA dehydrogenase, mitochondrial	ACADM
3-hydroxyisobutyryl-CoA hydrolase, mitochondrial	HIBCH
ATP synthase subunit delta, mitochondrial	ATP5F1D
UPF0598 protein C8orf82	C8orf82
Cytochrome b-c1 complex subunit 2, mitochondrial	UQCRC2
Stomatin-like protein 2, mitochondrial	STOML2
NADH-ubiquinone oxidoreductase 75 kDa subunit, mitochondria	NDUFS1
ATP synthase subunit alpha, mitochondrial	ATP5F1A
Coenzyme Q-binding protein COQ10 homolog B, mitochondrial	COQ10B
NADH dehydrogenase [ubiquinone] flavoprotein 1, mitochondria	NDUFV1
NADH dehydrogenase [ubiquinone] 1 alpha subcomplex assembl	NDUFAF2
Thioredoxin, mitochondrial	TXN2
Haloacid dehalogenase-like hydrolase domain-containing 5	HDHD5
Sterol-4-alpha-carboxylate 3-dehydrogenase, decarboxylating	NSDHL
Iron-sulfur cluster assembly 1 homolog, mitochondrial	ISCA1
Leucine-rich PPR motif-containing protein, mitochondrial	LRPPRC
3-oxoacyl-[acyl-carrier-protein] synthase, mitochondrial	OXSM
Methylcrotonoyl-CoA carboxylase beta chain, mitochondrial	MCCC2
Dolichyl-diphosphooligosaccharide--protein glycosyltransferase s	STT3B
NADH dehydrogenase [ubiquinone] iron-sulfur protein 5	NDUFS5
Alpha-ketoglutarate-dependent dioxygenase alkB homolog 7, mi	ALKBH7
NADH dehydrogenase [ubiquinone] 1 beta subcomplex subunit 1	NDUFB10
Dehydrogenase/reductase SDR family member 4	DHRS4
Serine/threonine-protein kinase 38-like	STK38L
Leucine-rich repeat-containing protein 59	LRRC59
Protein NCBP2AS2	NCBP2AS2
ATP synthase subunit gamma, mitochondrial	ATP5F1C
Dehydrogenase/reductase SDR family member 7	DHRS7
Cyclic GMP-AMP synthase	CGAS
Thiosulfate sulfurtransferase	TST
Dolichyl-diphosphooligosaccharide--protein glycosyltransferase s	DAD1
Carnitine O-palmitoyltransferase 2, mitochondrial	CPT2
Long-chain-fatty-acid--CoA ligase 4	ACSL4
Complex III assembly factor LYRM7	LYRM7
Prohibitin 1	PHB1
Kunitz-type protease inhibitor 2	SPINT2
Malectin	MLEC
Branched-chain-amino-acid aminotransferase, mitochondrial	BCAT2
Iron-sulfur cluster co-chaperone protein HscB	HSCB
GTP:AMP phosphotransferase AK3, mitochondrial	AK3
Long-chain fatty acid transport protein 3	SLC27A3
Ubiquinone biosynthesis O-methyltransferase, mitochondrial	COQ3
Bifunctional UDP-N-acetylglucosamine 2-epimerase/N-acetylmar	GNE
Cytochrome c oxidase subunit 5B, mitochondrial	COX5B
Vesicle-associated membrane protein-associated protein B/C	VAPB

von Willebrand factor A domain-containing protein 8	VWA8
Glutaredoxin-related protein 5, mitochondrial	GLRX5
Reticulon-3	RTN3
NADH dehydrogenase [ubiquinone] 1 alpha subcomplex subunit	NDUFA8
Peroxisomal multifunctional enzyme type 2	HSD17B4
Microsomal glutathione S-transferase 1	MGST1
Transcription intermediary factor 1-alpha	TRIM24
Peptidyl-prolyl cis-trans isomerase F, mitochondrial	PPIF
pre-rRNA 2'-O-ribose RNA methyltransferase FTSJ3	FTSJ3
Testis-specific Y-encoded-like protein 1	TSPYL1
Mitochondrial ribosome-associated GTPase 1	MTG1
Protein timeless homolog	TIMELESS
Endoplasmic reticulum junction formation protein lunapark	LNPK
Cohesin subunit SA-2	STAG2
Adenylate kinase 4, mitochondrial	AK4
G/T mismatch-specific thymine DNA glycosylase	TDG
Netrin receptor UNC5C	UNC5C
BRI3-binding protein	BRI3BP
ATP-dependent RNA helicase DDX18	DDX18
Phosphate carrier protein, mitochondrial	SLC25A3
Thioredoxin-related transmembrane protein 1	TMX1
Delta(24)-sterol reductase	DHCR24
ATP synthase subunit beta, mitochondrial	ATP5F1B
ATP synthase subunit f, mitochondrial	ATP5MF
Zinc finger MIZ domain-containing protein 1	ZMIZ1
Calcium-binding mitochondrial carrier protein SCaMC-1	SLC25A24
Oxidoreductase NAD-binding domain-containing protein 1	OXNAD1
Peptidyl-tRNA hydrolase 2, mitochondrial	PTRH2
Membrane-associated progesterone receptor component 1	PGRMC1
Dolichyl-diphosphooligosaccharide--protein glycosyltransferase s	STT3A
2-oxoglutarate dehydrogenase complex component E1	OGDH
Vitamin K epoxide reductase complex subunit 1	VKORC1
ADP/ATP translocase 2	SLC25A5
Voltage-dependent anion-selective channel protein 2	VDAC2
Cap-specific mRNA (nucleoside-2'-O-)-methyltransferase 2	CMTR2
Cytochrome b-c1 complex subunit 7	UQCRB
Transducin beta-like protein 2	TBL2
Pyrroline-5-carboxylate reductase 1, mitochondrial	PYCR1
COX assembly mitochondrial protein 2 homolog	CMC2
NADPH--cytochrome P450 reductase	POR
ATPase WRNIP1	WRNIP1
5'-AMP-activated protein kinase subunit beta-1	PRKAB1
Protein IWS1 homolog	IWS1
Minor histocompatibility antigen H13	HM13
Deoxynucleoside triphosphate triphosphohydrolase SAMHD1	SAMHD1
Cytochrome b-c1 complex subunit 1, mitochondrial	UQCRC1
Acyl-coenzyme A thioesterase 13	ACOT13
28S ribosomal protein S23, mitochondrial	MRPS23
Chromatin assembly factor 1 subunit B	CHAF1B
Polycomb protein EED	EED

E3 ubiquitin-protein ligase BRE1B	RNF40
Neurolysin, mitochondrial	NLN
Reticulon-4-interacting protein 1, mitochondrial	RTN4IP1
Putative heat shock protein HSP 90-alpha A4	HSP90AA4P
PRA1 family protein 3	ARL6IP5
MICOS complex subunit MIC19	CHCHD3
Beta-1,4-galactosyltransferase 1	B4GALT1
28S ribosomal protein S9, mitochondrial	MRPS9
U5 small nuclear ribonucleoprotein 40 kDa protein	SNRNP40
Probable peptidyl-tRNA hydrolase	PTRH1
Hydroxysteroid dehydrogenase-like protein 2	HSDL2
Putative lipid scramblase CLPTM1	CLPTM1
Chromobox protein homolog 1	CBX1
Vesicle-associated membrane protein-associated protein A	VAPA
Cell growth-regulating nucleolar protein	LYAR
Equilibrative nucleoside transporter 1	SLC29A1
28S ribosomal protein S2, mitochondrial	MRPS2
DnaJ homolog subfamily B member 12	DNAJB12
E3 SUMO-protein ligase PIAS4	PIAS4
28S ribosomal protein S18b, mitochondrial	MRPS18B
E3 ubiquitin-protein ligase UHRF1	UHRF1
Signal peptidase complex catalytic subunit SEC11A	SEC11A
PRELI domain-containing protein 1, mitochondrial	PRELID1
Nuclear factor 1 C-type	NFIC
Fatty acid CoA ligase Acsl3	ACSL3
Cytochrome c oxidase subunit 6B1	COX6B1
Sarcoplasmic/endoplasmic reticulum calcium ATPase 2	ATP2A2
Electron transfer flavoprotein subunit beta	ETFB
SPRY domain-containing protein 4	SPRYD4
POU domain, class 2, transcription factor 1	POU2F1
Emerin	EMD
Persulfide dioxygenase ETHE1, mitochondrial	ETHE1
Probable RNA-binding protein 23	RBM23
DDRGK domain-containing protein 1	DDRGK1
Integrator complex subunit 2	INTS2
Retinol dehydrogenase 11	RDH11
Calnexin	CANX
Peroxisomal leader peptide-processing protease	TYSND1
Metal cation symporter ZIP14	SLC39A14
Dehydrogenase/reductase SDR family member on chromosome	DHRSX
Uncharacterized protein C5orf34	C5orf34
Cytochrome c oxidase copper chaperone	COX17
Carnitine O-palmitoyltransferase 1, liver isoform	CPT1A
ATP synthase subunit e, mitochondrial	ATP5ME
M-phase inducer phosphatase 2	CDC25B
Protein regulator of cytokinesis 1	PRC1
RING-type E3 ubiquitin-protein ligase PPIL2	PPIL2
DNA polymerase subunit gamma-1	POLG
Dihydrolipoyllysine-residue succinyltransferase component of 2-	DLST
PAT complex subunit CCDC47	CCDC47

7-dehydrocholesterol reductase	DHCR7
Dolichol-phosphate mannosyltransferase subunit 3	DPM3
Atlastin-3	ATL3
Disintegrin and metalloproteinase domain-containing protein 10	ADAM10
Ras-related protein R-Ras	RRAS
Integrin beta-4	ITGB4
Frataxin, mitochondrial	FXN
Calcium uptake protein 2, mitochondrial	MICU2
Aladin	AAAS
Elongation of very long chain fatty acids protein 5	ELOVL5
Phosphatidylcholine transfer protein	PCTP
Extended synaptotagmin-1	ESYT1
Ubiquitin-conjugating enzyme E2 J1	UBE2J1
CDK-activating kinase assembly factor MAT1	MNAT1
General transcription factor 3C polypeptide 5	GTF3C5
Protein YIPF4	YIPF4
Breakpoint cluster region protein	BCR
WW domain-binding protein 11	WBP11
Oxygen-dependent coproporphyrinogen-III oxidase, mitochondri	CPOX
Immunoglobulin superfamily member 3	IGSF3
Spermatogenesis-associated protein 20	SPATA20
Dolichyl-diphosphooligosaccharide--protein glycosyltransferase s	RPN2
von Hippel-Lindau disease tumor suppressor	VHL
Adaptin ear-binding coat-associated protein 2	NECAP2
Extended synaptotagmin-2	ESYT2
Zinc finger CCCH-type with G patch domain-containing protein	ZGPAT
ATPase MORC2	MORC2
39S ribosomal protein L38, mitochondrial	MRPL38
Inactive tyrosine-protein kinase PRAG1	PRAG1
Reticulon-4	RTN4
Axin interactor, dorsalization-associated protein	AIDA
ER membrane protein complex subunit 3	EMC3
Lymphoid-specific helicase	HELLS
6-pyruvoyl tetrahydrobiopterin synthase	PTS
Outer dense fiber protein 2	ODF2
Myeloid leukemia factor 2	MLF2
Dolichyl-diphosphooligosaccharide--protein glycosyltransferase s	RPN1
Adipocyte plasma membrane-associated protein	APMAP
Zinc fingers and homeoboxes protein 2	ZHX2
Kinesin-like protein KIFC1	KIFC1
Atlastin-2	ATL2
RRP15-like protein	RRP15
Receptor expression-enhancing protein 4	REEP4
Dynamin-like 120 kDa protein, mitochondrial	OPA1
Proteasome assembly chaperone 1	PSMG1
5'-3' exoribonuclease 2	XRN2
G patch domain-containing protein 11	GPATCH11
Squalene monooxygenase	SQLE
Histone H4	H4C16
Sterol carrier protein 2	SCP2

Transmembrane protein 214	TMEM214
AT-rich interactive domain-containing protein 2	ARID2
Tetraspanin-15	TSPAN15
Signal transducing adapter molecule 2	STAM2
Uncharacterized protein KIAA0930	KIAA0930
Synembryn-B	RIC8B
mRNA-decapping enzyme 1A	DCP1A
Squalene synthase	FDFT1
ADP-ribosylation factor-like protein 6-interacting protein 1	ARL6IP1
Beta-2-microglobulin	B2M
Kinesin-like protein KIF20A	KIF20A
GTP cyclohydrolase 1	GCH1
Solute carrier family 52, riboflavin transporter, member 2	SLC52A2
Dolichyl-diphosphooligosaccharide--protein glycosyltransferase (	DDOST
Paxillin	PXN
Small integral membrane protein 7	SMIM7
Secretory carrier-associated membrane protein 2	SCAMP2
Anillin	ANLN
E3 ubiquitin-protein ligase RNF220	RNF220
DNA polymerase delta subunit 3	POLD3
Mitochondrial import inner membrane translocase subunit TIM5	TIMM50
COX assembly mitochondrial protein homolog	CMC1
Rab-like protein 3	RABL3
Prenylated Rab acceptor protein 1	RABAC1
BTB/POZ domain-containing protein KCTD12	KCTD12
H/ACA ribonucleoprotein complex subunit 1	GAR1
Elongation of very long chain fatty acids protein 1	ELOVL1
Retinoblastoma-associated protein	RB1
Sister chromatid cohesion protein DCC1	DSCC1
DNA ligase 3	LIG3
FERM domain-containing protein 8	FRMD8
Cation-dependent mannose-6-phosphate receptor	M6PR
Tetratricopeptide repeat protein 19, mitochondrial	TTC19
Ribonucleases P/MRP protein subunit POP1	POP1
Casein kinase I isoform epsilon	CSNK1E
Translocon-associated protein subunit delta	SSR4
NADH dehydrogenase [ubiquinone] iron-sulfur protein 6, mitoch	NDUFS6
Protein FAM83B	FAM83B
DNA repair and recombination protein RAD54B	RAD54B
Integrator complex subunit 13	INTS13
AMMECR1-like protein	AMMECR1L
Signal recognition particle receptor subunit beta	SRPRB
Signal peptidase complex subunit 3	SPCS3
Ubiquitin carboxyl-terminal hydrolase 40	USP40
Cholinephosphotransferase 1	CHPT1
Probable ATP-dependent RNA helicase DDX27	DDX27
Replication factor C subunit 3	RFC3
Protein mono-ADP-ribosyltransferase PARP4	PARP4
RRP12-like protein	RRP12
Nucleolar protein 9	NOP9

Regulation of nuclear pre-mRNA domain-containing protein 2	RPRD2
KH domain-containing, RNA-binding, signal transduction-associat	KHDRBS1
GDNF family receptor alpha-1	GFRA1
Histone RNA hairpin-binding protein	SLBP
COUP transcription factor 2	NR2F2
CD166 antigen	ALCAM
Tumor-associated calcium signal transducer 2	TACSTD2
Charged multivesicular body protein 6	CHMP6
Retinol dehydrogenase 13	RDH13
Transcription elongation factor SPT6	SUPT6H
DNA-directed RNA polymerase I subunit RPA34	POLR1G
Ras-related protein Rap-2c	RAP2C
Nucleolar protein 58	NOP58
Conserved oligomeric Golgi complex subunit 2	COG2
ATP-dependent RNA helicase DDX24	DDX24
RAD50-interacting protein 1	RINT1
Inorganic pyrophosphatase 2, mitochondrial	PPA2
Muscleblind-like protein 1	MBNL1
60S ribosomal protein L6	RPL6
Protein SOGA1	SOGA1
Proteasome assembly chaperone 2	PSMG2
Pre-mRNA-splicing factor RBM22	RBM22
Polyamine-modulated factor 1	PMF1
Interferon-related developmental regulator 1	IFRD1
Centrosomal protein of 97 kDa	CEP97
Cyclin-dependent kinase 7	CDK7
Methionine-R-sulfoxide reductase B2, mitochondrial	MSRB2
U3 small nucleolar RNA-interacting protein 2	RRP9
Glycine cleavage system H protein, mitochondrial	GCSH
Coiled-coil-helix-coiled-coil-helix domain-containing protein 5	CHCHD5
Selenocysteine insertion sequence-binding protein 2-like	SECISBP2L
General transcription factor IIF subunit 1	GTF2F1
Centromere protein H	CENPH
Sodium-coupled neutral amino acid symporter 1	SLC38A1
Replication initiator 1	REPIN1
Dolichol-phosphate mannosyltransferase subunit 1	DPM1
WD repeat and HMG-box DNA-binding protein 1	WDHD1
Cell division cycle protein 20 homolog	CDC20
Ribosomal oxygenase 2	RIOX2
Fanconi anemia group D2 protein	FANCD2
Folylpolyglutamate synthase, mitochondrial	FPGS
Glycerol-3-phosphate dehydrogenase, mitochondrial	GPD2
Zinc finger Ran-binding domain-containing protein 2	ZRANB2
Poly(A)-specific ribonuclease PARN	PARN
Heme oxygenase 2	HMOX2
DNA repair protein RAD51 homolog 1	RAD51
Pleiotropic regulator 1	PLRG1
Leucine-rich repeat-containing protein 58	LRRC58
Cyclin-D1-binding protein 1	CCNDBP1
mRNA-capping enzyme	RNGTT

ETS-related transcription factor Elf-1	ELF1
Sperm-associated antigen 5	SPAG5
Transcription factor Sp1	SP1
Carbonic anhydrase 12	CA12
Glyoxalase domain-containing protein 4	GLOD4
Cell division control protein 45 homolog	CDC45
DNA-(apurinic or apyrimidinic site) endonuclease 2	APEX2
Lamin-B1	LMNB1
Ribosome biogenesis protein BOP1	BOP1
Myc-associated zinc finger protein	MAZ
Pre-mRNA-splicing factor 38B	PRPF38B
Proteasome activator complex subunit 3	PSME3
NADH dehydrogenase [ubiquinone] 1 alpha subcomplex subunit	NDUFA12
Mediator of DNA damage checkpoint protein 1	MDC1
Serine/threonine-protein phosphatase PGAM5, mitochondrial	PGAM5
RNA-binding protein 12	RBM12
Endonuclease G, mitochondrial	ENDOG
Protein MIX23	MIX23
Zinc finger protein 217	ZNF217
U1 small nuclear ribonucleoprotein 70 kDa	SNRNP70
SWI/SNF-related matrix-associated actin-dependent regulator of	SMARCB1
Thyroid hormone receptor-associated protein 3	THRAP3
Uracil-DNA glycosylase	UNG
Protein JTB	JTB
Kinesin-like protein KIF23	KIF23
Spindle and kinetochore-associated protein 3	SKA3
General transcription factor IIF subunit 2	GTF2F2
Kinesin-like protein KIF2C	KIF2C
Mortality factor 4-like protein 2	MORF4L2
Arginine/serine-rich coiled-coil protein 2	RSRC2
Serine/arginine repetitive matrix protein 1	SRRM1
HCLS1-associated protein X-1	HAX1
Interferon regulatory factor 2-binding protein 1	IRF2BP1
Ribonucleoprotein PTB-binding 1	RAVER1
Serrate RNA effector molecule homolog	SRRT
Protein DENND6A	DENND6A
Prostaglandin E synthase 2	PTGES2
Occludin	OCLN
Golgi apparatus protein 1	GLG1
Heterogeneous nuclear ribonucleoprotein H	HNRNPH1
UBX domain-containing protein 4	UBXN4
Zinc phosphodiesterase ELAC protein 2	ELAC2
Nuclear transcription factor Y subunit gamma	NFYC
Ribosomal L1 domain-containing protein 1	RSL1D1
Centrosomal protein of 85 kDa	CEP85
Kinesin-like protein KIF22	KIF22
ARF GTPase-activating protein GIT2	GIT2
Copper homeostasis protein cutC homolog	CUTC
Tyrosine-protein phosphatase non-receptor type 2	PTPN2
Serine/threonine-protein kinase PLK1	PLK1

Targeting protein for Xklp2	TPX2
A-kinase anchor protein 11	AKAP11
Exocyst complex component 6	EXOC6
CD151 antigen	CD151
Ubiquitin-like protein 3	UBL3
Ubiquitin-conjugating enzyme E2 S	UBE2S
Nucleolar RNA helicase 2	DDX21
5'-3' exoribonuclease 1	XRN1
Condensin-2 complex subunit G2	NCAPG2
Myoferlin	MYOF
Secretory carrier-associated membrane protein 4	SCAMP4
Protein ITPRID2	ITPRID2
RNA demethylase ALKBH5	ALKBH5
WD repeat-containing protein 5	WDR5
Glutathione S-transferase Mu 4	GSTM4
Cyclin-H	CCNH
Telomeric repeat-binding factor 2-interacting protein 1	TERF2IP
RNA-binding protein 25	RBM25
Transmembrane emp24 domain-containing protein 2	TMED2
ATP-dependent DNA helicase Q1	RECQL
Transcriptional repressor p66-alpha	GATAD2A
Mitochondrial Rho GTPase 2	RHOT2
Transducin beta-like protein 3	TBL3
THO complex subunit 6 homolog	THOC6
Parafibromin	CDC73
Sodium/potassium-transporting ATPase subunit beta-3	ATP1B3
tRNA-splicing endonuclease subunit Sen54	TSEN54
Conserved oligomeric Golgi complex subunit 3	COG3
Transcription activator BRG1	SMARCA4
Leucyl-cystinyl aminopeptidase	LNPEP
Spastin	SPAST
Ras-associated and pleckstrin homology domains-containing pro	RAPH1
Polyadenylate-binding protein 2	PABPN1
Proliferation marker protein Ki-67	MKI67
CUGBP Elav-like family member 1	CELF1
Transferrin receptor protein 1	TFRC
WD repeat and FYVE domain-containing protein 3	WDFY3
Polymerase delta-interacting protein 3	POLDIP3
Centromere protein M	CENPM
Microfibrillar-associated protein 1	MFAP1
DNA topoisomerase 2-beta	TOP2B
Cleavage and polyadenylation specificity factor subunit 1	CPSF1
Zinc finger CCCH-type antiviral protein 1-like	ZC3HAV1L
Protein YIPF6	YIPF6
Palmitoyltransferase ZDHHC20	ZDHHC20
AP-5 complex subunit mu-1	AP5M1
Transcription initiation factor IIB	GTF2B
Pseudouridylate synthase 7 homolog	PUS7
E3 ubiquitin-protein ligase UBR5	UBR5
Phosducin-like protein	PDCL

WD40 repeat-containing protein SMU1	SMU1
Neuronal calcium sensor 1	NCS1
Ras-related protein Rap-2b	RAP2B
Adrenocortical dysplasia protein homolog	ACD
Basigin	BSG
tRNA-uridine aminocarboxypropyltransferase 1	DTWD1
Centromere protein F	CENPF
Centromere-associated protein E	CENPE
Replication factor C subunit 1	RFC1
Probable dimethyladenosine transferase	DIMT1
Ras-related protein Rab-2A	RAB2A
Activated RNA polymerase II transcriptional coactivator p15	SUB1
Protein kinase C-binding protein 1	ZMYND8
SAGA-associated factor 29	SGF29
DNA polymerase alpha catalytic subunit	POLA1
WD repeat-containing protein 62	WDR62
DNA (cytosine-5)-methyltransferase 1	DNMT1
DNA topoisomerase 2-alpha	TOP2A
Pumilio homolog 3	PUM3
DNA polymerase alpha subunit B	POLA2
RNA-binding Raly-like protein	RALYL
Histone PARylation factor 1	HPF1
RNA-binding E3 ubiquitin-protein ligase MEX3C	MEX3C
Pre-mRNA-processing factor 6	PRPF6
Peroxisomal targeting signal 1 receptor	PEX5
DNA mismatch repair protein Msh6	MSH6
RNA-binding protein Raly	RALY
Peptidyl-prolyl cis-trans isomerase-like 4	PPIL4
Heterogeneous nuclear ribonucleoprotein H3	HNRNPH3
RING finger protein 214	RNF214
Probable ATP-dependent RNA helicase DDX17	DDX17
Double-strand-break repair protein rad21 homolog	RAD21
Probable ATP-dependent RNA helicase DDX23	DDX23
Transmembrane 9 superfamily member 2	TM9SF2
Probable 28S rRNA (cytosine(4447)-C(5))-methyltransferase	NOP2
Fanconi anemia group I protein	FANCI
Nucleolar transcription factor 1	UBTF
rRNA 2'-O-methyltransferase fibrillarin	FBL
Alpha- and gamma-adaptin-binding protein p34	AAGAB
6-phosphofructo-2-kinase/fructose-2,6-bisphosphatase 3	PFKFB3
Flap endonuclease 1	FEN1
Rho family-interacting cell polarization regulator 1	RIPOR1
S1 RNA-binding domain-containing protein 1	SRBD1
Transcription initiation factor IIE subunit beta	GTF2E2
Low-density lipoprotein receptor	LDLR
Cleavage stimulation factor subunit 2	CSTF2
Non-POU domain-containing octamer-binding protein	NONO
DDB1- and CUL4-associated factor 7	DCAF7
Lysine-specific histone demethylase 1A	KDM1A
RNA-binding protein 14	RBM14

Adenylate kinase 2, mitochondrial	AK2
DNA polymerase delta catalytic subunit	POLD1
Nuclear inhibitor of protein phosphatase 1	PPP1R8
Transcriptional regulator QRICH1	QRICH1
Suppressor APC domain-containing protein 2	SAPCD2
tRNA (guanine(37)-N1)-methyltransferase	TRMT5
DNA repair protein RAD51 homolog 3	RAD51C
Intermembrane lipid transfer protein VPS13A	VPS13A
Splicing factor 3A subunit 1	SF3A1
Cap-specific mRNA (nucleoside-2'-O-)-methyltransferase 1	CMTR1
5'-AMP-activated protein kinase catalytic subunit alpha-1	PRKAA1
Aurora kinase A	AURKA
Poly [ADP-ribose] polymerase 1	PARP1
RNA-binding protein FUS	FUS
DnaJ homolog subfamily B member 6	DNAJB6
Serine/threonine-protein kinase 11-interacting protein	STK11IP
Conserved oligomeric Golgi complex subunit 1	COG1
ATP-dependent RNA helicase DDX42	DDX42
SPRY domain-containing protein 7	SPRYD7
Syntaxin-4	STX4
Probable ATP-dependent RNA helicase DDX49	DDX49
Lupus La protein	SSB
DNA replication complex GINS protein PSF1	GINS1
Ras-related protein Rab-27A	RAB27A
Ethanolamine kinase 1	ETNK1
E3 UFM1-protein ligase 1	UFL1
Proteolipid protein 2	PLP2
Probable ATP-dependent RNA helicase DDX46	DDX46
Sister chromatid cohesion protein PDS5 homolog A	PDS5A
Twinfilin-1	TWF1
DNA-3-methyladenine glycosylase	MPG
ADP-ribosylation factor-like protein 6-interacting protein 4	ARL6IP4
General transcription factor 3C polypeptide 3	GTF3C3
28S rRNA (cytosine-C(5))-methyltransferase	NSUN5
RPA-interacting protein	RPAIN
Squamous cell carcinoma antigen recognized by T-cells 3	SART3
E3 ubiquitin-protein ligase Itchy homolog	ITCH
UBX domain-containing protein 7	UBXN7
DNA primase large subunit	PRIM2
G2/mitotic-specific cyclin-B1	CCNB1
Transcription intermediary factor 1-beta	TRIM28
Splicing factor YJU2	YJU2
Leucine-rich repeat and WD repeat-containing protein 1	LRWD1
Pleckstrin homology-like domain family A member 2	PHLDA2
Retrotransposon-derived protein PEG10	PEG10
Nonsense-mediated mRNA decay factor SMG7	SMG7
Septin-10	SEPTIN10
Chromosome transmission fidelity protein 18 homolog	CHTF18
AP-2 complex subunit mu	AP2M1
Ribosomal RNA small subunit methyltransferase NEP1	EMG1

Myotubularin-related protein 12	MTMR12
Kinetochore protein Nuf2	NUF2
N6-adenosine-methyltransferase catalytic subunit	METTL3
Prelamin-A/C	LMNA
Retinoic acid receptor RXR-alpha	RXRA
Laminin subunit beta-2	LAMB2
Dystrobrevin alpha	DTNA
Rac GTPase-activating protein 1	RACGAP1
Histone H1,10	H1-10
Serine/threonine-protein kinase Chk2	CHEK2
Serine/threonine-protein kinase tousled-like 2	TLK2
Heterogeneous nuclear ribonucleoproteins C1/C2	HNRNPC
DNA replication licensing factor MCM7	MCM7
U4/U6,U5 tri-snRNP-associated protein 2	USP39
Heterogeneous nuclear ribonucleoprotein U	HNRNPU
Telomere-associated protein RIF1	RIF1
Kanadaptin	SLC4A1AP
Splicing factor U2AF 65 kDa subunit	U2AF2
Treacle protein	TCOF1
40S ribosomal protein S2	RPS2
Heterogeneous nuclear ribonucleoprotein D-like	HNRNPDL
Dual specificity protein kinase CLK3	CLK3
BUB3-interacting and GLEBS motif-containing protein ZNF207	ZNF207
Cystathionine gamma-lyase	CTH
CGG triplet repeat-binding protein 1	CGGBP1
Heat shock protein HSP 90-alpha	HSP90AA1
Protein DEK	DEK
AN1-type zinc finger protein 3	ZFAND3
Cyclin-dependent kinase 9	CDK9
GTP-binding protein 4	GTPBP4
Heterogeneous nuclear ribonucleoprotein L	HNRNPL
Tyrosine-protein phosphatase non-receptor type 1	PTPN1
Myotubularin-related protein 4	MTMR4
Nucleoporin p58/p45	NUP58
Cell cycle and apoptosis regulator protein 2	CCAR2
Programmed cell death protein 2	PDCD2
DNA replication licensing factor MCM4	MCM4
tRNA-splicing endonuclease subunit Sen34	TSEN34
ADP-ribosylation factor GTPase-activating protein 3	ARFGAP3
Protein FRG1	FRG1
60S ribosome subunit biogenesis protein NIP7 homolog	NIP7
RNA-binding protein 47	RBM47
Splicing factor 3B subunit 1	SF3B1
Protein Red	IK
Nuclear receptor coactivator 3	NCOA3
Dihydropyrimidinase-related protein 5	DPYSL5
Heterogeneous nuclear ribonucleoproteins A2/B1	HNRNPA2B1
Periodic tryptophan protein 1 homolog	PWP1
H/ACA ribonucleoprotein complex subunit DKC1	DKC1
Ubiquitin-conjugating enzyme E2 T	UBE2T

Heterogeneous nuclear ribonucleoprotein A0	HNRNPA0
Hyaluronan mediated motility receptor	HMMR
Lariat debranching enzyme	DBR1
Kinetochore protein NDC80 homolog	NDC80
Splicing factor, proline- and glutamine-rich	SFPQ
Fanconi anemia group J protein	BRIP1
DNA replication licensing factor MCM2	MCM2
Y-box-binding protein 2	YBX2
Transformer-2 protein homolog beta	TRA2B
Renin receptor	ATP6AP2
Pre-mRNA-splicing factor ATP-dependent RNA helicase PRP16	DHX38
Matrin-3	MATR3
Protein Spindly	SPDL1
5'-AMP-activated protein kinase subunit gamma-1	PRKAG1
Structural maintenance of chromosomes protein 3	SMC3
AP-2 complex subunit sigma	AP2S1
Nucleolar and spindle-associated protein 1	NUSAP1
DNA topoisomerase 1	TOP1
Heterogeneous nuclear ribonucleoprotein M	HNRNPM
Protein FAM83D	FAM83D
Bifunctional epoxide hydrolase 2	EPHX2
Trans-acting T-cell-specific transcription factor GATA-3	GATA3
Histone H1,5	H1-5
DnaJ homolog subfamily C member 17	DNAJC17
Heterogeneous nuclear ribonucleoprotein F	HNRNPF
Tubulin epsilon and delta complex protein 1	TEDC1
RNA-binding protein EWS	EWSR1
ELAV-like protein 1	ELAVL1
Mitotic checkpoint serine/threonine-protein kinase BUB1 beta	BUB1B
Serine/arginine-rich splicing factor 1	SRSF1
Ubiquitin-conjugating enzyme E2 C	UBE2C
DDB1- and CUL4-associated factor 13	DCAF13
Conserved oligomeric Golgi complex subunit 4	COG4
GA-binding protein alpha chain	GABPA
Helicase with zinc finger domain 2	HELZ2
DNA replication licensing factor MCM5	MCM5
U4/U6 small nuclear ribonucleoprotein Prp4	PRPF4
Protein transport protein Sec24D	SEC24D
Long-chain-fatty-acid--CoA ligase 1	ACSL1
Zinc finger transcription factor Trps1	TRPS1
DNA replication licensing factor MCM6	MCM6
FACT complex subunit SPT16	SUPT16H
Lamina-associated polypeptide 2, isoform alpha	TMPO
Splicing factor 3A subunit 3	SF3A3
Centrosomal protein of 78 kDa	CEP78
Mitotic checkpoint protein BUB3	BUB3
Brefeldin A-inhibited guanine nucleotide-exchange protein 1	ARFGEF1
Ribosome-binding protein 1	RRBP1
Lysosomal Pro-X carboxypeptidase	PRCP
F-box only protein 21	FBXO21

Mitochondrial protein C2orf69	C2orf69
D-3-phosphoglycerate dehydrogenase	PHGDH
Molybdopterin synthase catalytic subunit	MOCS2
Aminoacylase-1	ACY1
Serine/threonine-protein kinase ULK1	ULK1
Transmembrane protein 179B	TMEM179B
Serine--tRNA ligase, cytoplasmic	SARS1
tRNA wybutosine-synthesizing protein 5	TYW5
N(G),N(G)-dimethylarginine dimethylaminohydrolase 2	DDAH2
CCR4-NOT transcription complex subunit 6	CNOT6
Phosphoserine phosphatase	PSPH
TSC22 domain family protein 2	TSC22D2
Coiled-coil domain-containing protein 43	CCDC43
Ras-specific guanine nucleotide-releasing factor RalGPS2	RALGPS2
WW domain-binding protein 2	WBP2
EH domain-containing protein 1	EHD1
Protein FAM102A	FAM102A
Annexin A9	ANXA9
Protein S100-A6	S100A6
Thiamine-triphosphatase	THTPA
Histamine N-methyltransferase	HNMT
Nuclear factor of activated T-cells, cytoplasmic 2	NFATC2
Tubulin-specific chaperone cofactor E-like protein	TBCEL
Ubiquitin-conjugating enzyme E2 variant 1	UBE2V1
Molybdopterin synthase sulfur carrier subunit	MOCS2
Stathmin	STMN1
Threonylcarbamoyl-AMP synthase	YRDC
Asparagine synthetase [glutamine-hydrolyzing]	ASNS
Serine/threonine-protein phosphatase 2A 65 kDa regulatory sub	PPP2R1B
Biotinidase	BTD
Protein C10	C12orf57
Fos-related antigen 1	FOSL1
Cellular retinoic acid-binding protein 1	CRABP1
Calretinin	CALB2
Stathmin-2	STMN2
Phosphomannomutase 1	PMM1
Serine/threonine-protein kinase B-raf	BRAF
Adapter SH3BGRL	SH3BGRL
Archaemetzincin-1	AMZ1
Trinucleotide repeat-containing gene 6B protein	TNRC6B
m7GpppN-mRNA hydrolase	DCP2
Kinesin light chain 4	KLC4
Costars family protein ABRACL	ABRACL
RISC-loading complex subunit TARBP2	TARBP2
Sentrin-specific protease 8	SENP8
Glucoside xylosyltransferase 1	GXYLT1
Myoglobin	MB
Cingulin	CGN
Tumor protein p63-regulated gene 1-like protein	TPRG1L
Melanoregulin	MREG

Histone deacetylase 7	HDAC7
Protein OSCP1	OSCP1
Tripeptidyl-peptidase 1	TPP1
Nucleobindin-2	NUCB2
Protein S100-A13	S100A13
Nucleolar protein 3	NOL3
Protein phosphatase 1 regulatory subunit 14B	PPP1R14B
Hydroxylysine kinase	HYKK
Ubiquitin/ISG15-conjugating enzyme E2 L6	UBE2L6
Zinc finger CCHC domain-containing protein 3	ZCCHC3
Ectopic P granules protein 5 homolog	EPG5
Pseudouridine-5'-phosphatase	PUDP
Selenoprotein F	SELENOF
Tropomyosin alpha-4 chain	TPM4
EF-hand domain-containing protein D2	EFHD2
NF-kappa-B inhibitor-interacting Ras-like protein 1	NKIRAS1
Rhophilin-2	RHPN2
Ester hydrolase C11orf54	C11orf54
Programmed cell death protein 4	PDCD4
Pyruvate kinase PKLR	PKLR
Protein argonaute-2	AGO2
Coiled-coil domain-containing protein 120	CCDC120
Protein argonaute-1	AGO1
Prefoldin subunit 6	PFDN6
NHL repeat-containing protein 3	NHLRC3
Ribonuclease T2	RNASET2
Pyroglutamyl-peptidase 1	PGPEP1
RAB6A-GEF complex partner protein 2	RGP1
Lysosomal thioesterase PPT2	PPT2
Trinucleotide repeat-containing gene 6A protein	TNRC6A
Trypsin-3	PRSS3
Protein N-lysine methyltransferase METTL21D	VCPKMT
Cofilin-2	CFL2
1-phosphatidylinositol 3-phosphate 5-kinase	PIKFYVE
Desmoglein-1	DSG1
Endoribonuclease Dicer	DICER1
Selenoprotein H	SELENOH
Serine/threonine-protein kinase Sgk3	SGK3
N(G),N(G)-dimethylarginine dimethylaminohydrolase 1	DDAH1
Tetratricopeptide repeat protein 38	TTC38
DENN domain-containing protein 2A	DENND2A
Polyadenylate-binding protein-interacting protein 2	PAIP2
Phospholipid hydroperoxide glutathione peroxidase	GPX4
Protein S100-P	S100P
Cytosolic arginine sensor for mTORC1 subunit 1	CASTOR1
Transcriptional coactivator YAP1	YAP1
Sestrin-2	SESN2
BTB/POZ domain-containing adapter for CUL3-mediated RhoA d	TNFAIP1
Kynurenine--oxoglutarate transaminase 1	KYAT1
Chloride intracellular channel protein 6	CLIC6

Supplementary figure 1 : (A) Impact of CELSR1 and CELSR3 on metastasis free survival of all breast cancers and each breast cancer subtype. (B-C) CELSR1 and CELSR3 expression change respectively between paired primary tumors and metastasis.

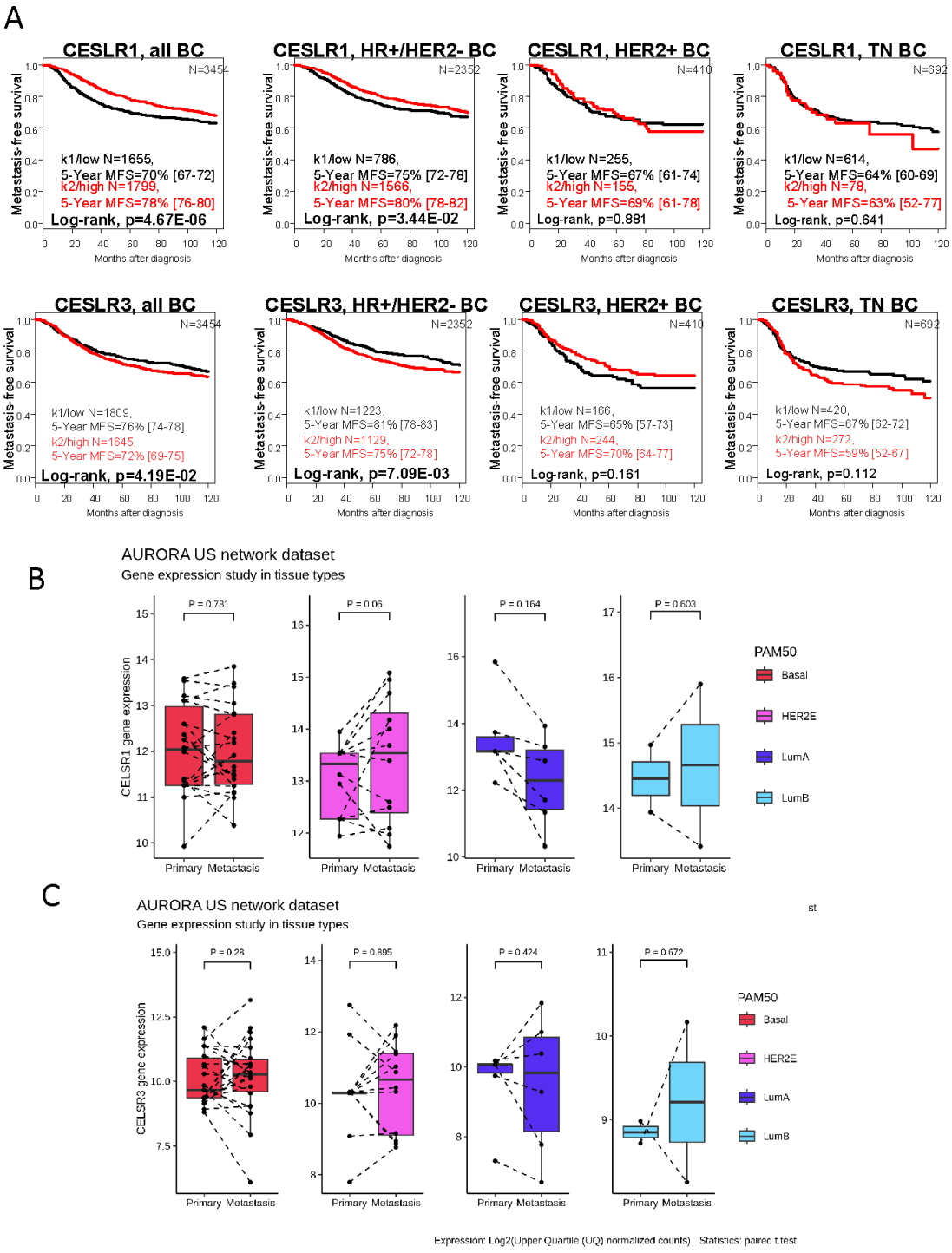

Supplementary figure 2 : Bioluminescence quantification in lymph nodes, ovaries, spleen, kidneys, liver and lungs in shSCR and shCELSR2 tumors.

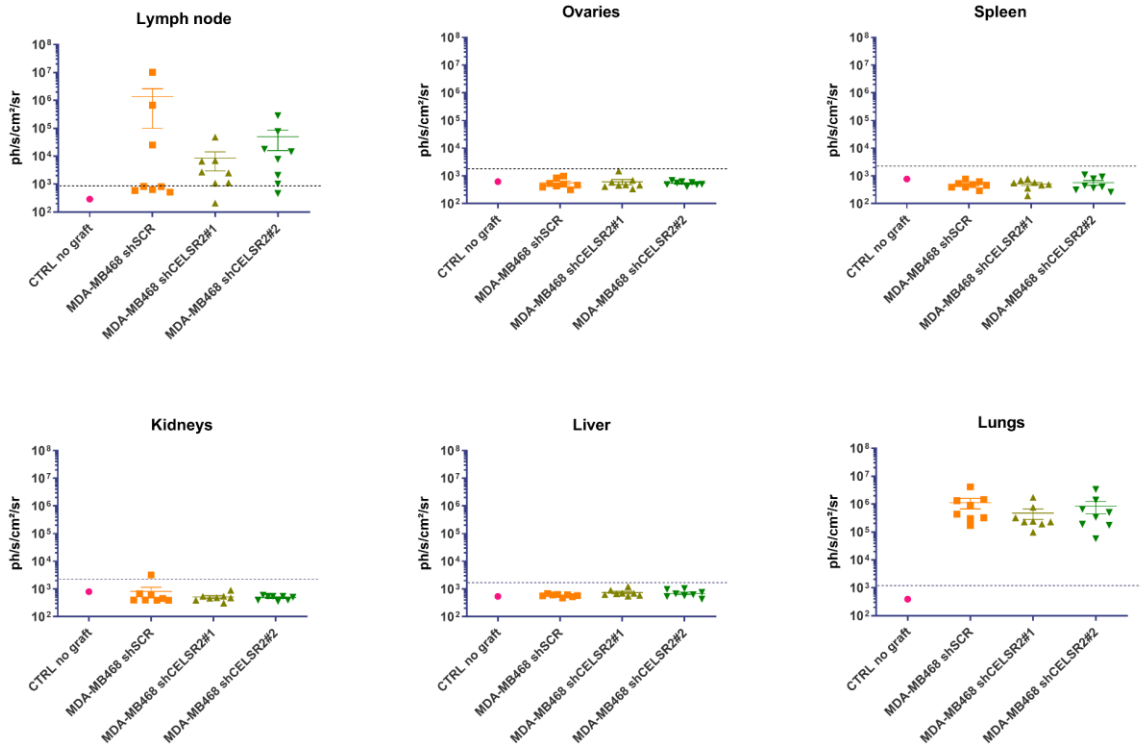

Supplementary figure 3 : (A) Histograms of nanobodies D7 and G6 surface staining in cell lines with decreasing level of CELSR2 expression. (B) mRNA levels of CELSR1, CELSR2 and CELSR3 in the cell lines used in (A).

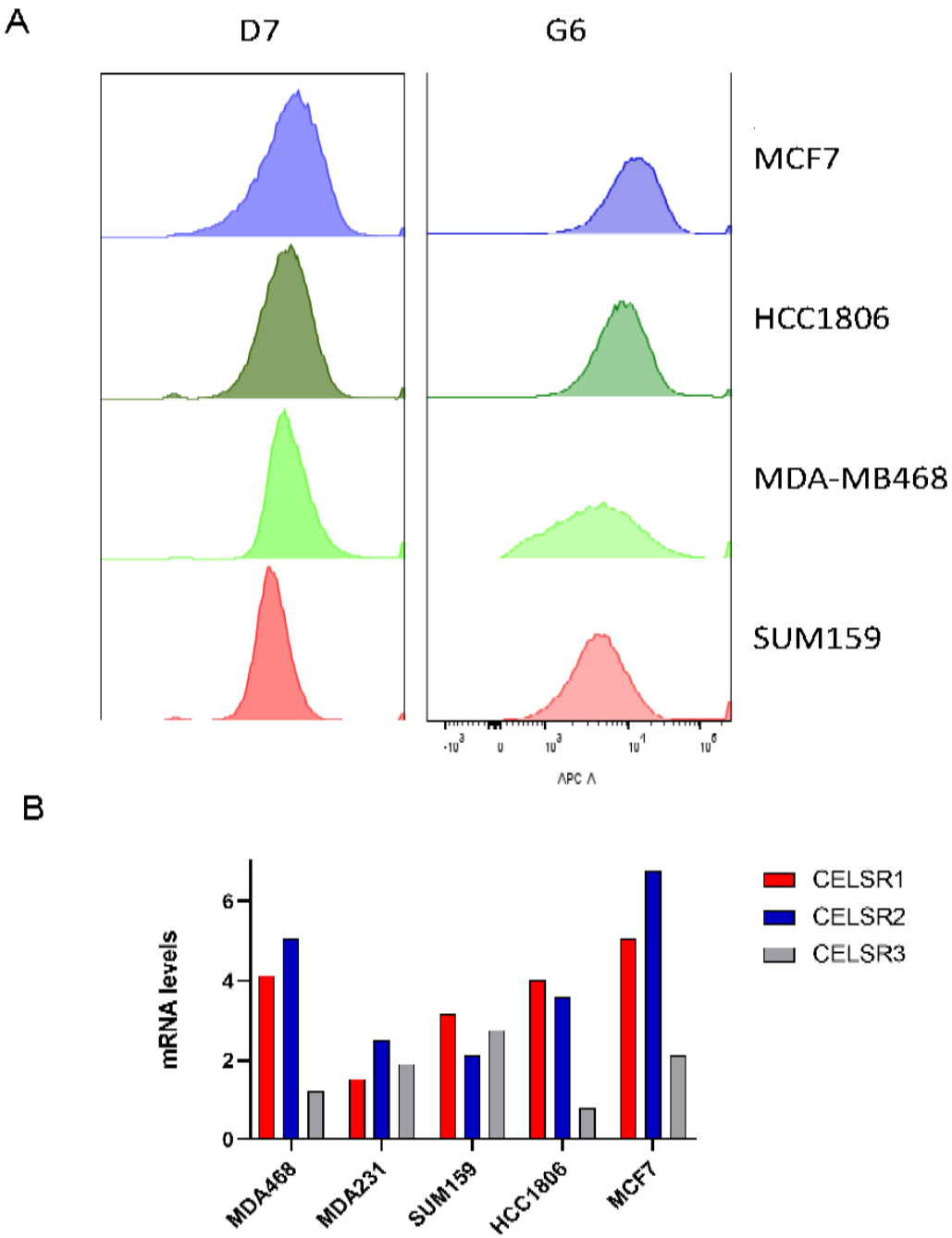

References :

1. Foulkes, W. D., Smith, I. E. & Reis-Filho, J. S. Triple-Negative Breast Cancer. *N. Engl. J. Med.* **363**, 1938–1948 (2010).

2. Almansour, N. M. Triple-Negative Breast Cancer: A Brief Review About Epidemiology, Risk Factors, Signaling Pathways, Treatment and Role of Artificial Intelligence. *Front. Mol. Biosci.* **9**, 836417 (2022).

3. Lehmann, B. D. *et al.* Identification of human triple-negative breast cancer subtypes and preclinical models for selection of targeted therapies. *J. Clin. Invest.* **121**, 2750–2767 (2011).

4. Zhu, X. *et al.* The prognostic and predictive potential of Ki-67 in triple-negative breast cancer. *Sci. Rep.* **10**, 225 (2020).

5. Dent, R. *et al.* Triple-negative breast cancer: clinical features and patterns of recurrence. *Clin. Cancer Res. Off. J. Am. Assoc. Cancer Res.* **13**, 4429–4434 (2007).

6. Chaffer, C. L. & Weinberg, R. A. A perspective on cancer cell metastasis. *Science* **331**, 1559–1564 (2011).

7. Derakhshan, F. & Reis-Filho, J. S. Pathogenesis of Triple-Negative Breast Cancer. *Annu. Rev. Pathol.* **17**, 181–204 (2022).

8. Liu, Z., Li, M., Jiang, Z. & Wang, X. A Comprehensive Immunologic Portrait of Triple-Negative Breast Cancer. *Transl. Oncol.* **11**, 311–329 (2018).

9. Li, Y. *et al.* Recent advances in therapeutic strategies for triple-negative breast cancer. *J. Hematol. Oncol.J Hematol Oncol* **15**, 121 (2022).

10. Han, H. S. *et al.* Early-Stage Triple-Negative Breast Cancer Journey: Beginning, End, and Everything in Between. *Am. Soc. Clin. Oncol. Educ. Book* e390464 (2023) doi:10.1200/EDBK_390464.

11. Takebe, N., Warren, R. Q. & Ivy, S. P. Breast cancer growth and metastasis: interplay between cancer stem cells, embryonic signaling pathways and epithelial-to-mesenchymal transition. *Breast Cancer Res. BCR* **13**, 211 (2011).

12. Sanz-Ezquerro, J. J., Münsterberg, A. E. & Stricker, S. Editorial: Signaling Pathways in Embryonic Development. *Front. Cell Dev. Biol.* **5**, 76 (2017).

13. Angers, S. & Moon, R. T. Proximal events in Wnt signal transduction. *Nat. Rev. Mol.*

Cell Biol. **10**, 468–477 (2009).

14. Daulat, A. M. *et al.* PRICKLE1 Contributes to Cancer Cell Dissemination through Its Interaction with mTORC2. *Dev. Cell* **37**, 311–325 (2016).

15. Anastas, J. N. *et al.* A protein complex of SCRIB, NOS1AP and VANGL1 regulates cell polarity and migration, and is associated with breast cancer progression. *Oncogene* **31**, 3696–3708 (2012).

16. Puvirajesinghe, T. M. *et al.* Identification of p62/SQSTM1 as a component of non-canonical Wnt VANGL2–JNK signalling in breast cancer. *Nat. Commun.* **7**, 10318 (2016).

17. Gujral, T. S. *et al.* A noncanonical Frizzled2 pathway regulates epithelial-mesenchymal transition and metastasis. *Cell* **159**, 844–856 (2014).

18. Boutin, C., Goffinet, A. M. & Tissir, F. Celsr1-3 cadherins in PCP and brain development. *Curr. Top. Dev. Biol.* **101**, 161–183 (2012).

19. Butler, M. T. & Wallingford, J. B. Planar cell polarity in development and disease. *Nat. Rev. Mol. Cell Biol.* **18**, 375–388 (2017).

20. Wang, X.-J. *et al.* Understanding CELSRs - Cadherin EGF LAG seven-pass G-type receptors. *J. Neurochem.* **131**, 699–711 (2014).

21. Bui, D. L. H. *et al.* The adhesion GPCRs CELSR1-3 and LPHN3 engage G proteins via distinct activation mechanisms. *Cell Rep.* **42**, 112552 (2023).

22. Xu, M., Zhu, S., Xu, R. & Lin, N. Identification of CELSR2 as a novel prognostic biomarker for hepatocellular carcinoma. *BMC Cancer* **20**, 313 (2020).

23. Suarez-Arnedo, A. *et al.* An image J plugin for the high throughput image analysis of in vitro scratch wound healing assays. *PLOS ONE* **15**, e0232565 (2020).

24. Vinci, M., Box, C. & Eccles, S. A. Three-Dimensional (3D) Tumor Spheroid Invasion Assay. *JoVE J. Vis. Exp.* e52686 (2015) doi:10.3791/52686.

25. Garcia-Recio, S. *et al.* Multiomics in primary and metastatic breast tumors from the AURORA US network finds microenvironment and epigenetic drivers of metastasis. *Nat.*

Cancer **4**, 128–147 (2023).

26. Evans, K. W. *et al.* Oxidative Phosphorylation Is a Metabolic Vulnerability in Chemotherapy-Resistant Triple-Negative Breast Cancer. *Cancer Res.* **81**, 5572–5581 (2021).

27. Mertens, R. T. *et al.* A gold-based inhibitor of oxidative phosphorylation is effective against triple negative breast cancer. *Biomed. Pharmacother.* **170**, 116010 (2024).

28. Uslu, C., Kapan, E. & Lyakhovich, A. Cancer resistance and metastasis are maintained through oxidative phosphorylation. *Cancer Lett.* **587**, 216705 (2024).

29. Pal, S. K., Childs, B. H. & Pegram, M. Triple negative breast cancer: unmet medical needs. *Breast Cancer Res. Treat.* **125**, 627–636 (2011).

30. Guihurt Santiago, J. *et al.* Adhesion G protein-coupled receptor, ELTD1, is a potential therapeutic target for retinoblastoma migration and invasion. *BMC Cancer* **21**, 53 (2021).

31. Stephan, G., Ravn-Boess, N. & Placantonakis, D. G. Adhesion G protein-coupled receptors in glioblastoma. *Neuro-Oncol. Adv.* **3**, vdab046 (2021).

32. Schiöth, H. B., Nordström, K. J. V. & Fredriksson, R. The adhesion GPCRs; gene repertoire, phylogeny and evolution. *Adv. Exp. Med. Biol.* **706**, 1–13 (2010).

33. Abdulkareem, N. M. *et al.* A novel role of ADGRF1 (GPR110) in promoting cellular quiescence and chemoresistance in human epidermal growth factor receptor 2-positive breast cancer. *FASEB J. Off. Publ. Fed. Am. Soc. Exp. Biol.* **35**, e21719 (2021).

34. Nam, H.-J., Kim, Y.-J., Kang, J.-H. & Lee, S.-J. GPR110 promotes progression and metastasis of triple-negative breast cancer. *Cell Death Discov.* **8**, 271 (2022).

35. Guo, D. *et al.* GPR116 receptor regulates the antitumor function of NK cells via Gαq/HIF1α/NF-κB signaling pathway as a potential immune checkpoint. *Cell Biosci.* **13**, 51 (2023).

36. Chen, Z. *et al.* Genetic analysis of Wnt/PCP genes in neural tube defects. *BMC Med. Genomics* **11**, 38 (2018).

37. Zhou, X. *et al.* Silencing Celsr2 inhibits the proliferation and migration of Schwann

cells through suppressing the Wnt/β-catenin signaling pathway. *Biochem. Biophys. Res. Commun.* **533**, 623–630 (2020).

38. Shima, Y. *et al.* Differential expression of the seven-pass transmembrane cadherin genes Celsr1-3 and distribution of the Celsr2 protein during mouse development. *Dev. Dyn. Off. Publ. Am. Assoc. Anat.* **223**, 321–332 (2002).

39. Kimura, H., Usui, T., Tsubouchi, A. & Uemura, T. Potential dual molecular interaction of the Drosophila 7-pass transmembrane cadherin Flamingo in dendritic morphogenesis. *J. Cell Sci.* **119**, 1118–1129 (2006).

40. Shima, Y. *et al.* Opposing roles in neurite growth control by two seven-pass transmembrane cadherins. *Nat. Neurosci.* **10**, 963–969 (2007).

41. Tissir, F. *et al.* Lack of cadherins Celsr2 and Celsr3 impairs ependymal ciliogenesis, leading to fatal hydrocephalus. *Nat. Neurosci.* **13**, 700–707 (2010).

42. Li, C. *et al.* Planar cell polarity protein Celsr2 maintains structural and functional integrity of adult cortical synapses. *Prog. Neurobiol.* **219**, 102352 (2022).

43. Qu, Y. *et al.* Genetic evidence that Celsr3 and Celsr2, together with Fzd3, regulate forebrain wiring in a Vangl-independent manner. *Proc. Natl. Acad. Sci. U. S. A.* **111**, E2996-3004 (2014).

44. Chaudhary, P. K. & Kim, S. An Insight into GPCR and G-Proteins as Cancer Drivers. *Cells* **10**, 3288 (2021).

45. Hanahan, D. & Weinberg, R. A. Hallmarks of Cancer: The Next Generation. *Cell* **144**, 646–674 (2011).

46. Pavlova, N. N. & Thompson, C. B. THE EMERGING HALLMARKS OF CANCER METABOLISM. *Cell Metab.* **23**, 27–47 (2016).

47. Yap, T. A. *et al.* First-in-human biomarker-driven phase I trial of the potent and selective glutaminase-1 (GLS1) inhibitor IACS-6274 (IPN60090) in patients (pts) with molecularly selected advanced solid tumors. *J. Clin. Oncol.* **39**, 3001–3001 (2021).

48. Mullard, A. Cancer metabolism pipeline breaks new ground. *Nat. Rev. Drug Discov.*

15, 735–737 (2016).

49. Goodwin, P. J. *et al.* Effect of metformin vs placebo on and metabolic factors in NCIC CTG MA.32. *J. Natl. Cancer Inst.* **107**, djv006 (2015).

50. Stine, Z. E., Schug, Z. T., Salvino, J. M. & Dang, C. V. Targeting cancer metabolism in the era of precision oncology. *Nat. Rev. Drug Discov.* **21**, 141–162 (2022).

51. Winter, M. *et al.* Mitochondrial adaptation decreases drug sensitivity of persistent triple negative breast cancer cells surviving combinatory and sequential chemotherapy. *Neoplasia N. Y. N* **46**, 100949 (2023).

52. El-Botty, R. *et al.* Oxidative phosphorylation is a metabolic vulnerability of endocrine therapy and palbociclib resistant metastatic breast cancers. *Nat. Commun.* **14**, 4221 (2023).

53. Ramchandani, D. *et al.* Copper depletion modulates mitochondrial oxidative phosphorylation to impair triple negative breast cancer metastasis. *Nat. Commun.* **12**, 7311 (2021).

54. Matrella, M. L. *et al.* High OXPHOS efficiency in RA-FUdr-differentiated SH-SY5Y cells: involvement of cAMP signalling and respiratory supercomplexes. *Sci. Rep.* **14**, 7411 (2024).

55. De Rasmo, D., Signorile, A., Roca, E. & Papa, S. cAMP response element-binding protein (CREB) is imported into mitochondria and promotes protein synthesis. *FEBS J.* **276**, 4325–4333 (2009).

56. Simula, L. *et al.* Mitochondrial metabolism sustains CD8+ T cell migration for an efficient infiltration into solid tumors. *Nat. Commun.* **15**, 2203 (2024).

57. Ren, L. *et al.* PHB2 promotes colorectal cancer cell proliferation and tumorigenesis through NDUFS1-mediated oxidative phosphorylation. *Cell Death Dis.* **14**, 1–11 (2023).

58. Yang, E. Y. & Shah, K. Nanobodies: Next Generation of Cancer Diagnostics and Therapeutics. *Front. Oncol.* **10**, 1182 (2020).

59. Rossotti, M. A., Bélanger, K., Henry, K. A. & Tanha, J. Immunogenicity and

humanization of single-domain antibodies. *FEBS J.* **289**, 4304–4327 (2022).

60. Kang, W. *et al.* Nanobody Conjugates for Targeted Cancer Therapy and Imaging. *Technol. Cancer Res. Treat.* **20**, 15330338211010117 (2021).

61. Ahl, P. J. *et al.* Met-Flow, a strategy for single-cell metabolic analysis highlights dynamic changes in immune subpopulations. *Commun. Biol.* **3**, 305 (2020).

62. Argüello, R. J. *et al.* SCENITH: A flow cytometry based method to functionally profile energy metabolism with single cell resolution. *Cell Metab.* **32**, 1063-1075.e7 (2020).

63. Sørlie, T. *et al.* Gene expression patterns of breast carcinomas distinguish tumor subclasses with clinical implications. *Proc. Natl. Acad. Sci. U. S. A.* **98**, 10869–10874 (2001).

Other results :

CELSR2 mediates cell adhesion to the matrix :

Considering that CELSR2 is both classified as an atypical cadherin, an adhesion GPCR and the presence of 9 cadherins repeats, which make up a third of CELSR2 protein and half of the extracellular fragment, we sought to investigate the possible role of the receptor in mediating cell adhesion. We coated 96 well plates with a matrix then seeded 5000 cells either wild type or silenced for CELSR2. Wells were washed and adhered cells were fixed and stained with crystal violet. It was then dissolved with SDS 1% and the absorbance, which reflects the number of adhered cells, was measured at OD570nm. These assays reveal an impaired adhesion capacity of the cells to the matrix upon the knockdown of CELSR2 (Figure 39). The same phenotype was observed with MCF7 cells, a non TNBC cell line, suggesting a cancer type independent role. Additionally, it has been elegantly demonstrated that CELSR1 plays a potent role in mediating cell-cell junctions, while CELSR2 is less efficiently recruited to the junctions[269]. These results, together with our findings, hint at possible different adhesive properties of the two paralogs, where CELSR1 promotes cell-cell adhesion while CELSR2 plays a more potent role in mediating cell-matrix adhesion.

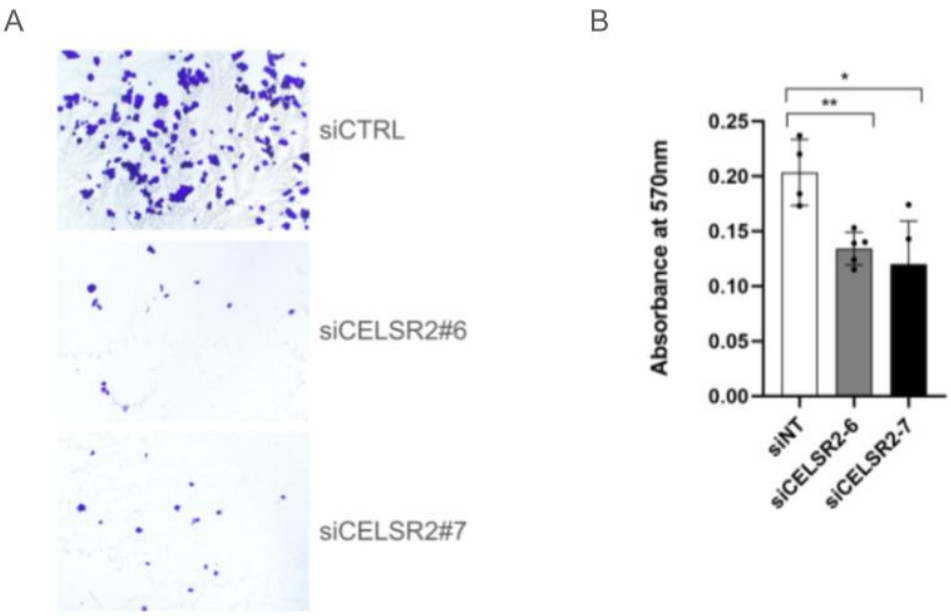

Figure 39 : CELSR2 mediates cell adhesion to the extracellular matrix. (A) representative snaps of cells adhered to the collagen matrix following treatment with siCTRL or siCELSR2. (B) bar chart of the quantification of adhered cells presented as mean ± SEM (n=3)

Tethered agonist exposure does not induce CELSR2 activation :

As described above, aGPCRs have an autoproteolytic site and harbor a tethered agonist within the GAIN domain. The cleavage of the NTF fragment and the subsequent exposure of the tethered agonist induces the receptor activation. This phenomenon has been observed for a number of GPCRs of which GPR126, GPR133 and VLGR1[248,424]. First, we wanted to determine if a cleavage of the receptor takes place. We collected the supernatant of wild type cells and CELSR2 knockout cells. By utilizing a commercial antibody recognizing the residues around the amino acid at position 1781 within the extracellular fragment (Figure 40A), we found that CELSR2 is present in the supernatant of wild type cells while being absent as expected in the knockout cells (Figure 40C). The size of the CELSR2 fragment revealed by western blot in the supernatant corresponds to the size of the NTF. Based on this finding, we aimed to investigate whether CELSR2 can be activated by an acute exposure to the tethered agonist. We synthesized a 19 amino acids long Stachel peptide and a Scramble peptide (Table 7). The Stachel peptide had a 95% purity and the scramble had a 75% purity. We treated HEK293 cells transfected, with an empty vector or full length CELSR2, with concentrations of the peptides ranging from 1µM to 10nM and conducted a luciferase reporter assay of the previously reported downstream pathways. When compared to the scramble peptide, the Stachel peptide did not induce the activation of any of the pathways (Figure 40D). Our experimental settings could be improved by testing different lengths of the Stachel peptide, as it has been reported that a shorter length could induce a greater receptor activation. Specifically, an optimization of the length is necessary as the most efficient Stachel peptide can vary between 7 and 18 amino acids[247,248,425,426]. Moreover, the concentrations we used in our study are lower than what is described in the literature. Moreover, in a study where the full length CELSR2 was shown to couple to Gαs in BRET assays, a PAR-CELSR2 construct, which allows for an acute tethered agonist exposure following treatment with thrombin, did not show an efficient coupling to Gαs, other G proteins, as well arrestins recruitment[354]. Recently, another independent study which assessed the tethered agonist signaling in aGPCRs corroborated that an acute exposure to the tethered agonist of CELSR2 does not translate onto a signaling activity. Moreover, the

study showed that about half of aGPCRs are not activated by their predicted internal agonist[427].

Table 7 : Stachel and Scramble peptides sequence

Stachel sequence	TSFAVLMDVSRRENGEILP
Scramble sequence	NSREVARIGLLMTVEDSFP

A

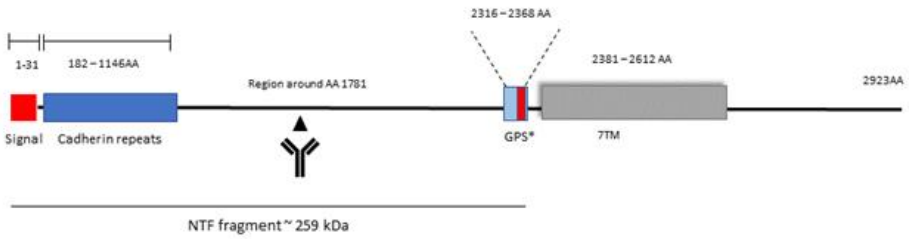
1-31
182 – 1146AA
Signal
Cadherin repeats
Region around AA 1781
2316 – 2368 AA
GPS*
2381 – 2612 AA
7TM
2923AA
NTF fragment ~ 259 kDa

B

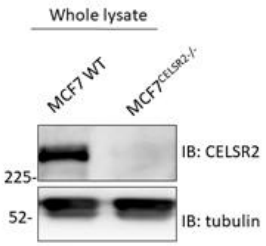
Whole lysate
MCF7 WT
MCF7CELSR2-/-
225-
IB: CELSR2
52-
IB: tubulin

C

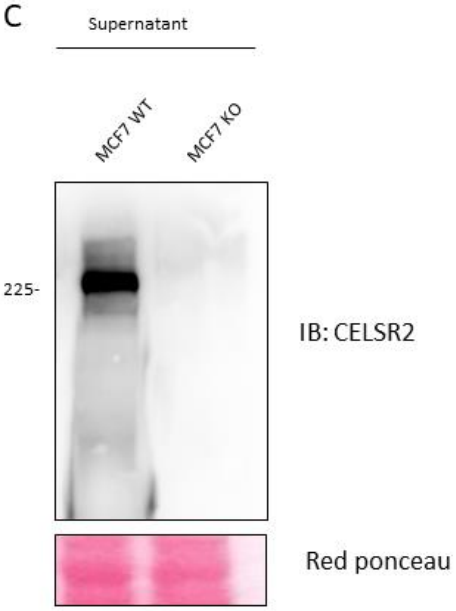
Supernatant
MCF7 WT
MCF7 KO
225-
IB: CELSR2
Red ponceau

D

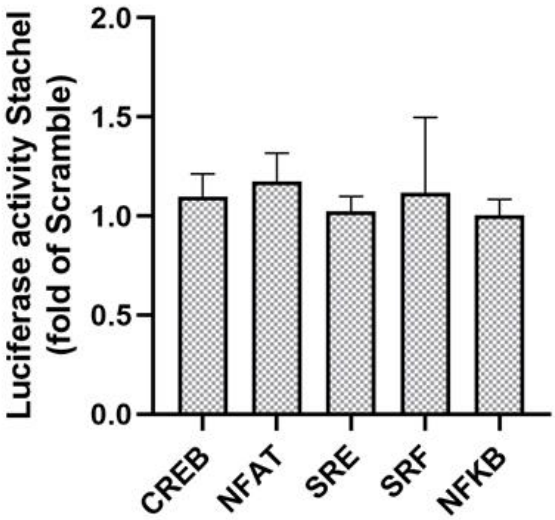
Luciferase activity Stachel (fold of Scramble)
2.0
1.5
1.0
0.5
0.0
CREB
NFAT
SRE
SRF
NFKB

Figure 40 : CELSR2 tethered agonist does not activate the canonical GPCR signaling (A) schematic representation of CELSR2 structure. The monoclonal antibody used to detect the receptor in the supernatant targets residues around the amino acid 1781. (B) CELSR2 detection by western blot in whole cell lysate of MCF7 WT and MCF7 KO cells. (C) CELSR2 detection by western blot in the supernatant of MCF7 WT and KO cells. (D) CRE, NFAT, SRE, SRF and NfKB luciferase reporter activity of cells treated with the Stachel peptide. Data normalized to the mean value of cells treated with a scramble peptide and are presented as mean ± SEM (n=3)

CELSR2 silencing does not sensitize cells to chemotherapies :

Currently, systemic cytotoxic chemotherapy is the mainstay of TNBC treatment. Although some targeted therapies have been approved, yet only a fraction of patients are eligible. Relapsed and metastatic TNBC tumors display an aggressive phenotype and a high resistance to chemotherapy. Many pathways contribute to the onset of drug resistance which remains a major challenge in oncology. Wnt signaling has been shown to induce drug resistance through various mechanisms of which maintaining cancer stem cell population, enhancing DNA damage repair and the promotion of immune evasion[428–430]. Equally importantly, OXPHOS has been reported to be implicated in the drug resistance process by providing tumor cells with very high loads of ATP for their survival, enhancing antioxidant defenses and detoxifying ROS, maintaining mitochondrial membrane potential, thus rendering cells less sensitive to apoptosis, and the upregulation of anti-apoptotic genes[431–435]. Given this background, the implication of CELSR2 as a core component of the Wnt/PCP pathway and its role in promoting OXPHOS, we postulated that the inactivation of CELSR2, thus its downstream signaling and cellular function, would render TNBC cells sensitive to standard chemotherapeutics currently used in the clinic.

We have selected a list of 21 drugs listed in table 8 :

Table 8 : list of used chemotherapeutic compounds to investigate drug resistance :

stock mM			dose max
10	1	Afatinib	50
10	2	Carboplatine	50
10	3	Cisplatine	50
10	4	Erlotinib	50
10	5	Everolimus	50
10	6	Gefitinib	50
10	7	Gemcitabine	50
10	8	Gilteritinib	50
10	9	lapatinib	50
10	10	Olaparib	50
10	11	palbociclib	50
10	12	Seliciclib	50
10	13	Trametinib	50
10	14	Doxorubicine	50
10	15	Paclitaxel	50
10	16	Masitinib	50
4	17	Bortezomib	20
10	18	Metformin DMSO	50
10	19	docetaxel	50
0.02	20	docetaxel	0.0005
1M	21	Metformin H2O	100 mM

3 TNBC cell lines were used in the assay : MDA-MB468, HCC1806 and BT20. Cells were transfected with siCELSR2 or siCTRL, treated with chemotherapeutics and seeded either in 384 and 96 well plates. Cell viability was assessed 72h later with cell titer glo. An initial screen of drugs reveals a gain of sensitivity to doxorubicin, docetaxel and everolimus (Figure 41A). A second screen focused on these specific drugs did not confirm the initial results, as no sensitivity gain was observed following CELSR2 knockdown (Figure 41B).

A

Drug	HCC1806		BT20		MDA-MB468	
	siCELSR2#1	siCELSR2#2	siCELSR2#1	siCELSR2#2	siCELSR2#1	siCELSR2#2
Afatinib	0.76	1.16	0.54	0.68	0.76	1.16
Carboplatine	1.00	1.00	1.00	1.00	1.00	1.00
Cisplatine			1.00	1.00		
Erlotinib	1.00	1.00	0.77	0.97	1.00	1.00
Gefitinib	0.96	1.00	0.79	0.68	0.96	1.00
Gemcitabine		0.71	0.91	0.62		0.71
Epirubicine	0.62	1.00	0.63	0.78	0.62	1.00
Epirubicine(exclu 2doses)	0.75	1.18	0.66	0.81	0.75	1.18
lapatinib	0.56	0.96	0.78	0.94	0.56	0.96
Olaparib	1.02	0.89	0.95	0.93	1.02	0.89
palbociclib	0.83	0.91	0.79	0.94	0.83	0.91
Seliciclib	0.67	0.80	0.66	1.00	0.67	0.80
Trametinib	0.55	1.06	0.71	0.81	0.55	1.06
Trametinib(exclu 2doses)	0.63	1.17	0.15	0.08	0.63	1.17
Doxorubicine	0.20	0.69	0.56	0.34	0.20	0.69
Masitinib	0.79	1.05	0.89	0.94	0.79	1.05
docetaxel	0.07	0.54	0.04	0.03	0.07	0.54
docetaxel	0.32	0.99	0.35	0.21	0.32	0.99
docetaxel(exc 1dose)	0.31	1.00	0.57	0.46	0.31	1.00
docetaxel	0.10	0.57	0.12	0.11	0.10	0.57
Metformin H2O	0.75	1.15	0.35	0.21	0.75	1.15
Paclitaxel			1.00	1.10		
Bortezomib	0.83	0.90	0.57	0.38	0.83	0.90
Everolimus 100	0.46	0.81	0.81	0.94	0.46	0.81
Everolimus 0.01	0.52	0.95	0.29	0.28	0.52	0.95
Everolimus mix	0.30	0.85	0.32	0.21	0.30	0.85

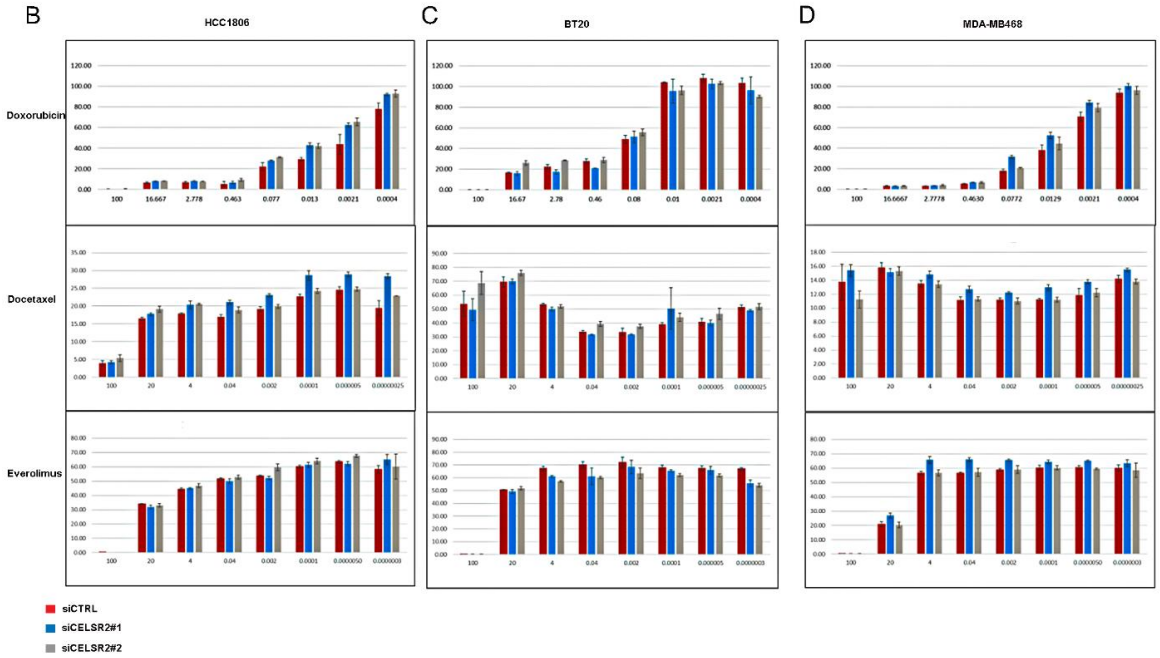

Figure 41 : CELSR2 inhibition does not sensitize cells to chemotherapies used in TNBC. (A) results of the first drug screen on HCC1806, BT20 and MDA-MB468

following CELSR2 silencing. Values represent cell viability of treated cells over control (DMSO). Green values indicate a sensitivity gain of silenced cells compared with the wild type (n=2). (B) Cell viability of the second drug screen with doxorubicin, docetaxel and everolimus. Data presented as mean ± SEM (n=4).

Our data did not conclude on a sensitivity nor a resistance gain to chemotherapies used for the treatment of TNBC following CELSR2 knockdown. The assay could be broadened to investigate the possible synergies with other chemotherapies. Assay ready plates could be used for large scale drug screens[436–438]. Moreover, further refinement should consider the use of 3D models as these can better recapitulate the biology of tumors, and they have been shown to respond in a substantially different manner than 2D cultures[439,440]. Furthermore, it would be a valuable to test the synergies of chemotherapeutics with our nanobodies targeting CELSR2 in controlling tumor growth and metastasis formation.

Discussion

Triple negative breast cancer poses up to date a difficult public health burden both on patients and care providers. As discussed in the opening of this work, several factors including the tumor heterogeneity both between patients and within the same patient, the high metastatic potential and the lack of targeted therapies all collude together to significantly diminish therapeutic choices and life expectancy of patients. There have been considerable efforts deployed to better understand the biology of TNBC. Briefly, we could cite all the funding allocated by the different research agencies worldwide and the wide application of multi omics approaches to identify vulnerabilities. Unfortunately, the complex technical approaches only revealed complex tumors, as reported by Lehmann and colleagues[77]. The approval to clinical use of the anti-TROP2 ADC, the ICIs and the PARP inhibitors benefits a defined proportion of patients but is still insufficient, as no drug can fit all patients.. Indeed, given the large heterogeneity

observed in TNBC patients, identifying new targets will help overcome gray zones of therapy and unmet needs.

It is in this overall context that we investigated whether CELSR2 could be a potent target in TNBC. This receptor has a dual affiliation, one with the GPCR superfamily, and the other with the developmental pathways, specifically the Wnt/planar cell polarity. Very few works have been conducted on the receptor for various reasons. First, the limited interest in the involvement of embryonic pathways in cancer development. In contrast, other research areas such as the immunology of tumors, genomic instability and tumor associated antigens draw much more attention both from the academic community and the pharmaceutical industry. This can be reflected in the number of academic papers published every year and the approval of multiple drugs accounting for more than a third of marketed drugs for cancer care for the last 20 years (Figure 15). On the other hand, drugging developmental pathways such as the Wnt related pathways did not result in much success as it's been challenging to find the proper balance between safety and efficacy[441]. Additionally, CELSR2 as an adhesion GPCR did not attract the same attention as other members such as CD97, EMR1, GPR56…etc. Working with large receptors such as CELSR2 can be particularly challenging due to the limited availability of tools and the difficult task of manipulating large proteins.

Amid this challenging, yet stimulating research niche, we have been able to identify the potent role played by CELSR2 in various processes of tumorigenesis both in vitro and in vivo. We unveiled the probable mechanism by which CELSR2 promotes tumor progression. CELSR2 signaling was found to induce the activation of the cAMP/PKA/CREB pathway to promote energy metabolism and the expression of a number of oxidative phosphorylation related genes to enable tumor cell processes. Finally, by immunizing a llama, we have been able to discover nanobodies specific to CELSR2. Their use in vitro showed that they potently inhibited cell migration thus hyping future investigations on the potential targeting of CELSR2 for therapeutic ends.

CELSR2 expression in TNBC tumors :

Starting from a survival analysis of CELSR2 in TNBC patient data from the Institut Paoli Calmettes and the TCGA, we found a significantly decreased overall survival and metastasis free survival in patients with an upregulated expression (Paper figure 1 C-D). A further analysis of the publicly available data of the AURORA cohort in which a total of 55 tumors of female patients presenting a metastatic TNBC were sequenced. The study also included the sequencing of the metastatic site. Similarly to the TCGA data, no overexpression was observed in the TNBC patients of the cohort. Upon pairing the expression between the primary site and the metastatic site, we find an upregulation of CELSR2 expression. The upregulation in the metastatic site was exclusive to TNBC patients (Paper figure 1E). Moreover, this trend was not observed with the two other paralogs CELSR1 and CELSR3, nor with some other proteins of Wnt/PCP pathways, such as VANGL2, PTK7 and Prickle-1. These findings hint at a possible proper role for CELSR2 in the metastatic site. To deepen our understanding of the receptor, we analyzed single cell RNA-sequencing data of both healthy tissues and TNBC tumors. In adult healthy tissues, we found a concentrated expression in the brain, specifically in oligodendrocytes, while the expression in all other tissues was significantly lower. Very interestingly, the expression of CELSR2 in tumors seemed to be restricted to the malignant cells of TNBC tumors (Figure 1 F-G). These findings are a first concerning the involvement of CELSR2 in tumor development and the compartmentalization of its expression. The low expression in healthy tissues opens a promising therapeutic window in which a targeting of the receptor would be highly concentrated on the tumor, therefore a receptor targeting with an ADC or CAR-T cells will in theory induce limited undesired toxicity.

A new role for CELSR2 in breast tumor development:

The results of this study indicate that CELSR2 is involved in various functions that cooperate to promote tumor development. Upon knockdown of CELSR2 by siRNA or shRNA, we found a significantly decreased cell motility in wound healing of multiple TNBC cell lines : MDA-MB468, BT20, HCC1806 (Paper figure 3E-G) and also a luminal cell line MCF7(data not reported here). A similar result was observed in Boyden chamber migration assay, in which MDA-MB468 in suspension was assessed

for its migration through the chamber membrane (Figure 3H). Additionally to the involvement in migration, a similar silencing strategy reveals a decreased proliferation of cells and invasion through the matrix (Paper figure 3I-J). All these processes which were altered by the silencing of CELSR2 are critical for tumor development. A targeting of CELSR2 would render tumor cells highly vulnerable and open a window for tumor neutralization by cytotoxic chemotherapies. The observations made in vitro were partially echoed in vivo. Indeed, an orthotopic xenograft of MDA-MB468 cells transduced with CELSR2 targeting shRNA showed a slower tumor growth when compared with scramble shRNA, mimicking the slower proliferation rate observed in vitro. The IHC staining of the proliferation marker Ki67 was significantly reduced in shCELSR2 tumors when compared with wild type controls. Yet we did not observe a significant differential in metastasis formation, owing to the very high metastatic potential of the cell line, known also for its distinctive overexpression of EGFR[442]. Indeed, while tumor volumes were relatively low at the endpoint (less than 100mm^3 in all conditions), metastasis to the lungs and lymph nodes was observed in both experimental conditions, although some tendencies were observed (Paper supplementary figure 2) . An alternative strategy to demonstrate the involvement of the receptor in metastasis formation would be to xenograft a less aggressive cell line and optimize the endpoint of the protocol in order to identify the finest moment to assess metastatic formation.

CELSR2 acting as an adhesion molecule :

An interesting aspect that we investigated briefly at the beginning of this project was the role of CELSR2 in mediating the adhesion to the extracellular matrix. Given the presence of 9 cadherin repeats in the extracellular fragment of CELSR2, one could easily postulate the involvement of the receptor in adhesion processes. When we silenced the receptor with siRNA, we observed a decreased adhesion to different matrices such as collagen, laminin and matrigel. These experiments were carried out both in MDA-MB468, a TNBC cell line, and MCF7, a luminal cell line (Figure 39) . We then revisited our mass spectrometry data in which we downregulated CELSR2 and analyzed the whole proteome of cells, we found Integrin beta 4 and Paxillin among the significantly downregulated proteins(Figure 42).

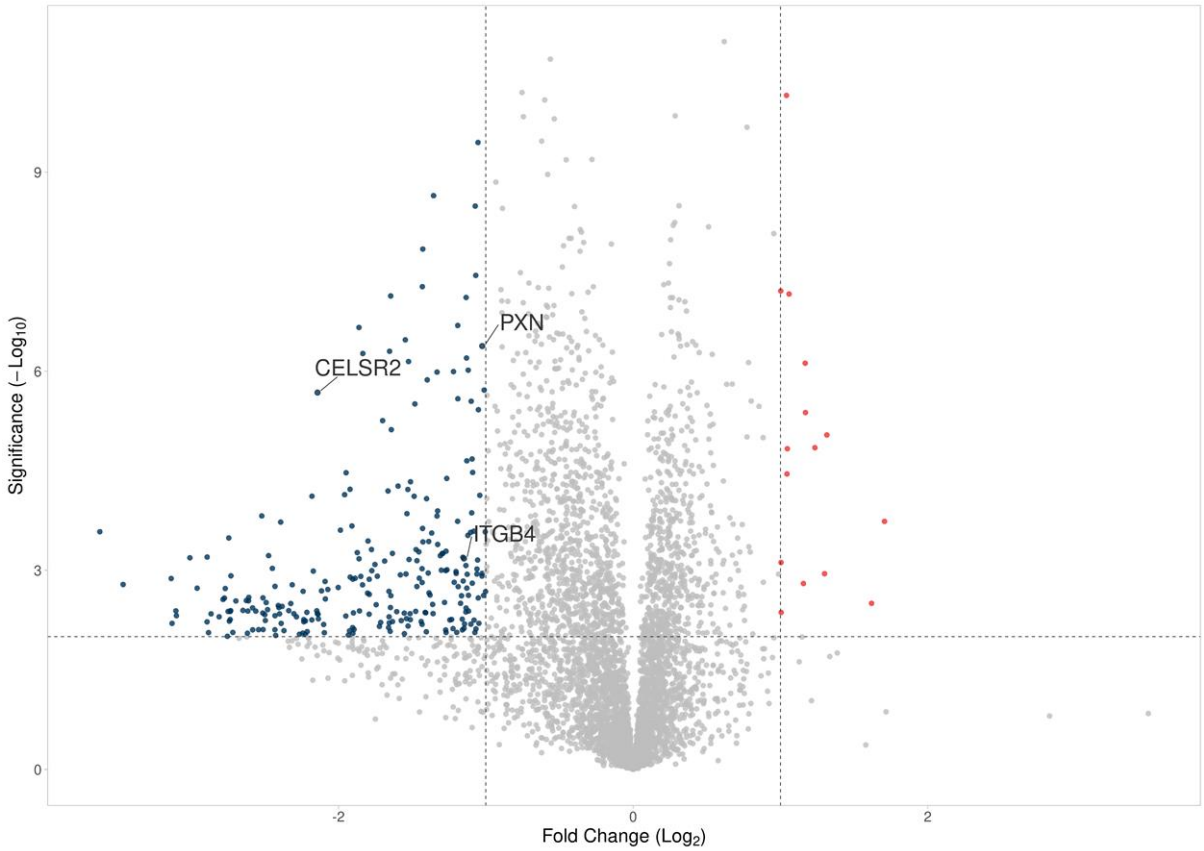

Figure 42 :

The adhesion properties of CELSR2 could further be reflected in the reported interaction of the receptor with various adhesive proteins as reported on Biogrid (https://thebiogrid.org/) such as Cadherins 8 and 16, protocadherins 12 and 20, CEACAM21, FLRT1…etc (Figure 43). Cell adhesion and migration are tightly intertwined[443]. Cells have been reported to have the capacity to migrate collectively without the disruption of cell-cell junctions, with the support of E-cadherin and integrins which bind to the extracellular matrix, supporting cell cohesion[444]. It is in this overall landscape that CELSR2 adhesive properties would contribute to binding to the extracellular matrix and facilitate the migration phenotype observed in in vitro assays reported in this study (Paper figure 3E-G).

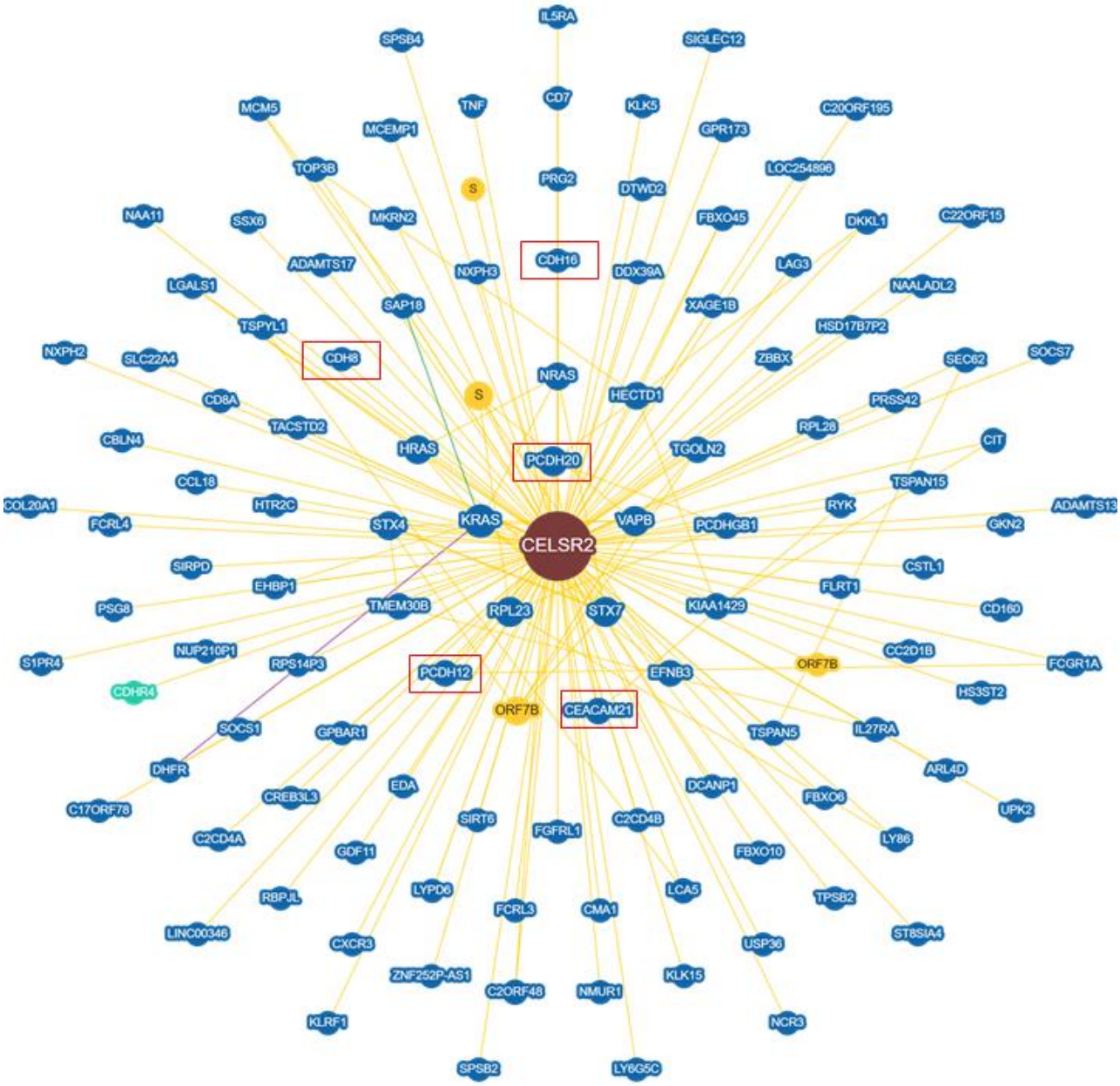

Figure 43 : Network map of CELSR2 interactors (thebiogrid.org)

Biased agonism of CELSR2 :

The ability selectively to activate one of the G-proteins (Gαs, Gαq/11, Gαi/o, or Gα12/13) is a distinctive feature of a biased GPCR ligand. This allows the ligand to selectively mobilize and exploit a particular GPCR conformation and GPCR-mediated downstream signaling pathway in a variety of metabolic disease systems, including cancer[445]. aGPCRs have been shown to be activated by different G-proteins depending on the context. For example, VLGR1 was found to be activated by Gαi,

Gαs and Gαq[446,447]. One of the best examples of the implications of biased agonism in cancer progression is the signaling of chemokines. These are chemotactic cytokines which orchestrate cell migration along a certain path. The path is set by increasing concentrations of the chemokines[448]. Mechanistically, chemokines bind their cognate receptors which are GPCRs and trigger a calcium influx. Intriguingly, the chemokines induce chemotaxis in range above a certain minimum and below a maximum in a biphasic manner[449]. The suggested underlying mechanism is that high concentration of a chemokine induces the formation of complexes comprising two molecules of the cytokine[450]. The binding of a single chemokine molecule or a complex of two molecules has been shown to induce different signaling cascades and cellular functions (Figure 45). Indeed, the single molecule can induce the activation of both Gαi and β-arrestin signaling. The activation of both pathways is capable of promoting cell motility. On the other hand, the binding of a complex inhibits β-arrestin signaling which results in a decreased cell migration[451]. Biased agonism can be exploited to target a specific signaling pathway of a GPCR in order to maximize the therapeutic effects of compounds or biologics. In our study, we find that CELSR2 activates not only Gαs, but also G12/13. Further studies could investigate how the inhibition of a specific signaling pathway affects tumor cells and assess whether exploiting a biased agonist strategy could potentiate more a therapy targeting CELSR2.

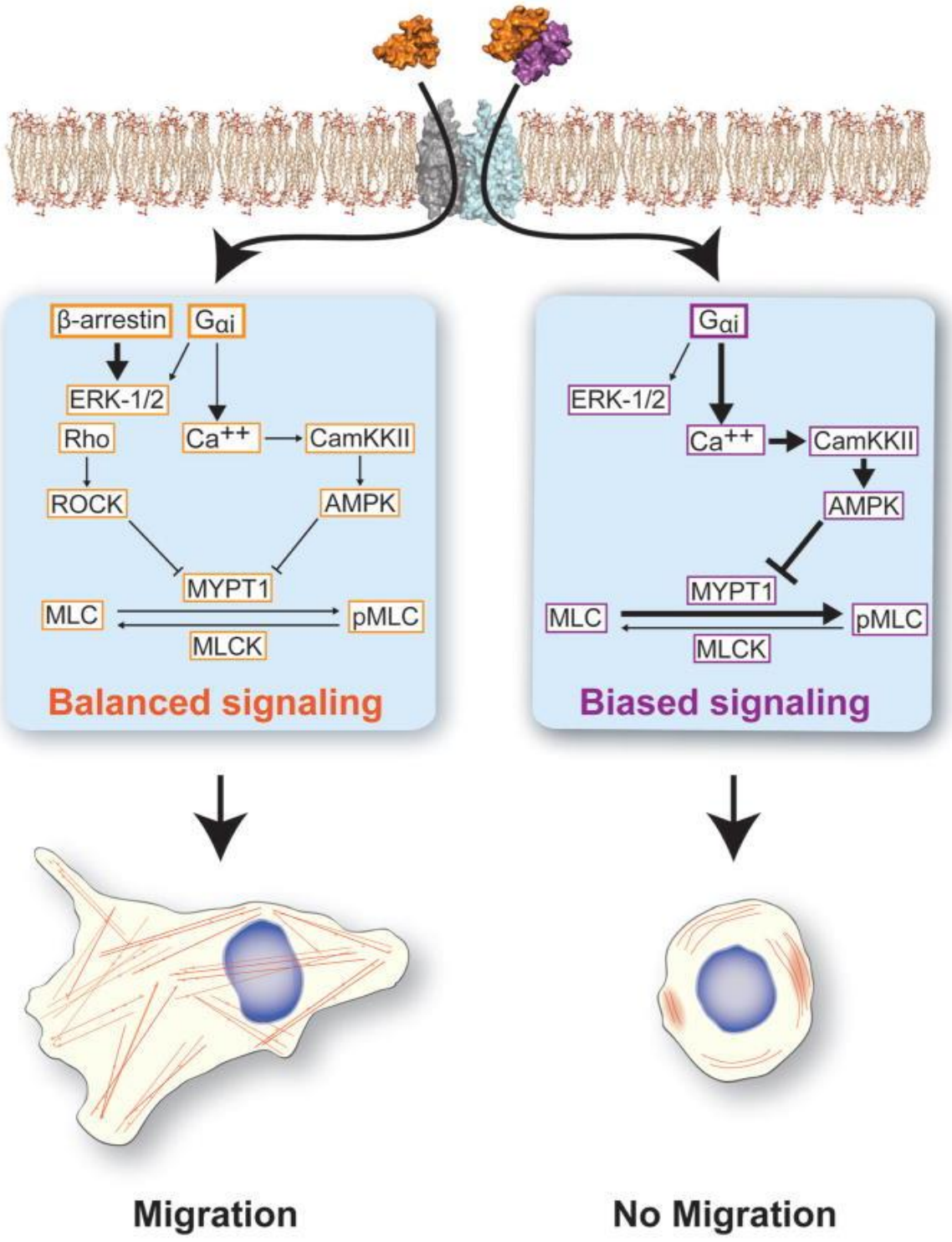

Figure 45 : ligand binding to a GPCR dictates a given downstream signaling[451]

Mechanism of CELSR2 in orchestrating tumor cells metabolism, proliferation and migration:

Considering the reports outlining that CELSR2 couples to Gαs[354], we investigated the signaling cascade downstream of Gαs. We found that CELSR2 ectopic expression activates CREB. Conversely, receptor silencing suppressed CREB signaling (Paper figure 4A, D). In order to gain an overview of the functions of CELSR2, we analyzed the total proteome of cells following CELSR2 silencing by mass spectrometry and compared with wild type cells. Interestingly, very few proteins were upregulated while a few hundreds were downregulated along with CELSR2 (Paper figure 5B). Most of these proteins were localized in the mitochondria and upon running a pathway analysis, it shows that the downregulated proteins mostly regulated the Krebs cycle and oxidative phosphorylation. In line with the literature, It has been reported that Gαs coupled GPCRs exert a function of gluconeogenesis and glycogenolysis by activating PKA, which in turn induces the expression of glucose-6-phosphatase (G6pc) and phosphoenolpyruvate carboxykinase (PCK)[452]. Interestingly, PCK2 is found to be downregulated as we silence CELSR2 in our experiments among other TCA and OXPHOS proteins such as NUBPL, ALDH1, IDH3, OGDH…etc. The activation of the cAMP/PKA/CREB pathway induces the expression of a number of CREB target gene products which are found to be downregulated in our study following CELSR2 silencing. Indeed, proteins such as OGDH, NUBPL, NDUFV3, ARG2, ATP5D play a role in the oxidative phosphorylation process and are found to be significantly downregulated. It suggests a direct effect between the inhibition of signaling through CREB, following celsr2 silencing, and the OXPHOS state of the cells. It could be interesting to further investigate whether our observations are reflected in other tumors and non cancerous study models.

Accordingly, in vitro assessment of cell bioenergetics upon CELSR2 knockdown reveals a decreased maximal respiration of cells (Paper figure 5H-I). Moreover, CELSR2 transcripts are found to be highly correlated with transcripts of OXPHOS genes and negatively correlated with glycolytic transcripts. Therefore, our data suggest an important role of CELSR2 in the regulation of cellular metabolism in particular oxidative phosphorylation.

OXPHOS has been demonstrated to be the top pathway associated with worse TNBC patient outcomes. Moreover, specific inhibition of the OXPHOS pathway neutralizes tumor growth[453]. OXPHOS implication in cell proliferation both in vitro and in vivo has been reported in multiple studies covering a wide range of cancers and cells[433,454–456]. OXPHOS stimulates proliferation by mediating the production of energy and the supply of metabolic intermediates such as lipids, amino acids and nucleotides[456]. The connection between energy metabolism and cell motility has been well documented in various cell types[457–459]. Indeed, it has been shown that migratory cells, especially leader cells may upregulate OXPHOS genes in order to ensure sufficient ATP is produced even in conditions where low glucose levels are available[460]. In this context, CELSR2 likely plays complementary functions of mediating adhesion to the extracellular matrix and potentiating the OXPHOS to enhance the migratory capacity of cells.

CELSR2 specific nanobodies discovery :

As we progressed in the understanding of the biology of CELSR2 in TNBC, we aimed to develop tools that can effectively target the receptor. We chose to work on discovering nanobodies, given the relatively low cost, the ease of manipulation, the novelty of using such fragments for cancer care and the expertise of our core facility “Antibody targeting and immunomodulation” in discovering nanobodies against tumor antigens. For my work, we decided to proceed with an immunization strategy of llama with the company Biotem. We isolated plasma membranes of MCF7 cells, which were previously selected for their high levels of CELSR2 mRNA and protein expression. Indeed, a search on DepMap (https://depmap.org/portal/) reveals that MCF7 was among the top CELSR2 expressing cell lines across all tumors. In total, we isolated the plasma membranes of 400 million cells concentrated in a total of 1mL. The isolated membrane fraction had relatively good purity with a high concentration of the receptor (Figure 6 of the paper). The immunization comprised 1 initial shot and 3 boosts. Biotem collected the PBMCs and isolated the mRNA which were sent back. The steps performed in our laboratory for library construction are described above. The selection of nanobodies consisted of depleting the phages on CELSR2 knockout MCF7 cells,

then a positive selection on wild type cells. The output of this first round was incubated with the recombinant extracellular CELSR2 that was produced in Expi293. The second output was re-infected in TG-1 bacteria. A total of 380 individual colonies encoding, in theory, unique nanobodies were picked for screening. The screening consisted of testing the selected nanobodies on MCF7 wild type cells, knockout cells, cell lines with varying levels of expression and recombinant protein. Out of the screen, we were able to identify two nanobodies with different sequences. The nanobodies exhibited different affinities in the submicromolar range. The number of specific nanobodies and their affinities were disappointing, as some nanobodies reported in the literature are in the subnanomolar range[461,462]. Nevertheless, it is worth considering the conserved nature of the GPCR family across species and therefore their low immunogenicity[463,464]. The discovery of these nanobodies is a foundational start to further studies in which attempts to improve affinity by site directed mutagenesis, somatic hypermutation or the design of a biparatopic construction. As discussed above, nanobodies offer a therapeutic platform with an outstanding potential due to their small size and high tissue penetration. Moreover, given the expression gain of CELSR2 in the metastatic sites of TNBC patients, it could offer an attractive opportunity to target not only the primary tumor but also brain metastasis, where other big molecules such as antibodies are excluded at the blood-brain barrier. The nanobodies can be used to target CELSR2 systemically but can be also utilized as part of CAR-T cell strategy, as this possibility only requires a receptor recognition instead of a functional nanobody. The possibility of using these nanobodies as ADCs is subject to the condition of internalization, which should be assessed in future investigations.

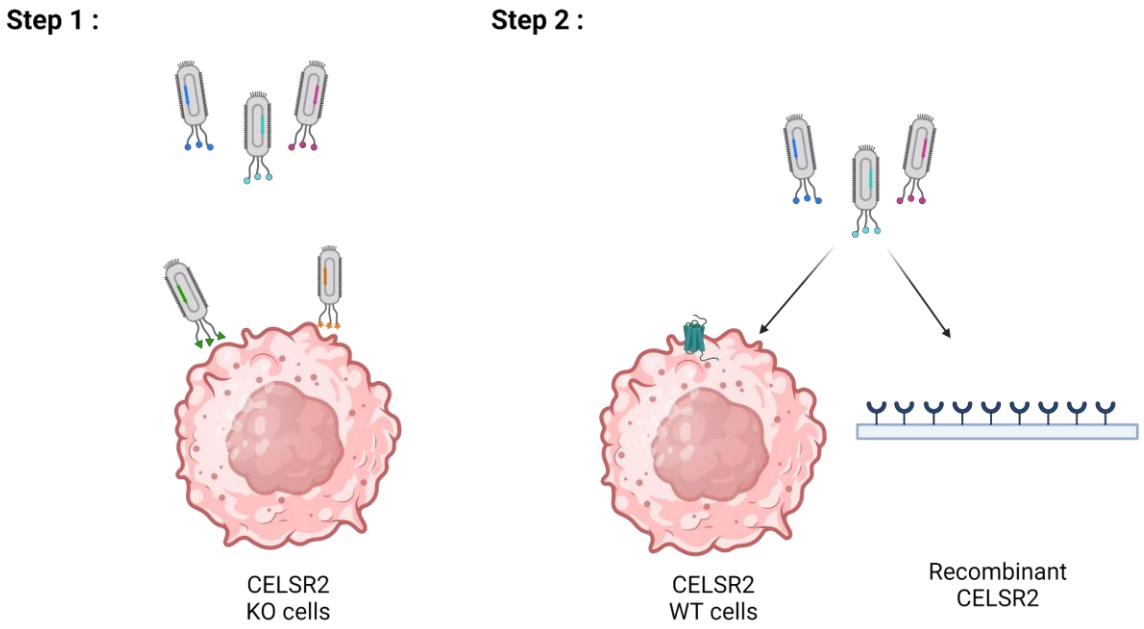

Figure 46 : Schematic representation of the selection strategy of the nanobodies. Step consists of non-specific phages depletion on knockout cells. Step 2 consists of a selection of the output phages from step 1 on WT cells and then on the recombinant extracellular fragment of CELSR2.

CELSR2 variants :

Surface proteins such as CELSR2 can be perceived as interfaces which scan the extracellular content and play a role in transducing a biochemical message. While more than half of all GPCRs have a single exon in their coding gene, aGPCRs have a median number of exons of 18, leaving an important window for alternative splicing[465]. As previously discussed, CELSR2 has a total of 35 exons and at least 7 transcript variants that are reported in the literature[466]. In the normal breast, there are two splice variants identified on Splice-O-Mat online application (https://tools.hornlab.org/Splice-O-Mat/), while 4 are found in fallopian tubes, 1 in each of the uterus, the ovaries and the cervix. Interestingly, the variants found in regions of the brain and other body sites are different. The study presented by Kuhn and colleagues incorporated only healthy tissues. So far, we do not have insight whether tumors produce a splice variant which is tumor specific. Variant consideration is important in a cancerous context, especially if the aim is to target the receptor with nanobodies or antibodies, as these, if raised against a variant non-existent in tumors, might not recognize the tumor antigen.

Conversely, it can be a valuable target to target a tumor specific splice variant, as this coils highly reduce off target effects and damage on healthy tissues[467].

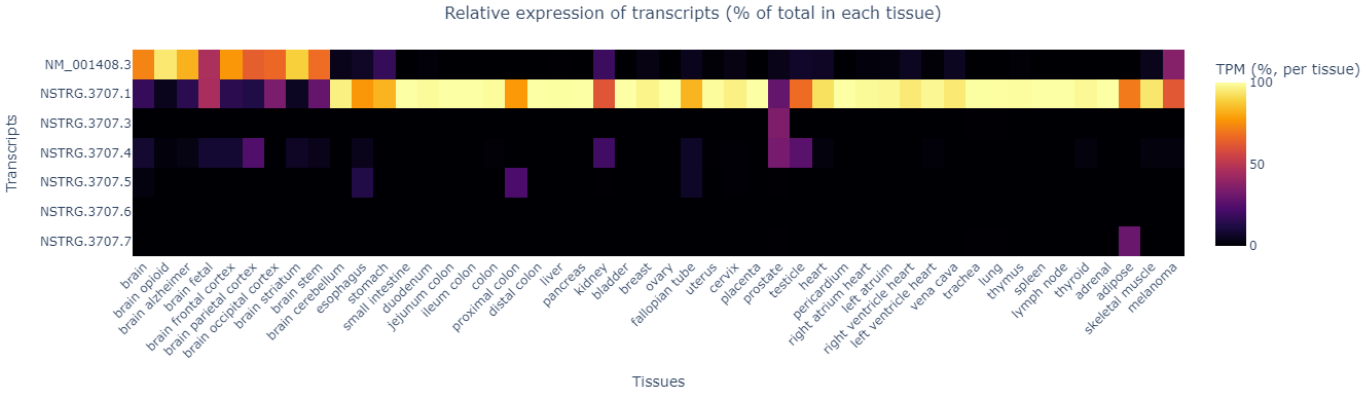

Figure 47 : Heatmap of the expression of splice variants of CELSR2 in different body sites.

Study limitations :

A cancer cell centered approach :

One of the limitations of the study is the tumor centered approach. Indeed, we have witnessed a shift in views and paradigms about carcinogenesis since the 1980s. The introduction of the tumor microenvironment as a central player proved to be a major leap forward in understanding cancer progression and developing therapeutic strategies. The role that CELSR2 plays in the tumor microenvironment remains elusive. How the expression of CELSR2 in tumor cells is influenced by clues from the microenvironment, and what the function of the receptor is in different cells remain unclear. Moreover, as much as this founding study on the role of CELSR2 in cancer provided insights about some functions and signaling cascade, receptor repression was only tested in immunodeficient mice. Moving to immunocompetent models could prove to be more challenging as the modulation of the activity of the receptor would incorporate many more variables thus making the resulting landscape unpredictable. Translating the use of CELSR2 to the clinic is even more unpredictable, as most trials fail to deliver the expected outcomes[468] . Altogether, these limitations hint at the limited resources, approaches and disciplines engaged in the discovery of novel therapeutic targets.

Additionally, as discussed above, the aGPCRs have large extracellular fragments with specific subdomains. The subdomains could potentially play specific roles in cell physiology. The investigation of the subdomains and subsequently attempting to target specific parts of the receptors can be a potent therapeutic strategy.

CELSR2 orphan status :

Moreover, as of now CELSR2 remains an orphan receptor. The identification of a natural ligand, whatever its function would be, can help understand better the biology of the receptor and unravel its potential implication in different physiological and pathological contexts. In our experience, the synthetic peptide of the Stachel sequence did not induce activation of the receptor even at very high concentrations. The possible limitation of our experiments might be the use of a single length of the peptide. Indeed, It has been demonstrated by Liebscher's lab and others that different peptide lengths could have an impact on the signaling induction[248]. It is not necessarily the full length Stachel peptide that is the most potent, it appears that physicochemical variables influence the binding and the activation. Therefore it will be with testing different lengths of the Stachel peptide and assess the activation of the receptor. If the Stachel is identified as a tethered agonist for CELSR2, it can be a valuable tool in elucidating other mechanisms of the receptor and could be used in other nanobodies discovery assays biased towards the identification of an agonist which competes with the Stachel[469].

Risks and limitations of targeting CELSR2 with nanobodies :

The use of nanobodies in clinical practice has so far been approved for at least two indications. The first being a nanobody directed at Von Wilbrand factor for the treatment of acquired thrombotic thrombocytopenic purpura[320]. The second is a BCMA-specific nanobody used as the targeting domain of CAR-T cells for the treatment of multiple myeloma[470]. Many Other nanobodies are currently at various phases of clinical trials for the treatment of various diseases, of which solid tumors and

hematological malignancies (Table 6)[398]. Other nanobodies are currently at various phases of clinical trials for the treatment of various diseases, of which solid tumors and hematological malignancies[471]. As discussed previously, nanobodies have a much shorter half-life when compared with antibodies. While it could prevent the advent of side effects due to a long exposure to the drug, it can also be a limiting factor. Nanobodies can be engineered to have an extended half-life, but might lose properties such as penetration in pockets inaccessible to conventional antibodies. Another challenge proper to the biology of CELSR2 is the receptor shedding. As we have demonstrated in the present study, the extracellular fragment is cleaved, most probably at the predicted GPS motif. This property of the receptor can alter the efficacy of the nanobodies as these can be neutralized in circulation even before reaching the tumor site. Moreover, it should not be ruled out that in the event of a therapeutic targeting, the shedding phenomenon would be intensified and become a resistance mechanism. Nevertheless, it is worth mentioning that many receptors that are currently targeted therapeutically in the clinic with antibodies or nanobodies are also reported to be shed such as EGFR and HER2[472,473].

References :

1. The Edwin Smith Surgical Papyrus, Volume 1: Hieroglyphic Transliteration, Translation, and Commentary | Institute for the Study of Ancient Cultures. https://isac.uchicago.edu/research/publications/oip/edwin-smith-surgical-papyrus-volume-1-hieroglyphic-transliteration.
2. van Middendorp, J. J., Sanchez, G. M. & Burridge, A. L. The Edwin Smith papyrus: a clinical reappraisal of the oldest known document on spinal injuries. *Eur. Spine J.* **19**, 1815–1823 (2010).
3. Cooper, W. A. The History of the Radical Mastectomy*From the Department of Surgery of the New York Hospital and Cornell Medical College. Done under a grant from the National Advisory Cancer Council of the U. S. Public Health Service, Washington, D. C. *Ann. Med. Hist.* **3**, 36–54 (1941).
4. Bland, K. I., Copeland, E. M. & Klimberg, V. S. *The Breast E-Book: Comprehensive Management of Benign and Malignant Diseases*. (Elsevier Health Sciences, 2009).
5. Allegra, J. C. & Lippman, M. E. Estrogen Receptor Status and the Disease-Free Interval in Breast Cancer. in *Endocrine Treatment of Breast Cancer: A New Approach* (eds. Henningsen, B., Linder, F. & Steichele, C.) 20–25 (Springer, Berlin, Heidelberg, 1980). doi:10.1007/978-3-642-81406-8_6.
6. Lynham, J. E. A. Pre- and Post-Operative Treatment of Cancer of the Breast by Radiation (Metastasis Excluded). *Br. J. Radiol.* (2014) doi:10.1259/0007-1285-4-47-534.
7. Geffen, D. B. & Man, S. New drugs for the treatment of cancer, 1990-2001. *Isr. Med. Assoc. J. IMAJ* **4**, 1124–1131 (2002).
8. Somogyi, R. B., Ziolkowski, N., Osman, F., Ginty, A. & Brown, M. Breast

reconstruction. *Can. Fam. Physician* **64**, 424–432 (2018).

9. Ahn, S. kyung, Oh, S., Kim, J., Choi, J.-S. & Hwang, K.-T. Psychological Impact of Type of Breast Cancer Surgery: A National Cohort Study. *World J. Surg.* **46**, 2224–2233 (2022).
10. Sevensma, K. E. & Lewis, C. R. Axillary Sentinel Lymph Node Biopsy. in *StatPearls* (StatPearls Publishing, Treasure Island (FL), 2023).
11. Burguin, A., Diorio, C. & Durocher, F. Breast Cancer Treatments: Updates and New Challenges. *J. Pers. Med.* **11**, 808 (2021).
12. Mattiuzzi, C. & Lippi, G. Current Cancer Epidemiology. *J. Epidemiol. Glob. Health* **9**, 217–222 (2019).
13. Sung, H. *et al.* Global Cancer Statistics 2020: GLOBOCAN Estimates of Incidence and Mortality Worldwide for 36 Cancers in 185 Countries. *CA. Cancer J. Clin.* **71**, 209–249 (2021).
14. Recommendations by age and resource setting. in *WHO Position Paper on Mammography Screening* (World Health Organization, 2014).
15. Francies, F. Z., Hull, R., Khanyile, R. & Dlamini, Z. Breast cancer in low-middle income countries: abnormality in splicing and lack of targeted treatment options. *Am. J. Cancer Res.* **10**, 1568–1591 (2020).
16. Alcohol is one of the biggest risk factors for breast cancer. https://www.who.int/europe/news/item/20-10-2021-alcohol-is-one-of-the-biggest-risk-factors-for-breast-cancer.
17. Lynch, B. M., Neilson, H. K. & Friedenreich, C. M. Physical activity and breast cancer prevention. *Recent Results Cancer Res. Fortschritte Krebsforsch. Progres Dans Rech. Sur Cancer* **186**, 13–42 (2011).
18. Rahib, L. *et al.* Projecting Cancer Incidence and Deaths to 2030: The

Unexpected Burden of Thyroid, Liver, and Pancreas Cancers in the United States. *Cancer Res.* **74**, 2913–2921 (2014).

19. McIntosh, S. A. *et al.* Global funding for cancer research between 2016 and 2020: a content analysis of public and philanthropic investments. *Lancet Oncol.* **24**, 636–645 (2023).
20. Sun, Y.-S. *et al.* Risk Factors and Preventions of Breast Cancer. *Int. J. Biol. Sci.* **13**, 1387–1397 (2017).
21. SEER Cancer Statistics Review 1975-2000 - Previous Version - SEER Cancer Statistics. *SEER* https://seer.cancer.gov/archive/csr/1975_2000/index.html.
22. Kohler, B. A. *et al.* Annual Report to the Nation on the Status of Cancer, 1975-2011, Featuring Incidence of Breast Cancer Subtypes by Race/Ethnicity, Poverty, and State. *J. Natl. Cancer Inst.* **107**, djv048 (2015).
23. DeSantis, C. E. *et al.* Breast cancer statistics, 2015: Convergence of incidence rates between black and white women. *CA. Cancer J. Clin.* **66**, 31–42 (2016).
24. Menarche, menopause, and breast cancer risk: individual participant meta-analysis, including 118 964 women with breast cancer from 117 epidemiological studies. *Lancet Oncol.* **13**, 1141–1151 (2012).
25. Apter, D., Reinilä, M. & Vihko, R. Some endocrine characteristics of early menarche, a risk factor for breast cancer, are preserved into adulthood. *Int. J. Cancer* **44**, 783–787 (1989).
26. Knudson, A. G. Mutation and cancer: statistical study of retinoblastoma. *Proc. Natl. Acad. Sci. U. S. A.* **68**, 820–823 (1971).
27. Nowell, P. C., Rowley, J. D. & Knudson, A. G. Cancer genetics, cytogenetics--defining the enemy within. *Nat. Med.* **4**, 1107–1111 (1998).
28. Stoppa-Lyonnet, D. The biological effects and clinical implications of BRCA

mutations: where do we go from here? *Eur. J. Hum. Genet.* **24**, S3–S9 (2016).

29. Chen, S. & Parmigiani, G. Meta-analysis of BRCA1 and BRCA2 penetrance. *J. Clin. Oncol. Off. J. Am. Soc. Clin. Oncol.* **25**, 1329–1333 (2007).
30. Kauff Noah D. *et al.* Risk-Reducing Salpingo-oophorectomy in Women with a BRCA1 or BRCA2 Mutation. *N. Engl. J. Med.* **346**, 1609–1615 (2002).
31. Torabi Dalivandan, S., Plummer, J. & Gayther, S. A. Risks and Function of Breast Cancer Susceptibility Alleles. *Cancers* **13**, 3953 (2021).
32. IARC. *Ionizing Radiation, Part 1: X- and Gamma (γ)-Radiation, and Neutrons*.
33. November 8, 1895: Roentgen's Discovery of X-Rays. http://www.aps.org/publications/apsnews/200111/history.cfm.
34. Tokunaga, M. *et al.* Incidence of Female Breast Cancer among Atomic Bomb Survivors, 1950-1985. *Radiat. Res.* **138**, 209–223 (1994).
35. L'indemnisation des victimes des essais nucléaires français : une loi qui n'a pas encore atteint ses objectifs. *Sénat* https://www.senat.fr/rap/r12-856/r12-856.html (2023).
36. Belmouhoub, N. D'Hiroshima à Reggane et de Nagasaki à In M'guel, en passant par Oued Namous. *Mediapart* https://blogs.mediapart.fr/nourredine-belmouhoub/blog/050820/d-hiroshima-reggane-et-de-nagasaki-m-guel-en-passant-par-oued-namous (2020).
37. Jartti, P., Pukkala, E., Uitti, J. & Auvinen, A. Cancer incidence among physicians occupationally exposed to ionizing radiation in Finland. *Scand. J. Work. Environ. Health* **32**, 368–373 (2006).
38. Al-Naggar, R. A. & Anil, S. Artificial Light at Night and Cancer: Global Study. *Asian Pac. J. Cancer Prev. APJCP* **17**, 4661–4664 (2016).
39. Videnros, C. *et al.* Investigating the risk of breast cancer among women

exposed to chemicals: a nested case–control study using improved exposure estimates. *Int. Arch. Occup. Environ. Health* **93**, 261–269 (2020).

40. Collaborative Group on Hormonal Factors in Breast Cancer. Breast cancer and hormonal contraceptives: collaborative reanalysis of individual data on 53 297 women with breast cancer and 100 239 women without breast cancer from 54 epidemiological studies. *Lancet Lond. Engl.* **347**, 1713–1727 (1996).
41. Mørch, L. S. *et al.* Contemporary Hormonal Contraception and the Risk of Breast Cancer. *N. Engl. J. Med.* **377**, 2228–2239 (2017).
42. Lee, J., Lee, J., Lee, D., Kim, H. & Kang, M. Sedentary work and breast cancer risk: A systematic review and meta- analysis. *J. Occup. Health* **63**, e12239 (2021).
43. Kyu, H. H. *et al.* Physical activity and risk of breast cancer, colon cancer, diabetes, ischemic heart disease, and ischemic stroke events: systematic review and dose-response meta-analysis for the Global Burden of Disease Study 2013. *The BMJ* **354**, i3857 (2016).
44. Picon- Ruiz, M., Morata- Tarifa, C., Valle- Goffin, J. J., Friedman, E. R. & Slingerland, J. M. Obesity and adverse breast cancer risk and outcome: Mechanistic insights and strategies for intervention. *Ca* **67**, 378–397 (2017).
45. Wang, X. *et al.* Body Mass Index at Diagnosis as a Prognostic Factor for Early-Stage Invasive Breast Cancer after Surgical Resection. *Oncol. Res. Treat.* **42**, 195–201 (2019).
46. Lyons, T. R., Schedin, P. J. & Borges, V. F. Pregnancy and Breast Cancer: when They Collide. *J. Mammary Gland Biol. Neoplasia* **14**, 87–98 (2009).
47. Islami, F. *et al.* Breastfeeding and breast cancer risk by receptor status—a systematic review and meta-analysis. *Ann. Oncol.* **26**, 2398–2407 (2015).

48. Holm, J. *et al.* Assessment of Breast Cancer Risk Factors Reveals Subtype Heterogeneity. *Cancer Res.* **77**, 3708–3717 (2017).
49. Elsevier eBooks+: Endocrine and Reproductive Physiology. https://bookshelf.health.elsevier.com/reader/books/9780323595759/epubcfi/6/34[%3Bvnd.vst.idref%3DB9780323595735000118]!/4/2/10/20/6/4[p0585]/9:489[rom%2Ca.].
50. Elsevier eBooks+: Gray's Anatomy for Students E-Book. https://bookshelf.health.elsevier.com/reader/books/9780323508520/epubcfi/6/84[%3Bvnd.vst.idref%3Did_chp00003_s2]!/4/2/2/2[s0135]/12/2[s0140]/10/2[s0145]/6/2[f0085]/2[ln0090]%4051:96.
51. On cancer of the breast / by Thomas William Nunn. *Wellcome Collection* https://wellcomecollection.org/works/jduf3za3.
52. Tan, P. H. *et al.* The 2019 World Health Organization classification of tumours of the breast. *Histopathology* **77**, 181–185 (2020).
53. SR, L., IO, E., SJ, S., PH, T. & MJ, van de V. *WHO Classification of Tumours of the Breast*.
54. Invasive breast cancer of no special type (NST). https://www.pathologyoutlines.com/topic/breastmalignantductalnos.html.
55. Limaiem, F., Khan, M. & Lotfollahzadeh, S. Lobular Breast Carcinoma. in *StatPearls* (StatPearls Publishing, Treasure Island (FL), 2024).
56. Chamalidou, C. *et al.* Survival patterns of invasive lobular and invasive ductal breast cancer in a large population-based cohort with two decades of follow up. *Breast Off. J. Eur. Soc. Mastology* **59**, 294–300 (2021).
57. Timbres, J. *et al.* Survival Outcomes in Invasive Lobular Carcinoma Compared to Oestrogen Receptor-Positive Invasive Ductal Carcinoma. *Cancers* **13**, 3036

(2021).

58. Yang, C. *et al.* Comparison of Overall Survival Between Invasive Lobular Breast Carcinoma and Invasive Ductal Breast Carcinoma: A Propensity Score Matching Study Based on SEER Database. *Front. Oncol.* **10**, 590643 (2020).
59. Bansal, C. *et al.* Comparative evaluation of the modified Scarff-Bloom-Richardson grading system on breast carcinoma aspirates and histopathology. *CytoJournal* **9**, 4 (2012).
60. Cserni, G. Histological type and typing of breast carcinomas and the WHO classification changes over time. *Pathologica* **112**, 25–41 (2020).
61. Amin, M. B. *et al.* The Eighth Edition AJCC Cancer Staging Manual: Continuing to build a bridge from a population-based to a more ‘personalized’ approach to cancer staging. *CA. Cancer J. Clin.* **67**, 93–99 (2017).
62. Edge, S. B. & Compton, C. C. The American Joint Committee on Cancer: the 7th edition of the AJCC cancer staging manual and the future of TNM. *Ann. Surg. Oncol.* **17**, 1471–1474 (2010).
63. Perou, C. M. *et al.* Molecular portraits of human breast tumours. *Nature* **406**, 747–752 (2000).
64. Sørlie, T. *et al.* Gene expression patterns of breast carcinomas distinguish tumor subclasses with clinical implications. *Proc. Natl. Acad. Sci. U. S. A.* **98**, 10869–10874 (2001).
65. Hu, Z. *et al.* The molecular portraits of breast tumors are conserved across microarray platforms. *BMC Genomics* **7**, 96 (2006).
66. Park, S. *et al.* Characteristics and outcomes according to molecular subtypes of breast cancer as classified by a panel of four biomarkers using immunohistochemistry. *The Breast* **21**, 50–57 (2012).

67. Fujii, T. *et al.* Revisiting the definition of estrogen receptor positivity in HER2-negative primary breast cancer. *Ann. Oncol. Off. J. Eur. Soc. Med. Oncol.* **28**, 2420–2428 (2017).

68. Slamon, D. J. *et al.* Use of chemotherapy plus a monoclonal antibody against HER2 for metastatic breast cancer that overexpresses HER2. *N. Engl. J. Med.* **344**, 783–792 (2001).

69. Vogel, C. L. *et al.* Efficacy and safety of trastuzumab as a single agent in first-line treatment of HER2-overexpressing metastatic breast cancer. *J. Clin. Oncol. Off. J. Am. Soc. Clin. Oncol.* **20**, 719–726 (2002).

70. Cobleigh, M. A. *et al.* Multinational study of the efficacy and safety of humanized anti-HER2 monoclonal antibody in women who have HER2-overexpressing metastatic breast cancer that has progressed after chemotherapy for metastatic disease. *J. Clin. Oncol. Off. J. Am. Soc. Clin. Oncol.* **17**, 2639–2648 (1999).

71. Carey, L. A. *et al.* Race, breast cancer subtypes, and survival in the Carolina Breast Cancer Study. *JAMA* **295**, 2492–2502 (2006).

72. Bauer, K. R., Brown, M., Cress, R. D., Parise, C. A. & Caggiano, V. Descriptive analysis of estrogen receptor (ER)-negative, progesterone receptor (PR)-negative, and HER2-negative invasive breast cancer, the so-called triple-negative phenotype: a population-based study from the California cancer Registry. *Cancer* **109**, 1721–1728 (2007).

73. Foulkes, W. D., Smith, I. E. & Reis-Filho, J. S. Triple-Negative Breast Cancer. *N. Engl. J. Med.* **363**, 1938–1948 (2010).

74. Dent, R. *et al.* Triple-negative breast cancer: clinical features and patterns of recurrence. *Clin. Cancer Res. Off. J. Am. Assoc. Cancer Res.* **13**, 4429–4434 (2007).

75. Kassam, F. *et al.* Survival outcomes for patients with metastatic triple-negative breast cancer: implications for clinical practice and trial design. *Clin. Breast Cancer* **9**, 29–33 (2009).

76. O'Reilly, D., Sendi, M. A. & Kelly, C. M. Overview of recent advances in metastatic triple negative breast cancer. *World J. Clin. Oncol.* **12**, 164–182 (2021).

77. Lehmann, B. D. *et al.* Identification of human triple-negative breast cancer subtypes and preclinical models for selection of targeted therapies. *J. Clin. Invest.* **121**, 2750–2767 (2011).

78. Lehmann, B. D. *et al.* Refinement of Triple-Negative Breast Cancer Molecular Subtypes: Implications for Neoadjuvant Chemotherapy Selection. *PloS One* **11**, e0157368 (2016).

79. Karaayvaz, M. *et al.* Unravelling subclonal heterogeneity and aggressive disease states in TNBC through single-cell RNA-seq. *Nat. Commun.* **9**, 3588 (2018).

80. Curtis, C. *et al.* The genomic and transcriptomic architecture of 2,000 breast tumours reveals novel subgroups. *Nature* **486**, 346–352 (2012).

81. Burstein, M. D. *et al.* Comprehensive Genomic Analysis Identifies Novel Subtypes and Targets of Triple-Negative Breast Cancer. *Clin. Cancer Res.* **21**, 1688–1698 (2015).

82. Masuda, H. *et al.* Differential response to neoadjuvant chemotherapy among 7 triple-negative breast cancer molecular subtypes. *Clin. Cancer Res. Off. J. Am. Assoc. Cancer Res.* **19**, 5533–5540 (2013).

83. Wang, G., Yao, Y., Huang, H., Zhou, J. & Ni, C. Multiomics technologies for comprehensive tumor microenvironment analysis in triple-negative breast

cancer under neoadjuvant chemotherapy. *Front. Oncol.* **13**, 1131259 (2023).

84. Harris, M. A. *et al.* Towards targeting the breast cancer immune microenvironment. *Nat. Rev. Cancer* 1–24 (2024) doi:10.1038/s41568-024-00714-6.
85. Nejman, D. *et al.* The human tumor microbiome is composed of tumor type-specific intracellular bacteria. *Science* **368**, 973–980 (2020).
86. Sidaway, P. Immunoscore provides a more accurate prognosis. *Nat. Rev. Clin. Oncol.* **15**, 471 (2018).
87. Arima, Y., Matsueda, S. & Saya, H. Significance of Cancer-Associated Fibroblasts in the Interactions of Cancer Cells with the Tumor Microenvironment of Heterogeneous Tumor Tissue. *Cancers* **15**, 2536 (2023).
88. Garaud, S. *et al.* Tumor infiltrating B-cells signal functional humoral immune responses in breast cancer. *JCI Insight* **5**, e129641, 129641 (2019).
89. Broz, M. L. *et al.* Dissecting the Tumor Myeloid Compartment Reveals Rare Activating Antigen-Presenting Cells Critical for T Cell Immunity. *Cancer Cell* **26**, 638–652 (2014).
90. Danenberg, E. *et al.* Breast tumor microenvironment structures are associated with genomic features and clinical outcome. *Nat. Genet.* **54**, 660–669 (2022).
91. Savas, P. *et al.* Single-cell profiling of breast cancer T cells reveals a tissue-resident memory subset associated with improved prognosis. *Nat. Med.* **24**, 986–993 (2018).
92. Galon, J. *et al.* Type, density, and location of immune cells within human colorectal tumors predict clinical outcome. *Science* **313**, 1960–1964 (2006).
93. Brummel, K., Eerkens, A. L., de Bruyn, M. & Nijman, H. W. Tumour-infiltrating lymphocytes: from prognosis to treatment selection. *Br. J. Cancer* **128**, 451–458

(2023).

94. Kim, A. *et al.* The prognostic significance of tumor-infiltrating lymphocytes assessment with hematoxylin and eosin sections in resected primary lung adenocarcinoma. *PLoS ONE* **14**, e0224430 (2019).
95. Mullinax, J. E. *et al.* Expanded Tumor-infiltrating Lymphocytes From Soft Tissue Sarcoma Have Tumor-specific Function. *J. Immunother. Hagerstown Md 1997* **44**, 63–70 (2021).
96. Leon-Ferre, R. A. *et al.* Tumor-Infiltrating Lymphocytes in Triple-Negative Breast Cancer. *JAMA* **331**, 1135–1144 (2024).
97. Cardoso, F. *et al.* Early breast cancer: ESMO Clinical Practice Guidelines for diagnosis, treatment and follow-up†. *Ann. Oncol.* **30**, 1194–1220 (2019).
98. Shang, L. *et al.* Subverted macrophages in the triple-negative breast cancer ecosystem. *Biomed. Pharmacother.* **166**, 115414 (2023).
99. Harris, R. J. *et al.* Tumor-Infiltrating B Lymphocyte Profiling Identifies IgG-Biased, Clonally Expanded Prognostic Phenotypes in Triple-Negative Breast Cancer. *Cancer Res.* **81**, 4290–4304 (2021).
100. Disis, M. L. & Stanton, S. E. Triple-Negative Breast Cancer: Immune Modulation as the New Treatment Paradigm. *Am. Soc. Clin. Oncol. Educ. Book* e25–e30 (2015) doi:10.14694/EdBook_AM.2015.35.e25.
101. Charafe-Jauffret, E. *et al.* Gene expression profiling of breast cell lines identifies potential new basal markers. *Oncogene* **25**, 2273–2284 (2006).
102. Dai, X., Cheng, H., Bai, Z. & Li, J. Breast Cancer Cell Line Classification and Its Relevance with Breast Tumor Subtyping. *J. Cancer* **8**, 3131–3141 (2017).
103. Forozan, F. *et al.* Comparative genomic hybridization analysis of 38 breast cancer cell lines: a basis for interpreting complementary DNA microarray data.

Cancer Res. **60**, 4519–4525 (2000).

104. Dvořánková, B. *et al.* Fibroblasts prepared from different types of malignant tumors stimulate expression of luminal marker keratin 8 in the EM-G3 breast cancer cell line. *Histochem. Cell Biol.* **137**, 679–685 (2012).
105. Fan, Y. & He, S. The Characteristics of Tumor Microenvironment in Triple Negative Breast Cancer. *Cancer Manag. Res.* **14**, 1–17 (2022).
106. Emerman, J. T., Burwen, S. J. & Pitelka, D. R. Substrate properties influencing ultrastructural differentiation of mammary epithelial cells in culture. *Tissue Cell* **11**, 109–119 (1979).
107. Perova, Z. *et al.* PDCM Finder: an open global research platform for patient-derived cancer models. *Nucleic Acids Res.* **51**, D1360–D1366 (2022).
108. Ben-David, U. *et al.* Patient-derived xenografts undergo murine-specific tumor evolution. *Nat. Genet.* **49**, 1567–1575 (2017).
109. Abdolahi, S. *et al.* Patient-derived xenograft (PDX) models, applications and challenges in cancer research. *J. Transl. Med.* **20**, 206 (2022).
110. Usary, J., Darr, D. B., Pfefferle, A. D. & Perou, C. M. Overview of Genetically Engineered Mouse Models of Distinct Breast Cancer Subtypes. *Curr. Protoc. Pharmacol.* **72**, 14.38.1-14.38.11 (2016).
111. Roberts, P. J. *et al.* Combined PI3K/mTOR and MEK inhibition provides broad antitumor activity in faithful murine cancer models. *Clin. Cancer Res. Off. J. Am. Assoc. Cancer Res.* **18**, 5290–5303 (2012).
112. Pfefferle, A. D. *et al.* Transcriptomic classification of genetically engineered mouse models of breast cancer identifies human subtype counterparts. *Genome Biol.* **14**, R125 (2013).
113. Lamballe, F. *et al.* Modeling Heterogeneity of Triple- Negative Breast Cancer

Uncovers a Novel Combinatorial Treatment Overcoming Primary Drug Resistance. *Adv. Sci.* **8**, 2003049 (2020).

114. Doha, Z. O. *et al.* MYC Deregulation and PTEN Loss Model Tumor and Stromal Heterogeneity of Aggressive Triple-Negative Breast Cancer. *Nat. Commun.* **14**, 5665 (2023).
115. Cancer of the Breast (Female) - Cancer Stat Facts. *SEER* https://seer.cancer.gov/statfacts/html/breast.html.
116. Fisher, B. *et al.* Twenty-year follow-up of a randomized trial comparing total mastectomy, lumpectomy, and lumpectomy plus irradiation for the treatment of invasive breast cancer. *N. Engl. J. Med.* **347**, 1233–1241 (2002).
117. Effect of radiotherapy after breast-conserving surgery on 10-year recurrence and 15-year breast cancer death: meta-analysis of individual patient data for 10 801 women in 17 randomised trials. *Lancet* **378**, 1707–1716 (2011).
118. Fisher, B. *et al.* Surgical adjuvant chemotherapy in cancer of the breast: results of a decade of cooperative investigation. *Ann. Surg.* **168**, 337–356 (1968).
119. Polychemotherapy for early breast cancer: an overview of the randomised trials. Early Breast Cancer Trialists' Collaborative Group. *Lancet Lond. Engl.* **352**, 930–942 (1998).
120. Rastogi, P. *et al.* Preoperative chemotherapy: updates of National Surgical Adjuvant Breast and Bowel Project Protocols B-18 and B-27. *J. Clin. Oncol. Off. J. Am. Soc. Clin. Oncol.* **26**, 778–785 (2008).
121. Marra, A. & Curigliano, G. Adjuvant and Neoadjuvant Treatment of Triple-Negative Breast Cancer With Chemotherapy. *Cancer J.* **27**, 41 (2021).
122. Berry, D. A. *et al.* Estrogen-receptor status and outcomes of modern chemotherapy for patients with node-positive breast cancer. *JAMA* **295**, 1658–

1667 (2006).

123. Petruolo, O. *et al.* How Often Does Modern Neoadjuvant Chemotherapy Downstage Patients to Breast-Conserving Surgery? *Ann. Surg. Oncol.* **28**, 287–294 (2021).

124. Petrelli, F. *et al.* Adjuvant chemotherapy for resected triple negative breast cancer patients: A network meta-analysis. *Breast Off. J. Eur. Soc. Mastology* **67**, 8–13 (2022).

125. Ge, J., Zuo, W., Chen, Y., Shao, Z. & Yu, K. The advance of adjuvant treatment for triple-negative breast cancer. *Cancer Biol. Med.* **19**, 187–201 (2022).

126. Dear, R. F. *et al.* Combination versus sequential single agent chemotherapy for metastatic breast cancer. *Cochrane Database Syst. Rev.* **2013**, CD008792 (2013).

127. Gennari, A. *et al.* ESMO Clinical Practice Guideline for the diagnosis, staging and treatment of patients with metastatic breast cancer. *Ann. Oncol. Off. J. Eur. Soc. Med. Oncol.* **32**, 1475–1495 (2021).

128. Scott, E. C. *et al.* Trends in the approval of cancer therapies by the FDA in the twenty-first century. *Nat. Rev. Drug Discov.* **22**, 625–640 (2023).

129. Perez, E. A. *et al.* Trastuzumab plus adjuvant chemotherapy for human epidermal growth factor receptor 2-positive breast cancer: planned joint analysis of overall survival from NSABP B-31 and NCCTG N9831. *J. Clin. Oncol. Off. J. Am. Soc. Clin. Oncol.* **32**, 3744–3752 (2014).

130. Robson Mark *et al.* Olaparib for Metastatic Breast Cancer in Patients with a Germline BRCA Mutation. *N. Engl. J. Med.* **377**, 523–533 (2017).

131. Litton Jennifer K. *et al.* Talazoparib in Patients with Advanced Breast Cancer and a Germline BRCA Mutation. *N. Engl. J. Med.* **379**, 753–763 (2018).

132. Olivares-Hernández, A. *et al.* Immune checkpoint inhibitors in non-small cell lung cancer: from current perspectives to future treatments—a systematic review. *Ann. Transl. Med.* **11**, 354 (2023).
133. Herrscher, H. & Robert, C. Immune checkpoint inhibitors in melanoma in the metastatic, neoadjuvant, and adjuvant setting. *Curr. Opin. Oncol.* **32**, 106–113 (2020).
134. Xu, Z. *et al.* Assessment of tumor mutation burden calculation from gene panel sequencing data. *OncoTargets Ther.* **12**, 3401–3409 (2019).
135. Zappasodi, R., Wolchok, J. D. & Merghoub, T. Strategies for Predicting Response to Checkpoint Inhibitors. *Curr. Hematol. Malig. Rep.* **13**, 383–395 (2018).
136. Schmid Peter *et al.* Pembrolizumab for Early Triple-Negative Breast Cancer. *N. Engl. J. Med.* **382**, 810–821 (2020).
137. Cortes, J. *et al.* Pembrolizumab plus chemotherapy versus placebo plus chemotherapy for previously untreated locally recurrent inoperable or metastatic triple-negative breast cancer (KEYNOTE-355): a randomised, placebo-controlled, double-blind, phase 3 clinical trial. *Lancet Lond. Engl.* **396**, 1817–1828 (2020).
138. Bardia, A. *et al.* Sacituzumab Govitecan in Metastatic Triple-Negative Breast Cancer. *N. Engl. J. Med.* **384**, 1529–1541 (2021).
139. Rizzo, A., Cusmai, A., Acquafredda, S., Rinaldi, L. & Palmiotti, G. Ladiratuzumab vedotin for metastatic triple negative cancer: preliminary results, key challenges, and clinical potential. *Expert Opin. Investig. Drugs* **31**, 495–498 (2022).
140. Brufsky, A. *et al.* A phase II randomized trial of cobimetinib plus chemotherapy,

with or without atezolizumab, as first-line treatment for patients with locally advanced or metastatic triple-negative breast cancer (COLET): primary analysis. *Ann. Oncol. Off. J. Eur. Soc. Med. Oncol.* **32**, 652–660 (2021).

141. Pimentel, I. *et al.* A phase II randomized clinical trial of the effect of metformin versus placebo on progression-free survival in women with metastatic breast cancer receiving standard chemotherapy. *Breast Edinb. Scotl.* **48**, 17–23 (2019).
142. Tutt, A. *et al.* 161O VIOLETTE: Randomised phase II study of olaparib (ola) + ceralasertib (cer) or adavosertib (ada) vs ola alone in patients (pts) with metastatic triple-negative breast cancer (mTNBC). *Ann. Oncol.* **33**, S194–S195 (2022).
143. Turner, N. *et al.* Ipatasertib plus paclitaxel for PIK3CA/AKT1/PTEN-altered hormone receptor-positive HER2-negative advanced breast cancer: primary results from cohort B of the IPATunity130 randomized phase 3 trial. *Breast Cancer Res. Treat.* **191**, 565–576 (2022).
144. Bachelot, T. *et al.* Durvalumab compared to maintenance chemotherapy in metastatic breast cancer: the randomized phase II SAFIR02-BREAST IMMUNO trial. *Nat. Med.* **27**, 250–255 (2021).
145. Geyer, C. E. *et al.* Long-term efficacy and safety of addition of carboplatin with or without veliparib to standard neoadjuvant chemotherapy in triple-negative breast cancer: 4-year follow-up data from BrighTNess, a randomized phase III trial. *Ann. Oncol.* **33**, 384–394 (2022).
146. Javed, A. & Lteif, A. Development of the Human Breast. *Semin. Plast. Surg.* **27**, 5–12 (2013).
147. Angers, S. & Moon, R. T. Proximal events in Wnt signal transduction. *Nat. Rev.*

Mol. Cell Biol. **10**, 468–477 (2009).

148. Aiello, N. M. & Stanger, B. Z. Echoes of the embryo: using the developmental biology toolkit to study cancer. *Dis. Model. Mech.* **9**, 105–114 (2016).
149. Berman, D. M. *et al.* Widespread requirement for Hedgehog ligand stimulation in growth of digestive tract tumours. *Nature* **425**, 846–851 (2003).
150. Jeng, K.-S., Sheen, I.-S., Leu, C.-M., Tseng, P.-H. & Chang, C.-F. The Role of Smoothened in Cancer. *Int. J. Mol. Sci.* **21**, 6863 (2020).
151. Wang, C.-Y. *et al.* Mutation of the PTCH1 gene predicts recurrence of breast cancer. *Sci. Rep.* **9**, 16359 (2019).
152. Duman-Scheel, M., Weng, L., Xin, S. & Du, W. Hedgehog regulates cell growth and proliferation by inducing Cyclin D and Cyclin E. *Nature* **417**, 299–304 (2002).
153. Yoon, J. W. *et al.* Noncanonical regulation of the Hedgehog mediator GLI1 by c-MYC in Burkitt lymphoma. *Mol. Cancer Res. MCR* **11**, 604–615 (2013).
154. Słowińska, M. *et al.* Analysis of efficacy and safety of vismodegib therapy in patients with advanced basal cell carcinoma – real world multicenter cohort study. *J. Eur. Acad. Dermatol. Venereol.* **36**, 1219–1228 (2022).
155. Villani, A., Fabbrocini, G., Costa, C. & Scalvenzi, M. Sonidegib: Safety and Efficacy in Treatment of Advanced Basal Cell Carcinoma. *Dermatol. Ther.* **10**, 401–412 (2020).
156. Harper, J. A., Yuan, J. S., Tan, J. B., Visan, I. & Guidos, C. J. Notch signaling in development and disease. *Clin. Genet.* **64**, 461–472 (2003).
157. Wang, Z., Li, Y., Banerjee, S. & Sarkar, F. H. Emerging Role of Notch in Stem Cells and Cancer. *Cancer Lett.* **279**, 8–12 (2009).
158. Dontu, G. *et al.* Role of Notch signaling in cell-fate determination of human

mammary stem/progenitor cells. *Breast Cancer Res.* **6**, R605–R615 (2004).

159. Bolós, V., Grego-Bessa, J. & de la Pompa, J. L. Notch Signaling in Development and Cancer. *Endocr. Rev.* **28**, 339–363 (2007).

160. Kontomanolis, E. N. *et al.* The Notch Pathway in Breast Cancer Progression. *Sci. World J.* **2018**, 2415489 (2018).

161. Aster, J. C., Pear, W. S. & Blacklow, S. C. Notch Signaling in Leukemia. *Annu. Rev. Pathol.* **3**, 587–613 (2008).

162. Lobry, C., Oh, P., Mansour, M. R., Look, A. T. & Aifantis, I. Notch signaling: switching an oncogene to a tumor suppressor. *Blood* **123**, 2451–2459 (2014).

163. Cook, N. *et al.* A phase I trial of the γ-secretase inhibitor MK-0752 in combination with gemcitabine in patients with pancreatic ductal adenocarcinoma. *Br. J. Cancer* **118**, 793–801 (2018).

164. DeAngelo, D. J. *et al.* Phase 1 clinical results with tandutinib (MLN518), a novel FLT3 antagonist, in patients with acute myelogenous leukemia or high-risk myelodysplastic syndrome: safety, pharmacokinetics, and pharmacodynamics. *Blood* **108**, 3674–3681 (2006).

165. Shimogori, T., Banuchi, V., Ng, H. Y., Strauss, J. B. & Grove, E. A. Embryonic signaling centers expressing BMP, WNT and FGF proteins interact to pattern the cerebral cortex. *Dev. Camb. Engl.* **131**, 5639–5647 (2004).

166. Yang, Y. Wnts and wing: Wnt signaling in vertebrate limb development and musculoskeletal morphogenesis. *Birth Defects Res. Part C Embryo Today Rev.* **69**, 305–317 (2003).

167. Chen, A. E., Ginty, D. D. & Fan, C.-M. Protein kinase A signalling via CREB controls myogenesis induced by Wnt proteins. *Nature* **433**, 317–322 (2005).

168. Zi, X. *et al.* Expression of Frzb/secreted Frizzled-related protein 3, a secreted

Wnt antagonist, in human androgen-independent prostate cancer PC-3 cells suppresses tumor growth and cellular invasiveness. *Cancer Res.* **65**, 9762–9770 (2005).

169. Anastas, J. N. & Moon, R. T. WNT signalling pathways as therapeutic targets in cancer. *Nat. Rev. Cancer* **13**, 11–26 (2013).
170. Petersen, C. P. & Reddien, P. W. Wnt Signaling and the Polarity of the Primary Body Axis. *Cell* **139**, 1056–1068 (2009).
171. Slusarski, D. C., Corces, V. G. & Moon, R. T. Interaction of Wnt and a Frizzled homologue triggers G-protein-linked phosphatidylinositol signalling. *Nature* **390**, 410–413 (1997).
172. De, A. Wnt/Ca2+ signaling pathway: a brief overview. *Acta Biochim. Biophys. Sin.* **43**, 745–756 (2011).
173. Bovolenta, P., Rodriguez, J. & Esteve, P. Frizzled/RYK mediated signalling in axon guidance. *Dev. Camb. Engl.* **133**, 4399–4408 (2006).
174. Menck, K., Heinrichs, S., Baden, C. & Bleckmann, A. The WNT/ROR Pathway in Cancer: From Signaling to Therapeutic Intervention. *Cells* **10**, 142 (2021).
175. Shafer, B., Onishi, K., Lo, C., Colakoglu, G. & Zou, Y. Vangl2 promotes Wnt/Planar Cell Polarity-like signaling by antagonizing Dvl1-mediated feedback inhibition in growth cone guidance. *Dev. Cell* **20**, 177–191 (2011).
176. Dreyer, C. A., VanderVorst, K. & Carraway, K. L. Vangl as a Master Scaffold for Wnt/Planar Cell Polarity Signaling in Development and Disease. *Front. Cell Dev. Biol.* **10**, 887100 (2022).
177. Daulat, A. M. & Borg, J.-P. Wnt/Planar Cell Polarity Signaling: New Opportunities for Cancer Treatment. *Trends Cancer* **3**, 113–125 (2017).
178. Chen, Y., Chen, Z., Tang, Y. & Xiao, Q. The involvement of noncanonical Wnt

signaling in cancers. *Biomed. Pharmacother.* **133**, 110946 (2021).

179. Chae, W.-J. & Bothwell, A. L. M. Canonical and Non-Canonical Wnt Signaling in Immune Cells. *Trends Immunol.* **39**, 830–847 (2018).

180. Dale, H. Modes of drug action. General introductory address. *Trans. Faraday Soc.* **39**, 319b–3322 (1943).

181. Kent, R. S., De Lean, A. & Lefkowitz, R. J. A quantitative analysis of beta-adrenergic receptor interactions: resolution of high and low affinity states of the receptor by computer modeling of ligand binding data. *Mol. Pharmacol.* **17**, 14–23 (1980).

182. Randall, M. H., Altman, L. J. & Lefkowitz, R. J. Structure and biological activity of (-)-[3H]-dihydroalprenolol, a radioligand for studies of .beta.-adrenergic receptors. *J. Med. Chem.* **20**, 1090–1094 (1977).

183. De Lean, A., Stadel, J. M. & Lefkowitz, R. J. A ternary complex model explains the agonist-specific binding properties of the adenylate cyclase-coupled beta-adrenergic receptor. *J. Biol. Chem.* **255**, 7108–7117 (1980).

184. Ross, E. M. & Gilman, A. G. Resolution of some components of adenylate cyclase necessary for catalytic activity. *J. Biol. Chem.* **252**, 6966–6969 (1977).

185. Ya, O. The complete amino acid sequence of visual rhodopsin. *Bioorg Khim* **8**, 1011–1014 (1982).

186. Dixon, R. A. *et al.* Cloning of the gene and cDNA for mammalian beta-adrenergic receptor and homology with rhodopsin. *Nature* **321**, 75–79 (1986).

187. Kobilka, B. K. *et al.* Cloning, sequencing, and expression of the gene coding for the human platelet alpha 2-adrenergic receptor. *Science* **238**, 650–656 (1987).

188. Cotecchia, S. *et al.* Molecular cloning and expression of the cDNA for the hamster alpha 1-adrenergic receptor. *Proc. Natl. Acad. Sci. U. S. A.* **85**, 7159–

7163 (1988).

189. Fargin, A. *et al.* The genomic clone G-21 which resembles a beta-adrenergic receptor sequence encodes the 5-HT1A receptor. *Nature* **335**, 358–360 (1988).

190. Schwinn, D. A. *et al.* Molecular cloning and expression of the cDNA for a novel alpha 1-adrenergic receptor subtype. *J. Biol. Chem.* **265**, 8183–8189 (1990).

191. The Nobel Prize in Chemistry 2012. *NobelPrize.org* https://www.nobelprize.org/prizes/chemistry/2012/lefkowitz/facts/.

192. Venter, J. C. *et al.* The sequence of the human genome. *Science* **291**, 1304–1351 (2001).

193. Fredriksson, R., Lagerström, M. C., Lundin, L.-G. & Schiöth, H. B. The G-protein-coupled receptors in the human genome form five main families. Phylogenetic analysis, paralogon groups, and fingerprints. *Mol. Pharmacol.* **63**, 1256–1272 (2003).

194. Leysen, H. *et al.* GPCRs Are Optimal Regulators of Complex Biological Systems and Orchestrate the Interface between Health and Disease. *Int. J. Mol. Sci.* **22**, 13387 (2021).

195. Sharma, N., Akhade, A. S. & Qadri, A. Sphingosine-1-phosphate suppresses TLR-induced CXCL8 secretion from human T cells. *J. Leukoc. Biol.* **93**, 521–528 (2013).

196. Wang, J., Gareri, C. & Rockman, H. A. G-Protein–Coupled Receptors in Heart Disease. *Circ. Res.* **123**, 716–735 (2018).

197. Hauser, A. S., Attwood, M. M., Rask-Andersen, M., Schiöth, H. B. & Gloriam, D. E. Trends in GPCR drug discovery: new agents, targets and indications. *Nat. Rev. Drug Discov.* **16**, 829–842 (2017).

198. Wishart, D. S. *et al.* DrugBank 5.0: a major update to the DrugBank database

for 2018. *Nucleic Acids Res.* **46**, D1074–D1082 (2018).

199. Hollenstein, K. *et al.* Insights into the structure of class B GPCRs. *Trends Pharmacol. Sci.* **35**, 12–22 (2014).

200. Liebscher, I. *et al.* A guide to adhesion GPCR research. *FEBS J.* **289**, 7610–7630 (2022).

201. Sriram, K. & Insel, P. A. G Protein-Coupled Receptors as Targets for Approved Drugs: How Many Targets and How Many Drugs? *Mol. Pharmacol.* **93**, 251–258 (2018).

202. Malbon, C. C. Frizzleds: new members of the superfamily of G-protein-coupled receptors. *Front. Biosci.-Landmark* **9**, 1048–1058 (2004).

203. Ruat, M., Hoch, L., Faure, H. & Rognan, D. Targeting of Smoothened for therapeutic gain. *Trends Pharmacol. Sci.* **35**, 237–246 (2014).

204. Yang, D. *et al.* G protein-coupled receptors: structure- and function-based drug discovery. *Signal Transduct. Target. Ther.* **6**, 1–27 (2021).

205. Pándy-Szekeres, G. *et al.* GPCRdb in 2018: adding GPCR structure models and ligands. *Nucleic Acids Res.* **46**, D440–D446 (2018).

206. Tang, X., Wang, Y., Li, D., Luo, J. & Liu, M. Orphan G protein-coupled receptors (GPCRs): biological functions and potential drug targets. *Acta Pharmacol. Sin.* **33**, 363–371 (2012).

207. Chan, H. C. S., Li, Y., Dahoun, T., Vogel, H. & Yuan, S. New Binding Sites, New Opportunities for GPCR Drug Discovery. *Trends Biochem. Sci.* **44**, 312–330 (2019).

208. Hilger, D., Masureel, M. & Kobilka, B. K. Structure and dynamics of GPCR signaling complexes. *Nat. Struct. Mol. Biol.* **25**, 4–12 (2018).

209. Downes, G. B. & Gautam, N. The G Protein Subunit Gene Families. *Genomics*

62, 544–552 (1999).

210. Zeghal, M., Laroche, G., Freitas, J. D., Wang, R. & Giguère, P. M. Profiling of basal and ligand-dependent GPCR activities by means of a polyvalent cell-based high-throughput platform. *Nat. Commun.* **14**, 3684 (2023).
211. Wacker, D., Stevens, R. C. & Roth, B. L. How ligands illuminate GPCR molecular pharmacology. *Cell* **170**, 414–427 (2017).
212. Kristiansen, K. Molecular mechanisms of ligand binding, signaling, and regulation within the superfamily of G-protein-coupled receptors: molecular modeling and mutagenesis approaches to receptor structure and function. *Pharmacol. Ther.* **103**, 21–80 (2004).
213. Gurevich, V. V. & Gurevich, E. V. GPCR Signaling Regulation: The Role of GRKs and Arrestins. *Front. Pharmacol.* **10**, (2019).
214. Hoare, S. R. J. & Hughes, T. E. Biosensor Assays for Measuring the Kinetics of G-Protein and Arrestin-Mediated Signaling in Live Cells. in *Assay Guidance Manual* (eds. Markossian, S. et al.) (Eli Lilly & Company and the National Center for Advancing Translational Sciences, Bethesda (MD), 2004).
215. Moscat, J., Diaz-Meco, M. T. & Rennert, P. NF-κB activation by protein kinase C isoforms and B-cell function. *EMBO Rep.* **4**, 31–36 (2003).
216. Yang, Y. M., Kuen, D.-S., Chung, Y., Kurose, H. & Kim, S. G. Gα12/13 signaling in metabolic diseases. *Exp. Mol. Med.* **52**, 896–910 (2020).
217. Kumari, P. *et al.* Functional competence of a partially engaged GPCR–β-arrestin complex. *Nat. Commun.* **7**, 13416 (2016).
218. Shapiro, D. A. *et al.* Aripiprazole, a novel atypical antipsychotic drug with a unique and robust pharmacology. *Neuropsychopharmacol. Off. Publ. Am. Coll. Neuropsychopharmacol.* **28**, 1400–1411 (2003).

219. Palczewski, K. *et al.* Crystal Structure of Rhodopsin: A G Protein-Coupled Receptor. *Science* **289**, 739–745 (2000).
220. Cherezov, V. *et al.* High-Resolution Crystal Structure of an Engineered Human β2-Adrenergic G Protein–Coupled Receptor. *Science* **318**, 1258–1265 (2007).
221. Rasmussen, S. G. F. *et al.* Crystal structure of the β2 adrenergic receptor–Gs protein complex. *Nature* **477**, 549–555 (2011).
222. Hanson, M. A. *et al.* Profiling of membrane protein variants in a baculovirus system by coupling cell-surface detection with small-scale parallel expression. *Protein Expr. Purif.* **56**, 85–92 (2007).
223. Rasmussen, S. G. F. *et al.* Structure of a nanobody-stabilized active state of the β2 adrenoceptor. *Nature* **469**, 175–180 (2011).
224. Munk, C. *et al.* An online resource for GPCR structure determination and analysis. *Nat. Methods* **16**, 151–162 (2019).
225. Weis, W. I. & Kobilka, B. K. The Molecular Basis of G Protein–Coupled Receptor Activation. *Annu. Rev. Biochem.* **87**, 897–919 (2018).
226. Neumann, E., Khawaja, K. & Müller-Ladner, U. G protein-coupled receptors in rheumatology. *Nat. Rev. Rheumatol.* **10**, 429–436 (2014).
227. Rehman, S., Rahimi, N. & Dimri, M. Biochemistry, G Protein Coupled Receptors. in *StatPearls* (StatPearls Publishing, Treasure Island (FL), 2024).
228. Baud, V. *et al.* EMR1, an unusual member in the family of hormone receptors with seven transmembrane segments. *Genomics* **26**, 334–344 (1995).
229. Hamann, J. *et al.* Expression cloning and chromosomal mapping of the leukocyte activation antigen CD97, a new seven-span transmembrane molecule of the secretion receptor superfamily with an unusual extracellular domain. *J. Immunol. Baltim. Md 1950* **155**, 1942–1950 (1995).

230. McKnight, A. J. & Gordon, S. EGF-TM7: a novel subfamily of seven-transmembrane-region leukocyte cell-surface molecules. *Immunol. Today* **17**, 283–287 (1996).
231. Hadjantonakis, A. K., Formstone, C. J. & Little, P. F. mCelsr1 is an evolutionarily conserved seven-pass transmembrane receptor and is expressed during mouse embryonic development. *Mech. Dev.* **78**, 91–95 (1998).
232. Shiratsuchi, T., Nishimori, H., Ichise, H., Nakamura, Y. & Tokino, T. Cloning and characterization of BAI2 and BAI3, novel genes homologous to brain-specific angiogenesis inhibitor 1 (BAI1). *Cytogenet. Cell Genet.* **79**, 103–108 (1997).
233. Lin, H. H., Stacey, M., Hamann, J., Gordon, S. & McKnight, A. J. Human EMR2, a novel EGF-TM7 molecule on chromosome 19p13.1, is closely related to CD97. *Genomics* **67**, 188–200 (2000).
234. Matsushita, H., Lelianova, V. G. & Ushkaryov, Y. A. The latrophilin family: multiply spliced G protein-coupled receptors with differential tissue distribution. *FEBS Lett.* **443**, 348–352 (1999).
235. Krasnoperov, V. *et al.* Post-translational proteolytic processing of the calcium-independent receptor of alpha-latrotoxin (CIRL), a natural chimera of the cell adhesion protein and the G protein-coupled receptor. Role of the G protein-coupled receptor proteolysis site (GPS) motif. *J. Biol. Chem.* **277**, 46518–46526 (2002).
236. Prömel, S. *et al.* The GPS motif is a molecular switch for bimodal activities of adhesion class G protein-coupled receptors. *Cell Rep.* **2**, 321–331 (2012).
237. Araç, D. *et al.* A novel evolutionarily conserved domain of cell-adhesion GPCRs mediates autoproteolysis. *EMBO J.* **31**, 1364–1378 (2012).
238. Scholz, N. *et al.* The adhesion GPCR latrophilin/CIRL shapes

mechanosensation. *Cell Rep.* **11**, 866–874 (2015).

239. Lin, H.-H., Ng, K.-F., Chen, T.-C. & Tseng, W.-Y. Ligands and Beyond: Mechanosensitive Adhesion GPCRs. *Pharm. Basel Switz.* **15**, 219 (2022).
240. Langenhan, T. Adhesion G protein–coupled receptors—Candidate metabotropic mechanosensors and novel drug targets. *Basic Clin. Pharmacol. Toxicol.* **126**, 5–16 (2020).
241. Langenhan, T., Aust, G. & Hamann, J. Sticky signaling--adhesion class G protein-coupled receptors take the stage. *Sci. Signal.* **6**, re3 (2013).
242. Frenster, J. D. *et al.* PTK7 is a positive allosteric modulator of GPR133 signaling in glioblastoma. *Cell Rep.* **42**, 112679 (2023).
243. Aguilar, A. Development: Celsr1 and Vangl2 team up to pattern the kidney. *Nat. Rev. Nephrol.* **12**, 651 (2016).
244. Liu, D. *et al.* CD97 promotes spleen dendritic cell homeostasis through the mechanosensing of red blood cells. *Science* **375**, eabi5965 (2022).
245. Demberg, L. M. *et al.* Activation of Adhesion G Protein-coupled Receptors: AGONIST SPECIFICITY OF STACHEL SEQUENCE-DERIVED PEPTIDES. *J. Biol. Chem.* **292**, 4383–4394 (2017).
246. Wang, F. *et al.* Crystal Structure of the Extracellular Domains of GPR110. *J. Mol. Biol.* **435**, 167979 (2023).
247. Wilde, C. *et al.* The constitutive activity of the adhesion GPCR GPR114/ADGRG5 is mediated by its tethered agonist. *FASEB J. Off. Publ. Fed. Am. Soc. Exp. Biol.* **30**, 666–673 (2016).
248. Liebscher, I. *et al.* A tethered agonist within the ectodomain activates the adhesion G protein-coupled receptors GPR126 and GPR133. *Cell Rep.* **9**, 2018–2026 (2014).

249. Kaczmarek, I. *et al.* The relevance of adhesion G protein-coupled receptors in metabolic functions. *Biol. Chem.* **403**, 000010151520210146 (2021).
250. Hamann, J. *et al.* International Union of Basic and Clinical Pharmacology. XCIV. Adhesion G Protein–Coupled Receptors. *Pharmacol. Rev.* **67**, 338–367 (2015).
251. Matúš, D., Post, W. B., Horn, S., Schöneberg, T. & Prömel, S. Latrophilin-1 drives neuron morphogenesis and shapes chemo- and mechanosensation-dependent behavior in *C. elegans* via a *trans* function. *Biochem. Biophys. Res. Commun.* **589**, 152–158 (2022).
252. Dietzsch, A. N. *et al.* Dysfunction of the adhesion G protein-coupled receptor latrophilin 1 (ADGRL1/LPHN1) increases the risk of obesity. *Signal Transduct. Target. Ther.* **9**, 1–14 (2024).
253. Sugita, S., Ichtchenko, K., Khvotchev, M. & Südhof, T. C. α-Latrotoxin Receptor CIRL/Latrophilin 1 (CL1) Defines an Unusual Family of Ubiquitous G-protein-linked Receptors: G-PROTEIN COUPLING NOT REQUIRED FOR TRIGGERING EXOCYTOSIS*. *J. Biol. Chem.* **273**, 32715–32724 (1998).
254. Lee, C.-S. *et al.* The G Protein-Coupled Receptor Latrophilin-2, A Marker for Heart Development, Induces Myocardial Repair After Infarction. *Stem Cells Transl. Med.* **11**, 332–342 (2022).
255. Zhang, R. S., Liakath-Ali, K. & Südhof, T. C. Latrophilin-2 and latrophilin-3 are redundantly essential for parallel-fiber synapse function in cerebellum. *eLife* **9**, e54443.
256. Mortimer, N. *et al.* Dissociation of impulsivity and aggression in mice deficient for the ADHD risk gene *Adgrl3*: Evidence for dopamine transporter dysregulation. *Neuropharmacology* **156**, 107557 (2019).
257. Legrand, F. *et al.* Eosinophil surface receptor EMR1: a novel therapeutic target

for eosinophilic disorders. *J. Allergy Clin. Immunol.* **133**, 1439-1447.e8 (2014).

258. Boyden, S. E. *et al.* Vibratory Urticaria Associated with a Missense Variant in ADGRE2. *N. Engl. J. Med.* **374**, 656–663 (2016).

259. Wei, M. *et al.* Monozygotic Twins Discordant for Immunoglobulin A Nephropathy Display Differences in DNA Methylation and Gene Expression. *Kidney Dis. Basel Switz.* **7**, 200–209 (2021).

260. Matmati, M. *et al.* The human EGF-TM7 receptor EMR3 is a marker for mature granulocytes. *J. Leukoc. Biol.* **81**, 440–448 (2007).

261. Visser, L. *et al.* Expression of the EGF-TM7 receptor CD97 and its ligand CD55 (DAF) in multiple sclerosis. *J. Neuroimmunol.* **132**, 156–163 (2002).

262. de Groot, D. M. *et al.* Therapeutic Antibody Targeting of CD97 in Experimental Arthritis: the Role of Antigen Expression, Shedding, and Internalization on the Pharmacokinetics of Anti-CD97 Monoclonal Antibody 1B21. *J. Immunol.* **183**, 4127–4134 (2009).

263. Pickering, C. *et al.* The Adhesion GPCR GPR125 is specifically expressed in the choroid plexus and is upregulated following brain injury. *BMC Neurosci.* **9**, 97 (2008).

264. Sakurai, T. *et al.* GPR125 (ADGRA3) is an autocleavable adhesion GPCR that traffics with Dlg1 to the basolateral membrane and regulates epithelial apicobasal polarity. *J. Biol. Chem.* **298**, 102475 (2022).

265. Chang, J. *et al.* Gpr124 is essential for blood-brain barrier integrity in central nervous system disease. *Nat. Med.* **23**, 450–460 (2017).

266. Chen, D.-Y. *et al.* GPR124 facilitates pericyte polarization and migration by regulating the formation of filopodia during ischemic injury. *Theranostics* **9**, 5937–5955 (2019).

267. Zhang, X.-H. *et al.* ADGRA1 negatively regulates energy expenditure and thermogenesis through both sympathetic nervous system and hypothalamus-pituitary-thyroid axis in male mice. *Cell Death Dis.* **12**, 362 (2021).
268. Krasnova, O. A. *et al.* Essential Role of Adhesion GPCR, GPR123, for Human Pluripotent Stem Cells and Reprogramming towards Pluripotency. *Cells* **12**, 304 (2023).
269. Basta, L. P. *et al.* Celsr1 and Celsr2 exhibit distinct adhesive interactions and contributions to planar cell polarity. *Front. Cell Dev. Biol.* **10**, 1064907 (2022).
270. Chen, Z. *et al.* CELSR1 variants are associated with partial epilepsy of childhood. *Am. J. Med. Genet. Part B Neuropsychiatr. Genet. Off. Publ. Int. Soc. Psychiatr. Genet.* **189**, 247–256 (2022).
271. Tissir, F. *et al.* Lack of cadherins Celsr2 and Celsr3 impairs ependymal ciliogenesis, leading to fatal hydrocephalus. *Nat. Neurosci.* **13**, 700–707 (2010).
272. Sun, J.-X. *et al.* Upregulation of GPR133 expression impaired the phagocytosis of macrophages in recurrent spontaneous miscarriage. *Epigenetics* **19**, 2337087 (2024).
273. Bianchi, E. *et al.* Control of oviductal fluid flow by the G-protein coupled receptor Adgrd1 is essential for murine embryo transit. *Nat. Commun.* **12**, 1251 (2021).
274. Wu, M. *et al.* Amelioration of non-alcoholic fatty liver disease by targeting adhesion G protein-coupled receptor F1 (Adgrf1). *eLife* **12**, e85131 (2023).
275. Huang, B. X. *et al.* Interaction between GPR110 (ADGRF1) and tight junction protein occludin implicated in blood-brain barrier permeability. *iScience* **26**, 106550 (2023).
276. Chiba, Y. *et al.* Deficiency of G protein-coupled receptor Gpr111/Adgrf2 causes enamel hypomineralization in mice by alteration of the expression of kallikrein-

related peptidase 4 (Klk4) during pH cycling process. *FASEB J. Off. Publ. Fed. Am. Soc. Exp. Biol.* **37**, e22861 (2023).

277. LopezJimenez, N. D. *et al.* Two novel genes, Gpr113, which encodes a family 2 G-protein-coupled receptor, and Trcg1, are selectively expressed in taste receptor cells. *Genomics* **85**, 472–482 (2005).
278. Chiba, Y. *et al.* G protein-coupled receptor Gpr115 (Adgrf4) is required for enamel mineralization mediated by ameloblasts. *J. Biol. Chem.* **295**, 15328–15341 (2020).
279. Winkler, R. *et al.* The Adhesion G-Protein-Coupled Receptor GPR115/ADGRF4 Regulates Epidermal Differentiation and Associates with Cytoskeletal KRT1. *Cells* **11**, 3151 (2022).
280. Röthe, J. *et al.* The adhesion GPCR GPR116/ADGRF5 has a dual function in pancreatic islets regulating somatostatin release and islet development. *Commun. Biol.* **7**, 104 (2024).
281. Niaudet, C. *et al.* Adgrf5 contributes to patterning of the endothelial deep layer in retina. *Angiogenesis* **22**, 491–505 (2019).
282. Zhu, D. *et al.* BAI1 regulates spatial learning and synaptic plasticity in the hippocampus. *J. Clin. Invest.* **125**, 1497–1508 (2015).
283. Choi, J.-S., Bae, W.-Y., Nam, S. & Jeong, J.-W. New Targets for Parkinson's Disease: Adhesion G Protein-Coupled Receptor B1 is Downregulated by AMP-Activated Protein Kinase Activation. *OMICS J. Integr. Biol.* **22**, 493–501 (2018).
284. Okajima, D., Kudo, G. & Yokota, H. Antidepressant-like behavior in brain-specific angiogenesis inhibitor 2-deficient mice. *J. Physiol. Sci. JPS* **61**, 47–54 (2011).
285. Jeong, B. C. *et al.* Brain-specific angiogenesis inhibitor 2 regulates VEGF

through GABP that acts as a transcriptional repressor. *FEBS Lett.* **580**, 669–676 (2006).

286. Duman, J. G., Tu, Y.-K. & Tolias, K. F. Emerging Roles of BAI Adhesion-GPCRs in Synapse Development and Plasticity. *Neural Plast.* **2016**, 8301737 (2016).
287. Carneiro, F. *et al.* Case Report: Diffuse Polymicrogyria Associated With a Novel ADGRG1 Variant. *Front. Pediatr.* **9**, 728077 (2021).
288. Della Chiesa, M. *et al.* GPR56 as a novel marker identifying the CD56dull CD16+ NK cell subset both in blood stream and in inflamed peripheral tissues. *Int. Immunol.* **22**, 91–100 (2010).
289. Lu, Y. *et al.* A novel ADGRG2 truncating variant associated with X-linked obstructive azoospermia in a large Chinese pedigree. *J. Assist. Reprod. Genet.* **40**, 1747–1754 (2023).
290. Zhang, D.-L. *et al.* Gq activity- and β-arrestin-1 scaffolding-mediated ADGRG2/CFTR coupling are required for male fertility. *eLife* **7**, e33432 (2018).
291. Hsiao, C.-C. *et al.* The Adhesion G Protein-Coupled Receptor GPR97/ADGRG3 Is Expressed in Human Granulocytes and Triggers Antimicrobial Effector Functions. *Front. Immunol.* **9**, 2830 (2018).
292. Kieslich, B. *et al.* The dimerized pentraxin-like domain of the adhesion G protein-coupled receptor 112 (ADGRG4) suggests function in sensing mechanical forces. *J. Biol. Chem.* **299**, 105356 (2023).
293. Werder, R. B. *et al.* The COPD GWAS gene ADGRG6 instructs function and injury response in human iPSC-derived type II alveolar epithelial cells. *Am. J. Hum. Genet.* **110**, 1735–1749 (2023).
294. Li, Q. *et al.* Structure, ligands, and roles of GPR126/ADGRG6 in the development and diseases. *Genes Dis.* **11**, 294–305 (2023).

295. Iżykowska, K. *et al.* Genetic rearrangements result in altered gene expression and novel fusion transcripts in Sézary syndrome. *Oncotarget* **8**, 39627–39639 (2017).

296. Ni, Y.-Y. *et al.* Deletion of Gpr128 results in weight loss and increased intestinal contraction frequency. *World J. Gastroenterol.* **20**, 498–508 (2014).

297. Linnert, J., Güler, B. E., Krzysko, J. & Wolfrum, U. The adhesion G protein-coupled receptor VLGR1/ADGRV1 controls autophagy. *Basic Clin. Pharmacol. Toxicol.* **133**, 313–330 (2023).

298. Weston, M. D., Luijendijk, M. W. J., Humphrey, K. D., Möller, C. & Kimberling, W. J. Mutations in the VLGR1 gene implicate G-protein signaling in the pathogenesis of Usher syndrome type II. *Am. J. Hum. Genet.* **74**, 357–366 (2004).

299. Wang, Y. *et al.* Deficiency of very large G-protein-coupled receptor-1 is a risk factor of tumor-related epilepsy: a whole transcriptome sequencing analysis. *J. Neurooncol.* **121**, 609–616 (2015).

300. Arora, C. *et al.* The landscape of cancer-rewired GPCR signaling axes. *Cell Genomics* **4**, (2024).

301. Wu, V. *et al.* Illuminating the Onco-GPCRome: Novel G protein–coupled receptor-driven oncocrine networks and targets for cancer immunotherapy. *J. Biol. Chem.* **294**, 11062–11086 (2019).

302. De Francesco, E. M., Sotgia, F., Clarke, R. B., Lisanti, M. P. & Maggiolini, M. G Protein-Coupled Receptors at the Crossroad between Physiologic and Pathologic Angiogenesis: Old Paradigms and Emerging Concepts. *Int. J. Mol. Sci.* **18**, 2713 (2017).

303. Yan, H. *et al.* An Update of G-Protein-Coupled Receptor Signaling and Its

Deregulation in Gastric Carcinogenesis. *Cancers* **15**, 736 (2023).

304. Allen, L. F., Lefkowitz, R. J., Caron, M. G. & Cotecchia, S. G-protein-coupled receptor genes as protooncogenes: constitutively activating mutation of the alpha 1B-adrenergic receptor enhances mitogenesis and tumorigenicity. *Proc. Natl. Acad. Sci.* **88**, 11354–11358 (1991).
305. Young, D., Waitches, G., Birchmeier, C., Fasano, O. & Wigler, M. Isolation and characterization of a new cellular oncogene encoding a protein with multiple potential transmembrane domains. *Cell* **45**, 711–719 (1986).
306. Gutkind, J. S., Novotny, E. A., Brann, M. R. & Robbins, K. C. Muscarinic acetylcholine receptor subtypes as agonist-dependent oncogenes. *Proc. Natl. Acad. Sci. U. S. A.* **88**, 4703–4707 (1991).
307. Julius, D., Livelli, T. J., Jessell, T. M. & Axel, R. Ectopic Expression of the Serotonin 1c Receptor and the Triggering of Malignant Transformation. *Science* **244**, 1057–1062 (1989).
308. Coughlin, S. R. Thrombin signalling and protease-activated receptors. *Nature* **407**, 258–264 (2000).
309. Mollica Poeta, V., Massara, M., Capucetti, A. & Bonecchi, R. Chemokines and Chemokine Receptors: New Targets for Cancer Immunotherapy. *Front. Immunol.* **10**, (2019).
310. Jung, J. Role of G Protein-Coupled Estrogen Receptor in Cancer Progression. *Toxicol. Res.* **35**, 209–214 (2019).
311. Aust, G. *et al.* CD97: a dedifferentiation marker in human thyroid carcinomas. *Cancer Res.* **57**, 1798–1806 (1997).
312. Ravn-Boess, N. *et al.* The expression profile and tumorigenic mechanisms of CD97 (ADGRE5) in glioblastoma render it a targetable vulnerability. *Cell Rep.*

42, 113374 (2023).

313. Haubner, S. *et al.* Cooperative CAR targeting to selectively eliminate AML and minimize escape. *Cancer Cell* **41**, 1871-1891.e6 (2023).
314. Yasinska, I. M. *et al.* The Tim-3-Galectin-9 Pathway and Its Regulatory Mechanisms in Human Breast Cancer. *Front. Immunol.* **10**, 1594 (2019).
315. Sun, J., Zhang, Z., Chen, J., Xue, M. & Pan, X. ELTD1 promotes invasion and metastasis by activating MMP2 in colorectal cancer. *Int. J. Biol. Sci.* **17**, 3048–3058 (2021).
316. Niinivirta, M. *et al.* Tumor endothelial ELTD1 as a predictive marker for treatment of renal cancer patients with sunitinib. *BMC Cancer* **20**, 339 (2020).
317. Sheldon, H. *et al.* ADGRL4/ELTD1 Expression in Breast Cancer Cells Induces Vascular Normalization and Immune Suppression. *Mol. Cancer Res. MCR* **19**, 1957–1969 (2021).
318. Guihurt Santiago, J. *et al.* Adhesion G protein-coupled receptor, ELTD1, is a potential therapeutic target for retinoblastoma migration and invasion. *BMC Cancer* **21**, 53 (2021).
319. Maiga, A. *et al.* Transcriptome analysis of G protein-coupled receptors in distinct genetic subgroups of acute myeloid leukemia: identification of potential disease-specific targets. *Blood Cancer J.* **6**, e431 (2016).
320. Davies, J. Q. *et al.* Leukocyte adhesion-GPCR EMR2 is aberrantly expressed in human breast carcinomas and is associated with patient survival. *Oncol. Rep.* **25**, 619–627 (2011).
321. Feliciano, A. *et al.* miR-99a reveals two novel oncogenic proteins E2F2 and EMR2 and represses stemness in lung cancer. *Cell Death Dis.* **8**, e3141 (2017).
322. Kane, A. J., Sughrue, M. E., Rutkowski, M. J., Phillips, J. J. & Parsa, A. T. EMR-

3: a potential mediator of invasive phenotypic variation in glioblastoma and novel therapeutic target. *Neuroreport* **21**, 1018–1022 (2010).

323. Wobus, M., Huber, O., Hamann, J. & Aust, G. CD97 overexpression in tumor cells at the invasion front in colorectal cancer (CC) is independently regulated of the canonical Wnt pathway. *Mol. Carcinog.* **45**, 881–886 (2006).
324. HE, Z., WU, H., JIAO, Y. & ZHENG, J. Expression and prognostic value of CD97 and its ligand CD55 in pancreatic cancer. *Oncol. Lett.* **9**, 793–797 (2015).
325. Li, C. *et al.* CD97 promotes gastric cancer cell proliferation and invasion through exosome-mediated MAPK signaling pathway. *World J. Gastroenterol. WJG* **21**, 6215–6228 (2015).
326. Wobus, M. *et al.* Association of the EGF-TM7 receptor CD97 expression with FLT3-ITD in acute myeloid leukemia. *Oncotarget* **6**, 38804–38815 (2015).
327. Wang, Z., Li, Y., Zhou, F., Piao, Z. & Hao, J. β-elemene enhances anticancer bone neoplasms efficacy of paclitaxel through regulation of GPR124 in bone neoplasms cells. *Oncol. Lett.* **16**, 2143–2150 (2018).
328. Gao, Y. *et al.* miR-138-5p reverses gefitinib resistance in non-small cell lung cancer cells via negatively regulating G protein-coupled receptor 124. *Biochem. Biophys. Res. Commun.* **446**, 179–186 (2014).
329. Cherry, A. E. *et al.* GPR124 regulates microtubule assembly, mitotic progression, and glioblastoma cell proliferation. *Glia* **67**, 1558–1570 (2019).
330. Wu, Y. *et al.* Elevated G-Protein Receptor 125 (GPR125) Expression Predicts Good Outcomes in Colorectal Cancer and Inhibits Wnt/β-Catenin Signaling Pathway. *Med. Sci. Monit. Int. Med. J. Exp. Clin. Res.* **24**, 6608–6616 (2018).
331. Xu, M., Zhu, S., Xu, R. & Lin, N. Identification of CELSR2 as a novel prognostic biomarker for hepatocellular carcinoma. *BMC Cancer* **20**, 313 (2020).

332. Autry, R. J. *et al.* Integrative genomic analyses reveal mechanisms of glucocorticoid resistance in acute lymphoblastic leukemia. *Nat. Cancer* **1**, 329–344 (2020).
333. YANG, J., WU, S. & ALACHKAR, H. Characterization of upregulated adhesion GPCRs in acute myeloid leukemia. *Transl. Res. J. Lab. Clin. Med.* **212**, 26–35 (2019).
334. Lum, A. M. *et al.* Orphan receptor GPR110, an oncogene overexpressed in lung and prostate cancer. *BMC Cancer* **10**, 40 (2010).
335. Bhat, R. R. *et al.* GPCRs profiling and identification of GPR110 as a potential new target in HER2+ breast cancer. *Breast Cancer Res. Treat.* **170**, 279–292 (2018).
336. Liu, Z., Zhang, G., Zhao, C. & Li, J. Clinical Significance of G Protein-Coupled Receptor 110 (GPR110) as a Novel Prognostic Biomarker in Osteosarcoma. *Med. Sci. Monit. Int. Med. J. Exp. Clin. Res.* **24**, 5216–5224 (2018).
337. Yang, L. *et al.* High expression of GPR116 indicates poor survival outcome and promotes tumor progression in colorectal carcinoma. *Oncotarget* **8**, 47943–47956 (2017).
338. Tang, X. *et al.* GPR116, an adhesion G-protein-coupled receptor, promotes breast cancer metastasis via the Gαq-p63RhoGEF-Rho GTPase pathway. *Cancer Res.* **73**, 6206–6218 (2013).
339. Kang, G. *et al.* Exome sequencing identifies early gastric carcinoma as an early stage of advanced gastric cancer. *PloS One* **8**, e82770 (2013).
340. Kaur, B., Brat, D. J., Calkins, C. C. & Van Meir, E. G. Brain angiogenesis inhibitor 1 is differentially expressed in normal brain and glioblastoma independently of p53 expression. *Am. J. Pathol.* **162**, 19–27 (2003).

341. Fukushima, Y. *et al.* Brain-specific angiogenesis inhibitor 1 expression is inversely correlated with vascularity and distant metastasis of colorectal cancer. *Int. J. Oncol.* **13**, 967–970 (1998).
342. Meisen, W. H. *et al.* Changes in BAI1 and nestin expression are prognostic indicators for survival and metastases in breast cancer and provide opportunities for dual targeted therapies. *Mol. Cancer Ther.* **14**, 307–314 (2015).
343. Hatanaka, H. *et al.* Vascularization is decreased in pulmonary adenocarcinoma expressing brain-specific angiogenesis inhibitor 1 (BAI1). *Int. J. Mol. Med.* **5**, 181–183 (2000).
344. Yang, L. *et al.* GPR56 Regulates VEGF production and angiogenesis during melanoma progression. *Cancer Res.* **71**, 5558–5568 (2011).
345. Daga, S. *et al.* High GPR56 surface expression correlates with a leukemic stem cell gene signature in CD34-positive AML. *Cancer Med.* **8**, 1771–1778 (2019).
346. Ji, B. *et al.* GPR56 promotes proliferation of colorectal cancer cells and enhances metastasis via epithelial- mesenchymal transition through PI3K/AKT signaling activation. *Oncol. Rep.* **40**, 1885–1896 (2018).
347. Ahn, J. I. *et al.* G-protein coupled receptor 64 (GPR64) acts as a tumor suppressor in endometrial cancer. *BMC Cancer* **19**, 810 (2019).
348. Peeters, M. C. *et al.* The adhesion G protein-coupled receptor G2 (ADGRG2/GPR64) constitutively activates SRE and NFκB and is involved in cell adhesion and migration. *Cell. Signal.* **27**, 2579–2588 (2015).
349. Richter, G. H. S. *et al.* G-Protein coupled receptor 64 promotes invasiveness and metastasis in Ewing sarcomas through PGF and MMP1. *J. Pathol.* **230**, 70–81 (2013).

350. An, W. *et al.* Progesterone activates GPR126 to promote breast cancer development via the Gi pathway. *Proc. Natl. Acad. Sci. U. S. A.* **119**, e2117004119 (2022).
351. Cui, H. *et al.* GPR126 regulates colorectal cancer cell proliferation by mediating HDAC2 and GLI2 expression. *Cancer Sci.* **112**, 1798–1810 (2021).
352. Usui, T. *et al.* Flamingo, a seven-pass transmembrane cadherin, regulates planar cell polarity under the control of Frizzled. *Cell* **98**, 585–595 (1999).
353. Wang, X.-J. *et al.* Understanding CELSRs - Cadherin EGF LAG seven-pass G-type receptors. *J. Neurochem.* **131**, 699–711 (2014).
354. Bui, D. L. H. *et al.* The adhesion GPCRs CELSR1-3 and LPHN3 engage G proteins via distinct activation mechanisms. *Cell Rep.* **42**, 112552 (2023).
355. Shima, Y. *et al.* Differential expression of the seven-pass transmembrane cadherin genes Celsr1-3 and distribution of the Celsr2 protein during mouse development. *Dev. Dyn. Off. Publ. Am. Assoc. Anat.* **223**, 321–332 (2002).
356. Formstone, C. J., Barclay, J., Rees, M. & Little, P. F. Chromosomal localization of Celsr2 and Celsr3 in the mouse; Celsr3 is a candidate for the tippy (tip) lethal mutant on chromosome 9. *Mamm. Genome Off. J. Int. Mamm. Genome Soc.* **11**, 392–394 (2000).
357. Cortijo, C., Gouzi, M., Tissir, F. & Grapin-Botton, A. Planar cell polarity controls pancreatic beta cell differentiation and glucose homeostasis. *Cell Rep.* **2**, 1593–1606 (2012).
358. Kim, M. S. *et al.* Prioritization of therapeutic targets for dyslipidemia using integrative multi-omics and multi-trait analysis. *Cell Rep. Med.* **4**, 101112 (2023).
359. Small, A. M. *et al.* Multiancestry Genome-Wide Association Study of Aortic Stenosis Identifies Multiple Novel Loci in the Million Veteran Program.

Circulation **147**, 942–955 (2023).

360. Yu Chen, H. *et al.* Dyslipidemia, inflammation, calcification, and adiposity in aortic stenosis: a genome-wide study. *Eur. Heart J.* **44**, 1927–1939 (2023).
361. Shaheen, R. *et al.* Characterizing the morbid genome of ciliopathies. *Genome Biol.* **17**, 242 (2016).
362. Kimura, H., Usui, T., Tsubouchi, A. & Uemura, T. Potential dual molecular interaction of the Drosophila 7-pass transmembrane cadherin Flamingo in dendritic morphogenesis. *J. Cell Sci.* **119**, 1118–1129 (2006).
363. Li, C. *et al.* Planar cell polarity protein Celsr2 maintains structural and functional integrity of adult cortical synapses. *Prog. Neurobiol.* **219**, 102352 (2022).
364. Gaengel, K. & Mlodzik, M. Egfr signaling regulates ommatidial rotation and cell motility in the Drosophila eye via MAPK/Pnt signaling and the Ras effector Canoe/AF6. *Dev. Camb. Engl.* **130**, 5413–23 (2003).
365. Qu, Y. *et al.* Genetic evidence that Celsr3 and Celsr2, together with Fzd3, regulate forebrain wiring in a Vangl-independent manner. *Proc. Natl. Acad. Sci. U. S. A.* **111**, E2996-3004 (2014).
366. Collected studies on immunity / by Professor Paul Ehrlich, privy councilor and director of the Royal institute for experimental therapy, Frankfurt, Germany, and by his collaborators; with several new contributions, including including a chapter written expressly for this edition by Professor Ehrlich; tr. by Dr. Charles Bolduan. - Vanderbilt University. https://catalog.library.vanderbilt.edu/discovery/fulldisplay/alma991033108699703276/01VAN_INST:vanui.
367. Keller, M. A. & Stiehm, E. R. Passive immunity in prevention and treatment of infectious diseases. *Clin. Microbiol. Rev.* **13**, 602–614 (2000).

368. The Nobel Prize in Physiology or Medicine 1901. *NobelPrize.org* https://www.nobelprize.org/prizes/medicine/1901/behring/facts/.

369. Casadevall, A. & Scharff, M. D. Return to the Past: The Case for Antibody-Based Therapies in Infectious Diseases. *Clin. Infect. Dis. Off. Publ. Infect. Dis. Soc. Am.* **21**, 150–161 (1995).

370. Rostock, R. A., Klein, J. L., Leichner, P., Kopher, K. A. & Order, S. E. Selective tumor localization in experimental hepatoma by radiolabeled antiferritin antibody. *Int. J. Radiat. Oncol.* **9**, 1345–1350 (1983).

371. McLaughlin, P. *et al.* Rituximab chimeric anti-CD20 monoclonal antibody therapy for relapsed indolent lymphoma: half of patients respond to a four-dose treatment program. *J. Clin. Oncol. Off. J. Am. Soc. Clin. Oncol.* **16**, 2825–2833 (1998).

372. Garcia, J. *et al.* Bevacizumab (Avastin®) in cancer treatment: A review of 15 years of clinical experience and future outlook. *Cancer Treat. Rev.* **86**, 102017 (2020).

373. von Arx, C. *et al.* The evolving therapeutic landscape of trastuzumab-drug conjugates: Future perspectives beyond HER2-positive breast cancer. *Cancer Treat. Rev.* **113**, 102500 (2023).

374. Moolten, F. L. & Cooperband, S. R. Selective destruction of target cells by diphtheria toxin conjugated to antibody directed against antigens on the cells. *Science* **169**, 68–70 (1970).

375. FitzGerald, D. J., Waldmann, T. A., Willingham, M. C. & Pastan, I. Pseudomonas exotoxin-anti-TAC. Cell-specific immunotoxin active against cells expressing the human T cell growth factor receptor. *J. Clin. Invest.* **74**, 966–971 (1984).

376. Thorpe, P. E. *et al.* Abrogation of the non-specific toxicity of abrin conjugated to anti-lymphocyte globulin. *Clin. Exp. Immunol.* **43**, 195–200 (1981).
377. Krolick, K. A., Villemez, C., Isakson, P., Uhr, J. W. & Vitetta, E. S. Selective killing of normal or neoplastic B cells by antibodies coupled to the A chain of ricin. *Proc. Natl. Acad. Sci. U. S. A.* **77**, 5419–5423 (1980).
378. Cooper, N. *et al.* Synthesis of novel C2-aryl pyrrolobenzodiazepines (PBDs) as potential antitumour agents. *Chem. Commun. Camb. Engl.* 1764–1765 (2002) doi:10.1039/b205136b.
379. Shen, B.-Q. *et al.* Conjugation site modulates the in vivo stability and therapeutic activity of antibody-drug conjugates. *Nat. Biotechnol.* **30**, 184–189 (2012).
380. Iodine-131 Tositumomab. *BioDrugs* **17**, 290–295 (2003).
381. Leonard, J. P. *et al.* Effects of single-dose interleukin-12 exposure on interleukin-12-associated toxicity and interferon-gamma production. *Blood* **90**, 2541–2548 (1997).
382. Waldhauer, I. *et al.* Simlukafusp alfa (FAP-IL2v) immunocytokine is a versatile combination partner for cancer immunotherapy. *mAbs* **13**, 1913791.
383. Roulleaux Dugage, M., Nassif, E. F., Italiano, A. & Bahleda, R. Improving Immunotherapy Efficacy in Soft-Tissue Sarcomas: A Biomarker Driven and Histotype Tailored Review. *Front. Immunol.* **12**, 775761 (2021).
384. Atiq, M. O. *et al.* Safety evaluation of M9241 in combination with docetaxel in metastatic prostate cancer. *J. Clin. Oncol.* **40**, 93–93 (2022).
385. Wagner, K., Schulz, P., Scholz, A., Wiedenmann, B. & Menrad, A. The targeted immunocytokine L19-IL2 efficiently inhibits the growth of orthotopic pancreatic cancer. *Clin. Cancer Res. Off. J. Am. Assoc. Cancer Res.* **14**, 4951–4960

(2008).

386. Chames, P., Van Regenmortel, M., Weiss, E. & Baty, D. Therapeutic antibodies: successes, limitations and hopes for the future. *Br. J. Pharmacol.* **157**, 220–233 (2009).

387. Greenberg, A. S. *et al.* A new antigen receptor gene family that undergoes rearrangement and extensive somatic diversification in sharks. *Nature* **374**, 168–173 (1995).

388. Hamers-Casterman, C. *et al.* Naturally occurring antibodies devoid of light chains. *Nature* **363**, 446–448 (1993).

389. Vilá, B. & Arzamendia, Y. South American Camelids: their values and contributions to people. *Sustain. Sci.* **17**, 707–724 (2022).

390. Lafaye, P., Achour, I., England, P., Duyckaerts, C. & Rougeon, F. Single-domain antibodies recognize selectively small oligomeric forms of amyloid beta, prevent Abeta-induced neurotoxicity and inhibit fibril formation. *Mol. Immunol.* **46**, 695–704 (2009).

391. Muyldermans, S. & Lauwereys, M. Unique single-domain antigen binding fragments derived from naturally occurring camel heavy-chain antibodies. *J. Mol. Recognit. JMR* **12**, 131–140 (1999).

392. Bannas, P., Hambach, J. & Koch-Nolte, F. Nanobodies and Nanobody-Based Human Heavy Chain Antibodies As Antitumor Therapeutics. *Front. Immunol.* **8**, 1603 (2017).

393. Flicker, S., Zettl, I. & Tillib, S. V. Nanobodies—Useful Tools for Allergy Treatment? *Front. Immunol.* **11**, 576255 (2020).

394. Nambulli, S. *et al.* Inhalable Nanobody (PiN-21) prevents and treats SARS-CoV-2 infections in Syrian hamsters at ultra-low doses. *Sci. Adv.* **7**, eabh0319 (2021).

395. Svecova, D. *et al.* A randomized, double-blind, placebo-controlled phase 1 study of multiple ascending doses of subcutaneous M1095, an anti-interleukin 17A/F nanobody, in moderate-to-severe psoriasis. *J. Am. Acad. Dermatol.* **81**, 196–203 (2019).
396. Vincke, C. *et al.* General strategy to humanize a camelid single-domain antibody and identification of a universal humanized nanobody scaffold. *J. Biol. Chem.* **284**, 3273–3284 (2009).
397. Wang, J. *et al.* Research Progress and Applications of Multivalent, Multispecific and Modified Nanobodies for Disease Treatment. *Front. Immunol.* **12**, (2022).
398. Duggan, S. Caplacizumab: First Global Approval. *Drugs* **78**, 1639–1642 (2018).
399. Li, D. *et al.* Camel nanobody-based B7-H3 CAR-T cells show high efficacy against large solid tumours. *Nat. Commun.* **14**, 5920 (2023).
400. Keam, S. J. Ozoralizumab: First Approval. *Drugs* **83**, 87–92 (2023).
401. Markham, A. Envafolimab: First Approval. *Drugs* **82**, 235–240 (2022).
402. Yang, E. Y. & Shah, K. Nanobodies: Next Generation of Cancer Diagnostics and Therapeutics. *Front. Oncol.* **10**, 1182 (2020).
403. Araste, F., Ebrahimizadeh, W., Rasooli, I., Rajabibazl, M. & Mousavi Gargari, S. L. A novel VHH nanobody against the active site (the CA domain) of tumor-associated, carbonic anhydrase isoform IX and its usefulness for cancer diagnosis. *Biotechnol. Lett.* **36**, 21–28 (2014).
404. Van Impe, K. *et al.* A nanobody targeting the F-actin capping protein CapG restrains breast cancer metastasis. *Breast Cancer Res. BCR* **15**, R116 (2013).
405. Krasniqi, A. *et al.* Theranostic Radiolabeled Anti-CD20 sdAb for Targeted Radionuclide Therapy of Non-Hodgkin Lymphoma. *Mol. Cancer Ther.* **16**, 2828–2839 (2017).

406. Romão, E. *et al.* Identification of Nanobodies against the Acute Myeloid Leukemia Marker CD33. *Int. J. Mol. Sci.* **21**, 310 (2020).
407. Wan, R. *et al.* Screening and antitumor effect of an anti- CTLA- 4 nanobody. *Oncol. Rep.* **39**, 511–518 (2018).
408. Benloucif, A. *et al.* Rapid nanobody-based imaging of mesothelin expressing malignancies compatible with blocking therapeutic antibodies. *Front. Immunol.* **14**, 1200652 (2023).
409. Roovers, R. C. *et al.* Efficient inhibition of EGFR signaling and of tumour growth by antagonistic anti-EFGR Nanobodies. *Cancer Immunol. Immunother. CII* **56**, 303–317 (2007).
410. Omidfar, K. *et al.* Efficient growth inhibition of EGFR over-expressing tumor cells by an anti-EGFR nanobody. *Mol. Biol. Rep.* **40**, 6737–6745 (2013).
411. Omidfar, K. *et al.* Production of a novel camel single-domain antibody specific for the type III mutant EGFR. *Tumour Biol. J. Int. Soc. Oncodevelopmental Biol. Med.* **25**, 296–305 (2004).
412. Mo, F. *et al.* Nanobody-based chimeric antigen receptor T cells designed by CRISPR/Cas9 technology for solid tumor immunotherapy. *Signal Transduct. Target. Ther.* **6**, 80 (2021).
413. Zhang, X. *et al.* High Efficacy and Safety of Nanobody Based Anti-BCMA CAR-T Cell Therapy in Treating Patients with Relapsed or Refractory Multiple Myeloma. *Blood* **142**, 2107 (2023).
414. Zhang, M. *et al.* First-in-human clinical trial of the autologous CD7-CART for relapsed/refractory ACUTE lymphoblastic leukemia/lymphoma. *J. Clin. Oncol.* **38**, 3026–3026 (2020).
415. Zhang, T. *et al.* Nanobody-based anti-CD22-chimeric antigen receptor T cell

immunotherapy exhibits improved remission against B-cell acute lymphoblastic leukemia. *Transpl. Immunol.* **71**, 101538 (2022).

416. Li, D. *et al.* EpCAM-targeting CAR-T cell immunotherapy is safe and efficacious for epithelial tumors. *Sci. Adv.* **9**, eadg9721.

417. Definition of anti-VEGF/ANG2 nanobody BI 836880 - NCI Drug Dictionary - NCI. https://www.cancer.gov/publications/dictionaries/cancer-drug/def/anti-vegf-ang2-nanobody-bi-836880 (2011).

418. Li, Q. *et al.* The anti-PD-L1/CTLA-4 bispecific antibody KN046 in combination with nab-paclitaxel in first-line treatment of metastatic triple-negative breast cancer: a multicenter phase II trial. *Nat. Commun.* **15**, 1015 (2024).

419. Ma, Y. *et al.* Phase I trial of KN046, a novel bispecific antibody targeting PD-L1 and CTLA-4 in patients with advanced solid tumors. *J. Immunother. Cancer* **11**, e006654 (2023).

420. Xiong, A. *et al.* Efficacy and safety of KN046, a novel bispecific antibody against PD-L1 and CTLA-4, in patients with non-small cell lung cancer who failed platinum-based chemotherapy: a phase II study. *Eur. J. Cancer Oxf. Engl. 1990* **190**, 112936 (2023).

421. Muyldermans, S. A guide to: generation and design of nanobodies. *FEBS J.* **288**, 2084–2102 (2021).

422. Liu, W. *et al.* Recent advances in the selection and identification of antigen-specific nanobodies. *Mol. Immunol.* **96**, 37–47 (2018).

423. webmaster. L'IPC classé 5ème dans la prise en charge du cancer du sein. *Institut Paoli-Calmettes* https://www.institutpaolicalmettes.fr/lipc-classe-5eme-dans-la-prise-en-charge-du-cancer-du-sein/ (2020).

424. Kusuluri, D. K. *et al.* Adhesion G protein-coupled receptor VLGR1/ADGRV1

regulates cell spreading and migration by mechanosensing at focal adhesions. *iScience* **24**, 102283 (2021).

425. Stoveken, H. M., Hajduczok, A. G., Xu, L. & Tall, G. G. Adhesion G protein-coupled receptors are activated by exposure of a cryptic tethered agonist. *Proc. Natl. Acad. Sci. U. S. A.* **112**, 6194–6199 (2015).
426. Demberg, L. M., Rothemund, S., Schöneberg, T. & Liebscher, I. Identification of the tethered peptide agonist of the adhesion G protein-coupled receptor GPR64/ADGRG2. *Biochem. Biophys. Res. Commun.* **464**, 743–747 (2015).
427. Dates, A. N. *et al.* Heterogeneity of tethered agonist signaling in adhesion G protein-coupled receptors. *Cell Chem. Biol.* **0**, (2024).
428. Karimaian, A., Majidinia, M., Bannazadeh Baghi, H. & Yousefi, B. The crosstalk between Wnt/β-catenin signaling pathway with DNA damage response and oxidative stress: Implications in cancer therapy. *DNA Repair* **51**, 14–19 (2017).
429. Zhong, Z. & Virshup, D. M. Wnt Signaling and Drug Resistance in Cancer. *Mol. Pharmacol.* **97**, 72–89 (2020).
430. Martin-Orozco, E., Sanchez-Fernandez, A., Ortiz-Parra, I. & Ayala-San Nicolas, M. WNT Signaling in Tumors: The Way to Evade Drugs and Immunity. *Front. Immunol.* **10**, 2854 (2019).
431. Zhao, Z., Mei, Y., Wang, Z. & He, W. The Effect of Oxidative Phosphorylation on Cancer Drug Resistance. *Cancers* **15**, 62 (2022).
432. Uslu, C., Kapan, E. & Lyakhovich, A. Cancer resistance and metastasis are maintained through oxidative phosphorylation. *Cancer Lett.* **587**, 216705 (2024).
433. Hong, H. S. *et al.* OXPHOS promotes apoptotic resistance and cellular persistence in TH17 cells in the periphery and tumor microenvironment. *Sci. Immunol.* **7**, eabm8182 (2022).

434. Okon, I. S. & Zou, M.-H. Mitochondrial ROS and cancer drug resistance: Implications for therapy. *Pharmacol. Res.* **100**, 170–174 (2015).
435. Zhou, X. *et al.* Molecular mechanisms of ROS-modulated cancer chemoresistance and therapeutic strategies. *Biomed. Pharmacother.* **165**, 115036 (2023).
436. Assay-ready drug plates | Drug Discovery, Chemical Biology and Screening | University of Helsinki. https://www.helsinki.fi/en/infrastructures/drug-discovery-chemical-biology-and-screening/infrastructures/high-throughput-biomedicine/assay-ready-drug-plates.
437. Assay-Ready Plates. *Newcells Biotech* https://newcellsbiotech.co.uk/models/kidney-nephron-models/assay-ready-plates/.
438. UniSA Ventures | Assay ready plates - UniSA Ventures - University of South Australia. https://www.unisa.edu.au/connect/unisa-ventures/available-technologies/assay-ready-plates/.
439. Muguruma, M. *et al.* Differences in drug sensitivity between two-dimensional and three-dimensional culture systems in triple-negative breast cancer cell lines. *Biochem. Biophys. Res. Commun.* **533**, 268–274 (2020).
440. Kapałczyńska, M. *et al.* 2D and 3D cell cultures – a comparison of different types of cancer cell cultures. *Arch. Med. Sci. AMS* **14**, 910–919 (2018).
441. Sheridan, C. Wnt is back in drugmakers' sights, but is it druggable? *Nat. Biotechnol.* **36**, 1028–1029 (2018).
442. Chavez, K. J., Garimella, S. V. & Lipkowitz, S. Triple Negative Breast Cancer Cell Lines: One Tool in the Search for Better Treatment of Triple Negative Breast Cancer. *Breast Dis.* **32**, 35–48 (2010).

443. De Pascalis, C. & Etienne-Manneville, S. Single and collective cell migration: the mechanics of adhesions. *Mol. Biol. Cell* **28**, 1833–1846 (2017).
444. Friedl, P. & Mayor, R. Tuning Collective Cell Migration by Cell-Cell Junction Regulation. *Cold Spring Harb. Perspect. Biol.* **9**, a029199 (2017).
445. Chaudhary, P. K. & Kim, S. An Insight into GPCR and G-Proteins as Cancer Drivers. *Cells* **10**, 3288 (2021).
446. Shin, D., Lin, S.-T., Fu, Y.-H. & Ptácek, L. J. Very large G protein-coupled receptor 1 regulates myelin-associated glycoprotein via Gαs/Gαq-mediated protein kinases A/C. *Proc. Natl. Acad. Sci. U. S. A.* **110**, 19101–19106 (2013).
447. Hu, Q.-X. *et al.* Constitutive Gαi coupling activity of very large G protein-coupled receptor 1 (VLGR1) and its regulation by PDZD7 protein. *J. Biol. Chem.* **289**, 24215–24225 (2014).
448. Bennett, L. D., Fox, J. M. & Signoret, N. Mechanisms regulating chemokine receptor activity. *Immunology* **134**, 246–256 (2011).
449. Blanchet, X., Langer, M., Weber, C., Koenen, R. R. & von Hundelshausen, P. Touch of Chemokines. *Front. Immunol.* **3**, (2012).
450. Wu, B. *et al.* Structures of the CXCR4 chemokine receptor in complex with small molecule and cyclic peptide antagonists. *Science* **330**, 1066–1071 (2010).
451. Roy, I., Getschman, A. E., Volkman, B. F. & Dwinell, M. B. Exploiting Agonist Biased Signaling of Chemokines to Target Cancer. *Mol. Carcinog.* **56**, 804–813 (2017).
452. Janah, L. *et al.* Glucagon Receptor Signaling and Glucagon Resistance. *Int. J. Mol. Sci.* **20**, 3314 (2019).
453. Evans, K. W. *et al.* Oxidative Phosphorylation Is a Metabolic Vulnerability in Chemotherapy-Resistant Triple-Negative Breast Cancer. *Cancer Res.* **81**,

5572–5581 (2021).

454. Cheng, G. *et al.* Mitochondria-targeted magnolol inhibits OXPHOS, proliferation, and tumor growth via modulation of energetics and autophagy in melanoma cells. *Cancer Treat. Res. Commun.* **25**, 100210 (2020).

455. Ren, L. *et al.* PHB2 promotes colorectal cancer cell proliferation and tumorigenesis through NDUFS1-mediated oxidative phosphorylation. *Cell Death Dis.* **14**, 1–11 (2023).

456. Greene, J., Segaran, A. & Lord, S. Targeting OXPHOS and the electron transport chain in cancer; Molecular and therapeutic implications. *Semin. Cancer Biol.* **86**, 851–859 (2022).

457. Simula, L. *et al.* Mitochondrial metabolism sustains CD8+ T cell migration for an efficient infiltration into solid tumors. *Nat. Commun.* **15**, 2203 (2024).

458. Saurty-Seerunghen, M. S. *et al.* Glioblastoma cell motility depends on enhanced oxidative stress coupled with mobilization of a sulfurtransferase. *Cell Death Dis.* **13**, 1–12 (2022).

459. Zanotelli, M. R., Zhang, J. & Reinhart-King, C. A. Mechanoresponsive metabolism in cancer cell migration and metastasis. *Cell Metab.* **33**, 1307–1321 (2021).

460. Commander, R. *et al.* Subpopulation targeting of pyruvate dehydrogenase and GLUT1 decouples metabolic heterogeneity during collective cancer cell invasion. *Nat. Commun.* **11**, 1533 (2020).

461. Huo, J. *et al.* Neutralizing nanobodies bind SARS-CoV-2 spike RBD and block interaction with ACE2. *Nat. Struct. Mol. Biol.* **27**, 846–854 (2020).

462. Chi, X. *et al.* An ultrapotent RBD-targeted biparatopic nanobody neutralizes broad SARS-CoV-2 variants. *Signal Transduct. Target. Ther.* **7**, 1–10 (2022).

463. Webb, D. R., Handel, T. M., Kretz-Rommel, A. & Stevens, R. C. Opportunities for Functional Selectivity in GPCR Antibodies. *Biochem. Pharmacol.* **85**, 147–152 (2013).

464. Perez, D. M. From Plants to Man: The GPCR “Tree of Life”. *Mol. Pharmacol.* **67**, 1383–1384 (2005).

465. Markovic, D. & Challiss, R. A. J. Alternative splicing of G protein-coupled receptors: physiology and pathophysiology. *Cell. Mol. Life Sci. CMLS* **66**, 3337–3352 (2009).

466. Kuhn, C. K. *et al.* The repertoire and structure of adhesion GPCR transcript variants assembled from publicly available deep-sequenced human samples. *Nucleic Acids Res.* **52**, 3823–3836 (2024).

467. Oku, T., Ando, Y., Ogura, M. & Tsuji, T. Development of Splice Variant-Specific Monoclonal Antibodies Against Human α3 Integrin. *Monoclon. Antibodies Immunodiagn. Immunother.* **35**, 12–17 (2016).

468. The triple negative breast cancer drugs graveyard: a review of failed clinical trials 2017-2022. https://www-tandfonline-com.proxy.insermbiblio.inist.fr/doi/epdf/10.1080/13543784.2022.2151433?needAccess=true.

469. Staus, D. P. *et al.* Allosteric Nanobodies Reveal the Dynamic Range and Diverse Mechanisms of GPCR Activation. *Nature* **535**, 448–452 (2016).

470. Han, L. *et al.* Single VHH-directed BCMA CAR-T cells cause remission of relapsed/refractory multiple myeloma. *Leukemia* **35**, 3002–3006 (2021).

471. Jin, B., Odongo, S., Radwanska, M. & Magez, S. NANOBODIES®: A Review of Diagnostic and Therapeutic Applications. *Int. J. Mol. Sci.* **24**, 5994 (2023).

472. Wilken, J. A. *et al.* Shedding of soluble epidermal growth factor receptor

(sEGFR) is mediated by a metalloprotease/fibronectin/integrin axis and inhibited by cetuximab. *Biochemistry* **52**, 4531–4540 (2013).

473. Tsé, C., Gauchez, A.-S., Jacot, W. & Lamy, P.-J. HER2 shedding and serum HER2 extracellular domain: Biology and clinical utility in breast cancer. *Cancer Treat. Rev.* **38**, 133–142 (2012).